DOCTORAL THESIS

Dynamics of viscoelastic-magnetorheological sandwich structures: multiphysics analysis

Author:
Leire Irazu

Supervisor:
Dra. María Jesús Elejabarrieta

A thesis submitted
in fulfillment of the requirements for the degree of
Doctor by Mondragon Unibertsitatea

Department of Mechanical and Industial production
Mondragon Unibertsitatea

October 15, 2017

Aita eta Amari

Laburpena

Sektore industrial askoren helburua egiturazko bibrazioak murriztea da, honela, osagai mekanikoen bizitza erabilgarria luzatu eta erradiazio akustikoa murrizten baita. Sandwich biskoelastikoak oso erabiliak izan dira egiturazko bibrazioak moteltzeko, izan ere, inplementatzeko errazak eta kostu baxukoak baitira. Gaur egun, gero eta bibrazio-kontrol efikazagoa eskatzen denez, denbora errealean ausazko bibrazioetara egokitzeko gai diren estruktura adimendunetan ardaztu dira azken ikerketak. Material magnetoerreologikoak material adimendunak dira, zeinen propietate erreologikoak eremu magnetiko baten bidez aldatu daitezkeen. Hortaz, ohiko sandwichen nukleoa material magnetoerreologikoekin ordezkatu daiteke, sandwich estruktura adimenduak sortzeko.

Tesi doktoral honen helburu nagusia sandwich biskoelastiko-magnetoerreologiko meheen dinamika aztertzea da. Eremu magnetikorik aplikatu ezean, sandwich hauen izaera dinamikoa sandwich biskoelastikoen bera da. Eremu magnetikoak aplikatzean, berriz, sandwichen izaera dinamikoa aldatu egiten da, beraien azal eta nukleoetan sortzen diren fenomeno ezberdinen akoplamenduagatik.

Lehenik, sandwich biskoelastiko meheen jokaera dinamikoa aztertu da, sandwich biskoelastiko-magnetoerreologikoen jokaera eremu magnetikorik gabe analizatzeko asmoz. Horretarako, konposizio ezberdineko sandwich biskoelastikoak karakterizatu eta zenbakizko ereduak definitu dira. Itsasgarri biskoelastikoek eta azal metalikoek sandwicharen propietate dinamikoetan duten eragina zehaztu da emaitza esperimental eta zenbakizkoei esker.

Azal metalikoetan sortutako Foucault-en korronteen fenomenoa ere aztertu da, korronte hauek sandwich biskoelastiko-magnetorreologikoen jokaera dinamikoaren gain duten eragina zehazteko. Horretarako, metalezko habe baten analisi modal esperimentala gauzatu da, habeak Foucault-en korronteak induzituta eta induzitu gabe dituelarik. Jarraian Foucault-en korronteen moteltze-gaitasuna ikusirik, sandwich hibrido berria proposatu da, zeinak moteltze biskoelastikoa eta Foucault-ena batzen dituen. Ondoren, metodo alderantzikatu berria garatu da, korronte hauen eragina zenbatetsi eta modelatzeko.

Nukleo biskoelastiko-magnetoerreologikoetan sortutako fenomenoak ere aztertu dira, hau da, efektu magnetoerreologikoa eta indar magnetikoa. Horretarako, bi fenomeno hauek kontutan hartzen dituen sandwich biskoelastiko-magnetoerreologikoen eredu dinamikoa proposatu eta emaitza esperimentalekin egiaztatu da.

Azkenik, sandwich biskoelastiko-magnetoerreologiko meheen jokaera dinamikoa esperimentalki ebaluatu da. Partikula magnetikoek eta eremu magnetikoaren intentsitateak eta posizioak sandwicharen propietate dinamikoetan duten eragina aztertu da. Tesi doktoral honetan zehar sortutako ezagutzak, sandwich hauen erantzun magnetodinamikoa gidatzen duten fenomeno fisikoak ezagutzea ahalbidetu du.

Resumen

En la actualidad, numerosos sectores industriales tienen como objetivo disminuir la amplitud de las vibraciones con el fin de alargar la vida útil de los componentes y reducir la radiación acústica. Con este propósito se utilizan sándwich viscoelasticos, ya que son sencillos de implementar, de bajo coste y eficaces en la atenuación de vibraciones estructurales. Sin embargo, estos sándwich no tienen la capacidad de adaptarse en tiempo real a las condiciones de trabajo, por lo que las últimas investigaciones en control de vibraciones se centran en estructuras inteligentes. Los materiales magnetorreológicos son capaces de modificar sus propiedades reológicas en respuesta a campos magnéticos externos, y por tanto son idóneos para fabricar estructuras sándwich inteligentes.

El objetivo principal de la presente tesis doctoral es conocer la respuesta dinámica de sándwich viscoelasticos-magnetorreológicos finos. En ausencia de campo magnético el comportamiento dinámico de estos sándwich es análogo al de los sándwich viscoelasticos, sin embargo al aplicar un campo magnético su comportamiento dinámico se modifica como resultado del acoplamiento de múltiples fenómenos físicos generados en las pieles y en el núcleo.

Se ha analizado el comportamiento dinámico de los sándwich viscoelasticos finos para entender la respuesta de los sándwich viscoelasticos-magnetorreológicos en ausencia de campo magnético. Para ello, se han caracterizado sándwich de diferentes composiciones y se han generado modelos numéricos. Con estos análisis se ha establecido la influencia de la composición y del espesor tanto del adhesivo viscoelastico, como de las pieles metálicas en las propiedades dinámicas del sándwich.

Se han estudiado las corrientes de Foucault que se generan en las pieles metálicas de los sándwich. Dada la capacidad de amortiguación de estas corrientes, se ha propuesto un nuevo sándwich híbrido que combina el amortiguamiento viscoelastico, con las corrientes de Foucault. Además, se ha desarrollado un nuevo método inverso que estima la influencia de este fenómeno en la respuesta dinámica de los sándwich.

En el núcleo viscoelastico-magnetorreológico concurren dos fenómenos: el efecto magnetorreológico, propio de la inteligencia del núcleo, y la fuerza magnética que se origina por el acoplamiento de las vibraciones del núcleo magnetizado con el campo magnético aplicado. Ambos fenómenos se han incluido en un nuevo modelo numérico, que se ha validado con resultados experimentales, y se ha establecido su influencia en la dinámica del sándwich.

Por último, se ha estudiado experimentalmente la influencia de las partículas magnéticas, y de la intensidad y posición del campo magnético en el comportamiento dinámico de los sándwich viscoelastico-magnetorreológico finos. El conocimiento adquirido con esta tesis, ha permitido determinar los fenómenos físicos que rigen la dinámica del sándwich viscoelastico-magnetorreológico y explicar el comportamiento magneto-dinámico experimental observado.

Abstract

A fundamental aim of many industrial sectors is the reduction of structural vibration in order to increase the service life of mechanical components and diminish noise radiation. Viscoelastic sandwiches have been widely applied to attenuate structural vibration as they are cost-effective and simple to employ. However, the constantly increasing requirements for vibration control have made the latest research move towards smart structures able to adapt to random vibrations in real time. Magnetorheological materials are a class of smart materials able to modify their rheological properties in response to magnetic fields. Thus, they offer attractive features for constructing smart sandwich structure with enhanced vibration control.

The present thesis studies the dynamics of thin viscoelastic-magnetorheological sandwich structures. These sandwiches are analogous to thin viscoelastic sandwiches in the absence of a magnetic field, whereas when magnetic fields are applied their dynamic behaviour is modified as a result of the coupling of multiple physical phenomena generated in their skins and core.

The dynamic behaviour of thin viscoelastic sandwiches was analysed as a way of studying the behaviour of thin viscoelastic-magnetorheological sandwiches in the absence of a magnetic field. To that end, sandwiches of different compositions were characterized and numerical models were defined. From the joint analysis of the experimental and numerical results, the influence of the nature and thickness of both viscoelastic adhesive and metallic skins on the dynamic properties of the sandwich were determined.

The phenomenon of eddy currents generated in metallic skins was studied in order to determine its influence on the dynamic behaviour of viscoelastic-magnetorheological sandwiches. To do this, an experimental modal analysis with a metallic beam, with and without induced eddy currents, was carried out. Then, in view of the damping capacity of eddy currents, a new hybrid sandwich structure combining viscoelastic and eddy current damping was proposed. Afterwards, a new inverse method was developed to estimate and model the influence of eddy currents.

The phenomena generated in the viscoelastic-magnetorheological core, the magnetorheological effect and magnetic force, were studied. To that end, a magneto-dynamic model of viscoelastic-magnetorheological sandwiches including both phenomena was proposed and validated with experimental results.

Finally, the dynamic behaviour of a thin viscoelastic-magnetorheological sandwich was analysed experimentally, and the influence of the magnetic particles and the intensity and position of the magnetic field was studied. The knowledge acquired in the course of this research enables determining the physical phenomena governing the dynamics of thin viscoelastic-magnetorheological sandwiches and explain the experimentally observed magneto-dynamic behaviour.

Acknowledgements

Azkenean iritsi da tesi honi amariera emango dioten azken lerroak idazteko unea, eta hauek bide honetan lagundu nauten orori eskerrak emateko erabili nahi nituzke.

En primer lugar quiero agradecer a mi directora de tesis, Dra. María Jesús Elejabarrieta, por toda la dedicación mostrada durante estos años. Gracias por tu dirección en esta tesis, por las discusiones que hemos tenido con el fin de mejorar las cosas, por el apoyo mostrado en los momentos más difíciles y por enseñarme a trabajar con honestidad. En definitiva, ¡Gracias por haber hecho esto que esto sea posible!

Mila esker Mondragon Unibertsitateari tesia bertan egiteko aukera eta baliabideak eskaintzeagatik. Eskerrak ere bide honetan lagundutako bertako langile guztiei (irakasle, tailer edo laborategiko teknikari, administrazioko langile, etab.). En especial al Dr. M. Mounir Bou-Ali por apostar por mí e introducirme en el mundo de la investigación.

Eskerrik beroenak urte hauetan nire doktoretzako lankide izan eta lagun bilakatu diren guztiei. Estela, Iker, Ion, Maider, Gorka, Imanol, Unai, Irune, Naia, Aitor, Buru, etab., zuek gabe bide hau ez zen berdina izango! Elkarbanatutako mila txorrada, mila diskusioek, pintxo-pote luzeek, afari eta juergek bide hau polittagoa egin dute. Esker bereziak Ikerri urte hauetan eskeinitako laguntzagatik eta emandako aholku tekniko eta pertsonal guztiengatik.

I would like to thank the Interweave project from Erasmus Mundus for the scholarship provided to make a PhD mobility of 6 months in the Indian Institute of Technology Guwahati. Thank you to Professor S. K. Dwivedy for being my supervisor during the stay and the help provided. I would also like to thank all the special people known in India who made the stay a really enriching experience. Mikel, Inês, Nama, Beth, Phurpa, Gonzalo, Gonzalo, Take, Javi, Lisa, Adrian, Michael, Ben, etc. Thank you!

Esker berezia ere urte hauetan nere pixukide izan diren Irune, Irune, Asier, Haizea eta Aitorri. Unibertsitateko nire buruhausteak aditu eta ondoren alde batera uzten laguntzeagatik pisuan alaitasuna jarriz.

Nola ez eskerrik beroenak kuadrilako lagun guztiei, momentu on eta txarretan beti hor zaudetelako. Zuekin momentu onak are hobeak dira eta momentu txarrak askoz eramangarriagoak. Eskerrik asko Igelakputzuan!

Eskerrik asko Gorka azken urte t'erdi honetan eskenitako laguntza, animo, irrifar eta mimo guztiengatik. Azken hilabeteak ez dira errazak izan eta erortzen hasi orduko hor zenden ni altxatzeko prest. Mila esker! Eta ez... zure pazientziak ez du parekorik!

Azkenik, etxekoei eskertu nahi diet mugagabe eskeinitako laguntza eta animoengatik, nigan nik baino gehiago sinisteagatik eta nire aukeratan aurrera egiteko indarra emategatik. Nola ez, tesi hau zuei eskeinia da. Eskerrik asko bihotzez Aita, Ama eta Iñigo!

Contents

List of Figures

List of Tables

Nomenclature

List of Abbreviations

AL	Aluminium
AL-ED	Aluminium with induced eddy currents
CIP	Carbonyl iron powder
DOF	Degree of freedom
FEM	Finite element method
FEMM	Finite element method magnetics
MR	Magnetorheological
VE	Viscoelastic
VEMR	Viscoelastic-magnetorheological
VEMRS	Viscoelastic-magnetorheological sandwich
VES	Viscoelastic sandwich
VES-ED	Hybrid damping sandwich

List of Symbols

b	Coefficient of Moon and Pao's equation
B	Magnetic field density
c_{e}	Eddy damping coefficient
C	Magnetic body couple
$\mathbf{C}_{\mathrm{eddy}}$	Eddy damping matrix
d	Magnetic particle distance
E	Storage modulus
E^*	Complex modulus
E_0	Static modulus
E_∞	Asymptotic modulus
f	Frequency

$\mathbf{F}$	Force vector
$\mathbf{F}^*_{\mathrm{eddy}}$	Complex eddy force vector
G_0	Static shear modulus
G_{inf}	Asymptotic shear modulus
G^*_{v}	Shear complex modulus
G_{v_B}	Field induced change in shear modulus
h_1	Thickness of the top layer
h_2	Thickness of the core layer
h_3	Thickness of the bottom layer
H_{x}	Magnetic field intensity in axial direction
H_{z}	Magnetic field intensity in transverse direction
i	Imaginary unit
J_{p}	Induced polarisation of the particles
k	Wave number
$\mathbf{K}^*$	Complex stiffness matrix
$\mathbf{M}$	Mass matrix
$\mathbf{q}$	Displacement vector
$\dot{\mathbf{q}}$	Velocity vector
$\ddot{\mathbf{q}}$	Acceleration vector
$\mathbf{R}^*$	Complex amplitude vector of the reaction forces
$\ddot{s}$	Acceleration of the beam in the base
$\mathbf{S}^*$	Complex amplitude vector of the applied base displacement
S^*_{exp}	Complex Fourier transform of the applied base movement
S^*_i	Complex amplitude of the displacement at base point (ith DOF)
T^*_{ij}	Complex transfer function related to ith DOF and jth DOF
${}_{\mathrm{exp}}T^*$	Complex experimental transfer function
R	Magnetic particle radio
$\dot{u}$	Velocity of the beam in the free end
u_1	Axial displacement of the top layer
u_3	Axial displacement of the bottom layer
$\mathbf{U}^*$	Complex amplitude vector of the unknown displacements
U^*_{exp}	Complex Fourier transform of the response movement in the free end
U^*_j	Complex amplitude of the displacement at response point (jth DOF)
$\mathbf{v}^*_{\mathrm{z}}$	Complex transverse velocity vector
w	Transverse displacement
$\frac{\partial w}{\partial x}$	Rotational displacement
x_{m}	Distance of the magnets device to the free end of the beam
α	Fractional parameter
ϵ	Strain
η	Loss factor

η_{v}	Shear loss factor
μ_0	Magnetic permeability of the vacuum
μ_{m}	Relative magnetic permeability of the viscoelastic adhesive
μ_r	Relative magnetic permeability of the VEMR
π	Pi number
σ	Stress
τ	Relaxation time
φ	Volume fraction of magnetic particles
χ	Magnetic susceptibility
ψ	Mode shape
ψ_{norm}	Normalised mode shape to maximum displacement unit
$(\bullet)_1$	Referring to the top layer
$(\bullet)_2$	Referring to the core layer
$(\bullet)_3$	Referring to the bottom layer
$(\bullet)_{\mathrm{s}}$	Relative to the base displacement
$(\bullet)_{\mathrm{u}}$	Relative to the unknown displacements

Chapter 1

Introduction

This chapter introduces the motivation and background of the field of research and defines the scope of the present thesis.

1.1 Motivation and background

The reduction of structural vibration is a fundamental aim in many industrial sectors to enhance the performance of mechanical systems, and thus diminish noise radiation and increase the service life and reliability of mechanical components. Passive damping techniques using viscoelastic (VE) materials, have been one the most widely applied structural vibration control techniques as they are cost-effective and simple to implement (Rao 2003). VE material can be confined between two metallic layers to form a sandwich structure. The metallic skins provide a high degree of rigidity to the structure, whereas the VE core dissipates energy by shear deformation. These viscoelastic sandwiches (VES) are of special interest for applications where the mass of components is critical, such as the aeronautical, automotive, railroad and marine industries (Rao 2003).

The dynamic properties of VE materials depend on several factors, such as chemical composition, temperature, frequency, deformation level, static prestrain or prestress, etc. (Goodman 1996). In addition to the aforementioned factors, the dynamic properties of VESs also depend on the metallic skins properties and the sandwich configuration itself. Thus, the dynamic behaviour of VESs and their design are complex and have been studied since the mid-20^{th} century. Some authors have analysed the influence of the core and skin thicknesses, frequency, temperature and static prestrain on the damping efficiency of the sandwich (Teng and Hu 2001; Kergourlay et al. 2006; Sher and Moreira 2013), whereas others have proposed optimal design procedures for multi-layered structures (Araújo et al. 2010; Hamdaoui et al. 2015; Madeira et al. 2015b).

In recent years, conventional VE materials used to form the sandwich structures have been replaced by micron-size VE adhesives (Martinez-Agirre and Elejabarrieta 2010). The use of these thin VE adhesives and metallic skins results in sandwich structures with high stiffness-to-weight and damping-to-weight ratios. In addition, the total thickness of these sandwiches is similar to metal sheets, which makes it possible to use them in classic sheet metal forming processes to obtain damped parts with complex geometries. Although some authors have shown these thin sandwiches can be effective (Martinez-Agirre and Elejabarrieta 2010; Sher and Moreira 2013), there are not many works focused exclusively on the dynamic behaviour and design of thin sandwiches.

VES structures are unable to adapt to random sources of vibration in real time since their dynamic properties and damping characteristics are fixed by their design. The constantly increasing requirements for vibration control in recent years have made scientists and engineers propose different semi-active sandwiches. In these sandwiches the active control can be used to enhance the vibration attenuation of the structure when needed. Semi-active sandwiches can be obtained by attaching piezoelectric actuators to the sandwich structure (Trindade and Benjeddou 2002; Kumar and Singh

2009), or by replacing the viscoelastic core with a smart material, such as shape memory alloys (Butaud et al. 2016), electrorheological materials (Ramkumar and Ganesan 2009; Wei et al. 2011) or magnetorheological materials (Lara-Prieto et al. 2010; Aguib et al. 2014).

Magnetorheological (MR) materials are smart materials possessing the unique ability to modify their rheological properties in response to external magnetic fields. They are composed of micro or nanosized magnetic particles suspended in a non-magnetisable medium, and depending on the nature of the medium are classified into MR fluids, MR gels and MR elastomers (Carlson and Jolly 2000). These MR materials have variable stiffness and damping properties, attributed to the changes in their rheology when a magnetic field is applied, and so they offer attractive features for constructing smart sandwich structures with enhanced vibration control. However, the sandwiches composed of MR fluids present the disadvantages of sealing problems and the settling of magnetic particles (Goncalves et al. 2006). Those composed of MR elastomers, overcome these drawbacks, but they may not preserve the main advantages of conventional VESs as they are commonly comprised of thick elastomers (Choi et al. 2010; Aguib et al. 2014; Hu et al. 2011b).

The magneto-dynamic behaviour of MR sandwiches is the result of the coupling of multiple physical effects generated in their skins and core. Depending on the composition of the sandwich and the magnetic field configuration, the contribution of each is different and therefore the behaviour of the MR sandwich is different.

When a conductive material experiences a time-varying magnetic field electrical currents, known as eddy currents, are induced in the conductor. Thus, when applying magnetic fields to vibrating MR sandwiches eddy currents are induced in their metallic skins and by their interaction with the magnetic field a repulsive force is generated. Eddy currents dissipate into heat due to the electrical resistance of the metallic materials. However, in dynamic systems there is a constant change in magnetic flux and so these currents are constantly regenerated, allowing energy to be removed from the system (Sodano and Bae 2004).

When magnetic fields are applied to vibrating MR sandwiches two phenomena are generated in their core. On the one hand, the rheological properties of the MR core are modified due to the interactions generated between magnetic particles. A field-induced stiffening is given and the change of modulus is commonly termed as magnetorheological effect (Chen et al. 2008). On the other hand, the MR core is magnetized and the sandwich is subjected to a distributed magnetic force (Moon and Pao 1969).

Several authors have carried out experimental tests to study the magneto-dynamic behaviour of MR sandwich structures (Wei et al. 2008; Hu et al. 2011b; Choi et al. 2009; Bishay et al. 2010). However, most of these studies have focused on analysing the global behaviour of the sandwich, rather than studying the different phenomena generated in these sandwiches. At the time of writing, there is experimentally observed behaviour with MR sandwiches that is not fully understand (Lara-Prieto et al. 2010;

Bishay et al. 2010).

All the models proposed for MR sandwiches in the literature account for the magnetic field dependence of the dynamic properties of their core, that is to say the magnetorheological effect, but, few takes into account other phenomena generated in vibrating MR sandwiches (Eshaghi et al. 2016).

Within this context, the present dissertation aims to study the dynamics of thin viscoelastic-magnetorheological sandwich (VEMRS) structures. To that end, the physical effects generated in these sandwiches as a result of the interactions between electromagnetic and mechanical fields are analysed. The present thesis has been developed as a compendium of scientific publications and it is presented in an academic thesis format. The current dissertation comprises seven chapters, including the first one for the introduction, the second one for the experimental and numerical background and the seventh one for the conclusions and future lines. The four central chapters (*Thin viscoelastic sandwich*, *Eddy currents in metallic skins*, *Magnetorheological effect and magnetic force in viscoelastic-magnetorheological core* and *Thin viscoelastic magnetorheological sandwich*) provide a brief summary of the papers with which they are associated.

In Chapter 3, *Thin viscoelastic sandwich*, the dynamic behaviour of thin VESs and the influence of the design of the sandwich on it is analysed, as a way of studying the dynamic behaviour of thin VEMRS in the absence of a magnetic field. The influence of the nature and thickness of both VE adhesive and metallic skins on the dynamic properties of thin viscoelastic sandwiches are analysed.

Chapter 4, *Eddy currents generated in metallic skins*, is focused on the phenomenon of eddy currents and studies the influence of eddy currents induced in the metallic skins on the dynamic behaviour of the sandwich. The effect of eddy currents on the vibration attenuation and modal parameters, natural frequencies and mode shapes, of metallic structures is analysed. In addition, a new hybrid sandwich structure combining viscoelastic and eddy current damping is proposed. Finally, a new inverse method to estimate and model the influence of eddy currents is proposed.

Chapter 5, *Magnetorheological effect and magnetic force generated in viscoelastic-magnetorheological core*, is focused on the phenomena generated in the viscoelastic-magnetorheological cores and studies the influence of the magnetorheological effect and the magnetic force on the dynamic behaviour of the sandwich. A magnetic force model to describe the interaction generated in vibrating VEMRSs when exposed to magnetic fields is proposed. Then, a magneto-dynamic modelling of VEMRSs by finite element method including the magnetorheological effect and the magnetic force is put forward. Finally, in this chapter a physical explanation is given for an experimental behaviour with MR sandwiches observed in the literature.

In Chapter 6, *Thin viscoelastic-magnetorheological sandwich*, the dynamic behaviour of a thin VEMRS is experimentally studied. The influence of adding magnetic particles to a VE adhesive of a conventional sandwich in order to obtain a smart VEMRS on the dynamic properties of the sandwich is analysed. Then, the magneto-dynamic

behaviour of the thin VEMRS is studied, analysing the influence of the intensity and position of the magnetic field. The experimentally observed behaviours are related to the different phenomena generated in these sandwiches when magnetic fields are applied.

1.2 Scope of the thesis

The main goal of the present dissertation was to study the dynamics of thin viscoelastic-magnetorheological sandwich structures analysing the physical phenomena generated in these sandwiches when magnetic fields are applied. The study comprises the following specific objectives:

- Analyse the dynamic behaviour of thin viscoelastic sandwiches and the influence of the design of the sandwich on it.
- Determine the influence of eddy currents induced in the metallic skins on the dynamic behaviour of the sandwich.
- Determine the influence of the magnetorheological effect and magnetic force generated in the VEMR core on the dynamic behaviour of the sandwich.
- Analyse the dynamics of thin viscoelastic-magnetorheological sandwiches and the influence of magnetic particles and magnetic fields on it.

Chapter 2

Experimental and numerical background

In this chapter the experimental technique and the numerical modelling used along the thesis are summarized.

2.1 Introduction

The design of structural systems with viscoelastic-magnetorheological sandwiches (VEMRS) requires knowledge of material properties and definition of proper numerical models.

Viscoelastic-magnetorheological (VEMR) materials are obtained by adding magnetic particles to a viscoelastic (VE) adhesive. Their dynamic properties depend on the dynamic properties of the base VE adhesive, type and content of magnetic particles, curing conditions and intensity and position of the applied magnetic field (Li et al. 2008). The dynamic properties of VE materials in turn depend on several factors such as chemical composition, temperature, frequency, deformation level, static pre-strain or pre-stress, etc., being the most influential ones the chemical composition, temperature and frequency (Goodman 1996).

Different techniques are used to characterize VE materials depending on the range of temperature and frequency of interest, as well as the frequency and temperature superposition principle. In Figure 8.1 the characterization techniques of VE materials classified according to the frequency range under study are shown (Ward and Sweeney 2004): creep and stress relaxation tests, free oscillations tests, non-resonance forced vibrations tests, forced vibrations tests with resonance and wave propagation methods. The more remarkable feature of VEMR materials is the modification of their rheological properties under an applied magnetic field. Therefore, the dynamic properties of VEMR materials as function of magnetic field intensity must be characterized. For that the characterizations techniques of VE materials adapted with magnetic field devices can be used (Ubaidillah et al. 2015).

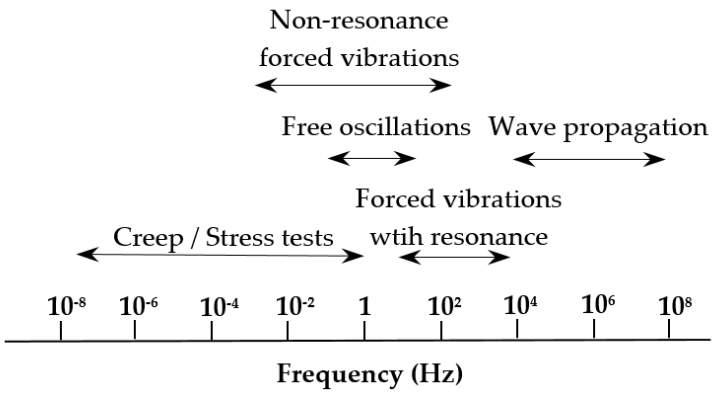

Figure 2.1. Viscoelastic materials characterization techniques classified according to the frequency range under study.

VE materials show both elastic and viscous characteristics. Simple differential viscoelastic models can be defined by the combination of discrete spring and dashpot elements, as well as more complex multi-element models, such as the generalised Maxwell or Kelvin-Voigt models. To reduce the number of terms required by

these models, the differential equation can be generalised by replacing the integer-order derivatives with fractional-order ones, and these models are known as fractional derivative models (Jones 2001). Bagley and Torvik (1983) and Bagley and Torvik (1986) analysed the fractional derivatives from molecular and thermodynamical points of view, and several authors have used the fractional derivative models to model the dynamic behaviour of VE materials successfully (Ouis 2003; Lu 2007; Rouleau et al. 2015). The magnetic field dependence of VEMR materials can be described by the dipole-dipole interaction models (Jolly et al. 1996a; Jolly et al. 1996b; Davis 1999; Shen et al. 2004).

Recently, Caliri et al. (2016) presented an extensive review on plate and shell theories for laminated and sandwich structures. In addition, they described the solution methods based on finite element method (FEM) with whom the dynamic behaviour of sandwich structures can be obtained.

This chapter has a double purpose. On the one hand, to show the experimental technique followed to characterize metallic, viscoelastic and viscoelastic-magnetorheological sandwich structures both in frequency domain and under magnetic fields. On the other hand, to present the numerical models used to describe their dynamic behaviour, which encompasses a constitutive viscoelastic model for the core and a finite element model for the sandwich beams.

2.2 Experimental technique

The dynamic properties of sandwich structures and their cores were characterized by forced vibrations tests with resonance according to the standard ASTM E 756 (2005) and the modification proposed by Cortés and Elejabarrieta (2007) in the bandwidth of 0-1 kHz. The magneto-dynamic behaviour of VEMRSs is the result of the coupling of different physical effects. Thus, different configurations of magnetic field were applied to the forced vibration tests to study each of these phenomena.

Next, the tested specimens are presented, the experimental set-up is described and the procedure to identify the materials' properties is detailed.

2.2.1 Specimens

In this thesis different metallic, viscoelastic and viscoelastic-magnetorheological sandwich structures were characterized.

In Chapter 3 thin viscoelastic sandwiches (VES) composed of different metallic skins and VE adhesives were characterized in order to analyse the dynamic behaviour of these thin sandwiches. In Chapter 4 a metallic beam and a thin VES were tested to study the influence of eddy currents induced in metallic skins on the dynamic behaviour of the sandwich and in Chapter 5 a thin VEMRS was tested to study the influence of the magnetorheological effect and magnetic force on the dynamic response of the sandwich. Finally, in Chapter 6 a VES and VEMRS composed of same metallic

skins and VE adhesives, but, with and without magnetic particles, were characterized in order to analyse the dynamic response of smart thin VEMRSs and their advantages over VESs.

The nomenclature used to name the different sandwich structures is the following:

- In Chapter 3, as VESs of different compositions were characterized, these are named by the metallic material followed by the VE material. In some cases the thickness of the VE core in dry is specified in order to differentiate among VESs with same composition, but different thicknesses.

- In Chapters 4, 5 and 6 a metallic, VES and VEMRS are tested and this are named by AL, VES and VEMRS, respectively for simplicity.

In Table 2.1 the composition of the analysed structures and the nomenclature used to name them throughout the thesis is shown and in Table 2.2 their geometrical and physical properties are detailed, where the deviations are the standard deviations among three specimens.

Table 2.1. Nomenclature and composition of the analysed structures

Type of specimen	Chapter	Nomenclature in the thesis	Composition	
			Skins	Core
VES	Chapter 3	SS1-VE1-36	Stainless steel AISI 316 -1	Polyester-based adhesive - 1
VES	Chapter 3	SS1-VE1-19	Stainless steel AISI 316 -1	Polyester-based adhesive - 1
VES	Chapter 3	SS1-VE1-7	Stainless steel AISI 316 -1	Polyester-based adhesive - 1
VES	Chapter 3	AL-VE1	Aluminium alloy 1050 H18 -1	Polyester-based adhesive - 1
VES	Chapter 3	SS2-VE2	Stainless steel AISI 316 -2	Polyester-based adhesive - 2
VES	Chapter 3	GS-VE2	Galvanised steel Z100	Polyester-based adhesive - 2
Metal	Chapter 4	AL	Aluminium alloy 2024-T3	-
VES	Chapter 4 - 6	VES	Aluminium alloy 1050 H18 -2	Polyester-based adhesive - 1
VEMRS	Chapter 5 - 6	VEMRS	Aluminium alloy 1050 H18 -2	Polyester-based adhesive - 1 + 12% CIP

Table 2.2. Geometrical and physical properties of the analysed structures and their constituents.

Nomenclature	Sandwich			Skin				Core	
	Thickness (mm)	Width (mm)	Density (g/cm^3)	Thickness (mm)	Density* (g/cm^3)	Storage modulus (GPa)	Loss factor	Thickness (μm)	Density* (g/cm^3)
SS1-VE1-36	0.552 ± 0.002	9.9 ± 0.1	7.51 ± 0.05	0.258 ± 0.002	7.95	185.24 ± 1.95	0.0025 ± 0.008	36 ± 2	1.13
SS1-VE1-19	0.521 ± 0.002	9.9 ± 0.1	7.70 ± 0.05	0.251 ± 0.002	7.95	185.24 ± 1.95	0.0025 ± 0.008	19 ± 2	1.13
SS1-VE1-7	0.523 ± 0.002	9.9 ± 0.1	7.86 ± 0.05	0.258 ± 0.002	7.95	185.24 ± 1.95	0.0025 ± 0.008	7 ± 2	1.13
AL-VE1	0.988 ± 0.002	9.9 ± 0.1	2.67 ± 0.05	0.483 ± 0.002	2.7	67.96 ± 0.75	0.0025 ± 0.008	21 ± 2	1.13
SS2-VE2	0.472 ± 0.002	9.9 ± 0.1	7.37 ± 0.05	0.216 ± 0.002	7.96	205.71 ± 0.36	0.0021 ± 0.009	41 ± 2	1.13
GS-VE2	1.219 ± 0.002	9.9 ± 0.1	7.54 ± 0.05	0.589 ± 0.002	7.76	177.96 ± 0.55	0.0033 ± 0.0021	40 ± 2	1.13
AL	-	-	-	0.404 ± 0.002	2.77	66.9 ± 0.4	0.0021 ± 0.0006	-	-
VES	1.146 ± 0.003	9.9 ± 0.1	2.675 ± 0.008	0.564 ± 0.002	2.7	68.11 ± 0.68	0.0024 ± 0.0008	18 ± 2	1.13
VEMRS	1.162 ± 0.003	9.9 ± 0.1	2.676 ± 0.008	0.564 ± 0.002	2.7	68.11 ± 0.68	0.0024 ± 0.0008	35 ± 2	1.91

*Data provided by the manufacturer, Replasa S.A.

2.2.2 Experimental procedure

The standard ASTM E 756 (2005) establishes the procedure to characterise the sandwich structures and their cores by measuring the frequency response function of sandwich beam specimens in a cantilever configuration. Cortés and Elejabarrieta (2007) proposed to replace the force excitation by a seismic base motion at the clamp and prove the procedure is equally applicable with transfer functions.

In Figure 8.2 the scheme of the experimental set-up used to measured the transfer functions is shown. The base motion was generated by an electrodynamic shaker and consisted on a white noise in the frequency range of 0-1 kHz in general. The acceleration of the base, $\ddot{s}$, was measured by a piezoelectric accelerometer with a charge conditioning amplifier and loopback controlled by a vibration controller. The velocity of the beam, $\dot{u}$, was measured in the point located to 5 mm from the free end by a laser vibrometer. The data acquisition and signal processing were performed with an analyser connected to a computer. The transfer function was obtained by relating the response movement of the beam's free end with that applied at the base so that

$$_{\exp}T^* = \frac{U^*_{\exp}}{S^*_{\exp}}\,, \tag{2.1}$$

where $U^*_{\exp}$ is the Fourier transform of the response movement measured at the free end and $S^*_{\exp}$ is the Fourier transform of the applied base movement.

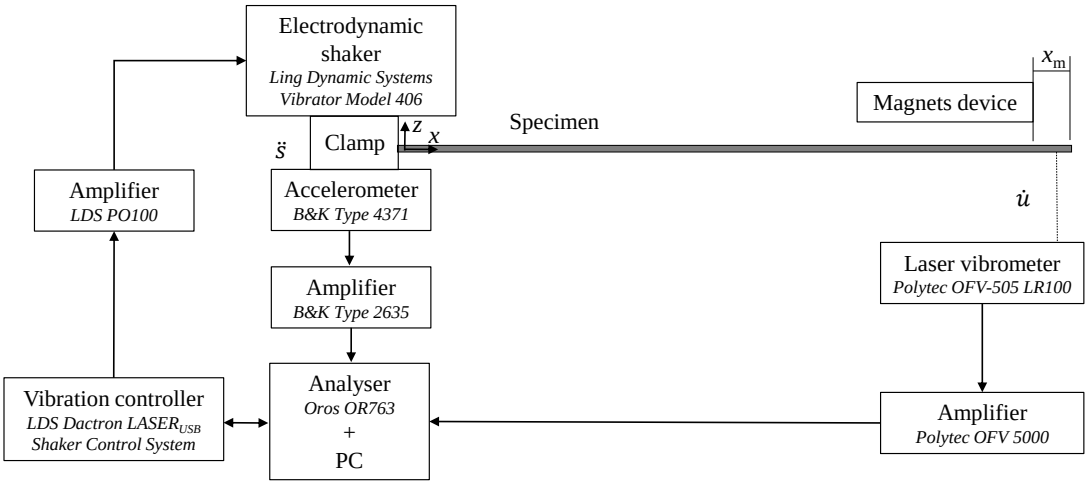

Figure 2.2. Experimental set-up.

Transfer functions were measured in the absence of magnetic fields in order to characterize the sandwich structures and their cores in frequency domain, and under different configurations of magnetic field to analyse the physical effects generated in VEMRSs.

Two devices were designed to apply three configurations of magnetic field to the experimental tests. In one device NdFeB 35 MGO neodymium magnets of 50 x 50 x 8 mm^3 sizes were used, and in the other one NdFeB 35 MGO neodymium magnets of

42 x 42 x 8 mm^3 sizes. Depending on the field configuration and intensity required more or less magnets were placed. Simulations with the free software Finite Element Method Magnetics 4.2 were held in order to characterize these magnetic fields, as well as measurements by the Gaussimeter FH-54. In Figure 2.3, Figure 2.4 and Figure 2.5 the applied three magnetic field configurations are shown. A photograph of the magnets device, the magnetic flux distribution and the magnetic field intensity in transverse, H_{z}, and axial, H_{x}, directions can be seen. Note, regardless of the free length of the beam specimen to be tested, the magnets devices were placed to 8 mm from the free end, $x_{\mathrm{m}} = 8$ in Figure 8.2. As an exception, the configuration shown in Figure 2.5 was placed in more positions.

The configuration shown in Figure 2.3 was used in Chapter 4 to analyse the effect of induced eddy currents, the one shown in Figure 2.4 was implemented in Chapter 5 to study the influence of the magnetorheological effect and magnetic force, and finally the configuration shown in Figure 2.5 was used in Chapter 6 to study the magnetodynamic behaviour of thin a VEMRS, and analyse the influence of the intensity and position of the magnetic field on its dynamic properties. Note, in this last magnets configuration the axial alignment of the magnets is not guaranteed and so the actual magnetic field will be less homogeneous than the one shown by the simulation.

In the experimental tests, first the transfer functions in the bandwidth of 0-1 kHz were measured and then the modal transfer functions in order to obtain a higher resolution. In general, from each analysed structure three specimens were tested, each one with three different free lengths in order to determine the dynamic properties of the structure all along the bandwidth.

All the experimental measurements, both in the absence of and under magnetic fields, were taken at environmental temperature, 20ºC, and within the linear range. To ensure this, a linearity analysis consisting on exciting the beam with different acceleration levels was carried out with each structure and with the longest free length. When the deformations are over the linear range, the stiffness of the structure decreases and the loss factor increases (Nashif et al. 1985). Thus, analysing the measured transfer functions the maximum acceleration applicable to ensure linearity was determined for each analysed structure. As an example, in Figure 8.3 the linearity analysis carried out with the VES beam is shown. It can ve observed that within the first three excitation levels, the same transmissibility function is obtained; whereas increasing the excitation, the modulus and the resonance frequency decrease meaning that the deformations go over the linear range.

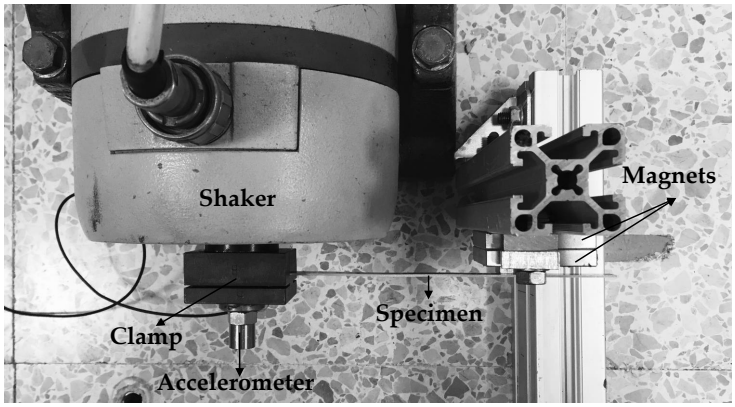

(a)

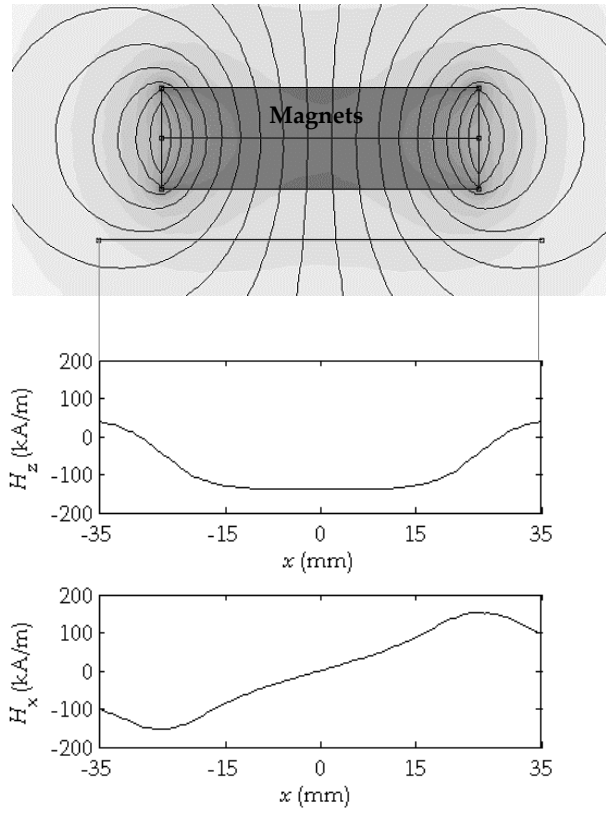

(b)

Figure 2.3. Magnetic field configuration implemented in Chapter 4, (a) photograph of the magnets device and (b) numerical magnetic flux distribution and magnetic field intensity in transverse, H_z, and axial, H_x, directions.

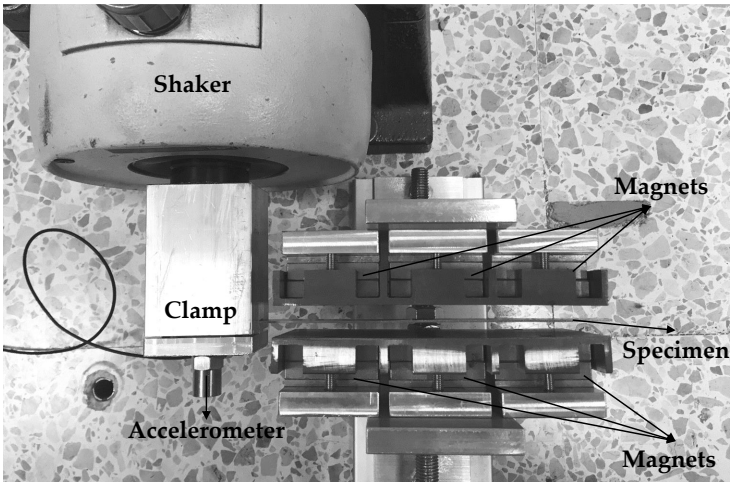

(a)

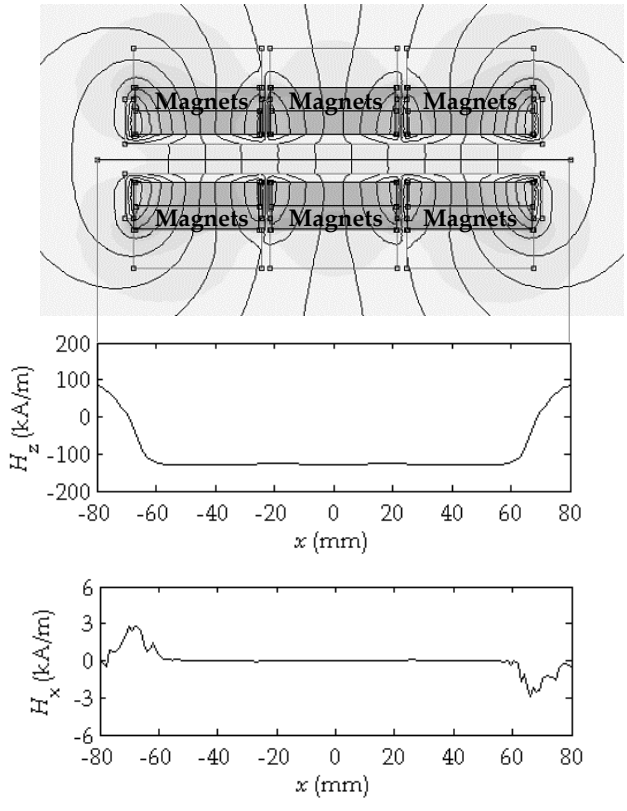

(b)

Figure 2.4. Magnetic field configuration implemented in Chapter 5, (a) photograph of the magnets device and (b) numerical magnetic flux distribution and magnetic field intensity in transverse, H_z, and axial, H_z, directions.

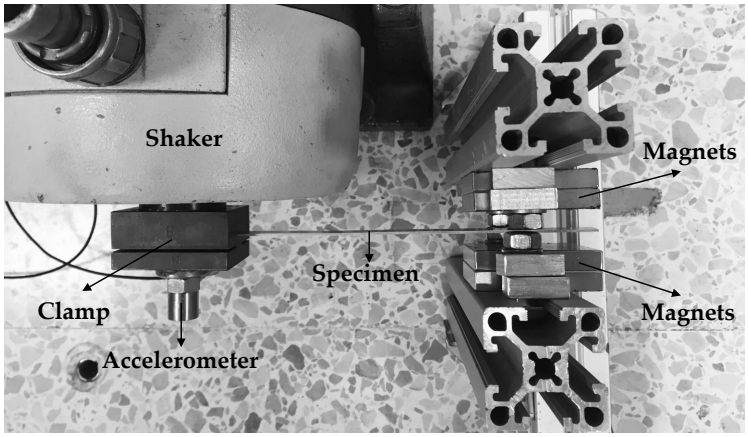

(a)

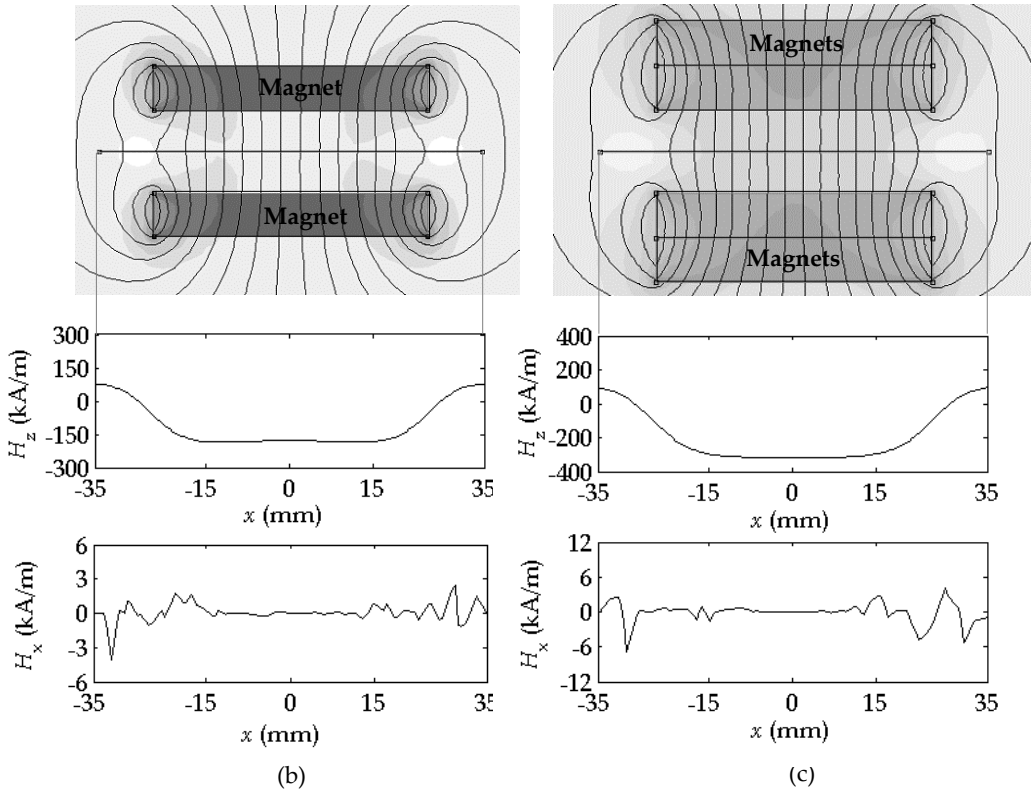

(b) (c)

Figure 2.5. Magnetic field configuration implemented in Chapter 6, (a) photograph of the magnets device, (b) numerical magnetic flux distribution and magnetic field intensity in transverse, H_z, and axial, H_z, directions with 4 magnets and (c) magnetic flux distribution and magnetic field intensity in transverse and axial directions with 2 magnets.

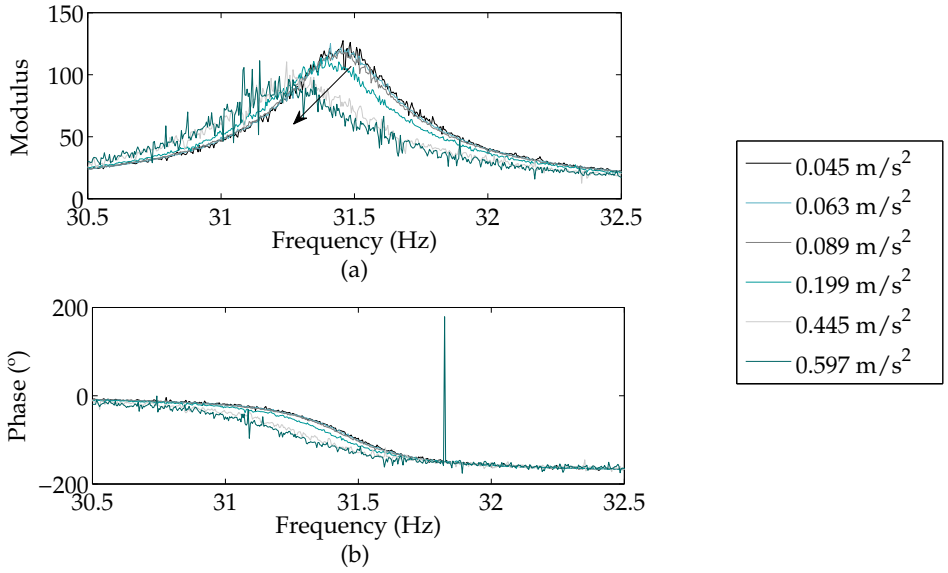

Figure 2.6. Experimental linearity analysis of the VES with 170 mm of free length. First mode transfer function, (a) modulus and (b) phase, under different excitation levels.

The dynamic properties of the sandwich structures and their cores are deduced from the experimental transfer functions in a two-step process according to the standard ASTM E 756 (2005). First, the complex modulus of the sandwich structure is determined from the transfer function, and then the shear complex modulus of the core is obtained from the Ross-Kerwin-Ungar equations (Ross et al. 1959).

Assuming a linear viscoelastic behaviour of the sandwich structure, its complex modulus, $E^*(f)$, is expressed as

$$E^*(f) = E(f)(1 + \mathrm{i}\eta(f))\,, \tag{2.2}$$

where $E(f)$ is the storage modulus and $\eta(f)$ is the loss factor. Assuming the Poisson's ratio of the viscoelastic core is real and constant in frequency (de Espíndola et al. 2005; Lakes and Wineman 2006), its shear complex modulus, $G_{\mathrm{v}}^*(f)$, is given by

$$G_{\mathrm{v}}^*(f) = G_{\mathrm{v}}(f)(1 + \mathrm{i}\eta_{\mathrm{v}}(f))\,, \tag{2.3}$$

where $G_{\mathrm{v}}(f)$ is the shear modulus and $\eta_{\mathrm{v}}(f)$ is the shear loss factor.

2.3 Numerical model

Next, the numerical models of the analysed metallic, VES and VEMRS structures, as well as their cores, is described.

A four-parameter fractional derivative model was considered for describing the frequency dependence of the shear dynamic properties of the VE adhesive. The most remarkable features of the fractional derivative models, are their ability for describing the frequency dependence of VE materials with a low number of parameters (Ouis

2003; Rouleau et al. 2015) and the physical interpretation of each of these. The four-parameter fractional derivative model, also known as the generalised Zener model, was thoroughly analysed by Pritz (1996) and it is represented by the following fractional differential equation

$$\sigma(t) + \tau^{\alpha}\frac{\partial^{\alpha}\sigma(t)}{\partial t^{\alpha}} = E_0\epsilon(t) + E_{\infty}\tau^{\alpha}\frac{\partial^{\alpha}\epsilon(t)}{\partial t^{\alpha}}\,, \tag{2.4}$$

where $\sigma(t)$ is the stress, $\epsilon(t)$ is the strain, E_0 is the static modulus, E_∞ is the asymptotic modulus, τ is the relaxation time and α is the fractional parameter. Assuming the Poisson's ratio is real and constant (de Espíndola et al. 2005; Lakes and Wineman 2006), the complex shear modulus yields

$$G^{*}_{\mathrm{v}}(\omega) = \frac{G_0 + G_{\infty}(\mathrm{i}\omega\tau)^{\alpha}}{1 + (\mathrm{i}\omega\tau)^{\alpha}}\,, \tag{2.5}$$

where $\omega = 2\pi f$, G_0 is the static shear modulus and G_∞ is the asymptotic shear modulus.

The four-parameters fractional derivative model was fitted to the experimental shear complex modulus data by the Nelder-Mead minization algorithm implemented in Matlab R2014a (Nelder and Mead 1965).

A beam finite element and a three-layer beam finite element were considered to model the dynamic behaviour of metallic and sandwich structures, respectively.

The beam finite element is based on the Euler-Bernoulli beam theory. The finite element is defined by two nodes and two degrees of freedom (DOF) per node, the transverse displacement, w, and the rotational displacement, $\frac{\partial w}{\partial x}$, and the generalised displacements are discretised by the Hermite cubic shape function.

The three-layer beam finite element is based on the following assumptions: the metallic skins bend according to Euler-Bernoulli beam theory, the VE or the VEMR core is subjected only to shear deformation, the transverse displacement is uniform on a cross section and all layers are assumed to be perfectly bonded. The finite element is defined by two nodes with four DOF per node, the axial displacements of the top and bottom layers, u_1 and u_3, the transverse displacement, w, and the rotational displacement, $\frac{\partial w}{\partial x}$. The element combines linear shape functions for the axial displacements of the top and bottom layers and the Hermite cubic shape function for the transverse displacement, which avoids the shear locking effects in the element. In Figure 8.4 the configuration of the sandwich and the assumed displacement field are shown. Note that, $(\bullet)_1$, $(\bullet)_2$ and $(\bullet)_3$ refer to the top layer, core and bottom layer, respectively.

The theoretical transfer function is obtained by the direct frequency method. The governing equation of motion of a cantilever beam in the finite element form is written as

$$\mathbf{M}\ddot{\mathbf{q}} + \mathbf{K}^{*}\mathbf{q} = \mathbf{F}\,, \tag{2.6}$$

where $\mathbf{q}$ and $\ddot{\mathbf{q}}$ are the displacement vector and the acceleration vector, and where $\mathbf{M}$, $\mathbf{K}^*$ and $\mathbf{F}$ are the global mass matrix, the global complex stiffness matrix and the

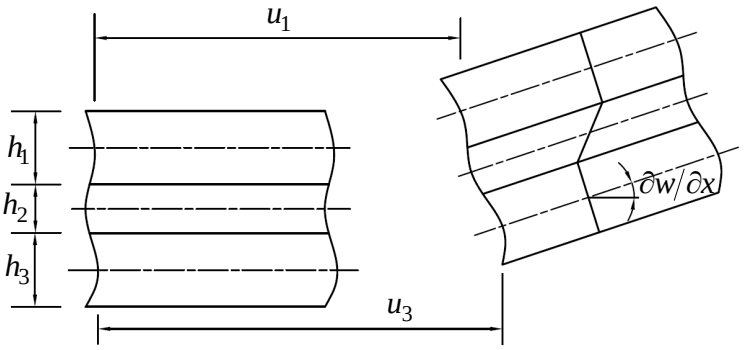

Figure 2.7. Displacement field of the sandwich beam.

global force vector. Note $\mathbf{K}^*$ depends on frequency due to the viscoelastic nature of the core. If a steady-state harmonic base excitation is considered, and the motion equation is written differentiating the DOF related to the base displacement vector, indicated by $(\bullet)_{\mathrm{s}}$, and the unknown displacement vector, indicated by $(\bullet)_{\mathrm{u}}$, the following is obtained

$$\left(-\omega^2\begin{bmatrix}\mathbf{M}_{\mathrm{ss}} & \mathbf{M}_{\mathrm{su}}\\ \mathbf{M}_{\mathrm{us}} & \mathbf{M}_{\mathrm{uu}}\end{bmatrix}+\begin{bmatrix}\mathbf{K}^*_{\mathrm{ss}} & \mathbf{K}^*_{\mathrm{su}}\\ \mathbf{K}^*_{\mathrm{us}} & \mathbf{K}^*_{\mathrm{uu}}\end{bmatrix}\right)\begin{Bmatrix}\mathbf{S}^*\\ \mathbf{U}^*\end{Bmatrix}=\begin{Bmatrix}\mathbf{R}^*\\ \mathbf{0}\end{Bmatrix}, \tag{2.7}$$

where $\mathbf{S}^*$, $\mathbf{U}^*$ and $\mathbf{R}^*$ are the complex amplitude vector of the applied base motion, unknown displacements and reaction forces of the base, respectively. The transfer function is determined by dividing the amplitude of the transverse displacement of the response point (jth DOF), U_j^*, by the amplitude of the transverse displacement applied at the base point (ith DOF), S_i^*, as

$$T_{ij}^* = \frac{U_j^*}{S_i^*}\,. \tag{2.8}$$

By way of example, the correlation of the SS2-VE2 sandwich in the bandwidth of 0-1 kHz is shown in Figure 8.5. It is observed the correlation in frequency and modulus is acceptable, being the biggest deviation in the first vibration mode. This is due to an overestimation of the shear modulus of the VE core at low frequencies. This result validates the constitutive viscoelastic model, the finite element and the numerical modelling of the cantilever beam by FEM.

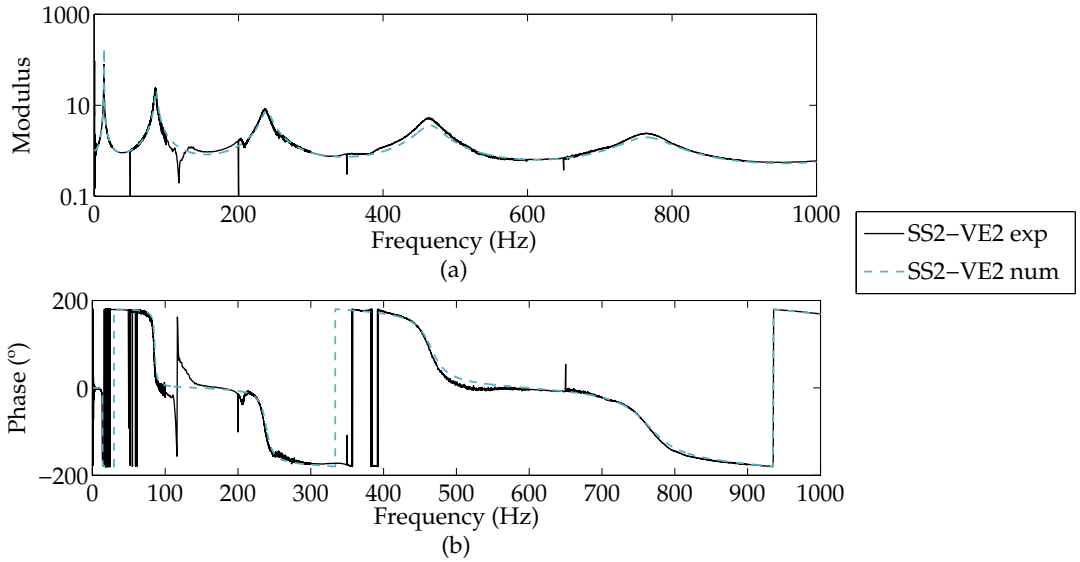

Figure 2.8. Experimental and numerical transfer function, (a) modulus and (b) phase, of the SS2-VE2 beam with 170 mm of free length in the bandwidth of 0-1 kHz.

Throughout the thesis, when showing results, if these were obtained experimentally, it will be indicated; otherwise they are numerical results.

Chapter 3

Thin viscoelastic sandwich

The smart viscoelastic-magnetorheological sandwiches which are the object of study of this thesis are analogous to thin viscoelastic sandwiches. This chapter analyses the dynamic behaviour of thin viscoelastic sandwiches and the influence of their design on it, as a way of studying the dynamic behaviour of thin viscoelastic-magnetorheological sandwiches in the absence of a magnetic field.

Irazu L and Elejabarrieta MJ (2017). The effect of the viscoelastic film and metallic skin on the dynamic properties of thin sandwich structures. *Composite Structures* 176:407-419. DOI: 10.1016/j.compstruct.2017.05.038.

Irazu L and Elejabarrieta MJ (2015). The influence of viscoelastic film thickness on the dynamic characteristics of thin sandwich structures. *Composite Structures* 134:421-428. DOI: 10.1016/j.compstruct.2015.07.086.

3.1 Introduction

Viscoelastic sandwiches (VES) constitute a cost-effective passive damping technique and have been used in different applications where the mass of components is critical (Rao 2003). In these sandwiches, the viscoelastic (VE) core is cyclically shear deformed due to the relative motion of the skins, dissipating energy into heat. In recent years, the conventional VE materials used in sandwich structures are being replaced by micron-size VE adhesive films (Martinez-Agirre and Elejabarrieta 2010) since the relative shear deformation developed within thin cores is significantly higher than the one developed within thick cores (Moreira and Dias Rodrigues 2010). The use of these thin VE adhesives and metallic skins results in sandwich structures with high stiffness-to-weight and damping-to-weight ratios. In addition, the total thickness of these sandwiches is similar to metal sheets, which makes it possible to use them in classic sheet metal forming processes.

The smart viscoelastic-magnetorheological sandwiches (VEMRS) on which this thesis is focused are analogous to thin VESs in order to preserve all their main characteristics. As thin VESs, these are composed of metallic skins and micron-size VE adhesives, with the difference that magnetic particles were added to their VE adhesive. In this chapter the dynamic behaviour of thin VESs and the influence of different design parameters on it is analysed, as a way of studying the dynamic performance of thin VEMRSs in the absence of a magnetic field. VESs composed of different metallic skins and VE adhesives were characterized in the bandwidth of 0-1 kHz in general. The influence of the nature and thickness of both VE core and metallic skins on the dynamic properties of thin sandwiches is analysed from the experimental and numerical results.

Next, a brief state of the art about dynamic properties and design of VESs is presented and the objectives of this chapter are defined. Then, the influence of the nature and thickness of both VE core and metallic skins on the dynamic properties of thin VESs is analysed from experimental and numerical results. Finally, the obtained conclusions are summarized and the scientific contributions are presented.

3.2 State of art

VE materials can be confined between two rigid layers to form sandwich structures. When these VES are subjected to cyclic flexural vibrations, the skin layers move relatively to each other, resulting in the VE material being highly deformed in shear and thus dissipating energy from the system. These VES structures are cost-effective to attenuate structural vibrations and simple to implement. Nevertheless, the optimal design of these sandwiches is complex since their dynamic performance and damping capacities depend upon the configuration of the sandwich, as well as the intrinsic dynamic properties of the viscoelastic and skin materials (Sher and Moreira 2013).

The dynamic properties and design of VES structures has been the subject of study since the mid-20th century and the first research in this field was pioneered by Kerwin (1959) and Ross et al. (1959), who presented an analytical model to predict the damping effectiveness of viscoelastic sandwiches. Lifshitz and Leibowitz (1987) and Leibowitz and Lifshitz (1990) solved a sixth-order equation of motion with complex coefficients for a sandwich beam numerically and analysed the influence of the VE core and skin thicknesses on the damping of the sandwich. They showed how depending on the conditions, a thinner or thicker VE core gives higher values of damping, and so they suggested the use of an optimization technique. Teng and Hu (2001) analysed the influence of frequency, temperature and thicknesses of both VE core and skins on the damping characteristics of the sandwich by employing the model presented by Ross et al. (1959). They observed symmetric sandwiches possess better damping efficiency than asymmetric ones, and temperature affects the damping of the sandwich, being the loss factor of the sandwich maximum in the transition region of the viscoelastic material. Kergourlay et al. (2006) analysed the influence of the static pre-strain on the dynamic properties of thin VE films. To that end, they built a dynamic test ring able to measure the complex shear modulus of VE cores of sandwich structures on which a static pre-strain have been induced and they observed that increasing the prestrain the modulus of the VE film increases and the loss factor decreases. Martinez-Agirre et al. (2014) analysed too the effect of the static prestrain on the viscoelastic film. In addition to the observations pointed by Kergourlay et al. (2006), they showed the frequency dependence of the VE material decreases with the static prestrain. Sher and Moreira (2013) performed an extensive parametric study to explore the effect of the design parameters on the sandwich efficiency. Specifically, they analysed the influence of the thickness to length ratio, skin layer thickness, material modulus, natural mode and boundary conditions. Finally, they highlighted the potential of sandwiches composed of thin VE films, specially if these are symmetric and with high skin thickness-length ratio.

The latest researches concerning the design of viscoelastic sandwiches have gradually shifted their focus towards optimal design procedures for multi-layered structures. Araújo et al. (2010) used the Feasible Arc Interior Point Algorithm to optimize the modal loss factor of sandwich structures, the design variables being the thicknesses and the laminate layer ply orientation angles. Hamdaoui et al. (2015) and Madeira et al. (2015a) proposed a multi-objective optimisation approach to minimize the mass and maximize the damping. The first ones used the viscoelastic material and the thickness of the viscoelastic and elastic layers as design variables, whereas the latter's considered the materials of the elastic layers and the thickness of viscoelastic and elastic layers to be variables. Later, Madeira et al. (2015b) went one step further and proposed a more general multi-objective optimization procedure in which the design variables allow for a full design of the sandwich structure, minimizing the weight and the material cost and maximizing the modal damping. The multi-objective optimization procedures are very useful since the optimal design of VESs is based on a

trade-off between damping, mechanical properties and added weight.

Some authors have shown thin VESs can be effective (Martinez-Agirre and Elejabarrieta 2010; Sher and Moreira 2013), however there are not many works focused exclusively on the dynamic behaviour and design of these thin sandwiches composed of micron-size VE adhesives.

3.3 Objectives

The main aim of this chapter is to study the dynamic behaviour of thin VESs and the influence of the design of the sandwich on it. To that end, the following is analysed:

- The influence of the nature and thickness of the VE adhesive on the dynamic properties of thin VESs.
- The influence of the nature and thickness of the metallic skins on the dynamic properties of thin VESs.

3.4 Results

Thin VESs composed of different metallic skins and VE adhesives were characterized. The obtained experimental results enabled to define numerical models with whom, once validated, the influence of design parameters on the dynamic behaviour of these thin VESs was studied. Specifically, six thin VESs were characterized composed of two viscoelastic adhesives, polyester-based adhesive-1 (VE1) and polyester-based adhesive-2 (VE2), and four metallic skins, stainless steel AISI 316-1 (SS1), stainless steel AISI 316-2 (SS2), aluminium alloy 1050 H18-1 (AL) and galvanised steel Z100 (GS).Their geometrical and physical properties are shown in Table 2.2.

The experimental characterization was carried out by the forced vibration tests with resonance according to the standard ASTM E 756 (2005) and the modification proposed by Cortés and Elejabarrieta (2007) in the bandwidth of 0-1 kHz. In some cases, the bandwidth was extended up to 4 kHz. The defined numerical models encompass a four-parameters fractional derivative model for the VE adhesives and a multi-layer finite element for the thin sandwich structure as detailed in Chapter 2.

3.4.1 Influence of viscoelastic core

Following, the influence of the nature and thickness of the VE core on the vibrational response and dynamic properties of thin VESs is studied.

Two VE films, VE1 and VE2, were characterized and in Figure 8.1 the constitutive viscoelastic model defined for each one are shown. The shear modulus of both VE films increases with frequency, the VE1 one being higher at low frequencies and the VE2 one at high frequencies. Concerning the loss factor, that for VE2 is bigger than the VE1 one over the whole frequency bandwidth.

Figure 8.7 compares the dynamic properties of thin VESs composed of VE1 and VE2 adhesives. The storage modulus of both sandwiches decreases in frequency being this tendency stronger in the sandwich composed of VE1 and the storage modulus of the sandwich composed of VE2 is bigger than the one composed of VE1. Regarding the loss factor, this increases with the frequency and the loss factor of the sandwich composed of VE2 is bigger than the one composed of VE1, being this difference constant in frequencies higher than 20 Hz. In analysing Figure 8.6 and Figure 8.7 together, it is concluded that the differences between the shear dynamic properties of both films become smaller in the dynamic properties of thin VESs composed of these films.

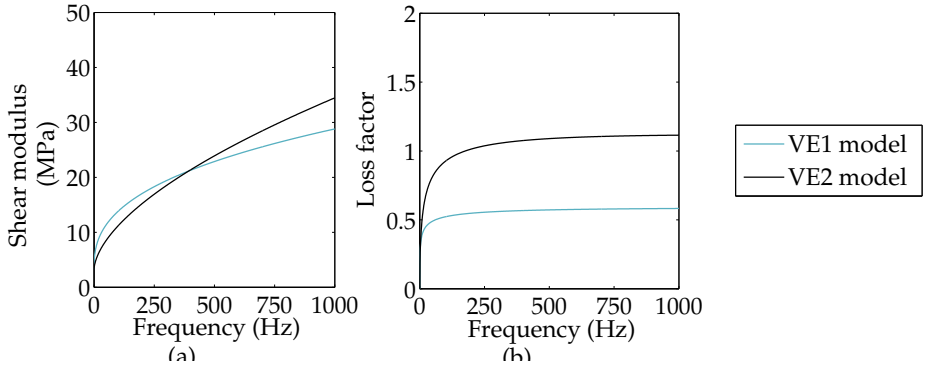

Figure 3.1. Shear complex modulus models, (a) shear modulus and (b) loss factor, of VE1 and VE2 films in the bandwidth of 0-1 kHz.

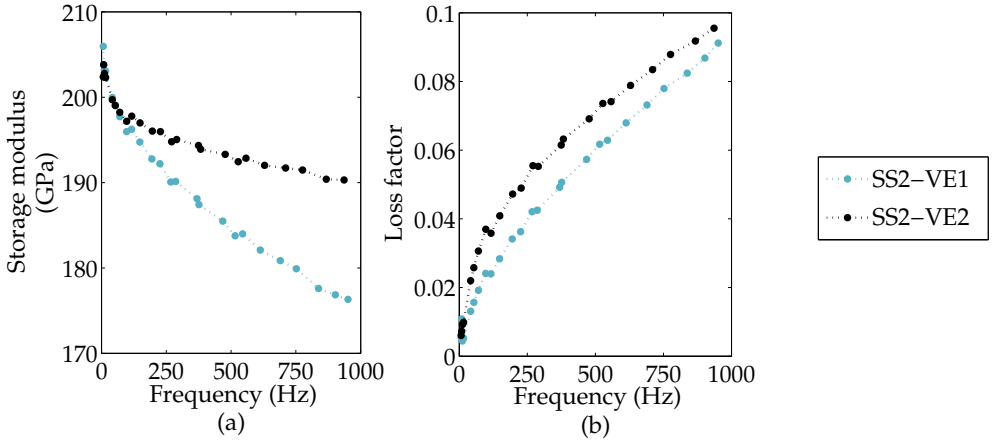

Figure 3.2. Influence of the VE film nature on the homogenised complex modulus, (a) storage modulus and (b) loss factor, of thin VESs in the bandwidth of 0-1 kHz. The composition of the sandwiches is the following: 0.25 mm of SS2 skins, and 40 µm of VE1 or VE2.

Next, the influence of the VE core thickness is analysed. Figure 8.8 shows the experimental transfer functions of thin VESs composed of three VE1 thicknesses in the bandwidth of 0-1 kHz. The bigger the core thickness, the lower the modulus of the transfer function and so the vibration amplitude. In contrast, the bending stiffness and so the resonance frequencies increases with the core thickness. Note the resonance frequencies of the SS1-VE1-19 are lower than the others, due to its thinner skin layers as specified in Table 2.2.

Sargianis and Suhr (2012) observed in sandwich structures the bending stiffness, which depends on core thickness, dominates the low frequency vibrational response, whereas at high frequencies the response is influenced mainly by the material properties of the core. In Figure 8.9 the frequency bandwidth is extended to 4 kHz exceptionally and unlike these authors it is observed in these thin VES structures the vibrational response is influenced by the VE core thickness in all the bandwidth from 0 to 4 kHz.

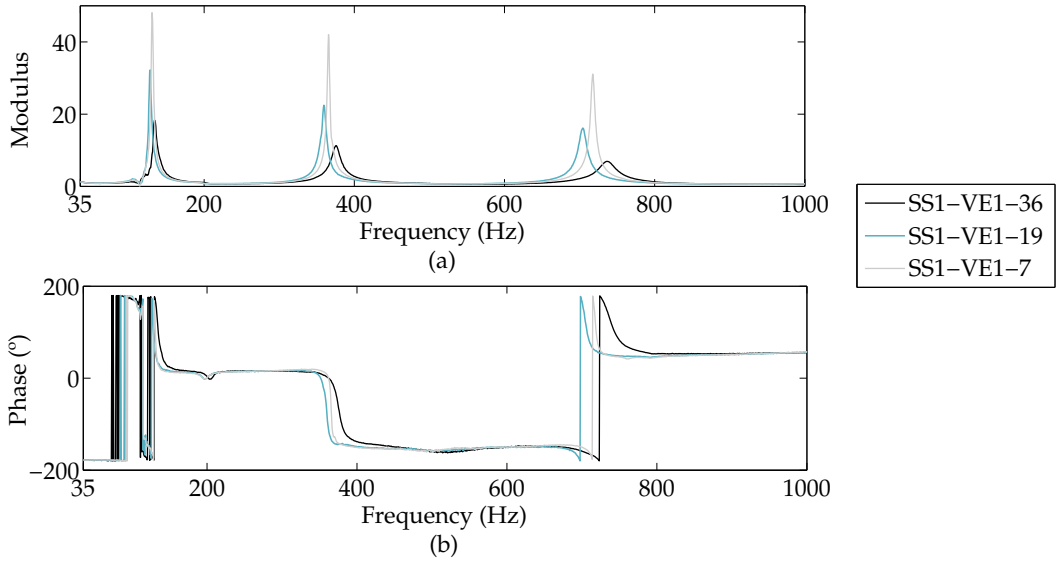

Figure 3.3. Experimental transfer functions, (a) Modulus and (b) Phase, of the SS1-VE1-36, SS1-VE1-19 and SS1-VE1-7 beams with with 140 mm of free length in the bandwidth of 35-1000 Hz.

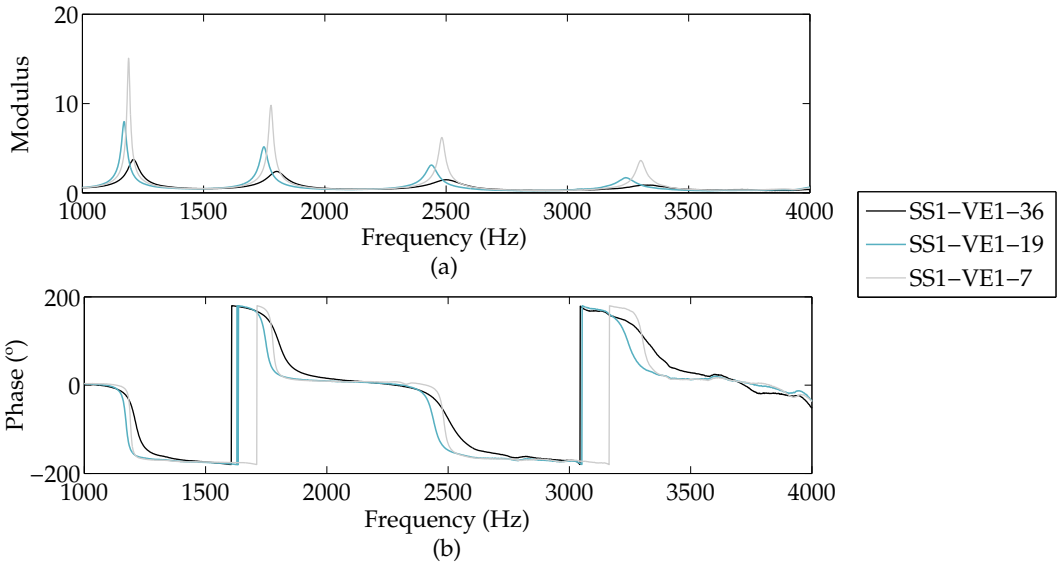

Figure 3.4. Experimental transfer functions, (a) Modulus and (b) Phase, of the SS1-VE1-36, SS1-VE1-19 and SS1-VE1-7 beams with with 140 mm of free length in the bandwidth of 1-4 kHz.

In Figure 8.10 the influence of the VE1 core thickness of the dynamic properties of thin VESs is shown. Increasing the VE core thickness, the storage modulus decreases

and the loss factor increases. In addition, both properties become more frequency dependent.

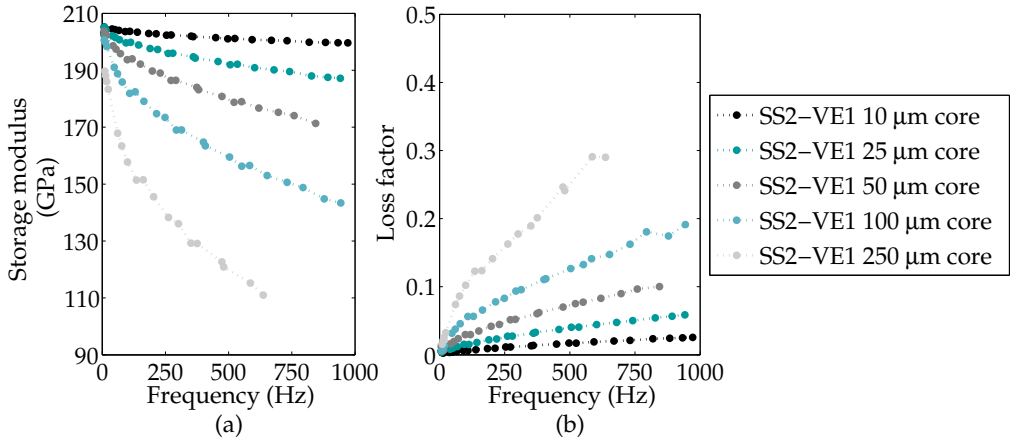

Figure 3.5. Influence of the VE1 film thickness on the homogenised complex modulus, (a) storage modulus and (b) loss factor, of thin VESs in the bandwidth of 0-1 kHz. The composition of the sandwiches is the following: 0.25 mm of SS2 skins, and 10 µm, 25 µm, 50 µm, 100 µm or 250 µm of VE1.

3.4.2 Influence of metallic skin

Following, the effect of the type of metallic skin and its thickness on the dynamic properties of thin VESs is analysed. In Figure 8.11, the influence of forming the sandwich structure with SS1, SS2, GS or AL metallic skins on its storage modulus and loss factor is shown. As expected, the bigger the storage modulus of the metallic material, the bigger the storage modulus of the VES. In addition, the bigger the storage modulus the bigger the loss factor of the VES, which means sandwiches composed of rigid skins dissipate more energy. The metallic material has no influence of the frequency dependence of thin VESs.

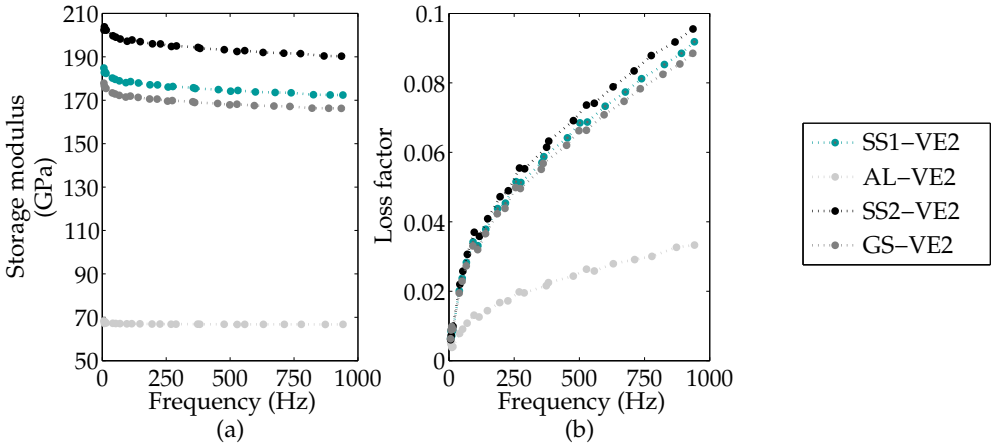

Figure 3.6. Influence of the type of metallic skin on the homogenised complex modulus, (a) storage modulus and (b) loss factor, of thin VESs in the bandwidth of 0-1 kHz. The composition of the sandwiches is the following: 0.25 mm of SS1, AL, SS2 or GS skins and 40 µm of VE2.

Regardless of the metallic material of which the sandwich is composed, the skin thickness does not have a remarkable influence on the dynamic properties of thin VESs. As an example, Figure 8.12 shows the influence of the AL skin thickness on the dynamic properties of VESs. However, it will modify the bending stiffness of the structure.

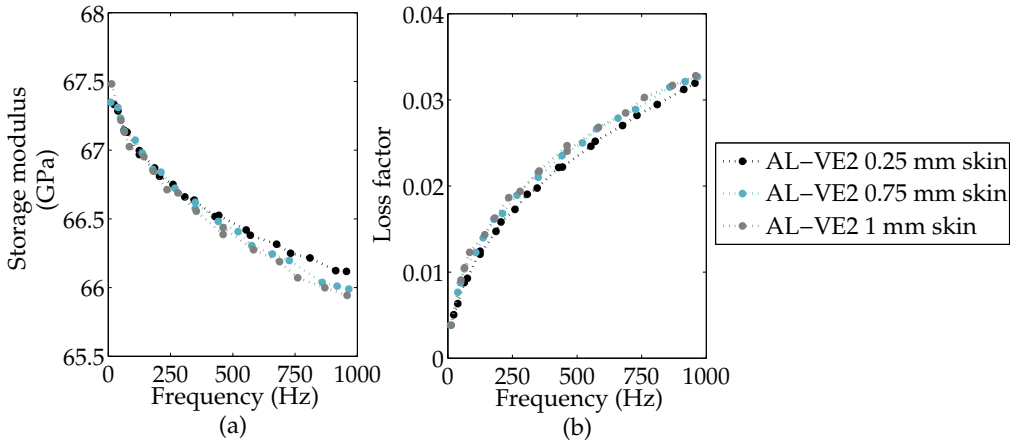

Figure 3.7. Influence of the AL skin thickness on the homogenised complex modulus, (a) storage modulus and (b) loss factor, of thin VESs in the bandwidht of 0-1 kHz. The composition of the sandwiches is the following: 0.25 mm, 0.75 mm or 1 mm of AL skins, and 40 µm of VE2.

3.5 Conclusions

In this chapter the dynamic behaviour of thin VESs was studied. To that end, thin VESs composed of different VE adhesives and metallic skins were characterized in the bandwidth of 0-1 kHz. Then, numerical models, consisting of a four-parameters fractional derivative model for the VE adhesives and a three-layer beam finite element for the thin VESs, were defined. The influence of the nature and thickness of both VE adhesive and metallic skins on the dynamic properties of thin VESs was analysed using experimental and numerical results.

The obtained results showed VE adhesives with high shear modulus and loss factor or metallic skins with high storage modulus lead to thin VESs with higher stiffness and damping. The thickness of the VE core influences the dynamic behaviour of the sandwich in the bandwidth up to 4 kHz. Increasing the core thickness, the loss factor of the sandwich increases and the vibration amplitude decreases. In contrast, the storage modulus decreases, whereas the bending stiffness increases. The thickness of the metallic skins has no remarkable influence on the dynamic properties of the sandwich. However, its thickness modifies the bending stiffness of the structure.

3.6 Scientific contribution

The effect of the viscoelastic film and metallic skin on the dynamic properties of thin sandwich structures

Leire Irazu and María Jesús Elejabarrieta
Mechanical & Manufacturing Department, Mondragon Unibertsitatea, Loramendi 4, 20500 Arrasate-Mondragon, Spain

Composite Structures (2017) 176:407-419
DOI: 10.1016/j.compstruct.2017.05.038.

Impact factor - JCR: 3.858
Ranking - JCR: 5/25

Composite Structures 176 (2017) 407–419

Contents lists available at ScienceDirect

Composite Structures

journal homepage: www.elsevier.com/locate/compstruct

The effect of the viscoelastic film and metallic skin on the dynamic properties of thin sandwich structures

Leire Irazu, Maria Jesus Elejabarrieta *

Mechanical and Manufacturing Department, Mondragon Unibertsitatea, Loramendi 4, 20500 Arrasate-Mondragon, Spain

ARTICLE INFO

Article history:
Received 24 February 2017
Revised 28 April 2017
Accepted 11 May 2017
Available online 17 May 2017

Keywords:
Thin sandwich
Viscoelastic film
Metallic skin
Vibration attenuation
Experimental characterization
Numerical model

ABSTRACT

In this work, the influence of design parameters on the dynamic properties of thin sandwich structures composed of micron-size viscoelastic adhesive layers is analysed. Sandwiches composed of different types of viscoelastic film and metallic skins are characterised in the frequency bandwidth of 0–1 kHz. The numerical modelling of thin sandwich structures is presented and validated with experimental results. A four-parameter fractional derivative model is used to describe the dynamic behaviour of the viscoelastic films, and a three-layer beam element is used to model the sandwich structures. The analysis of experimental and numerical results allows the establishment of design considerations to obtain thin sandwich structures with high stiffness and damping. The viscoelastic adhesive film should have a high shear modulus and loss factor, and the metallic skin should have a high storage modulus.

© 2017 Elsevier Ltd. All rights reserved.

1. Introduction

Passive damping techniques by means of viscoelastic materials are cost-effective ways to control structural vibrations and dissipate acoustic energies. The viscoelastic material can be confined between two rigid layers to form a sandwich structure in which the viscoelastic material deforms in shear mode dissipating energy. These structures are of special interest for applications in which the mass of components is critical, and high strength-to-weight and stiffness-to-weight ratios are desired, such as in aeronautical, automotive, railroad and marine industries [1].

The design of viscoelastic sandwich structures has been the subject of study since the mid-20th century, as the performance and damping capabilities of sandwiches depend on it. The first research in this field was pioneered by Kerwin [2] and Ross, Ungar and Kerwin [3], who presented an analytical model to predict the damping effectiveness of viscoelastic sandwiches. Teng and Hu [4] analysed the influence of the frequency, the temperature and the thicknesses of the viscoelastic core and skins on the vibration damping characteristics of sandwich structures by employing the model presented by Ross, Ungar and Kerwin [3]. Lifshitz and Leibowitz [5,6] solved a sixth-order equation of motion with complex coefficients of a sandwich beam for a large variety of boundary conditions, analysed the influence of the viscoelastic core and skin thicknesses on the damping and proposed an optimal design procedure for sandwich beams. The latest researches have gradually shifted their focus towards optimal design procedures for multi-layered structures. Araújo et al. [7] used the Feasible Arc Interior Point Algorithm to optimize the modal loss factor of sandwich structures, the design variables being the thicknesses and the laminate layer ply orientation angles. Hamdaoui et al. [8] and Madeira et al. [9] proposed a multi-objective optimisation approach to minimize the mass and maximize the damping. The first ones used the viscoelastic material and the thickness of the viscoelastic and elastic layers as design variables, whereas the latter's considered the materials of the elastic layers and the thickness of viscoelastic and elastic layers to be variables. Later, Madeira et al. [10] went one step further and proposed a more general multi-objective optimization procedure in which the design variables allow for a full design of the sandwich structure, minimizing the weight and the material cost and maximizing the modal damping.

Currently, the conventional viscoelastic materials used to form sandwich structures are being replaced by micron-size viscoelastic adhesive films [11–13]. The use of these adhesives and metallic constraining layers result in sandwich structures with high stiffness-to-weight and damping-to-weight ratios. In addition, the total thickness of the sandwich is similar to that of the metal sheets, which makes possible to use them on classic sheet metal forming processes. This feature is of special interest because damped pieces of complex geometries can be obtained with less manufacturing steps, saving time and costs.

* Corresponding author.
E-mail address: mjelejabarrieta@mondragon.edu (M.J. Elejabarrieta).

http://dx.doi.org/10.1016/j.compstruct.2017.05.038
0263-8223/© 2017 Elsevier Ltd. All rights reserved.

The main aim of this work is to study the dynamic response of thin sandwich structures composed of micron-size viscoelastic adhesive films, and analyse the influence of different design parameters on their dynamic properties. Four thin sandwich structures composed of different viscoelastic films and metallic skins are experimentally characterised in the bandwidth of 0–1 kHz. Then, the numerical modelling of thin viscoelastic sandwich structures is presented and validated. A four-parameter fractional derivative model is used to describe the dynamic behaviour of the viscoelastic adhesive films, and a three-layer beam finite element is used to model the sandwich structures. The numerical and experimental transmissibility functions of the analysed sandwich structures are compared and show good agreement in all of the bandwidth. Finally, the influence of the nature and thickness of the viscoelastic film and metallic skins on the dynamic properties of thin sandwich structures is studied from the experimental and numerical results.

2. Experimental characterization

The frequency-dependent dynamic properties of sandwich structures and their viscoelastic cores are characterised by forced vibration tests with resonance according to the standard ASTM E 756-05 [14] and the modification proposed by Cortés and Elejabarrieta [15] in the bandwidth of 0–1 kHz.

Next, the analysed sandwich structures are presented, the experimental technique is described and the procedure to identify the materials' properties is detailed.

2.1. Specimens

All of the analysed sandwich structures are symmetric and composed of thin viscoelastic films and metallic skins. Two polyester-based adhesive films are used as viscoelastic core, and stainless steel, galvanised steel and aluminium layers as metallic skins. From each sandwich structure, three specimens are characterised to obtain the average results. In Fig. 1, the configuration of the sandwich structures is shown, where L, b and H are the free length, the width and the thickness of the sandwich, and H_e and H_v are the thickness of the metallic skin and viscoelastic film, respectively. Note that $(\bullet_e)$ and $(\bullet_v)$ refer to the elastic and viscoelastic layers.

Table 1 shows the composition of the analysed sandwiches and the nomenclature used to name them, which is the metallic material (SS1, AL, SS2 or GS) followed by the viscoelastic material (VE1 or VE2). In Table 2, the geometrical and physical properties of the sandwich structures and their components are specified, in which E_e is the storage modulus of the skin, and ρ, ρ_e and ρ_v are the density of the sandwich structure, the metallic skin and the viscoelastic core, respectively.

2.2. Experimental technique

The standard ASTM E 756-05 [14] establishes the procedure to characterise the sandwich structures and their viscoelastic cores by measuring the frequency response function of sandwich beam specimens in a cantilever configuration. Cortés and Elejabarrieta [15] proposed to replace the excitation force by a seismic base motion at the clamp and prove the procedure is equally applicable with transmissibility functions.

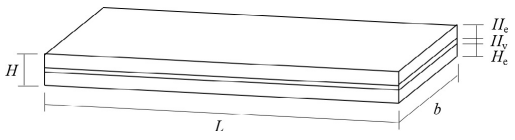

Fig. 1. Configuration of the sandwich structure.

Table 1
Nomenclature and composition of the analysed sandwich structures.

	Metallic skin	Viscoelastic layer
SS1-VE1	SS1: Stainless steel AISI 316-1	VE1: Polyester-based adhesive – 1
AL-VE1	AL: Aluminium alloy 1050 H18	
SS2-VE2	SS2: Stainless steel AISI 316-2	VE2: Polyester-based adhesive – 2
GS-VE2	GS: Galvanised steel Z100	

In the experimental tests, the transmissibility functions of all of the sandwich specimens with two or three different free lengths were measured. Fig. 2 shows the scheme of the experimental set-up. The base motion was generated by an electrodynamic shaker and consisted of a white noise in the frequency range of 0 to 1 kHz. The acceleration of the base, $\ddot{s}$, was measured by a piezoelectric accelerometer with a charge conditioning amplifier and loop-back controlled by a vibration controller. The velocity of the beam, $\dot{u}$, was measured in the point located 5 mm from the free end by a laser vibrometer. The data acquisition and signal processing were performed with an analyser connected to a PC. The transmissibility function, Eq. (1), was obtained by relating the acceleration of the beam's free end with that applied at the base, so that

$$\exp T^*(f) = \frac{U^*_{\exp}(f)}{S^*_{\exp}(f)}, \tag{1}$$

where $U^*_{\exp}(f)$ is the Fourier transform of the derivative of the velocity measured at the free end, $\dot{u}$, and $S^*_{\exp}(f)$ is the Fourier transform of the acceleration applied at the base, $\ddot{s}$. The resolution of the transmissibility function is higher at low frequencies than at higher frequencies to obtain more accurate measurements of the peaks of the first vibration modes. Specifically, the resolution goes from 0.02 Hz in the first vibration mode to 0.7 Hz in the last mode.

The dynamic properties of viscoelastic materials, besides depending on frequency, also depend on temperature and strain level. In this work, all the measurements were taken at environmental temperature and within the linear range. To ensure this, a linearity analysis consisting of exciting the sandwich beam with different acceleration levels was carried out with each sandwich structure and with the longest free length, since it is the most sensitive. When the deformations of the viscoelastic material are over the linear viscoelastic range, its stiffness decreases and the loss factor increases [16]. Thus, analysing the measured transmissibility functions the maximum acceleration applicable to ensure linearity was determined. For example, Fig. 3 shows the linearity analysis carried out with the GS-VE2 sandwich beam. It can be observed that within the first three excitation levels, the same transmissibility function is obtained; whereas increasing the excitation, the modulus and the resonance frequency are decreased meaning that the deformations go over the linear range.

2.3. Materials parameter extraction procedure

In the following, the procedure to obtain the dynamic properties of sandwich structures and their viscoelastic films from the experimental transmissibility functions is presented. The characterisation is done in a two-step process: the homogenised complex modulus of the sandwich structure is determined from the transmissibility function, and then the shear complex modulus of the viscoelastic film is obtained from the Ross-Kerwin-Ungar (RKU) equations [3] with Rao's correction [17,18].

Table 2
Geometrical and physical properties of the analysed sandwich structures.

	Sandwich			Metallic skin			Viscoelastic layer	
	H (±0.002 mm)	b (±0.1 mm)	ρ (±0.05 g/cm^3)	H_e (±0.002 mm)	ρ_e^* (g/cm^3)	E_e (GPa)	H_v (±2 μm)	ρ_v^* (g/cm^3)
SS1-VE1	0.552	9.9	7.51	0.258	7.95	185.24	36	1.13
AL-VE1	0.988	9.9	2.67	0.483	2.7	67.96	21	1.13
SS2-VE2	0.472	9.9	7.37	0.216	7.96	205.71	41	1.13
GS-VE2	1.219	9.9	7.54	0.589	7.76	177.95	40	1.13

*Data provided by the manufacturer, Replasa S.A.

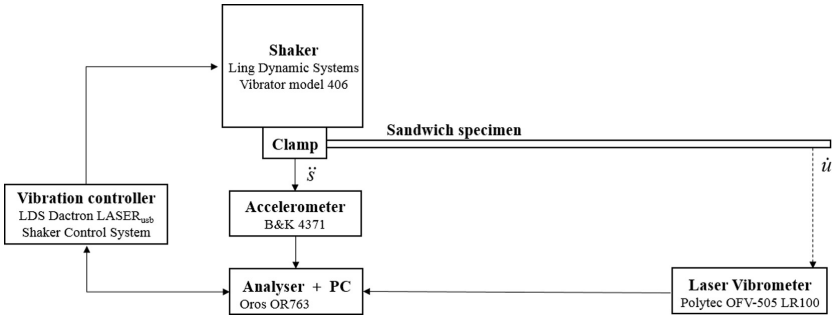

Fig. 2. Scheme of the experimental set-up.

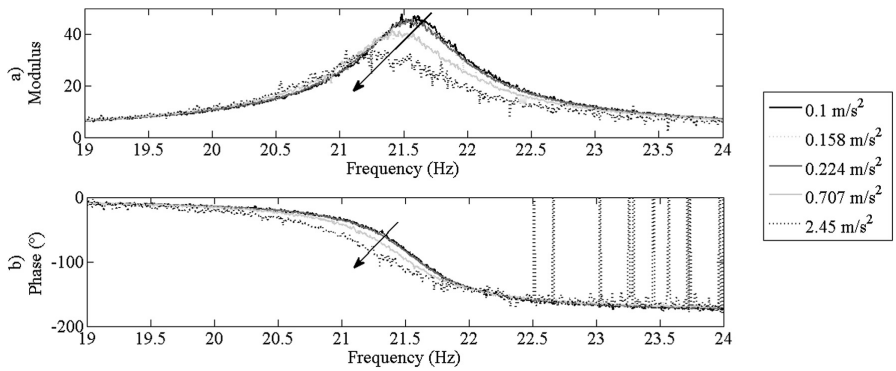

Fig. 3. Linearity analysis of the GS-VE2 sandwich specimen: first-mode transmissibility function of the sandwich beam with 210 mm of free length under different excitation levels.

The numerical procedure uses the classical analysis based on the Euler-Bernoulli beam theory, so the terms involving rotary inertia or shear deformation are not included, and it is assumed that the transversal section remains plane. This approximation is accurate as long as the dimensions of the beam's cross section are much shorter than the length of the beam. Moreover, the extensional terms of the core are not included, which is acceptable when the modulus of the viscoelastic layer is considerably lower than that of the metallic skin, and the loss factor of the base metal is assumed to be zero.

The storage modulus, E, of the sandwich structure is dependent on frequency and it is obtained from

$$E = \frac{12\rho L^4 f_n^2}{H^2 C_n^2} \tag{2}$$

where f_n is the resonance frequency of mode n of the sandwich beam, and C_n is the coefficient for mode n of clamped-free configuration, detailed in the standard ASTM E 756-05 [14]. The resonance frequency, f_n, is deduced from the modal transmissibility function, determining the frequency in which the real part of the function is zero, and the imaginary part has a maximum or minimum.

The loss factor, η, which is also frequency dependent, it is obtained by the half-power bandwidth (HPB) method, like the standard ASTM E 756-05 recommends [14]. As the loss factor values of the analysed sandwich structures are less than 0.1, the HPB method can be used to determine the loss factor with an error rate of less than 0.1% [12,15]. In the HPB method, the modal loss factor, η, is obtained by the division of the bandwidth where the amplitude of the peak is reduced 3 dB, Δf_n, with the resonance frequency such that

$$\eta = \frac{\Delta f_n}{f_n}. \tag{3}$$

Assuming a linear viscoelastic behaviour of the sandwich structure, the homogenised complex modulus, E^*, can be expressed as

$$E^* = E(1 + i\eta). \tag{4}$$

Once the homogenised complex modulus of the sandwich structure is known, the shear complex modulus of the viscoelastic film is obtained from the RKU equations with Rao's correction [18]. The RKU homogenised beam theory is strictly applicable to pinned-pinned beam configuration, and for other boundary conditions, an approximation is made. The standard ASTM E 756-05 [14] establishes to ignore the results obtained from the first vibration mode, since the approximation is not good for the lower modes. Rao studied this aspect and he proposed equations to correctly determine the resonance frequencies and loss factors of lower modes for different boundary conditions [17].

The RKU equations with Rao's correction are the following

$$E^* I = 2E_e I_e + E_e H_e (H_e + H_v)^2 \frac{g_n^*}{1 + 2g_n^*}, \tag{5}$$

$$g_n^* = \frac{G_v^* L^2}{E_e H_v H_e \xi_n^2 \sqrt{R_n}} \tag{6}$$

where I is the second moment of area of the sandwich $I = H^3/12$, I_e is the second moment of area of the metallic skin $I_e = H_e^3/12$, $\xi_n^2 = 2\pi C_n$ and R_n is the Rao's correction for mode n [18].

Finally, assuming a linear viscoelastic behaviour of the viscoelastic film and Poisson ratio is real and constant in frequency [19,20], the shear complex modulus, G_v^*, can be expressed as follows

$$G_v^* = G_v(1 + i\eta_v) \tag{7}$$

where G_v is the shear modulus and η_v is the loss factor of the core, both frequency dependent.

The experimental dynamic properties of the analysed sandwich structures and viscoelastic adhesive films can be seen in Tables 3–6. All of the results shown are an average of three specimens with the standard deviations. It can be observed the deviations obtained between the sandwiches composed of VE1 is bigger than between the ones composed of VE2. This is due to the nature of VE1 film that makes more difficult to obtain repeatable sandwich specimens.

3. Numerical modelling

The constitutive viscoelastic and the finite element model used to describe the dynamic behaviour of the analysed sandwich structures are presented, as well as the correlation with the experimental results.

3.1. Constitutive viscoelastic model

Viscoelastic materials show both elastic and viscous characteristics, and simple differential viscoelastic models can be defined by the combination of discrete spring and dashpot elements. Nevertheless, the actual behaviour of polymeric materials may not be represented in terms of simple differential relations, and multi-element models, such as the generalised Maxwell or the generalised Kelvin-Voigt, are required. To reduce the number of terms required by these models, the differential equation can be generalised by replacing the integer-order derivatives with fractional-order ones, and these models are known as fractional derivative models [16,18]. Bagley and Torvik [21,22] analysed the fractional derivatives from molecular and thermodynamical points of view, and several authors have used the fractional derivative models to model the dynamic behaviour of viscoelastic materials successfully [12,23–25]. The most known fractional derivative model is the four-parameter fractional derivative model or the generalised Zener model, which had been thoroughly analysed by Pritz [26]. This model is able to represent the shear dynamic behaviour of several viscoelastic materials with just four parameters, and each parameter has a physical interpretation.

The four-parameter fractional derivative model is represented by the fractional equation

$$\sigma(t) + \tau^\alpha \frac{\partial^\alpha \sigma(t)}{\partial t^\alpha} = E_0 \varepsilon(t) + E_\infty \tau^\alpha \frac{\partial^\alpha \varepsilon(t)}{\partial t^\alpha} \tag{8}$$

where $\sigma(t)$ is the stress and $\varepsilon(t)$ is the strain. The complex modulus in the frequency domain results in

$$E_v^* = \frac{E_0 + E_\infty (i\omega\tau)^\alpha}{1 + (i\omega\tau)^\alpha} \tag{9}$$

where E_0 is the static modulus, E_∞ is the asymptotic modulus, τ is the relaxation time and α is the fractional parameter.

Assuming that the Poisson ratio is real and constant in frequency in the analysed bandwidth [19,20], the shear complex modulus is expressed as

$$G_v^* = \frac{G_0 + G_\infty (i\omega\tau)^\alpha}{1 + (i\omega\tau)^\alpha} \tag{10}$$

where G_0 and G_∞ are the static and asymptotic shear modulus, respectively.

The four-parameter fractional model is fitted to the experimental shear complex modulus data by the Nerder-Mead minimisation algorithm. The minimised function is

$$\|G_{v,\text{fitted}} - G_{v,\text{exp}}\| + \|G_{v,\text{fitted}}\eta_{v,\text{fitted}} - G_{v,\text{exp}}\eta_{v,\text{exp}}\| \tag{11}$$

where $G_{v,\text{fitted}}$ and $\eta_{v,\text{fitted}}$ are obtained from Eqs. (7) and (10), and where $G_{v,\text{exp}}$ and $\eta_{v,\text{exp}}$ are the experimental shear modulus and the loss factor, respectively, shown in Tables 3–6. Finally, it must be verified whether the thermodynamic constrains are satisfied at

Table 3
The resonance frequencies and the homogenised complex modulus of SS1-VE1 sandwich structure and the shear complex modulus of the VE1 viscoelastic film.

SS1-VE1						
Sandwich					Core	
f (Hz)	Mode No.	L (mm)	E (GPa)	η	G_v (MPa)	η_v
21.27 ± 0.17	1	140	164.09 ± 2.59	0.0249 ± 0.0017	0.85 ± 0.12	0.2286 ± 0.0123
24.77 ± 0.15	1	130	165.58 ± 1.98	0.0196 ± 0.0013	1.08 ± 0.13	0.192 ± 0.0084
156.48 ± 1.19	2	130	168.2 ± 2.56	0.0238 ± 0.0037	8.23 ± 1.35	0.2681 ± 0.0071
378.68 ± 2.14	3	140	168.98 ± 1.91	0.0262 ± 0.0008	20.32 ± 2.4	0.3117 ± 0.0264
438.88 ± 1.18	3	130	168.75 ± 0.91	0.0229 ± 0.0019	23.53 ± 1.06	0.268 ± 0.0374
740.7 ± 2.84	4	140	168.36 ± 1.29	0.0274 ± 0.0028	38.01 ± 2.91	0.3141 ± 0.0399
858.72 ± 2.41	4	130	168.23 ± 0.94	0.0261 ± 0.0004	44.02 ± 2.31	0.2961 ± 0.0208

Table 4
The resonance frequencies and the homogenised complex modulus of AL-VE1 sandwich structure and the shear complex modulus of the VE1 viscoelastic film.

AL-VE1						
Sandwich					Core	
f (Hz)	Mode No.	L (mm)	E (GPa)	η	G_v (MPa)	η_v
30.89 ± 0.24	1	160	65.57 ± 1.03	0.0104 ± 0.0027	0.99 ± 0.34	0.3143 ± 0.0465
35.37 ± 0.12	1	150	66.39 ± 0.45	0.0086 ± 0.0023	1.58 ± 0.4	0.386 ± 0.0918
40.51 ± 0.10	1	140	66.07 ± 0.32	0.0093 ± 0.0014	1.47 ± 0.16	0.3536 ± 0.1211
194.76 ± 0.96	2	160	66.35 ± 0.65	0.0087 ± 0.0011	9.15 ± 2.78	0.3967 ± 0.0949
222.52 ± 0.46	2	150	66.90 ± 0.28	0.0091 ± 0.0020	12.89 ± 2.39	0.6109 ± 0.1736
254.62 ± 0.51	2	140	66.47 ± 0.27	0.0103 ± 0.0033	11.01 ± 0.75	0.5054 ± 0.2582
544.22 ± 4.91	3	160	66.08 ± 1.19	0.0109 ± 0.0049	24.39 ± 11.15	0.4276 ± 0.0678
622.19 ± 2.62	3	150	66.72 ± 0.56	0.0101 ± 0.0042	33.99 ± 11.87	0.583 ± 0.1694
713.22 ± 1.68	3	140	66.52 ± 0.31	0.0096 ± 0.0023	32.52 ± 1.85	0.4922 ± 0.2373

Table 5
The resonance frequencies and the homogenised complex modulus of SS2-VE2 sandwich structure and the shear complex modulus of the VE2 viscoelastic film.

SS2-VE2						
Sandwich					Core	
f (Hz)	Mode No.	L (mm)	E (GPa)	η	G_v (MPa)	η_v
8.89 ± 0.07	1	210	194.71 ± 3.22	0.0175 ± 0.0029	0.9 ± 0.26	0.3437 ± 0.0439
10.83 ± 0.01	1	190	193.73 ± 0.38	0.0207 ± 0.0009	0.95 ± 0.04	0.3671 ± 0.0049
13.53 ± 0.02	1	170	193.88 ± 0.67	0.0197 ± 0.0008	1.22 ± 0.07	0.3536 ± 0.0061
55.73 ± 0.38	2	210	194.96 ± 2.64	0.0253 ± 0.0012	5.33 ± 0.98	0.5168 ± 0.1045
67.93 ± 0.07	2	190	194.1 ± 0.4	0.0244 ± 0.0031	6.18 ± 0.41	0.4474 ± 0.0437
84.52 ± 0.02	2	170	192.6 ± 0.07	0.0281 ± 0.0004	6.71 ± 0.06	0.4595 ± 0.0037
236.84 ± 0.39	3	170	192.89 ± 0.64	0.0405 ± 0	16.1 ± 0.37	0.6897 ± 0.0352
304.83 ± 1.35	4	210	193.75 ± 1.72	0.0438 ± 0.0022	20.2 ± 1.67	0.8092 ± 0.0774
371.93 ± 0.22	4	190	193.28 ± 0.22	0.0517 ± 0.0027	21.23 ± 0.95	0.9273 ± 0.0719
462.08 ± 0.6	4	170	191.2 ± 0.49	0.0531 ± 0.0011	24.96 ± 0.69	0.8108 ± 0.0096
499.54 ± 2.07	5	210	190.42 ± 1.58	0.0492 ± 0.0028	27.96 ± 2.35	0.709 ± 0.0317
612.06 ± 0.78	5	190	191.55 ± 0.49	0.0642 ± 0.004	27.99 ± 1.7	1.0325 ± 0.1122
747.84 ± 1.81	6	210	191.24 ± 0.93	0.0628 ± 0.0038	35.03 ± 2.33	0.9813 ± 0.0001
762.07 ± 2.69	5	170	190.31 ± 1.34	0.0699 ± 0.0037	31.71 ± 1.49	1.0475 ± 0.1617
911.16 ± 4.42	6	190	190.23 ± 1.85	0.0721 ± 0.0005	36.74 ± 0.49	1.08 ± 0.1298

Table 6
The resonance frequencies and the homogenised complex modulus of GS-VE2 sandwich structure and the shear complex modulus of the VE2 viscoelastic film.

GS-VE2						
Sandwich					Core	
f (Hz)	Mode No.	L (mm)	E (GPa)	η	G_v (MPa)	η_v
21.2 ± 0.16	1	210	170.01 ± 2.49	0.0302 ± 0.0030	1.86 ± 0.35	0.7610 ± 0.17608
25.72 ± 0.25	1	190	167.60 ± 3.32	0.0333 ± 0.0010	1.84 ± 0.25	0.6806 ± 0.29797
32.31 ± 0.22	1	170	169.51 ± 2.29	0.0321 ± 0.0033	2.67 ± 0.47	0.7627 ± 0.17003
201.61 ± 0.12	2	170	168.08 ± 0.19	0.0390 ± 0.0010	14.36 ± 0.17	0.7645 ± 0.03579
452.68 ± 1.98	3	190	168.65 ± 1.48	0.0556 ± 0.0030	23.13 ± 1.15	1.2214 ± 0.13192
563.76 ± 1.24	3	170	167.64 ± 0.73	0.0614 ± 0.0049	26.15 ± 2.37	1.2086 ± 0.02841
727.12 ± 1.01	4	210	169.09 ± 0.47	0.0651 ± 0.0053	29.88 ± 2.87	1.5417 ± 0.06602
878.86 ± 4.79	4	190	165.54 ± 1.80	0.0683 ± 0.0059	36.55 ± 3.41	1.1253 ± 0.06826

Table 7
Identified parameters of the four-parameter fractional derivative model for VE1 and VE2 films.

	G_0 (Pa)	G_∞ (Pa)	τ (s)	α
VE1	$3.24{\cdot}10^6$	$5.64{\cdot}10^8$	$1.031{\cdot}10^{-7}$	0.390
VE2	$3.17{\cdot}10^6$	$1.15{\cdot}10^9$	$7.869{\cdot}10^{-7}$	0.587

the end of the minimisation procedure, which are the following: $G_\infty > G_0 > 0$, $\tau > 0$ and $\alpha > 0$.

The material parameters identified for both viscoelastic films, VE1 and VE2, are shown in Table 7. The static shear modulus of VE1 is bigger than VE2's, whereas the opposite happens with the asymptotic shear modulus. The relaxation time of VE1 is smaller than that of VE2, which means the loss factor maximum occurs for the former one at a higher frequency. Regarding the fractional parameter, α, the VE2's is bigger, which means the material presents more viscoelastic behaviour, and the slope of its dynamic modulus curve in the frequency domain at the inflexion point is bigger. Note that, if $\alpha = 0$, the material is purely elastic, and if $\alpha = 1$, the fractional derivative model, Eq. (9), yields to the original Zener model.

Figs. 4 and 5 show the experimental shear complex modulus with the fitted material models. Regarding VE1 film, the shear modulus is overestimated at low frequencies and is underestimated at high frequencies, whereas the loss factor is a bit overestimated in all of the bandwidth. Concerning VE2 film, the shear modulus is accurate in all of the bandwidth, and the loss factor is a bit overestimated in the mid-range frequencies.

3.2. Finite element model

In the literature, different finite element approaches to modelling sandwich structures are available, such as three-dimensional brick elements or multi-layer beam, plate and shell elements. Recently, Caliri et al. [27] presented an extensive review of plate and shell theories for laminated and sandwich structures solved by the Finite Element Method (FEM).

In this work, a three-layer sandwich beam finite element is considered, and the following assumptions based on the Mead and Markus theory [28] are taken into account:

1. The metallic skin layers bend according to Euler-Bernoulli beam theory.
2. The viscoelastic core is subjected only to shear deformation.
3. All layers are assumed to be incompressible through the thickness, so the transverse displacement is uniform on a cross section.
4. All layers are assumed to be perfectly bonded, so there is no slippage and delamination between the layers during deformation.

The finite element is defined by two nodes with four degrees of freedom (DOF) per node. The DOF include the axial displacements of the top and bottom skin layers, u_1 and u_3, the transverse displacement, w, and the rotational displacement of the beam, $\partial w/\partial x$. Linear shape functions are used for the axial displacement of the top and bottom skins, and the Hermite cubic shape function for the transverse displacement. In this way, the shear locking phenomenon is avoided, which consists of an excessive element stiffness as the element becomes long and thin [29]. The formulation of the finite element is shown in Appendix A.

3.3. Theoretical dynamic response

The numerical transmissibility function is obtained by the direct frequency method. The governing equation of motion of a cantilever beam in the frequency domain is written as

$$\mathbf{M}\ddot{\mathbf{q}} + \mathbf{K}^*\mathbf{q} = \mathbf{F}, \tag{12}$$

where $\mathbf{q}$ and $\ddot{\mathbf{q}}$ are the displacement vector and the acceleration vector, and where $\mathbf{M}$, $\mathbf{K}^*$ and $\mathbf{F}$ are the global mass matrix, the global stiffness matrix and the global force vector, obtained by assembling the corresponding matrices for all of the elements. If a steady-state harmonic base excitation is considered, and the motion equation is written differentiating the DOF related to the base displacement vector, indicated by $(\bullet_s)$, and the unknown displacement vector, indicated by $(\bullet_u)$, the following is obtained

$$\left(-(2\pi f)^2\begin{bmatrix}\mathbf{M}_{ss} & \mathbf{M}_{su}\\ \mathbf{M}_{us} & \mathbf{M}_{uu}\end{bmatrix} + \begin{bmatrix}\mathbf{K}^*_{ss} & \mathbf{K}^*_{su}\\ \mathbf{K}^*_{us} & \mathbf{K}^*_{uu}\end{bmatrix}\right)\begin{Bmatrix}\mathbf{S}^*\\ \mathbf{U}^*\end{Bmatrix} = \begin{Bmatrix}\mathbf{R}^*\\ 0\end{Bmatrix}, \tag{13}$$

where $\mathbf{S}^*$, $\mathbf{U}^*$ and $\mathbf{R}^*$ are the amplitude vector of the applied base motion, unknown displacements and reaction forces on the base, respectively. Note that $\mathbf{K}^*$ depends on frequency due to the viscoelastic core, so $\mathbf{U}^*$ and $\mathbf{R}^*$ depend on frequency, too.

The unknown displacement amplitude vector, $\mathbf{U}^*$, is obtained from

$$\mathbf{U}^* = \frac{\left((2\pi f)^2\mathbf{M}_{us} - \mathbf{K}^*_{us}\right)\mathbf{S}^*}{-(2\pi f)^2\mathbf{M}_{uu} + \mathbf{K}^*_{uu}}, \tag{14}$$

and the transmissibility function is determined by dividing the transverse displacement of the response DOF U_j^* by the transverse displacement applied at the base DOF S_i^*, as

$$T^*_{ij}(f) = \frac{U^*_j(f)}{S^*_i(f)}. \tag{15}$$

The dynamic properties, storage modulus and loss factor, of the sandwich structure are then obtained in the same way as from experimental transmissibility functions.

3.4. Model validation

The numerical transmissibility functions obtained by FEM are compared with the experimental ones measured in the forced vibration tests to validate the constitutive viscoelastic model, the sandwich beam element and the numerical modelling of the cantilever beam by FEM.

In numerical modelling, the sandwich beam is discretised by 2.5 mm long elements, and the direct transmissibility function is obtained with a 0.05 Hz resolution in the bandwidth of 0–250 Hz and with a 0.1 Hz resolution in the bandwidth of 250–1000 Hz.

Figs. 6 and 7 show the experimental and numerical transmissibility functions of the sandwiches composed of VE1, and Figs. 8 and 9 show the transmissibility functions of the ones composed of VE2. It is observed that the correlation in the frequency and modulus is acceptable for sandwiches composed of both viscoelastic films, with the biggest deviations in the first vibration mode of the

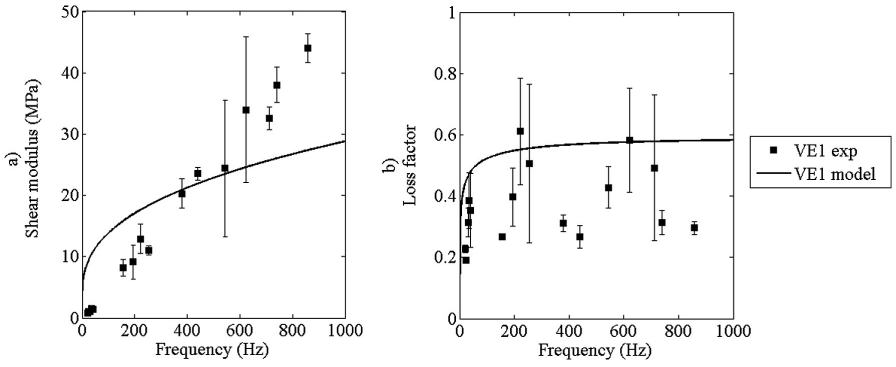

Fig. 4. The fitted shear complex modulus, a) shear modulus and b) loss factor, and the experimental results of VE1 viscoelastic film obtained from SS1-VE1 and AL-VE1 sandwich beams.

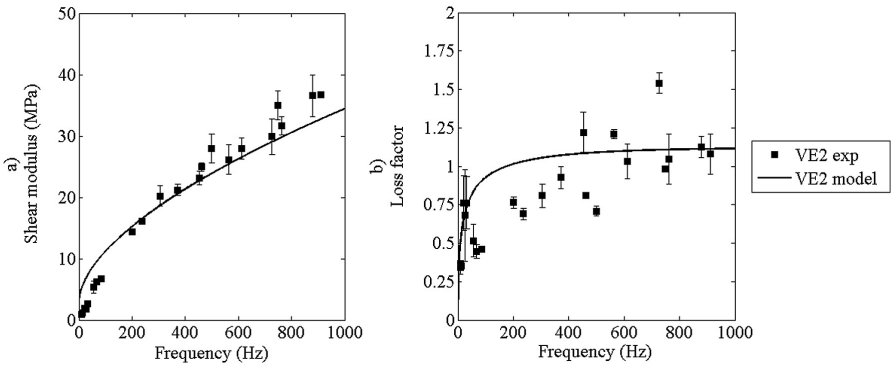

Fig. 5. The fitted shear complex modulus, a) shear modulus and b) loss factor, and the experimental results of VE2 viscoelastic film obtained from SS2-VE2 and GS-VE2 sandwich beams.

sandwiches composed of VE1 film. The deviations in the first vibration mode are, on the one hand, due to a lack of enough resolution to properly measure this mode, and in the other hand, due to the overestimation of the shear modulus at low frequencies, Figs. 4 and 5.

4. Design parameters

In this section, the influence of different design parameters on the dynamic properties, storage modulus, E, and loss factor, η, of thin sandwich structures is studied. The analysed parameters are the nature and thickness of viscoelastic films and metallic skins. This analysis is based on numerical results obtained by FEM with the previously defined four parameters fractional derivative models for VE1 and VE2, with the exception of Fig. 17 in which the experimental results shown in Tables 5 and 6 are plotted.

4.1. Viscoelastic film

Two viscoelastic films, VE1 and VE2, are analysed and their analytical shear dynamic models defined in Section 3.1 are compared in Fig. 10. The shear modulus of both viscoelastic films increases with frequency, the VE1 one being higher at low frequencies and the VE2 one at high frequencies. Concerning the loss factor, that for VE2 is bigger than the VE1 one over the whole frequency bandwidth.

Fig. 11 shows the influence of using VE1 or VE2 as the core of the sandwich structure on its dynamic properties. The storage modulus of sandwiches composed of both films decreases with the frequency this tendency being stronger in the sandwich composed of VE1. In addition, the storage modulus of the sandwich composed of VE2 is bigger than the one composed of VE1. Regarding the loss factor, it increases with the frequency, and VE2's loss factor is bigger than the VE1 ones, being this difference constant in frequencies higher than 20 Hz. This tendency matches the behaviour of both films' loss factor. In analysing Figs. 10 and 11, it is concluded that the differences between the shear dynamic properties of both films become smaller in the homogenised dynamic properties of the sandwiches composed of the films. For example, a difference of 17% in the shear modulus of both films at high frequencies turns into a difference of 7% in the storage modulus of the sandwiches, and a difference of 50% in the loss factor of both films results in a difference of 4% in the loss factor of the sandwiches.

Next, the influence of the viscoelastic film thickness on the dynamic properties of the sandwich is analysed. Figs. 12 and 13 show the influence of the VE1 and VE2 films' thicknesses on the storage modulus and loss factor of the sandwich. Regardless of the viscoelastic film of which the sandwich is composed, the

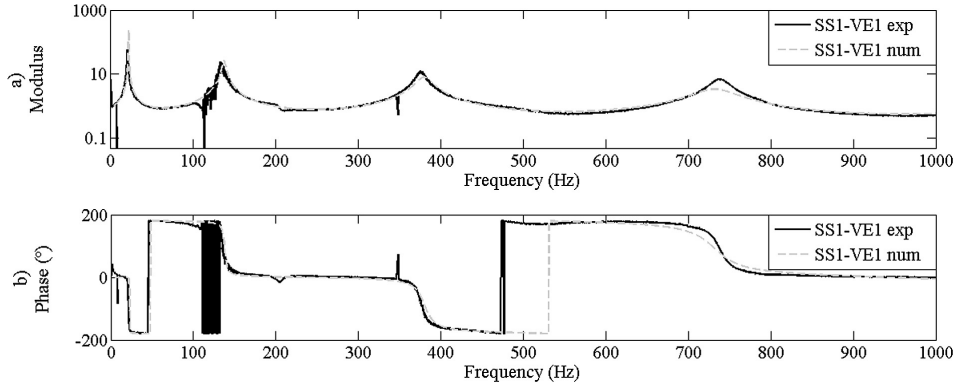

Fig. 6. Experimental and numerical transmissibility functions, a) modulus and b) phase, of SS1-VE1 sandwich beam with 140 mm of free length.

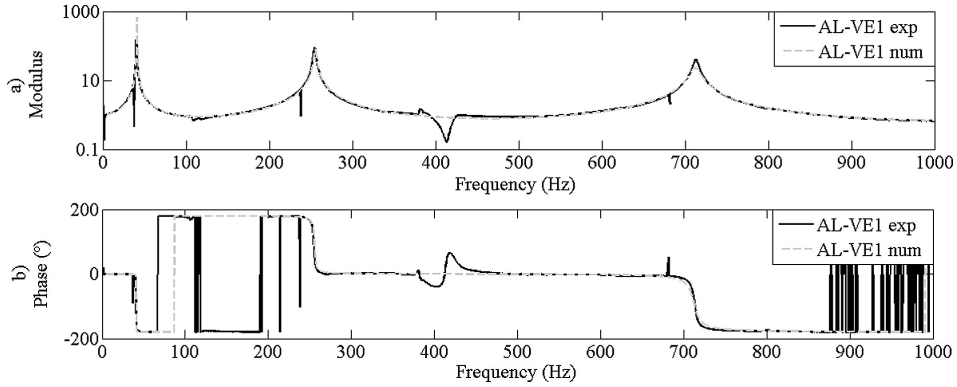

Fig. 7. Experimental and numerical transmissibility functions, a) modulus and b) phase, of AL-VE1 sandwich beam with 140 mm of free length.

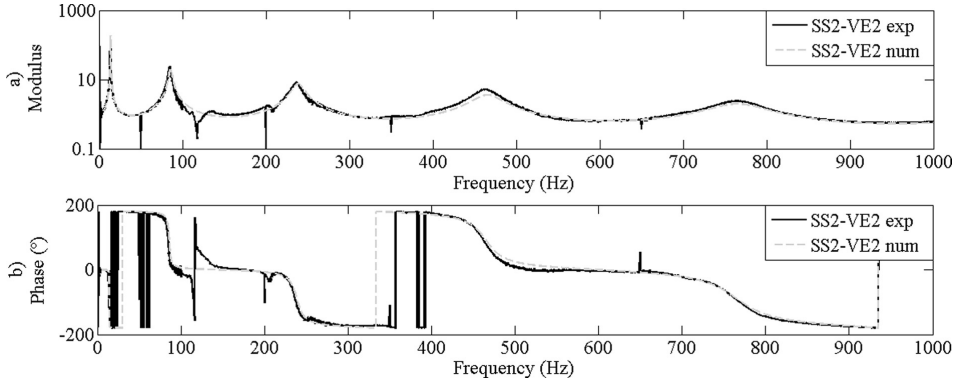

Fig. 8. Experimental and numerical transmissibility functions, a) modulus and b) phase, of SS2-VE2 sandwich beam with 170 mm of free length.

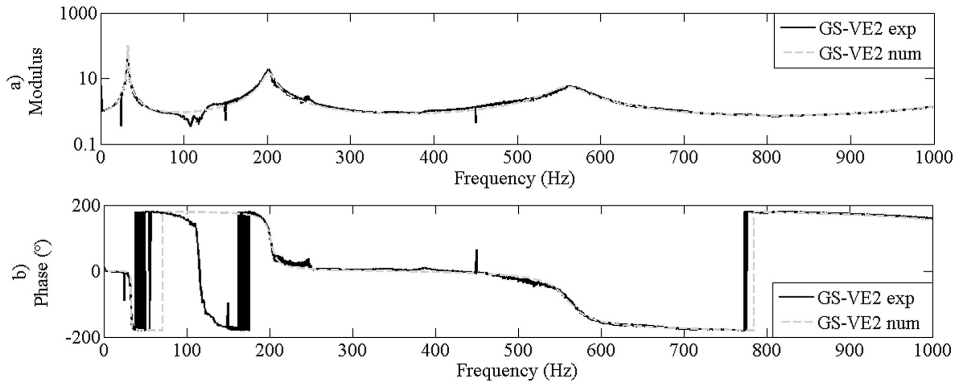

Fig. 9. Experimental and numerical transmissibility functions, a) modulus and b) phase, of GS-VE2 sandwich beam with 170 mm of free length.

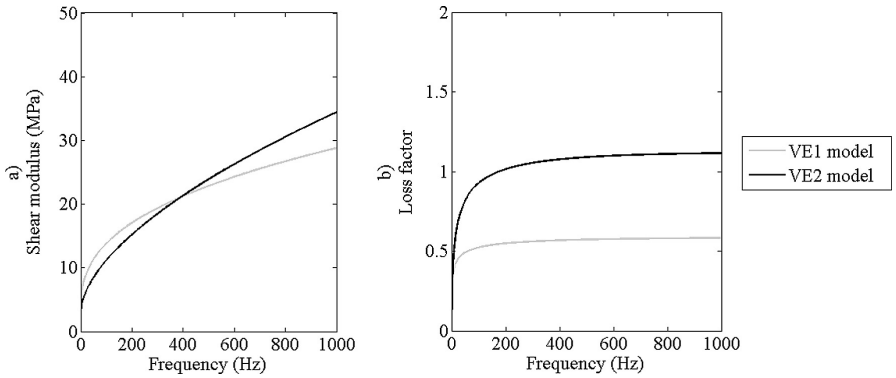

Fig. 10. Shear complex modulus models, a) shear modulus and b) loss factor, of VE1 and VE2 viscoelastic films.

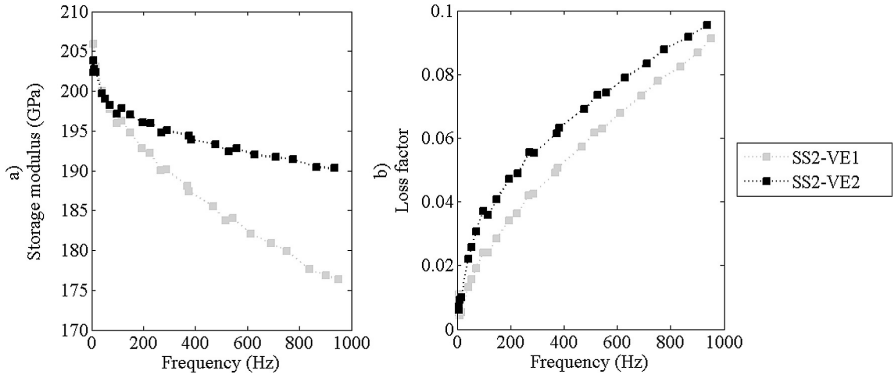

Fig. 11. Influence of the viscoelastic film on the homogenised complex modulus, a) storage modulus and b) loss factor, of sandwich structures in the frequency domain. The composition of the sandwiches is the following: 0.25 mm of SS2 skins, and 40 μm of VE1 or VE2.

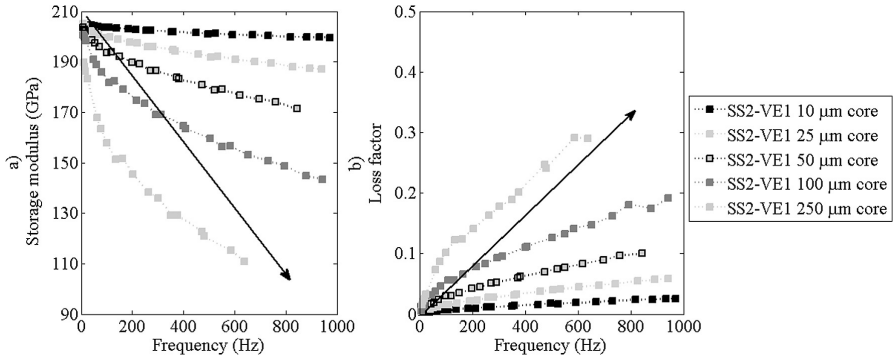

Fig. 12. Influence of the VE1 film thickness on the homogenised complex modulus, a) storage modulus and b) loss factor, of sandwich structures in the frequency domain. The composition of the sandwiches is the following: 0.25 mm of SS1 skins, and 5 μm, 25 μm, 50 μm, 100 μm or 250 μm of VE1.

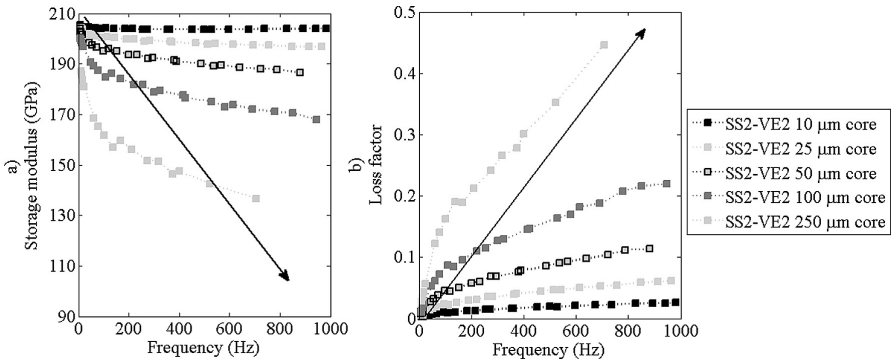

Fig. 13. Influence of the VE2 film thickness on the homogenised complex modulus, a) storage modulus and b) loss factor, of sandwich structures in the frequency domain. The composition of the sandwiches is the following: 0.25 mm of SS1 skins, and 5 μm, 25 μm, 50 μm, 100 μm or 250 μm of VE2.

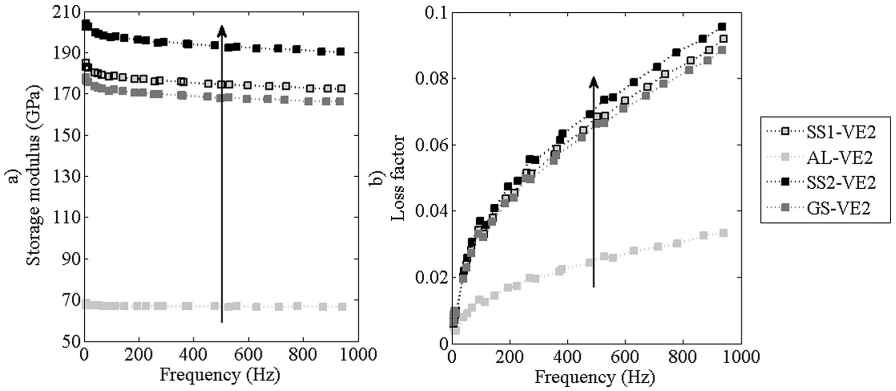

Fig. 14. Influence of the type of metallic skin on the homogenised complex modulus, a) storage modulus and b) loss factor, of sandwich structures in the frequency domain. The composition of the sandwiches is the following: 0.25 mm of SS1, AL, SS2 or GS skins and 40 μm of VE2.

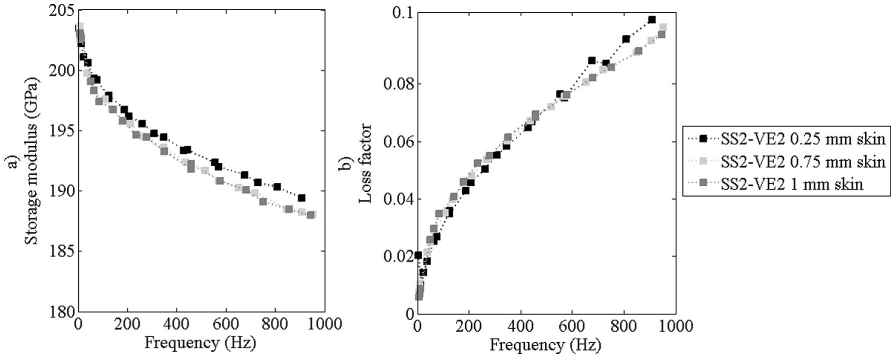

Fig. 15. Influence of the SS2 skin thickness on the homogenised complex modulus, a) storage modulus and b) loss factor, of sandwich structures in the frequency domain. The composition of the sandwiches is the following: 0.25 mm, 0.75 mm or 1 mm of SS2 skins, and 40 μm of VE2.

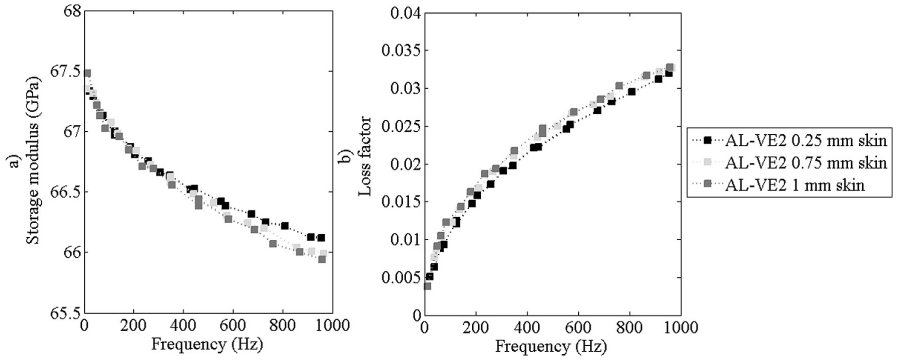

Fig. 16. Influence of the AL skin thickness on the homogenised complex modulus, a) storage modulus and b) loss factor, of sandwich structures in the frequency domain. The composition of the sandwiches is the following: 0.25 mm, 0.75 mm or 1 mm of AL skins, and 40 μm of VE2.

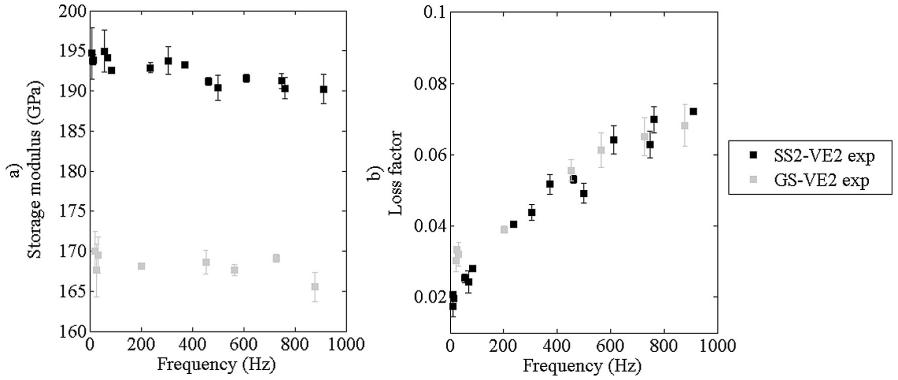

Fig. 17. Influence of the type and thickness of the metallic skin on the complex modulus, a) storage modulus and b) loss factor, of sandwich structures in the frequency domain. The composition of the sandwiches is: 0.216 mm of SS2 and 41 μm of VE2, 0.589 mm of GS and 40 μm of VE2.

storage modulus of the sandwich decreases and the loss factor increases with increasing the core thickness. In addition, both properties become more frequency dependent. Specifically, the storage modulus tends to decrease in frequency and the loss factor to increase. Depending on the nature of the viscoelastic film, its thickness can have a greater or lesser influence on the dynamic properties of the sandwich.

These results emphasise the advantages of using micron-sized viscoelastic adhesive films to form thin sandwich structures. For example, if a 0.5 mm thick SS2 beam is replaced by a sandwich beam composed of two SS2 skins with half thickness of the original beam, 0.25 mm, and 40 μm of VE2, the mass of the beam is increased just 1.14% per m^2. Regarding the dynamic properties, the damping of the beam is increased substantially, by 4000%, at an expense of a small decrement of the storage modulus, 7%.

4.2. Metallic skin

The sandwich structures characterised in this work are composed of different metallic materials, such as stainless steel, galvanised steel and aluminium. Following, the effect of the type of metallic skin and its thickness on the dynamic properties of thin viscoelastic sandwich structures is analysed. In Fig. 14, the influence of forming the sandwich structure with SS1, SS2, GS of AL metallic skins on its homogenised complex modulus is shown. As expected, the bigger the storage modulus of the metallic material, the bigger the storage modulus of the sandwich. In addition, the storage modulus of the metallic skin influences the loss factor of the sandwich. Specifically, the bigger the storage modulus of the metallic skin, the bigger the loss factor of the sandwich. This means that sandwiches composed of rigid skins dissipate more energy. The metallic skin material has no influence on the frequency dependence of the sandwich structure's dynamic properties because it is the viscoelastic core which exerts a major influence on the frequency.

Figs. 15 and 16 show the influence of the SS2 and AL skin thicknesses on the dynamic properties of sandwich structures. Regardless of the metallic material of which the sandwich is composed, the skin thickness does not have a remarkable influence on the dynamic properties of thin sandwich structures.

Finally, in Fig. 17, the experimental dynamic properties of the sandwich structures composed of the same viscoelastic films but different metallic skins are shown. In these experimental results, the combination of the numerical results shown in Figs. 15–17 can be seen. It is observed that the storage modulus of SS2-VE2 is bigger than that of GS-VE2, whereas the loss factor of both

sandwiches are identical over the whole bandwidth. The storage modulus of stainless steel SS2 is bigger than the galvanised steel GS ones; thus, a sandwich with a higher storage modulus and loss factor is expected. The thickness of metallic skin has no influence on the storage modulus and loss factor of the sandwich, nevertheless the bending stiffness of the GS-VE2 sandwich will be bigger than the SS2-VE2 due to its greater thickness.

5. Conclusions

In this work, four sandwich structures composed of different types and thicknesses of viscoelastic film and metallic skins are characterised in the bandwidth of 0–1 kHz. Then the numerical modelling of thin viscoelastic sandwich structures is presented and correlated with experimental results in all of the bandwidth. A four-parameter fractional derivative model is used to describe the dynamic behaviour of the viscoelastic films and a three-layer beam element for modelling the sandwich structures.

The influence of the design variables, the type and thickness of the viscoelastic film and the metallic skins, on the dynamic properties of thin sandwich structures is analysed. The nature of the viscoelastic adhesive film influences the overall behaviour of the sandwich structure even though its thickness is micrometric. Viscoelastic films with high shear modulus and loss factor are preferred to obtain sandwiches with high stiffness and damping. In increasing the core thickness, the loss factor is increased, and the storage modulus is decreased, with both properties becoming more frequency dependent. Regarding metallic skins, these must have a high storage modulus to obtain a stiffer sandwich with greater damping capabilities.

Acknowledgments

The present study has been partially supported by AVISANI (DPI2015-71198-R, Spanish Government) and AVISANI (PI_2016_1_0026, Basque Government) projects and Replasa S.A.

Appendix A. Finite element model

In Fig. A1 the assumed displacement field of the three-layer sandwich beam is shown. Note that $(\bullet_1)(\cdot)_1$, $(\bullet_2)(\cdot)_2$ and $(\bullet_3)(\cdot)_3$ refer to the top layer, core, and bottom layer, respectively.

The total angular rotation of the core is

$$\psi_2 = -\gamma_2 - \frac{\partial w}{\partial x} \tag{A.1}$$

and the shear strain in the core, γ_2, can be derived from [30]

$$\gamma_2 = \left(1 + \frac{H_{e1} + H_{e3}}{2H_{v2}}\right)\frac{\partial w}{\partial x} + \frac{u_1 - u_3}{H_{v2}}. \tag{A.2}$$

The sandwich beam element is defined by two nodes with four degrees of freedom (DOF) per node. The DOF include the axial displacements of the top and bottom skin layers, u_1 and u_3, the transverse displacement, w, and the rotational displacement of the beam, $\partial w/\partial x$. The generalised displacements, $\mathbf{u} = \{u_1 \quad u_3 \quad w\}^T$, are discretised with the Lagrange linear shape function, $\mathbf{N}_{u1}$ and $\mathbf{N}_{u3}$, for the displacements of the top and bottom skin layer, u_1 and u_3, and the Hermite cubic shape function, $\mathbf{N}_w$, for the transverse displacement, w. In this way, the shear locking phenomenon is avoided, which consists of an excessive element stiffness as the element becomes long and thin [29]. Thus, the relation between the generalised displacements and the elementary degrees of freedom is given by

$$\begin{Bmatrix} u_1 \\ u_3 \\ w \end{Bmatrix} = \begin{bmatrix} \mathbf{N}_{u1} \\ \mathbf{N}_{u3} \\ \mathbf{N}_w \end{bmatrix} \begin{Bmatrix} u_{1_1} \\ u_{3_1} \\ w_1 \\ \frac{\partial w_1}{\partial x} \\ u_{1_2} \\ u_{3_2} \\ w_2 \\ \frac{\partial w_2}{\partial x} \end{Bmatrix}. \tag{A.3}$$

The stiffness matrix for the sandwich element is obtained from the strain energy of the finite element and the mass matrix from the kinetic energy.

The total strain energy includes the bending and extension of the skin layers and the shear deformation of the core, given by

$$U = \int_0^l \tfrac{1}{2}(E_{e1}I_{e1} + E_{e3}I_{e3})\left(\tfrac{\partial^2 w}{\partial x^2}\right)^2 dx + \int_0^l \tfrac{1}{2}\left(E_{e1}A_{e1}\left(\tfrac{\partial u_1}{\partial x}\right)^2 + E_{e3}A_{e3}\left(\tfrac{\partial u_3}{\partial x}\right)^2\right)dx + \int_0^l \tfrac{1}{2}G^*_{v2}A_{v2}\gamma_2^2 dx, \tag{A.4}$$

where I_1 and I_3 are the second moment of inertia at the centroid of the skin layers, and A_1 and A_3 are the cross-sectional area of the skin layers.

The strain energy equation can be rewritten in nodal displacement variables for one element as follows

$$U^e = \frac{1}{2}\mathbf{q}^{e^T}\mathbf{k}^{e^*}\mathbf{q}^e, \tag{A.5}$$

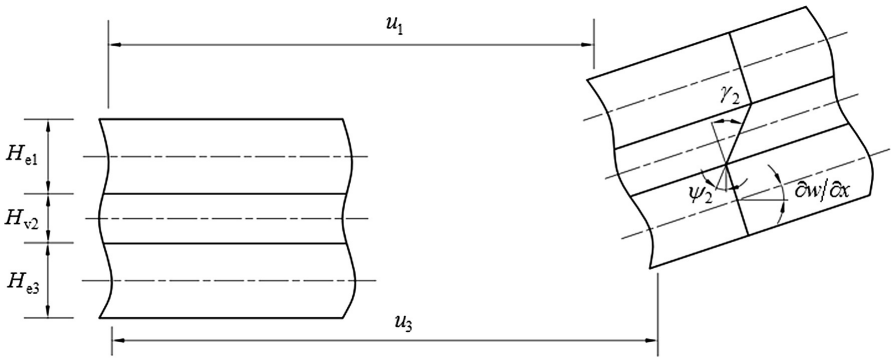

Fig. A1. Displacement field of the sandwich beam.

where the element stiffness matrix, $\mathbf{k}^{e^*}$, is given by

$$\begin{aligned}\mathbf{k}^{e^*} &= \int_0^{l_e}(E_{e1}I_{e1}+E_{e3}I_{e3})\frac{\partial^2\mathbf{N}_w^T}{\partial x^2}\frac{\partial^2\mathbf{N}_w}{\partial x^2}dx\\ &+\int_0^{l_e}\left(E_{e1}A_{e1}\frac{\partial\mathbf{N}_{u1}^T}{\partial x}\frac{\partial\mathbf{N}_{u1}}{\partial x}+E_{e3}A_{e3}\frac{\partial\mathbf{N}_{u3}^T}{\partial x}\frac{\partial\mathbf{N}_{u3}}{\partial x}\right)dx\\ &+\int_0^{l_e}G_{v2}^*A_{v2}\left(\left(1+\frac{H_{e1}+H_{e3}}{2H_{v2}}\right)\frac{\partial\mathbf{N}_w}{\partial x}+\frac{\mathbf{N}_{u1}-\mathbf{N}_{u3}}{H_{v2}}\right)^T\cdot\\ &\left(\left(1+\frac{H_{e1}+H_{e3}}{2H_{v2}}\right)\frac{\partial\mathbf{N}_w}{\partial x}+\frac{\mathbf{N}_{u1}-\mathbf{N}_{u3}}{H_{v2}}\right)dx\end{aligned} \tag{A.6}$$

The total kinetic energy includes the transverse displacement of all layers, the axial displacement of skin layers and the rotation of the core, given by

$$\begin{aligned}T=&\int_0^l\tfrac{1}{2}\rho A\left(\tfrac{\partial w}{\partial t}\right)^2dx+\int_0^l\tfrac{1}{2}\left(\rho_{e1}A_{e1}\left(\tfrac{\partial u_1}{\partial t}\right)^2+\rho_{e3}A_{e3}\left(\tfrac{\partial u_3}{\partial t}\right)^2\right)dx\\ &+\int_0^l\tfrac{1}{2}\rho_{v2}I_{v2}\left(\tfrac{\partial\psi_2}{\partial t}\right)^2dx\end{aligned} \tag{A.7}$$

As with the strain energy, the total kinetic energy equation can be rewritten in nodal displacement variables for one element as follows

$$T^e=\frac{1}{2}\dot{\mathbf{q}}^{eT}\mathbf{m}^e\dot{\mathbf{q}}^e, \tag{A.8}$$

where the element mass matrix, $\mathbf{m}^e$, is the following

$$\begin{aligned}\mathbf{m}^e=&\int_0^{l_e}\rho A\mathbf{N}_w^T\mathbf{N}_w dx+\int_0^{l_e}\left(\rho_{e1}A_{e1}\mathbf{N}_{u1}^T\mathbf{N}_{u1}+\rho_{e3}A_{e3}\mathbf{N}_{u3}^T\mathbf{N}_{u3}\right)dx\\ &+\int_0^{l_e}\rho_{v2}I_{v2}\left(-\left(\left(1+\frac{H_{e1}+H_{e3}}{2H_{v2}}\right)\frac{\partial\mathbf{N}_w}{\partial x}+\frac{\mathbf{N}_{u1}-\mathbf{N}_{u3}}{H_{v2}}\right)-\frac{\partial\mathbf{N}_w}{\partial x}\right)^T\cdot\\ &\left(-\left(\left(1+\frac{H_{e1}+H_{e3}}{2H_{v2}}\right)\frac{\partial\mathbf{N}_w}{\partial x}+\frac{\mathbf{N}_{u1}-\mathbf{N}_{u3}}{H_{v2}}\right)-\frac{\partial\mathbf{N}_w}{\partial x}\right)dx\end{aligned} \tag{A.9}$$

References

[1] Rao MD. Recent applications of viscoelastic damping for noise control in automobiles and commercial airplanes. J Sound Vib 2003;262:457–74. http://dx.doi.org/10.1016/S0022-460X(03)00106-8.

[2] Kerwin EM. Damping of flexural waves by a constrained viscoelastic layer. J Acoust Society Am 1959;31:952–62.

[3] Ross D, Ungar EE, Kerwin EMJ. Damping of plate flexural vibrations by means of viscoelastic laminae. Struct Damp 1959:49–87.

[4] Teng T, Hu N. Analysis of damping characteristics for viscoelastic laminated beams. Comput Methods Appl Mech Eng 2001;190:3881–92.

[5] Leibowitz M, Lisfshitz JM. Experimental verification of modal parameters for 3-layered sandwich beam. Int J Solids Struct 1990;26:175–84.

[6] Lisfshitz JM, Leibowitz M. Optimal sandwich beam design for maximum viscoelastic damping. Int J Solids Struct 1987;23:1027–34.

[7] Araújo AL, Soares CMM, Soares CAM, Herskovits J. Optimal design and parameter estimation of frequency dependent viscoelastic laminated sandwich composite plates. Compos Struct 2010;92:2321–7. http://dx.doi.org/10.1016/j.compstruct.2009.07.006.

[8] Hamdaoui M, Robin G, Jrad M, Daya EM. Optimal design of frequency dependent three-layered rectangular composite beams for low mass and high damping. Compos Struct 2015;120:174–82. http://dx.doi.org/10.1016/j.compstruct.2014.09.062.

[9] Madeira JFA, Araújo AL, Soares CMM, Soares CAM. Multiobjective optimization of viscoelastic laminated sandwich structures using the Direct MultiSearch method. Comput Struct 2015;147:229–35. http://dx.doi.org/10.1016/j.compstruc.2014.09.009.

[10] Madeira JFA, Araújo AL, Soares CMM, Soares CAM, Ferreira AJM. Multiobjective design of viscoelastic laminated composite sandwich panels. Compos Part B 2015;77:391–401. http://dx.doi.org/10.1016/j.compositesb.2015.03.025.

[11] Irazu L, Elejabarrieta MJ. The influence of viscoelastic film thickness on the dynamic characteristics of thin sandwich structures. Compos Struct 2015;134:421–8.

[12] Martinez-Agirre M, Elejabarrieta MJ. Characterisation and modelling of viscoelastically damped sandwich structures. Int J Mech Sci 2010;52:1225–33. http://dx.doi.org/10.1016/j.ijmecsci.2010.05.010.

[13] Martinez-Agirre M, Elejabarrieta MJ. Dynamic characterization of high damping viscoelastic materials from vibration test data. J Sound Vib 2011;330:3930–43. http://dx.doi.org/10.1016/j.jsv.2011.03.025.

[14] ASTM. ASTM E 756–05: Standard test method for measuring vibration-damping properties of materials 2005.

[15] Cortés F, Elejabarrieta MJ. Viscoelastic materials characterisation using the seismic response. Mater Des 2007;28:2054–62. http://dx.doi.org/10.1016/j.matdes.2006.05.032.

[16] Nashif AD, Jones DIG, Henderson JP. Vibration damping. New York: Wiley; 1985.

[17] Rao DK. Frequency and loss factors of sandwich beams under various boundary conditions. J Mech Eng Sci 1978;20:271–82.

[18] Jones DIG. Handbook of viscoelastic vibration damping. Chichester: John Wiley and Sons Ltd; 2001.

[19] Lakes RS, Wineman A. On Poisson's ratio in linearly viscoelastic solids. J Elast 2006;85:45–63. http://dx.doi.org/10.1007/s10659-006-9070-4.

[20] de Espíndola JJ, da Silva Neto JM, Lopes EMO. A generalised fractional derivative approach to viscoelastic material properties measurement. Appl Math Comput 2005;164:493–506. http://dx.doi.org/10.1016/j.amc.2004.06.099.

[21] Bagley RL, Torvik PJ, Bagley RL, Base WAF. On the fractional calculus model of viscoelastic behavior on the fractional calculus model of viscoelastic behavior. J Rheol (N Y N Y) 1986;133:133–55. http://dx.doi.org/10.1122/1.549887.

[22] Bagley RL, Torvik PJ. A theoretical basis for the application of fractional calculus to viscoelasticity. J Rheol (N Y N Y) 1983;27:201–10. http://dx.doi.org/10.1122/1.549724.

[23] Ouis D. Combination of a standard viscoelastic model and fractional derivate calculus to the characterization of polymers 2003:42–6. doi:10.1007/s10019-002-0223-1.

[24] Rouleau L, Pirk R, Pluymers B, Desmet W. Characterization and Modeling of the Viscoelastic Behavior of a Self-Adhesive Rubber Using Dynamic Mechanical Analysis Tests. J Aerosp Technol Manag 2015;7:200–8. http://dx.doi.org/10.5028/jatm.v7i2.474.

[25] Lu YC. Fractional derivative viscoelastic model for frequency-dependent complex moduli of automotive elastomers 2007:329–36. doi:10.1007/s10999-007-9039-x.

[26] Pritz T. Analysis of four-parameter fractional derivative model of real solid materials. J Sound Vib 1996;195:103–15.

[27] Jr MFC, Ferreira AJM, Tita V. A review on plate and shell theories for laminated and sandwich structures highlighting the finite element method. Compos Struct 2016;156:63–77. http://dx.doi.org/10.1016/j.compstruct.2016.02.036.

[28] Mead DJ. A comparison of some equations for the flexural vibration fo damped sandwich beams. J Sound Vib 1982;83:363–77.

[29] Zapfe JA, Lesieutre GA. A discrete layer beam finite element for the dynamic analysis of composite sandwich beams with integral damping layers. Comput Struct 1999;70:647–66. http://dx.doi.org/10.1016/S0045-7949(98)00212-0.

[30] Mead DJ, Markus S. The forced vibration of a three-layer, damped sandwich beam with arbitrary boundary conditions. J Sound Vib 1969;10:163–75. http://dx.doi.org/10.1016/0022-460X(69)90193-X.

The influence of viscoelastic film thickness on the dynamic characteristics of thin sandwich structures

Leire Irazu and María Jesús Elejabarrieta
Mechanical & Manufacturing Department, Mondragon Unibertsitatea, Loramendi 4, 20500 Arrasate-Mondragon, Spain

Composite Structures (2015) 134:421-428
DOI: 10.1016/j.compstruct.2015.07.086.

Impact factor - JCR: 3.853
Ranking - JCR: 2/25

Composite Structures 134 (2015) 421–428

Contents lists available at ScienceDirect

Composite Structures

journal homepage: www.elsevier.com/locate/compstruct

The influence of viscoelastic film thickness on the dynamic characteristics of thin sandwich structures

Leire Irazu, María Jesús Elejabarrieta *

Mech. & Manuf. Dept., Mondragon Unibertsitatea, 20500 Arrasate-Mondragon, Spain

ARTICLE INFO

Article history:
Available online 30 July 2015

Keywords:
Sandwich structure
Vibrations
Complex modulus
Characterisation
Numerical model

ABSTRACT

Passive damping techniques by means of viscoelastic materials are widely used for structural vibrations control. Sandwich structures composed of viscoelastic adhesive films and metallic constraining layers result in thin composite structures with improved dynamic capabilities. The nature and the small thickness of these sandwich structures enable them to be processed in conventional metal sheet transformation techniques to obtain components of complex geometries. In this work the influence of the viscoelastic film thickness on the dynamic properties, stiffness and damping, of thin sandwich structures is analysed from experimental and numerical results. Sandwich structures composed of same viscoelastic material but three different core thicknesses are tested and the dynamic properties of the viscoelastic film are obtained. From the experimental results a material model with fractional derivatives is proposed for the shear complex modulus of the viscoelastic adhesive film. The results show the viscoelastic film thickness has a greater influence in the loss factor than in the storage modulus, being this effect more pronounced at high frequencies. The bending stiffness of the sandwich structure is increased with core thickness even if the storage modulus is decreased. Therefore, the viscoelastic film thickness determines the vibrational response of thin sandwich structures.

© 2015 Elsevier Ltd. All rights reserved.

1. Introduction

The reduction of structural vibration amplitudes in mechanical systems has currently become a key objective in many industrial sectors in order to extend the life of components, reduce acoustic radiation or increase comfort and security. There are different techniques aimed at the control of structural vibration, classified into active, semiactive, adaptive and passive techniques [1]. Today, passive surface treatments by means of viscoelastic materials are the most common damping technique, because of their simplicity in implementation and lower cost. Viscoelastic materials can be used in three different configurations: free layer damping treatment (FLD), constrained layer damping treatment (CLD) and tuned viscoelastic damper (TVD). In the first two treatments, the energy dissipated depends on the superficial deformations and so they are effective in vibrations of plates and beam structures, while in the TVD treatment it depends on the local displacements. In the FLD treatment, the viscoelastic material is subjected to low tension/compression strains, whereas adding a constraining elastic layer, CLD treatment, the core undergoes high shear deformations that enables high energy losses [2,3]. Thus, the CLD treatment is more effective than FLD treatment for a given added weight.

Kervin [4] was one of the first to analyse the damping effectiveness of the CLD treatment or sandwich structure and since then, numerous studies have been carried out to understand and model the damping mechanism and characteristics of sandwich structures [5–12]. Besides, there are many studies that analyse the influence of the design parameters on the damping of sandwich structures, as well as, optimal design procedures to attain the maximum damping in the sandwich beams [13–20]. However, the influence of the design parameters on the stiffness of sandwich structures must be known too; since for a given application's design, equilibrium between damping and stiffness must be found to ensure proper operation. In addition, a gap concerning thin sandwich structures has been found.

The use of viscoelastic adhesive films and metallic constraining layers enables the production of thin sandwich structures. These sandwich structures provide higher damping than their metallic base layers for a low added weight and moreover they can be processed in conventional metal sheet transformation techniques to obtain pieces of complex geometries. The main aim of this paper is to analyse the influence of the viscoelastic film thickness on

* Corresponding author.
E-mail address: mjelejabarrieta@mondragon.edu (M.J. Elejabarrieta).

http://dx.doi.org/10.1016/j.compstruct.2015.07.086
0263-8223/© 2015 Elsevier Ltd. All rights reserved.

the dynamic properties, stiffness and damping, of thin sandwich structures.

Sandwich structures composed of same viscoelastic material and three core thicknesses are characterised by experimental dynamic tests according to the ASTM E 756-05 standard [21] with the modification proposed by Cortés and Elejabarrieta [22]. From these results the shear complex modulus of the viscoelastic film is determined and a material model based on the four parameter fractional derivative model with an empirical modification is proposed fitting it to the experimental data. The influence of the viscoelastic film and base layer thicknesses is analysed from the experimental results and numerical ones obtained from the proposed viscoelastic material model and RKU equations [23]. Lastly, this analysis allows proposing a methodology to design symmetric thin sandwich structures according to their final application's dynamic requirements.

2. Experimental characterisation

The frequency domain technique established by the ASTM E 756-05 standard [21] with the modification proposed by Cortés and Elejabarrieta [22] is applied to characterise the different sandwich structures and the viscoelastic film in a bandwidth from 0 to 1 kHz.

2.1. Specimens

The sandwich structures analysed in this work are provided by Replasa S.A. and they are manufactured in a continuous coating process called coil coating. All of them are symmetric and composed of two AISI 316 steel base layers and different thicknesses of a polyester-based adhesive core. The core thicknesses studied in this work are 40 μm, 80 μm and 100 μm in wet. In Fig. 1, the configuration of the analysed sandwich structures can be seen, where L is the free length, b is the width and H, H_e and H_v are the thickness of the sandwich, base layer and core. Note that $(\bullet)_e$ and $(\bullet)_v$ refer to the elastic and viscoelastic materials, respectively.

Three sandwich specimens from each core thickness are tested, each of them with free lengths of 140 mm, 150 mm and 160 mm. Tables 1 and 2 show the geometrical and physical properties of the analysed sandwich structures and their components; where $H_{v,dry}$ and $H_{v,wet}$, are the thickness of the core in dry and in wet, and ρ, ρ_e and $\rho_{v,dry}$ are the density of the sandwich, base layer and core ones in dry.

The nomenclature used is the following: the letter S refers to sandwich specimens and then the thickness of the core in wet is specified, 40 μm, 80 μm or 100 μm. The thickness of the viscoelastic core in wet is provided since it is the parameter controlled in the fabrication process of sandwich structures; nevertheless in the material properties extraction procedure, the geometrical and physical properties of the core once it is cured is used.

2.2. Experimental technique

The experimental characterisation is carried by a forced vibration test with resonance according to the ASTM E 756-05 standard [21] and the modification proposed by Cortés and Elejabarrieta [22].The dynamic properties of the sandwich structures and their

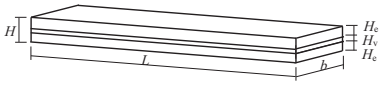

Fig. 1. Sandwich configuration.

Table 1
Geometrical and physical properties of the analysed sandwich structures.

	b (±0.002 mm)	H (±0.002 mm)	ρ (±0.05 g/cm^3)
S100	9.900	0.552	7.51
S80	9.900	0.521	7.70
S40	9.900	0.523	7.86

Table 2
Geometrical and physical properties of sandwich structure's components.

	H_e (±0.002 mm)	$H_{v,dry}$ (±2 μm)	$H_{v,wet}$* (μm)	ρ_e* (g/cm^3)	$\rho_{v,dry}$* (g/cm^3)
S100	0.258	36	100	7.95	1.13
S80	0.251	19	80	7.95	1.13
S40	0.258	7	40	7.95	1.13

* manufacturer's data, Replasa S.A..

cores are obtained in a two-step process. First, the sandwich beam is tested and the homogenised complex modulus, E^*, of the sandwich is obtained from the transmissibility function. Which assuming a linear viscoelastic behaviour is given by

$$E^*(f) = E(f) + iE'(f) = E(f)(1 + i\eta(f)), \quad (1)$$

where $E(f)$, $E'(f)$ and $\eta(f)$ are the storage modulus, the loss modulus and the loss factor of the sandwich structure, respectively [24]. After determining the homogenised complex modulus and the geometrical and physical properties of the sandwich components, the dynamic properties of the viscoelastic film can be identified [21]. Assuming the Poisson ratio is constant in frequency [25,26], the shear complex modulus, $G_v^*(f)$, of the viscoelastic film yields

$$G_v^*(f) = G_v(f) + iG_v'(f) = G_v(f)(1 + i\eta_v(f)), \quad (2)$$

where $G_v(f)$ is the shear modulus, $G_v'(f)$ is the loss modulus and $\eta_v(f)$ is the shear loss factor of the core.

In the extraction of the dynamic properties of the sandwich structure and core, the classical analysis based on the Euler–Bernoulli beam theory is used, so it must be ensured that the beam's cross section is much less than its length [21]. Moreover, the extensional terms for the core are not included since the storage modulus of the viscoelastic core is much lower than the base metal ones and the loss factor of the base metal is assumed to be zero. Furthermore, the results obtained from the first vibration mode are ignored as established by the ASTM E 756-05 standard [21,23].

Fig. 2 shows the experimental set-up used for measuring the transmissibility functions of the cantilever sandwich beams. The specimens are excited from the base by an electrodynamic shaker (Ling Dynamic Systems Vibrator, Model 406) and the base acceleration consists of a white noise in a bandwidth from 0 to 1 kHz generated by a vibration controller (LDS Dactron LASER Shaker Control System). The acceleration of the base, $\ddot{s}(t)$, is measured by a piezoelectric accelerometer (B&K, Type 4371) with a charge conditioning amplifier (B&K, Type 2635) and the velocity of the free end of the specimens, $\dot{u}(t)$, is measured by a laser vibrometer (Polytec OFV 505 LR100). Data acquisition and signal processing are performed with the OROS (OR763) analyser of four channels connected to a PC. The obtained transmissibility functions are the derivative of the velocity output of the beam's free end divided by the acceleration of the base.

In the experimental tests, first the transmissibility functions of each specimen in the bandwidth from 0 to 1 kHz are obtained and the resonant frequencies are identified. Then, the modal transmissibility functions are measured in order to obtain a better resolution. Finally, the analysed bandwidth is extended to 4 kHz in

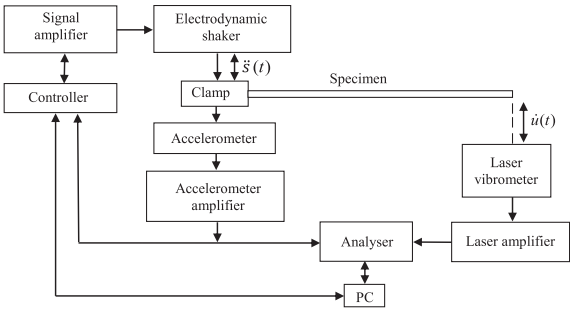

Fig. 2. Experimental set-up schematic.

order to study the vibration attenuation in frequency domain. All measurements are made in the linear range and at environmental temperature. Moreover, it is ensured the clamping system does not add damping to the system.

3. Results and discussion

In this section, the experimental results of the sandwich structures' homogenised complex modulus are presented and the effect of the viscoelastic film thickness on it is analysed. Then the viscoelastic film's shear complex modulus obtained from dynamic tests on sandwich structures is presented and a material model, based on the four parameters fractional derivative model with an empirical modification, is defined to model its dynamic behaviour from 0 to 1 kHz. Lastly, a numerical analysis of the influence of the core and base layer thickness ratio, base layer thickness and frequency, on the storage modulus and loss factor of the sandwich structure is carried out and a procedure to design symmetric thin sandwich structures for a given application's requirements is provided.

3.1. Experimental characterisation of sandwich structures

The experimental results of the sandwich structures' homogenised properties and the viscoelastic film's shear properties are presented in Tables 3, 4 and 5, all of which are an average of three specimens, and the deviations shown are the standard deviations. The homogenised storage modulus, E, and the loss factor, η, of sandwich structures, as well as the shear modulus, G_v, and the loss factor, η_v, of the viscoelastic film are determined from the modal transmissibility functions measured from the sandwich beams with different free lengths.

In Fig. 3, the homogenised complex modulus of sandwich structures with different core thicknesses are compared. Fig. 3(a) shows the homogenised storage modulus is constant in frequency regardless the core thickness and it decreases with the core thickness. In Fig. 3(b) it is observed the loss factor of the sandwich structure is increased with the core thickness. Moreover, the loss factor increases in frequency and this frequency dependence becomes greater with the core thickness, which means a greater viscous behaviour.

In addition of the results shown, it is observed the viscoelastic film thickness influence more the loss factor than the storage modulus Tables 3, 4 and 5. For example, in the third vibration mode with 140 mm of free length, the storage modulus decreases by 8%, whereas the loss factor increases by 79% when the core thickness is increased from 40 μm to 100 μm in wet.

Fig. 4 shows the transmissibility functions of the analysed three sandwich structures in the bandwidth from 35 to 1000 Hz. The amplitude of the transmissibility modulus gives an idea of the damping capabilities of the sandwich structure. It can be seen that regardless of the core thickness, the transmissibility modulus decreased in frequency. Furthermore, the bigger the core thickness, the lower the transmissibility modulus at all resonances. The resonance frequencies and so the bending stiffness increased with the core thicknesses. Note the reason why the S80 specimen's resonance frequencies are not between S40 and S100 ones is because its base layers are slightly thinner as specified in Table 2.

Sargianis and Suhr have observed in sandwich structures the bending stiffness, which depends on core thickness, dominates the low frequency vibrational response, whereas at high frequencies the response is influenced mainly by the core's material properties [18,27]. In Fig. 5 the frequency bandwidth has been extended to 4 kHz and unlike these authors it is observed in these thin sandwich structures the vibrational response is fully influenced by the viscoelastic film thickness in all the bandwidth from 0 to 4 kHz.

3.2. Viscoelastic material model

The experimental dynamic properties of the viscoelastic film are shown and a mathematical model based on a four-parameter fractional derivative model with an empirical modification is defined to model its behaviour.

The shear complex modulus of the polyester-based adhesive film is determined from the sandwich beams' experimental tests. In Fig. 6 the shear modulus and the loss factor of the viscoelastic film are shown. Here, as well as Tables 3, 4 and 5, demonstrate the validity of the experimental procedure since the obtained viscoelastic film's dynamic properties are the same regardless of the tested sandwich structure's core thickness. The shear modulus, as well as the loss factor of the viscoelastic film increase in frequency in the analysed bandwidth, which means in the bandwidth from 0 to 1 kHz and room temperature the viscoelastic core is working in the rubbery region and so the frequency where the damping is maximum has not yet been reached.

There are different mathematical models to represent the mechanical behaviour of viscoelastic materials, which can be classified into differential, hereditary and fractional models [24,28,29]. The four parameters fractional derivative model, known as the generalised Zener model, is commonly used to model the behaviour of viscoelastic materials. However, in some cases this model should be modified to better represent the viscoelastic material's real behaviour. In this work an additional fractional power term is added to the generalised Zener model as proposed in [28], in

Table 3
S100's resonant frequency, storage modulus and loss factor, and viscoelastic core's shear modulus and loss factor for each vibration mode with 140 mm of free length.

S100						
			Sandwich structure		Viscoelastic core	
f (Hz)	Mode No.	L (mm)	E (GPa)	η	G_v (MPa)	η_v
NA	2	140	NA	NA	NA	NA
380.57 ± 2.3	3	140	170.67 ± 2.1	0.033 ± 0.003	15.5 ± 1.7	0.294 ± 0.002
750.78 ± 3.7	4	140	172.97 ± 1.7	0.046 ± 0.001	31.0 ± 2.2	0.470 ± 0.035

NA: results unavailable.

Table 4
S80's resonant frequency, storage modulus and loss factor, and viscoelastic core's shear modulus and loss factor for each vibration mode and free length.

S80						
			Sandwich structure		Viscoelastic core	
f (Hz)	Mode No.	L (mm)	E (GPa)	η	G_v (MPa)	η_v
98.40 ± 1.0	2	160	175.64 ± 3.5	0.015 ± 0.003	3.0 ± 0.6	0.182 ± 0.071
111.24*	2	150	173.4*	NA	NA	NA
128.32 ± 0.6	2	140	175.08 ± 1.7	NA	NA	NA
276.26 ± 1.9	3	160	176.58 ± 2.4	0.012 ± 0.003	9.0 ± 1.4	0.146 ± 0.058
315.30 ± 4.0	3	150	177.70 ± 4.5	0.015 ± 0.008	11.0 ± 2.7	0.231 ± 0.163
360.80 ± 0.4	3	140	176.55 ± 0.4	0.015 ± 0.004	11.4 ± 0.1	0.185 ± 0.048
544.35 ± 4.8	4	160	178.55 ± 3.2	NA	NA	NA
620.78 ± 5.5	4	150	179.37 ± 3.2	0.019 ± 0.004	23.4 ± 4.6	0.303 ± 0.137
08.51 ± 1.9	4	140	177.29 ± 0.9	0.016 ± 0.006	23.3 ± 0.8	0.208 ± 0.091
5.59 ± 11.1	5	160	180.84 ± 4.4	0.026 ± 0.009	33.8 ± 5.6	0.508 ± 0.325

* Results identified from one specimen.
NA: results unavailable.

Table 5
S40's resonant frequency, storage modulus and loss factor, and viscoelastic core's shear modulus and loss factor for each vibration mode and free length.

S40						
			Sandwich structure		Viscoelastic core	
f (Hz)	Mode No.	L (mm)	E (GPa)	η	G_v (MPa)	η_v
100.18 ± 0.3	2	160	184.40 ± 1.1	0.007 ± 0.001	2.4 ± 0.3	0.167 ± 0.004
NA	2	150	NA	NA	NA	NA
131.06 ± 0.6	2	140	185.02 ± 1.7	NA	NA	NA
281.97 ± 0.8	3	160	186.34 ± 1.1	0.007 ± 0.001	8.6 ± 1.4	0.195 ± 0.004
321.20 ± 0.1	3	150	186.79 ± 0.1	0.006 ± 0.001	10.4 ± 0.2	0.185 ± 0.013
366.77 ± 0.9	3	140	184.81 ± 0.9	0.007 ± 0.001	9.1 ± 1.1	0.161 ± 0.008
552.67 ± 2.1	4	160	186.43 ± 1.4	NA	NA	NA
630.42 ± 0.3	4	150	187.38 ± 0.2	0.007 ± 0.001	22.2 ± 1.2	0.239 ± 0.043
720.56 ± 1.2	4	140	185.76 ± 0.6	0.011 ± 0.003	19.2 ± 2.2	0.284 ± 0.045
916.95 ± 2.1	5	160	187.80 ± 0.9	0.013 ± 0.003	30.2 ± 5.8	0.497 ± 0.032

NA: results unavailable.

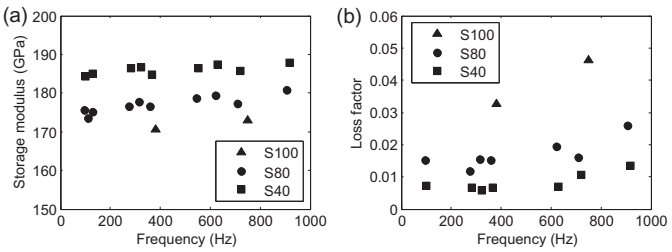

Fig. 3. The homogenised complex modulus, (a) Storage modulus and (b) Loss factor, of the sandwich beams with 40 μm, 80 μm and 100 μm of core thicknesses in the frequency domain.

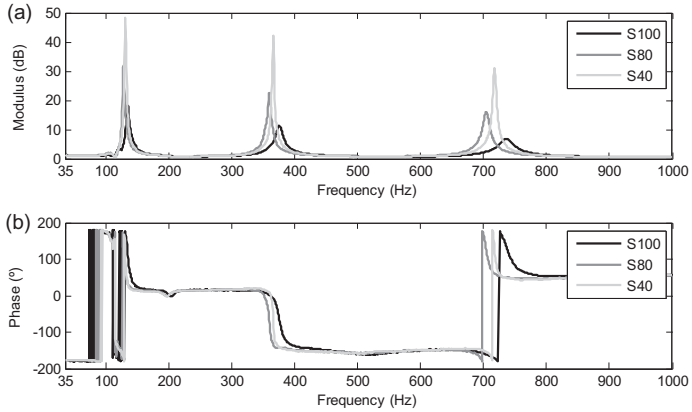

Fig. 4. Experimental transmissibility functions, (a) Modulus and (b) Phase, of the sandwich beams with 40 μm, 80 μm and 100 μm of core thicknesses with 140 mm of free length in the bandwidth from 35 to 1000 Hz.

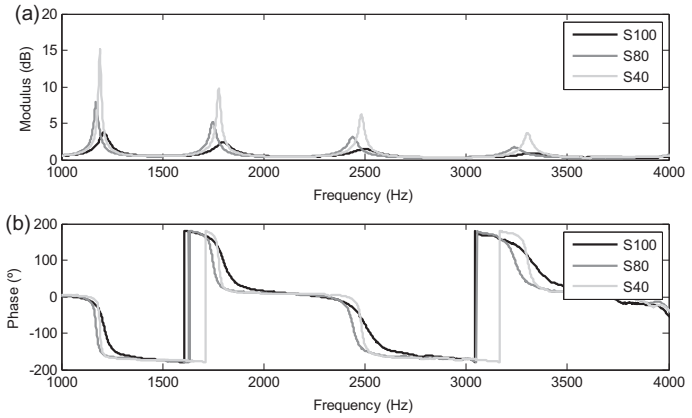

Fig. 5. Experimental transmissibility functions, (a) Modulus and (b) Phase, of the sandwich beams with 40 μm, 80 μm and 100 μm of core thicknesses with 140 mm of free length in the bandwidth from 1000 to 4000 Hz.

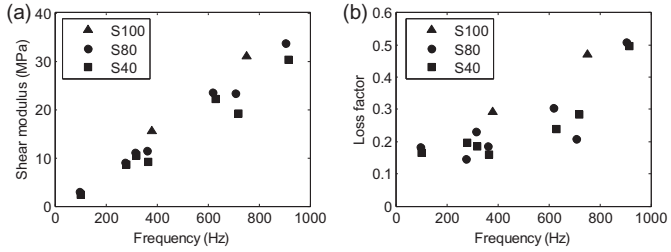

Fig. 6. The shear complex modulus, (a) Shear modulus and (b) Loss factor, of the 40 μm, 80 μm and 100 μm viscoelastic cores in the frequency domain.

order to add a small finite slope in the frequency domain, superimposed on the modulus values.

Assuming the Poisson ratio of the viscoelastic material is constant in frequency in the analysed bandwidth [25,26], the complex shear modulus can be expressed by

$$G_v^*(f) = G_v(f)(1 + i\eta_v(f)) = \frac{a + b(if)^\alpha}{1 + c(if)^\alpha} \cdot (f)^p, \tag{3}$$

where the parameters to define are a, b, c, α and p.

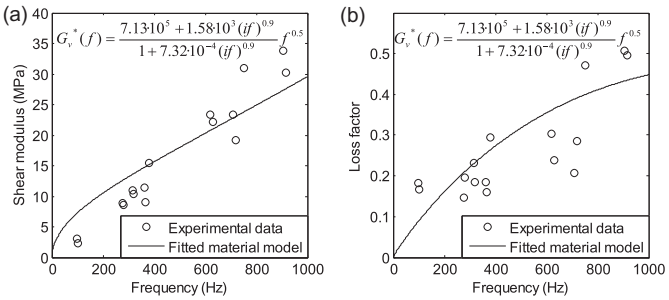

Fig. 7. The fitted shear complex modulus, (a) Shear modulus and (b) Loss factor, and experimental results of the polyester-based adhesive core.

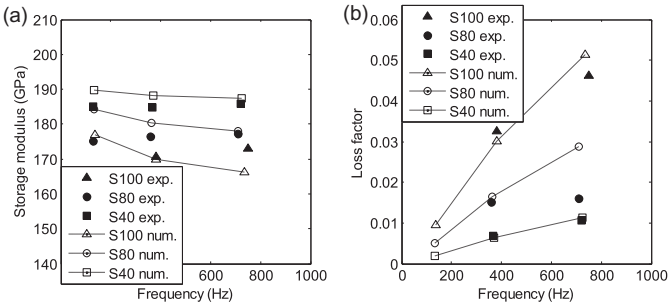

Fig. 8. Numerical homogenised complex modulus, (a) storage modulus and (b) loss factor, and experimental results of the S100, S80 and S40 sandwich specimens with 140 mm of free length.

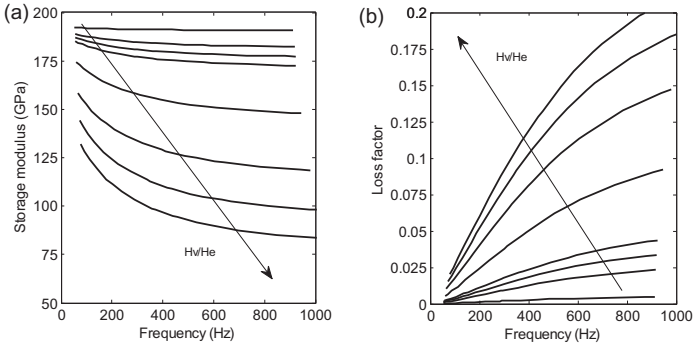

Fig. 9. The influence of the H_v/H_e thickness ratio, which goes from 0.01 to 1, on the homogenised properties, (a) Storage modulus and (b) Loss factor, of sandwich structures composed of H_e = 0.258 mm in the frequency domain.

The defined mathematical model is fitted to the experimental shear complex modulus data by the Nelder–Mead minimisation algorithm implemented in MATLAB. The minimised function is

$$\sum_{s}^{s_{max}} |(G_v(f_s) - G_{v,s}) + 2(G_v(f_s)\eta_v(f_s) - G_{v,s}\eta_{v,s})|, \quad (4)$$

where s is the summation index, s_{max} is the total number of experimental numbers, $G_v(f_s)$ and $\eta_v(f_s)$ are the value of the material model at the experimental frequency f_s given by Eq. (3) and $G_{v,s}$ and $\eta_{v,s}$ are experimental shear modulus and loss factor measured at the same frequency f_s shown in Tables 3, 4 and 5.

In Fig. 7, the experimental shear modulus and loss factor values, and the fitted fractional derivative model are shown.

3.3. Numerical analysis of the design parameters

Following, the influence of the core and base layer thicknesses and frequency, on the dynamic properties, storage modulus and loss factor, of sandwich structures is studied numerically and a

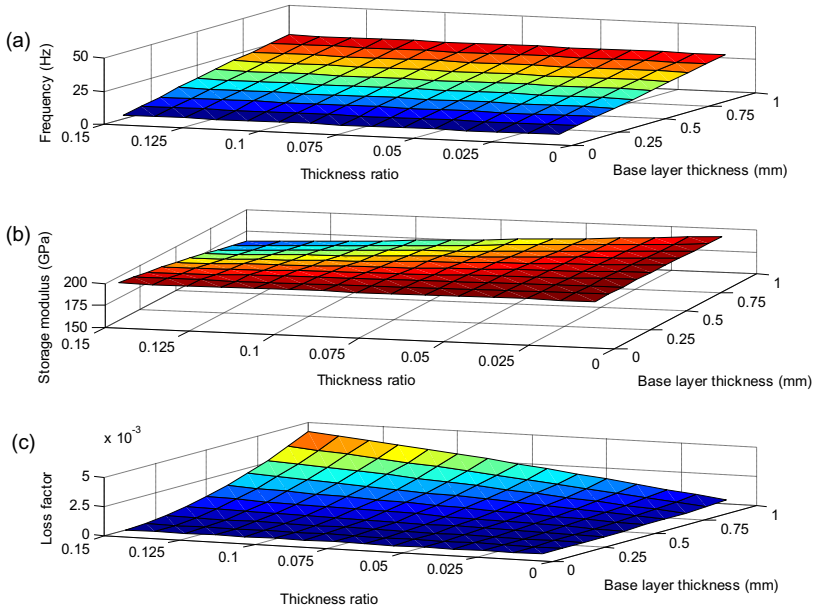

Fig. 10. The storage modulus (b) and loss factor (c) as a function of H_v/H_e thickness ratio and H_e, at low frequencies 0–30 Hz (a).

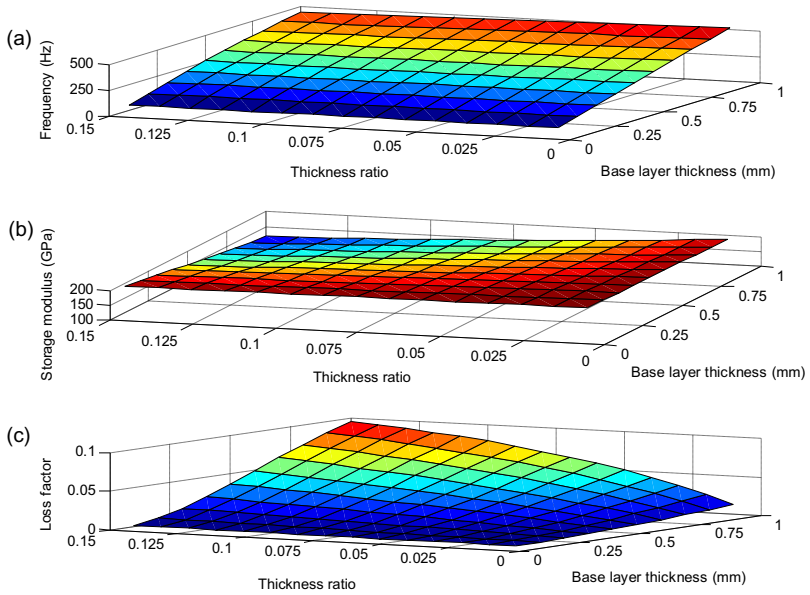

Fig. 11. The storage modulus (b) and loss factor (c) as a function of H_v/H_e thickness ratio and H_e, at high frequencies 30–450 Hz (a).

procedure to enable the design of symmetric sandwich structures is provided.

For that purpose an iterative numeric program is developed in MATLAB based on the RKU equations for symmetric sandwich configuration and on the defined polyester-based adhesive's shear complex modulus model [23]. Even if at first sight the RKU equations seems to be too simple, the results obtained numerically are correlated well with the experimental results, which means they constitute a powerful tool for the easy and quick design of sandwich structures.

In Fig. 8 the experimental homogenised results of the sandwich structures with different core thicknesses are compared with those obtained numerically. In general the biggest deviations are in the storage modulus at low frequencies due to the proposed model's shear modulus overestimation at low frequencies. The results show the validity of the proposed constitutive material model.

Fig. 9 shows the influence of the H_v/H_e thickness ratio on the homogenised properties of sandwich structures in the frequency domain with H_e = 0.258 mm. With small thickness ratios the storage modulus is nearly constant and the loss factor is not very frequency dependent, as has been observed experimentally in Fig. 3. However, by increasing the thickness ratio the frequency dependence of both, storage modulus and loss factor, is considerably increased, which means a greater viscoelastic behaviour of sandwich structures. Moreover, it is observed that by increasing H_v/H_e the storage modulus is decreased and the loss factor is increased in all the frequency bandwidth, being the influence bigger in the loss factor than in the storage modulus.

Finally, Figs. 10 and 11, are supplied to design thin symmetric sandwich structures for a given stiffness and damping specifications. In these graphics, the values of the storage modulus, E, and loss factor, η, are given as a function of the core and base layer thickness ratio, H_v/H_e, and base layer thickness, H_e at two different frequencies, at a low frequency and at a higher one.

The design procedure is the following:

(1) Define the minimum and maximum values of E and η and the working frequency bandwidth.
(2) Choose a H_v/H_e thickness ratio and a H_e value that best fulfil the E and η requirements from the low frequency range graphic or high frequency range graphic depending on the working frequency bandwidth.
(3) Analyse the frequency dependence of the designed sandwich structure comparing its dynamic properties at a low and a higher frequency. If the dynamic properties of the sandwich structure are highly frequency dependent so that the dynamic specifications may not be fulfilled in all the working bandwidth, new values of H_v/H_e and H_e must be chosen.

4. Conclusions

In this work the dynamic behaviour, stiffness and loss factor, of thin sandwich structures as a function of the viscoelastic film thickness is established. The experimental characterisation of three different core thicknesses thin sandwich structures is carried out and the homogenised dynamic properties of the sandwich structures are obtained in a bandwidth from 0 to 1 kHz. The influence of the viscoelastic film thickness on the dynamic properties of thin sandwich structures is analysed from the experimental and numerical results. The core thickness influence more the loss factor than the storage modulus. Increasing it, the loss factor is considerably increased at the expense of a decrement in the storage modulus, and both become more frequency dependent. Moreover, even if the storage modulus of the sandwich structure is decreased with core thickness the bending stiffness is increased and its vibrational response is fully influenced by the viscoelastic film thickness in the bandwidth up to 4 kHz.

The generalised Zener model with an empirical modification is proposed to describe the shear complex modulus of the viscoelastic film, polyester-based adhesive. The proposed model is valid up to 1 kHz.

The defined viscoelastic material model along with the RKU equations allow a numerical analysis of the geometrical design parameters, core and base layer thicknesses, on the stiffness, damping and frequency dependence of thin sandwich structures. From this analysis a procedure to design symmetric thin sandwich structures for a given application's dynamic specifications at different frequency bandwidths is proposed.

Acknowledgements

The present study is partially supported by MAGNETOBUSH (UE2013-09, Basque Government) and AVISUINT (DPI 2012-36366, Spanish Government) projects and Replasa S.A.

References

[1] Tomlinson GR. State of the art review: damping, structural dynamic @ 2000: current status and future directions. Baldock, Hertfordshire, England: Research Studies Press; 2001.
[2] Lifshitz JM, Leibowits M. Optimal sandwich beam design for maximum viscoelastic damping. Int J Solids Struct 1987;23:1207–34.
[3] Bangarubabu P, Kishore Kumar K, Krishna Y. Damping effect of viscoelastic materials on sandwich beams. In: Proceedings of the International Conference on Trends on Industrial and Mechanical Engineering (ICETIME 2012), Dubai, 24–25 March 2012. p. 171–173.
[4] Kerwin EM. Damping of flexural waves by a constrained viscoelastic layer. J Acoust Soc Am 1959;31:952–62.
[5] Nakra BC. Vibration control with viscoelastic materials. Shock Vib Dig 1976;8:3–12.
[6] Nakra BC. Vibration control with viscoelastic materials – II. Shock Vib Dig 1981;13:17–20.
[7] Nakra BC. Vibration control with viscoelastic materials – III. Shock Vib Dig 1984;16:17–22.
[8] Mead M. The forced vibration of a three-layer damped sandwich beam with arbitrary boundary conditions. J Sound Vib 1969;10(2):163–75.
[9] Rao DK. Frequency and loss factors of sandwich beams under various boundary conditions. J Mech Eng Sci 1978;20(5):271–82.
[10] Matter M, Gmür T, Cugnoni J, Schorderet A. Identification of the elastic and damping properties in sandwich structures with a low core-to-skin stiffness ratio. Compos Struct 2011;93(331):41.
[11] Hamdaoui M, Druesne F, Daya EM. Variability analysis of frequency dependent visco-elastic three-layered beams. Compos Struct 2015;131:238–47.
[12] Lima AMG, Faria AW, Rade DA. Sensitivity analysis of frequency response functions of composite sandwich plates containing viscoelastic layers. Compos Struct 2010;92:364–72.
[13] Leibowits M, Lifshitz JM. Experimental verification of modal parameters for 3-layered sandwich beams. Int J Solids Struct 1990;26:175–84.
[14] Teng TL, Hu NK. Analysis of damping characteristics for viscoelastic laminated beams. Comput Methods Appl Mech Eng 2001;190:3881–92.
[15] Hamdaoui M, Robin G, Jrad M, Daya EM. Optimal design of frequency dependent three-layered rectangular composite beams for low mass and high damping. Compos Struct 2015;120:174–82.
[16] Grewal JS, Sedaghati R, Esmailzadeh E. Vibration analysis and design optimization of sandwich beams with constrained viscoelastic core layer. J Sandw Struct Mater 2013;15:203–28.
[17] Sharma RS, Raghupathy VP. Influence of core density, core thickness, and rigid inserts on dynamic characteristics of sandwich panels with polyurethane foam as core. J Reinf Plast Compos 2010;29:3226–36.
[18] Sargianis J, Suhr J. Effect of core thickness on wave number and damping properties in sandwich composites. Compos Sci Technol 2012;72:724–30.
[19] Arvin H, Sasighi M, Ohadi AR. A numerical study of free and forced vibration of composite sandwich beam with viscoelastic core. Compos Struct 2010;92:996–1008.
[20] Arikoglu A, Ozkol I. Vibration analysis of composite sandwich beams with viscoelastic core by using differential transform method. Compos Struct 2010;92:3031–9.
[21] ASTM E 756–05. ASTM E 756–05. Standard Test Method for Measuring Vibration-Damping Properties of Materials, 2005.
[22] Cortes F, Elejabarrieta MJ. Viscoelastic materials characterisation using the seismic response. Mater Des 2007;28:2054–62.
[23] Ross D, Ungar EE, Kerwin EMJ. Damping of plate flexural vibrations by means of viscoelastic laminae. Struct damping 1960:49–87.
[24] Nashif AD, Jones DIG, Henderson JP. Vibration damping. New York: John Wiley and Sons; 1985.
[25] Lakes RS. On Poisson's ratio in linearly viscoelastic solids. J Elast 2006;85(1):45–63.
[26] Espíndola JJ, Silva Neto JM, Lopes EMO. A generalised fractional derivative approach to viscoelastic material properties measurement. Appl Math Comput 2005;164:493–506.
[27] Nilsson AC. Wave propagation in and sound transmission through sandwich plates. J Sound Vib 1990;183:73–94.
[28] Jones DIG. Handbook of viscoelastic vibration damping. England: John Wiley and Sons; 2001.
[29] Cortes F, Martinez M, Elejabarrieta MJ. On mechanical vibration control using viscoelastic surface treatments. In: Mechanical vibrations: measurements, effects and control. Nova Science Publisher Inc; 2009.

Chapter 4

Eddy currents generated in metallic skins

This chapter is focused on the skins of viscoelastic-magnetorheological sandwiches and studies the influence of eddy currents induced in the metallic skins on the dynamic behaviour of sandwich. The phenomenon of eddy currents is one of the physical phenomena generated in viscoelastic-magnetorheological sandwiches when exposed to magnetic fields.

Irazu L and Elejabarrieta MJ (Major revision). Analysis and numerical modelling of eddy current damper for vibration problems. *Journal of Sound and Vibration*.

Irazu L and Elejabarrieta MJ (Revision). A novel hybrid sandwich structure: viscoelastic and eddy current damping. *Materials and Design*.

4.1 Introduction

If a conductive material experiences a time-varying magnetic field, electrical currents, known as eddy currents, are induced in the conductor. Thus, when magnetic fields are applied to vibrating viscoelastic-magnetorheological sandwiches (VEMRS), eddy currents are induced in their metallic skins. These currents circulate in such a way that they induce their own magnetic field with opposite polarity to the change in magnetic flux. By the iteration of the eddy currents with the magnetic field, an electromagnetic repulsive force is generated. Due to the electrical resistance of the metallic material the induced currents are dissipated into heat and the force is disappeared. However, in dynamic systems, such as vibrating VEMRSs, there is a constant change in magnetic flux. Thus, eddy currents and force are constantly regenerated, allowing energy to be removed from the system (Sodano and Bae 2004).

The phenomenon of eddy currents is one of the physical phenomena generated in vibrating VEMRSs exposed to magnetic fields. Therefore, in this chapter the influence of eddy currents induced in conductive metallic beams is studied by means of an experimental modal analysis. The effect of these currents on the modal parameters and vibration attenuation is analysed. In view of the vibration attenuation potential of eddy currents, the combination of viscoelastic and eddy current damping is studied and a new hybrid sandwich structure is put forward. Then, a new inverse method is proposed in order to estimate and model the effect of eddy currents.

Following, the state of the art about the phenomenon of eddy currents is presented, focusing on its applications to dampen vibration and the approaches to model it. Then, the objectives of this chapter are defined. The experimental modal analysis carried out with an aluminium beam in the absence of and under a magnetic field is shown and the influence of the induced currents is studied. A new hybrid sandwich structure combining viscoelastic and eddy current damping is proposed and its dynamic properties are analysed. Afterwards, a new inverse method is proposed to estimate and model the influence of eddy currents on metallic and sandwich beams. Finally, the obtained conclusions are shown and the scientific contributions are presented.

4.2 State of art

The phenomenon of eddy current is caused when a conductive material experiences a time-varying magnetic field. Since in dynamic systems there is a constant change in magnetic flux, continuously eddy currents are induced in the conductor and energy is dissipated from the system in the form of heat. This phenomenon has been known since the late 1800s and many authors have proposed different uses of eddy currents for dynamic systems, such as braking systems, suppression of rotor vibration and damping of structural vibrations. Sodano and Bae (2004) presented an extensive review about the different applications proposed with eddy currents.

Matsuzaki et al. (1997) and Matsuzaki et al. (2000) were among the first to highlight the possibility of using electromagnetic forces to dampen vibration of beams. They proposed attenuating the vibration of a periodically magnetised beam using electromagnetic forces generated by the current passing between the magnetised sections. Sodano et al. (2005) analysed the vibration suppression capabilities of a cantilever beam by placing a magnet perpendicular to the beam motion and attaching a conductive sheet in the beam tip. In later works, they proposed the use of two magnets with the same polarity facing each other and the active movement of magnets to increase the damping added to the beam (Sodano et al. 2006; Sodano and Inman 2007). Kwak et al. (2003) proposed an eddy current damper consisting of a flexible linkage with two permanent magnets and a fixed copper plate attached to the end of the cantilever beam to be damped. Later, Bae et al. (2005) developed the theoretical model of such eddy current damper. Cheng and Oh (2009) and Cheng et al. (2010) introduced an electromagnetic shunt damper to attenuate vibration of beams using eddy currents. Stein et al. (2016) proposed the damping of transversal vibration of clamped-clamped beams with a centre mass loading by a ferro-magnetic circuit.

In recent years, the trend is to use the eddy current phenomenon to obtain hybrid dampers with improved damping performance. Bae et al. (2012) and Bae et al. (2014) suggested combining the classical tuned mass damper with the eddy current phenomenon using a permanent magnet as a concentrated mass of the tuned mass damper, Berardengo et al. (2015) proposed an adaptive tuned mass damper based on shape memory alloys and eddy currents, and recently Asghar Maddah et al. (2017) developed an hybrid damper consisting of an eddy current damper and a magnetorheological fluid damper.

With regard to modelling of the eddy current phenomenon, it is difficult to address it analytically while taking into account all the effects involved in the phenomenon, such as the determination of the magnetic flux density, boundary conditions of the conductor, surface charges (Coulomb charge), etc. Sodano et al. (2005) and Sodano et al. (2006) provided a theoretical model of the eddy current force generated on a vibrating beam exposed to a cylindrical permanent magnet. The surface charges were ignored, the edge effects were accounted by the image method and just the radial magnetic flux was considered since the deflection of the beam was assumed to be in the transverse direction. Zhou and Wang (2006a) addressed analytically the eddy loads generated on vibrating conductive beams exposed to steady-state homogenous transverse magnetic fields. However, the proposed analytical model was not validated with experimental results.

The majority of the works analysing the phenomenon of eddy current have focused on designing eddy current devices that magnifies significantly the damping added to the structure, which in same cases result also in a significant modification of the original structure to be damped. However, as stated by Sodano and Bae (2004) the eddy current phenomenon can be used to remove energy from the system without contacting the structure. It is known the contactless induced eddy currents do not

modify the resonance frequencies of the structure (Sodano et al. 2005; Sodano et al. 2006), however there are no works analysing in detail the influence of these currents on the dynamic behaviour and modal parameters of the structure. Moreover, even if several hybrid dampers have been proposed in recent years, the combination of viscoelastic and eddy current damping have not been analysed. Finally, it has been found a lack of simple numerical methods able to describe the influence of eddy currents induced by different magnetic field configurations.

4.3 Objectives

The purpose of this chapter is to determine the influence of eddy currents induced in the metallic skins of the dynamic behaviour of the sandwich. This involves:

- Analysing the effect of eddy currents on the modal parameters and vibration attenuation of metallic beams.
- Analysing the effect of eddy currents on the vibrational response of thin viscoelastic sandwiches.
- Proposing an eddy force model and developing a numerical method to estimate and model the influence of eddy currents.

4.4 Results

Two structures, a metallic beam and a thin viscoelastic sandwich beam, were analysed. On the one hand, the AL beam was used to study the influence of induced eddy currents on the modal parameters and vibration attenuation of metallic beams. On the other hand, the thin VES was used to analyse the effect of eddy currents on the vibrational response of thin sandwiches and to study the possibility of combining viscoelastic and eddy current damping to obtain a hybrid sandwich structure with enhanced vibration attenuation. The geometrical and physical properties of both structures are shown in Table 2.2

The dynamic response of both structures were measured by the experimental procedure detailed in Chapter 2, which consisted on forced vibrations tests with resonance in the absence of and under a magnetic field. The magnetic field was applied to the AL and VES beams by placing two neodymium magnets in one side of the beam at its free end, Figure 2.3. This configuration of magnets was chosen to maximize the induction of eddy currents and so their influence (Sodano et al. 2005).

4.4.1 Influence of eddy currents

Next, the effect of applying magnetic fields to vibrating non-magnetic metallic beams is studied. The results obtained on the experimental modal analysis with the AL beam

are shown and the influence of the induced eddy currents on modal parameters, natural frequencies and mode shapes, and vibration attenuation is discussed.

Table 4.1 shows the experimental values of the natural frequencies and transfer modulus of the aluminium beam with and without induced eddy currents, AL-ED and AL, in the bandwidth of 0-1 kHz. The natural frequencies of the AL beam are not modified when inducing eddy currents. The transfer modulus, instead, is decreased in all the resonances, which means the eddy currents attenuate the vibration of the beam in all the resonances within the bandwidth of 0-1 kHz. However, the relative attenuation of the beam is greater at low frequencies than at higher ones due to the greater velocity of the beam at low frequencies (Sodano et al. 2005; Sodano et al. 2006). Note the transfer modulus of the AL without eddy currents in the first vibration mode is lower than in the second one due to a lack of resolution to properly measure the first resonance of metallic beams.

Table 4.1. Experimental natural frequencies and modulus of the transfer function of the AL and AL-ED beams in its free end in the bandwidth of 0-1 kHz.

	Natural frequency (Hz)		Transfer modulus	
	AL	AL-ED	AL	AL-ED
Mode 1	9.9	9.8	232	21
Mode 2	61.9	61.9	356	101
Mode 3	173.6	173.7	190	92
Mode 4	340.9	341.0	88	57
Mode 5	564.4	564.6	53	35
Mode 6	845.0	845.1	39	31

In Figure 8.14 the experimental mode shapes, ψ , of the cantilever AL and AL-ED beams in the bandwidth of 0-1 kHz are shown. The mode shapes were obtained from the modal transfer functions measured every 5 mm along the length of the beam, Chapter 2. It is observed the vibration amplitude is notably decreased in the first three vibration modes when the magnetic field is applied to induce eddy currents, as seen in Table 4.1. In addition, the vibration is reduced in all the length of the beam even if the magnetic field is applied just in the free end, Figure 2.3. In Figure 8.15 the theoretical (Blevins 1979) and the experimental mode shapes of the cantilever AL and AL-ED beams normalised to maximum displacement unit, ψ_{nom}, are shown. It is concluded that even though the vibration amplitude of the beam is decreased, the mode shapes itself remain unmodified in all the analysed bandwidth.

These results show the phenomenon of eddy currents attenuates the vibration of conductive metallic structures without even contacting the structure to be damped and modifying its characteristics. Applying a magnetic field to a vibrating metallic beam eddy currents are induced in it and as a consequence the vibration amplitude is considerably decreased at resonances, while the natural frequencies and mode shapes remain unmodified. In addition, even if the magnetic field is applied in a partial region of the beam the vibration of all the length is attenuated.

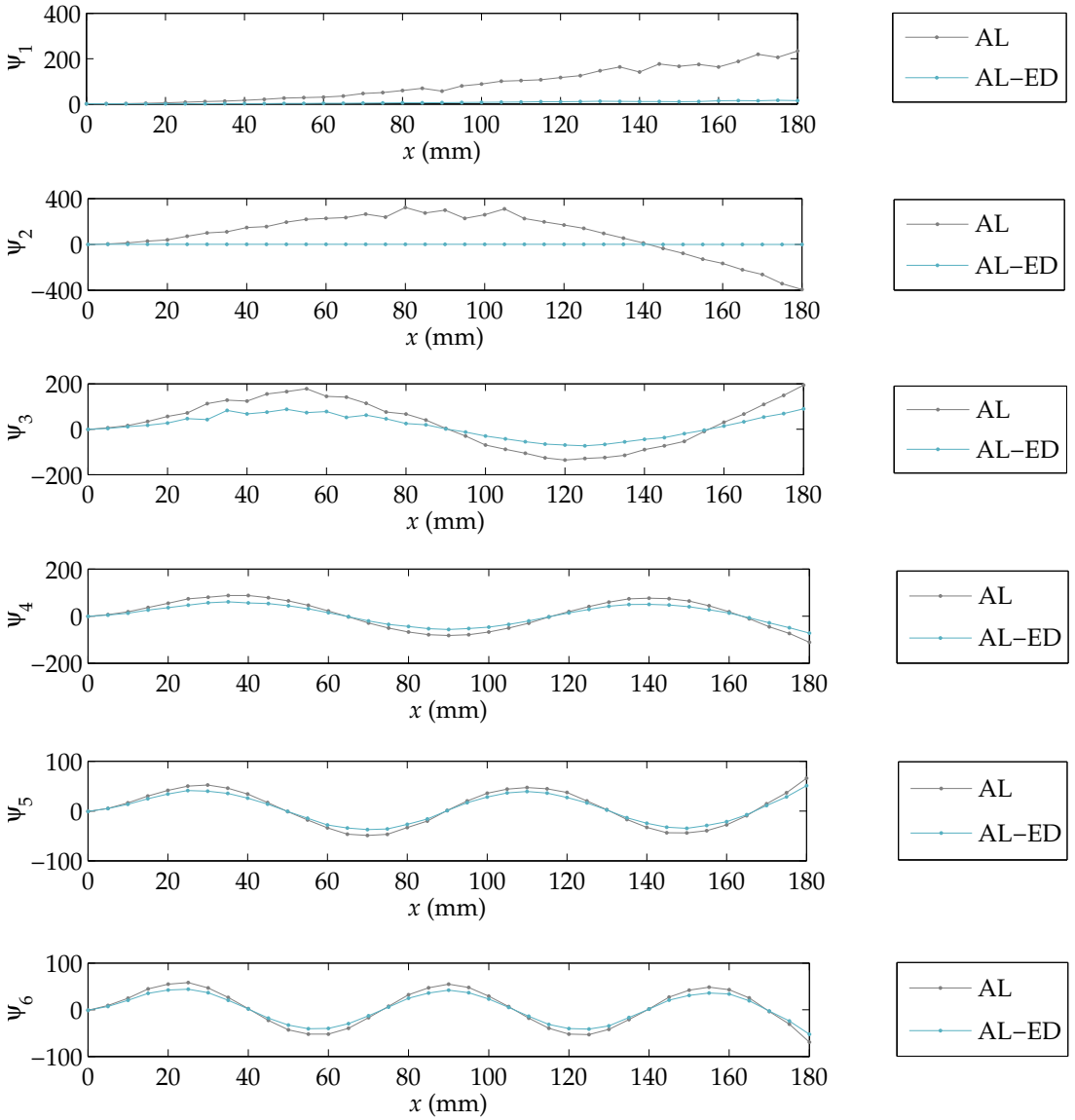

Figure 4.1. Experimental mode shapes of the AL and AL-ED cantilever beams with 180 mm of free length in the bandwidth of 0-1 kHz.

4.4.2 New hybrid sandwich structure

The studying of the phenomenon of eddy currents leads to propose a new hybrid damping sandwich with enhanced vibration characteristics. The design of viscoelastic sandwiches (VES) is based on a trade-off between damping, mechanical properties and added weight. In view of the potential of eddy currents to dampen structural vibration, the combination of viscoelastic and eddy current damping is studied in order to obtain a hybrid damping sandwich (VES-ED) structure able to attenuate structural vibration in a wide frequency bandwidth, without adding mass to the structure and compromising its mechanical properties. The hybrid damping VES-ED consists of placing permanent magnets near, but not in contact with, the thin VES in order to enable the induction of eddy currents in the metallic skins of the sandwich. Thus, when the sandwich begins vibrating, energy is dissipated by two mechanisms: shear

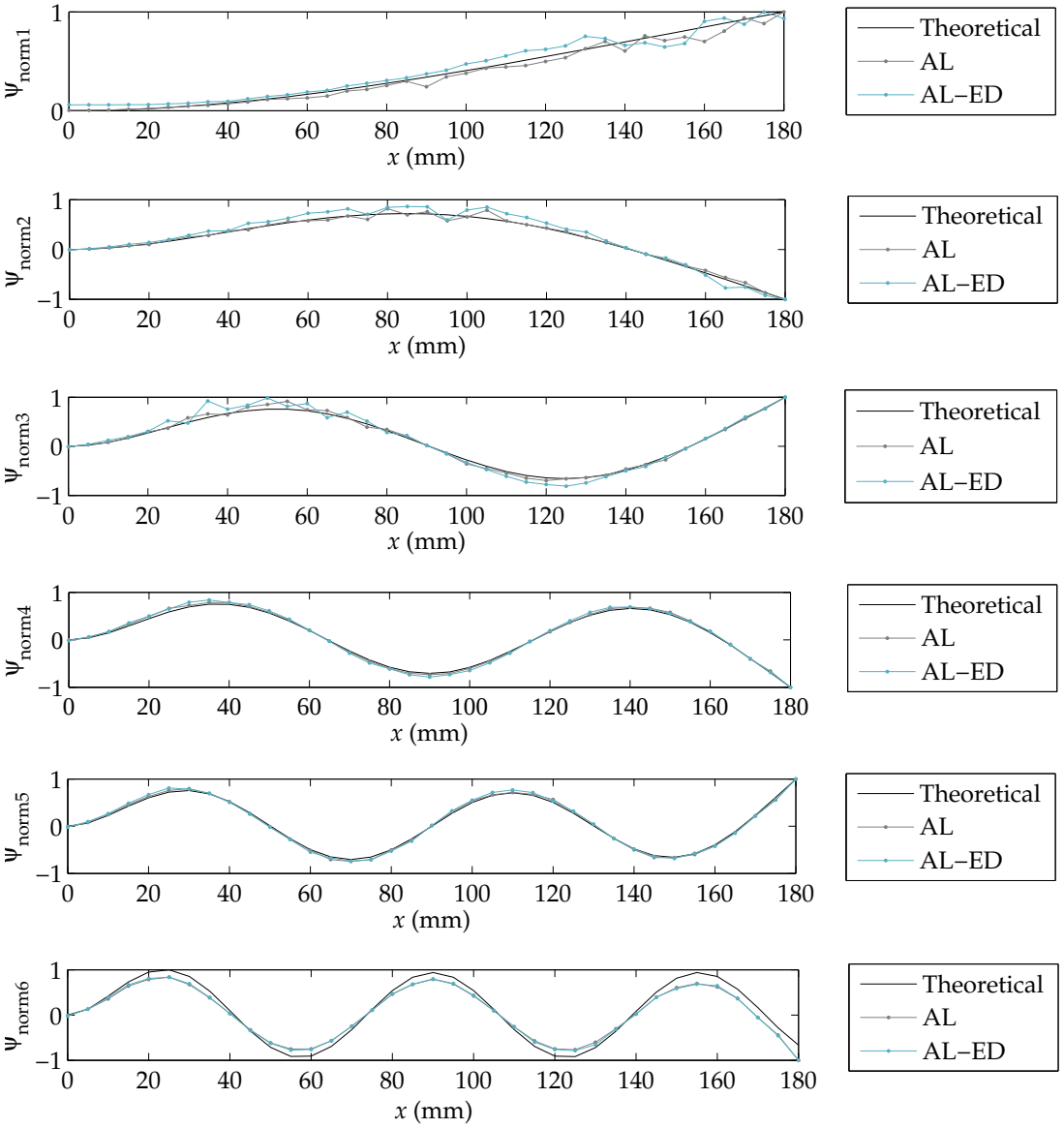

Figure 4.2. Experimental and theoretical mode shapes normalised to maximum displacement unit of the AL and AL-ED cantilever beams with 180 mm of free length in the bandwidth of 0-1 kHz (Blevins 1979)

deformation of the viscoelastic film and eddy currents.

Figure 8.16 shows the transfer functions of the resonances within the bandwidth of 0-1 kHz of the VES and VES-ED. It is observed the induced eddy currents do not modify the resonance frequencies of the sandwich, as in the case of the AL beam. However, the transfer modulus, and so the vibration amplitude, of the VES-ED is smaller than the VES ones in all the resonances, being this tendency being greater at low vibration modes.

In Table 4.2 the experimental dynamic properties of the VES and the VES-ED are shown. The results are an average of three specimens, with their corresponding standard deviations. It is observed the storage modulus of the VES and VES-ED are almost identical, whereas the loss factor of VES-ED is bigger than the VES ones. For example, by placing permanent magnets near the thin VES in order to induce eddy currents,

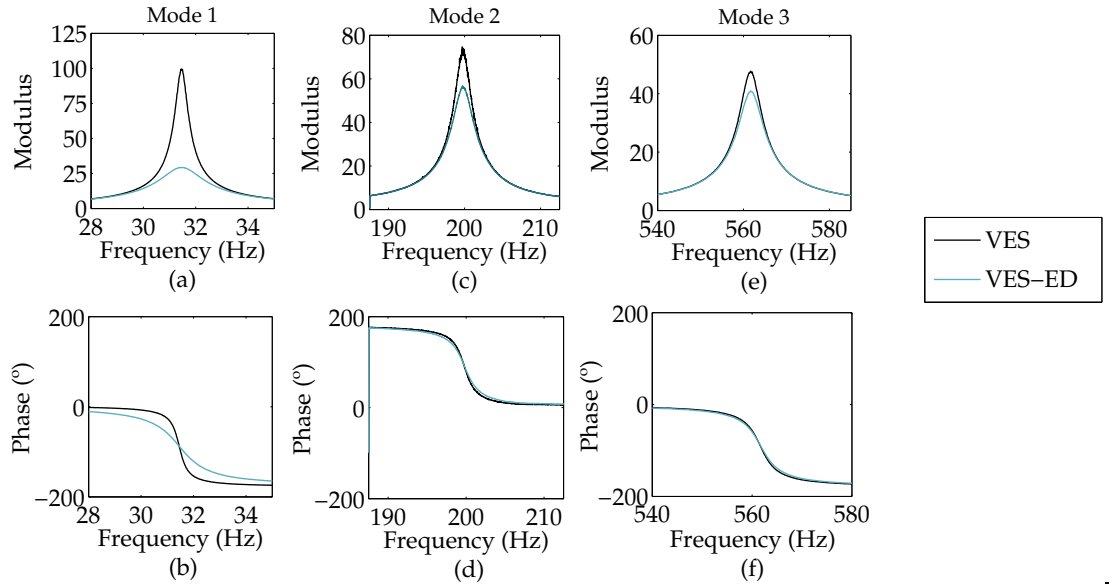

Figure 4.3. Experimental modal transfer functions, (a) modulus and (b) phase, of the VES and VES-ED beams with 170 mm of free length in the bandwidth of 0-1 kHz.

and thus obtain a hybrid damping VES-ED, the loss factor is increased by 260% in the first vibration mode, whereas te storage modulus remains constant.

Table 4.2. Experimental homogenised complex modulus, storage modulus and loss factor, of the VES and VES-ED obtained from the 170 mm long beams.

	E (GPa)		η	
	VES	VES-ED	VES	VES-ED
Mode 1	65.82 $\pm$ 1.83	65.91 $\pm$ 1.82	0.0131 $\pm$ 0.0020	0.0472 $\pm$ 0.0051
Mode 2	66.29 $\pm$ 1.13	66.30 $\pm$ 1.14	0.0105 $\pm$ 0.0012	0.0133 $\pm$ 0.0013
Mode 3	66.66 $\pm$ 0.93	66.68 $\pm$ 0.93	0.0086 $\pm$ 0.0004	0.0101 $\pm$ 0.0004

The experimental results shown highlight the efficiency of the VES-ED in attenuating structural vibration in a wide frequency bandwidth, without adding mass to the structure and compromising its mechanical properties. The proposed VES-ED constitutes a method of maximising the performance of thin VESs at low frequencies.

4.4.3 Inverse method to estimate the influence eddy currents

A new inverse method in order to estimate and model the influence of induced eddy currents is proposed. The inverse method serves for both cases, metallic and sandwich structures, the FEM model being different for each case. The inverse method and the eddy force model are based on the following assumptions:

- The influence of eddy currents on the vibrational response of the beam can be modelled by an eddy force parallel to the vibration direction.

- The eddy force exists only in the area where the magnetic field is applied.
- The eddy force is proportional to the velocity of the beam and can be expressed by a constant viscous damping matrix in the frequency domain.

The proposed eddy force, $\mathbf{F}^*_{\text{eddy}}$, consists of a lineal viscous force given by

$$\mathbf{F}^*_{\text{eddy}} = -c_{\text{e}}\mathbf{v}^*_{\text{z}}\,, \tag{4.1}$$

where c_{e} is the eddy damping coefficient and $\mathbf{v}^*_{\text{z}}$ is the complex transverse velocity of the metallic or sandwich structure. In the finite element form the eddy force can be expressed by an eddy damping matrix, $\mathbf{C}_{\text{eddy}}$, constant in frequency domain. Thus, the governing equation of motion of the metallic or sandwich structure incorporating the influence of eddy currents is given by

$$\mathbf{M}\ddot{\mathbf{q}} + \mathbf{C}_{\text{eddy}}\dot{\mathbf{q}} + \mathbf{K}^*\mathbf{q} = \mathbf{F}\,, \tag{4.2}$$

where $\mathbf{q}$, $\dot{\mathbf{q}}$ and $\ddot{\mathbf{q}}$ are the displacement, the velocity and the acceleration vectors, and where $\mathbf{M}$, $\mathbf{C}_{\text{eddy}}$, $\mathbf{K}^*$ and $\mathbf{F}$ are the global mass matrix, the global eddy damping matrix, the global complex stiffness matrix and the global force vector.

The proposed inverse method consists of minimising the residue between the experimental and numerical transfer functions at certain frequencies in order to identify the coefficient of the proposed eddy force model. The method departs from two experimental transfer functions, with and without induced eddy currents, of the same point of the beam. The transfer functions must include at least one resonance, not being necessary to measure the entire bandwidth under analysis. Then the control frequencies, frequencies where the residue between the experimental and numerical transfer functions will be minimized are selected and the minimization process starts. The numerical transfer function at the selected control frequencies is evaluated by FEM taking into account the proposed eddy force model. The minimization process is as follows: the value of c_{e} is initialised, the FEM model is updated, the numerical transfer function is computed for all the control frequencies, the error between the experimental and numerical transfer functions is obtained and the iterative process is repeated until the error becomes smaller than a certain specified tolerance or the maximum number of iterations is exceeded. The obtained value of c_{e} is unique and constant in frequency for a given system, and so the response of any point of the beam in any frequency bandwidth can be predicted. Figure 8.17 shows by way of summary a scheme of the inverse method.

In order to validate the proposed eddy force model and inverse method the numerical transfer function of the VES-ED was computed and compared with experimental one, Figure 8.18. The transfer functions of the second vibration mode were considered as the input data of the inverse method and with the determined c_{e} value the transfer function in the bandwidth of 0-1 kHz was computed. It is observed the correlation is good in all the bandwidth, the greatest deviation in the amplitude of transfer modulus

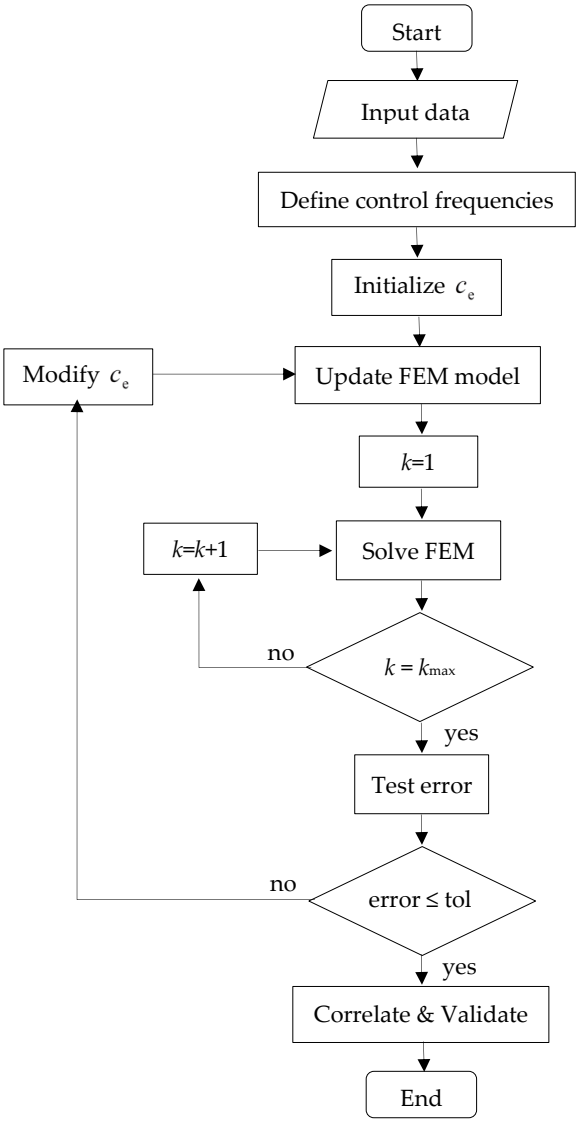

Figure 4.4. Scheme of the proposed inverse method for modelling the influence of induced eddy currents on conductive vibrating structures exposed to steady-state magnetic fields.

at the first resonance being due to the overestimated shear modulus of the viscoelastic film by the constitutive model at low frequencies.

4.5 Conclusions

This chapter analysed the influence of eddy currents induced in metallic skins on the dynamic behaviour of the sandwich. An experimental modal analysis with an aluminium cantilever beam in the absence of and under a magnetic field was carried out in the bandwidth of 0-1 kHz. The results reveal the induced eddy currents attenuate considerably the vibration of the beam in all the bandwidth without modifying its natural frequencies and mode shapes. In addition, the vibration of all the length of the

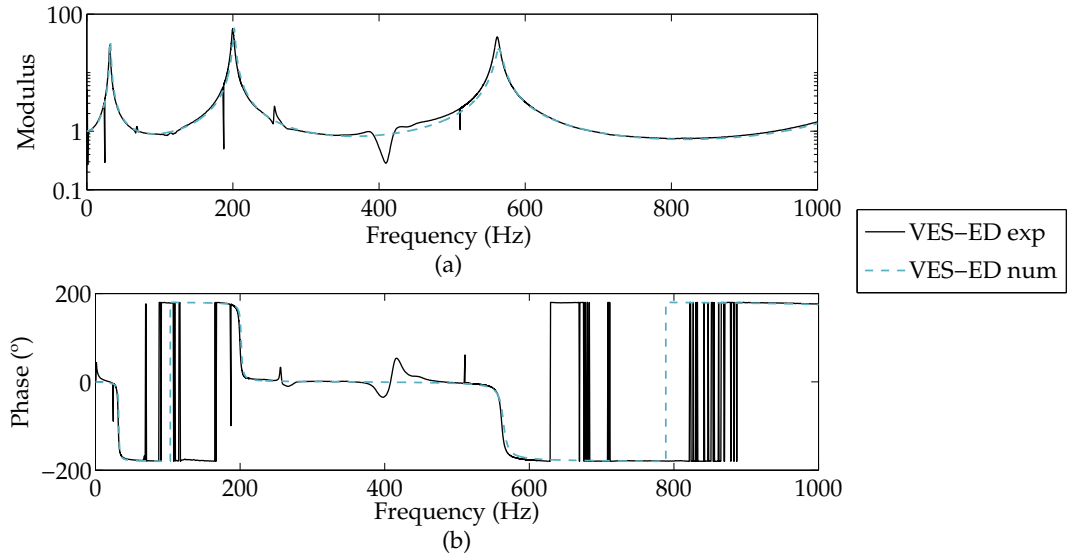

Figure 4.5. Experimental and numerical transfer function, (a) modulus and (b) phase, of the VES-ED beam with a free length of 170 mm in the bandwidth of 0-1 kHz.

beam is attenuated even if the magnetic field is applied only in a partial region.

A new hybrid sandwich structure combining viscoelastic and eddy current damping was proposed. The hybrid VES-ED consists of a thin VES and permanent magnets placed near, but not in contact with, the sandwich. Thus, when the VES-ED begins vibrating, energy is dissipated by two mechanisms: shear deformation of the viscoelastic film and eddy currents. The results highlighted the efficiency of the VES-ED attenuating structural vibration in a wide frequency bandwidth, without adding mass to the structure and compromising its mechanical properties. The proposed VES-ED constitutes a method of maximising the performance of thin VESs at low frequencies.

Finally, a new inverse method was developed in order to estimate and model the influence of induced eddy currents in metallic and sandwich structures.

4.6 Scientific contribution

Analysis and numerical modelling of eddy current damper for vibration problems

Leire Irazu and María Jesús Elejabarrieta
Mechanical & Manufacturing Department, Mondragon Unibertsitatea, Loramendi 4, 20500 Arrasate-Mondragon, Spain

Journal of Sound and Vibration
(Major revision)

Analysis and numerical modelling of eddy current damper for vibration problems

L. Irazu, M. J. Elejabarrieta*

Mechanical & Manufacturing Department, Mondragon Unibertsitatea, 20500 Arrasate-Mondragon, Spain

Abstract

This work deals with a contactless eddy current damper to attenuate structural vibration and has been motivated by two main issues. First, eddy currents have the potential to remove energy from dynamic systems without any contact and so without adding mass or modifying the rigidity of the structure. Second, there is a lack of analytical models to describe the complex multi-physics phenomenon involved. The dynamic properties of the contactless eddy current damper are analysed. To establish the influence of induced eddy currents on the dynamic response of the structure, an experimental modal analysis of a cantilever beam in absence of and under a partial magnetic field is carried out in the bandwidth of 0-1 kHz. The results show the eddy current phenomenon can attenuate the vibration of the whole structure without modifying the natural frequencies or the mode shapes of structure itself. A new inverse method to determine numerically the dynamic properties of the contactless eddy current damper is proposed. The proposed inverse method and the eddy current model based on a lineal viscous force are validated by a practical application. The numerically obtained transmissibility function correlates with the experimental one showing a good agreement in all the bandwidth of 0-1 kHz. The proposed method provides an easy and quick tool to model and predict the dynamic behaviour of the contactless eddy current damper, avoiding thus the use of complex analytical models.

Keywords: eddy current, vibration attenuation, modal analysis, inverse method

*Email address: mjelejabarrieta@mondragon.edu (Maria Jesus Elejabarrieta)

1. Introduction

The concept of eddy currents has been investigated since the late 1800s and many authors have proposed different uses of eddy currents for dynamic systems, such as braking systems, suppression of rotor vibration and damping of structural vibrations [1].

The main advantage of using the eddy current phenomenon to dampen structural vibration is the possibility to remove energy from the system without ever contacting the structure itself. This means that unlike in other damping techniques, such as viscoelastic materials or piezoelectric actuators, the system to be dampened remains unmodified and mass is not added to the structure.

Matsutzaki et al.[2, 3] were among the first to highlight the possibility of using electromagnetic forces to dampen vibrations of beams. They proposed attenuating the vibration of a periodically magnetised beam using electromagnetic forces generated by the current passing between the magnetised sections. Sodano et al. [4] analysed the vibration suppression capabilities of a cantilever beam by placing a magnet perpendicular to the beam motion and attaching a conductive sheet in the beam tip. In later works, they proposed the use of two magnets with the same polarity facing each other and the active movement of magnets to increase the damping added to the beam [5, 6]. Kwak et al. [7] proposed an eddy current damper consisting of a flexible linkage with two permanent magnets and a fixed copper plate attached to the end of the cantilever beam to be damped. Cheng et al. [8, 9] introduced an electromagnetic shunt damper to attenuate the vibrations of beams using eddy currents. Bae et al. [10, 11] suggested combining the classical tuned mass damper with the eddy current phenomenon using a permanent magnet as a concentrated mass of the tuned mass damper, while Berardengo et al. [12] proposed an adaptive tuned mass damper based on shape memory alloys and eddy currents. Stein et al. [13] proposed the damping of transversal vibrations of a clamped-clamped beams with a centre mass loading by a simple ferro-magnetic circuit. Recently, Maddah et al. [14] developed a hybrid damper consisting of an eddy current damper and a magnetorheological damper. Most of the works analysing the use of the eddy current phenomenon to attenuate vibration have focused on designing eddy current devices that magnify the damping added to the structure rather than focusing on the contactless characteristic of this phenomenon. Consequently, the proposed devices modify significantly the original structure to be damped.

In this work a contactless eddy current damper, which consists of applying steady state magnetic fields to conductive structures in order to dampen their vibration, is analysed. To the author's knowledge for the first time, an experimental modal analysis of a cantilever beam in absence of and under a partial magnetic field is carried out in the bandwidth of 0-1 kHz. The influence of the induced eddy currents on the natural frequencies and the mode shapes of the structure is studied, as well as the vibration attenuation. Once the dynamic behaviour of the contactless eddy current damper is known, a new inverse method is proposed to model it. The influence of induced eddy currents is modelled by a lineal viscous force which proportionality constant is named as eddy damping coefficient. The proposed inverse method determines the eddy damping coefficient of the contactless eddy current damper of any configuration.

The organisation of the paper is as follows: First the theoretical background of the eddy current phenomenon is presented. Then the experimental procedure and the analysis of the dynamic properties of the contactless eddy current damper is shown. Finally, the foundation of the inverse method is presented and a practical application is shown in order to validate the proposed eddy force model and inverse method.

2. Theoretical background

In this section the generation mechanism of eddy currents is described and the theoretical approaches proposed by other authors to model the eddy force generated on vibrating structures exposed to a steady-state magnetic field is reviewed.

When a conductive material experiences a time-varying magnetic field, electrical currents are induced. The induced current circulate in such a way that they induce their own magnetic field to oppose the change of magnetic field that created them. By the iteration of the induced eddy currents with the magnetic field a repulsive force is generated. Due to the electrical resistance of the conductor, eddy currents are dissipated into heat and so the force disappears. However, in dynamic systems with vibrating structures, there is a constant change in magnetic flux and the eddy currents are regenerated constantly allowing energy to be removed from the system.

The force generated due to eddy currents can be obtained from the Lorentz force law, given by

$$\mathbf{F} = \int_V \mathbf{J} \times \mathbf{B} \mathrm{d}V \,, \tag{1}$$

where $\mathbf{J}$ is the induced total eddy current density, $\mathbf{B}$ is the total magnetic flux density and V is the volume of the conductor.

In vibrating structures the eddy currents are induced through two different mechanisms:

- If the magnetic flux density varies in the space, the structure is exposed to a time-varying magnetic field when it starts vibrating. According to Faradays law of induction an electromotive force is induced in the conductor and an electric current flows through it, which can be obtained from

$$\mathbf{J} = \sigma \left(-\frac{\mathrm{d}}{\mathrm{d}t} \int_S \mathbf{B} \mathrm{d}S \right) \,, \tag{2}$$

  where σ is the conductivity of the conductor and S is the surface area.

- If the magnetic flux, $\mathbf{B}$, and the velocity of the beam, $\mathbf{v}$, are not parallel, a motional induced electromotive force is generated. The motional induced current density is given by

$$\mathbf{J} = \sigma \left(\mathbf{v} \mathbf{B} \right) \,. \tag{3}$$

The contactless eddy current damper analysed in this work consists of applying a steady-state magnetic field to a vibrating conductive beam. As an example, In Figure 1 a scheme of the contactless eddy current damper is shown composed of a cantilever beam and a permanent magnet placed in one side of the beam. In this system the eddy current is induced according to Equation 2 and Equation 3 and as a consequence the vibration is attenuated.

The contactless eddy current damper is a complex multi-physics phenomenon difficult to address analytically while taking into account all the effects involved in the phenomenon. In the bibliography, two different approaches are available. Sodano et al. [4, 5] provide a theoretical model of the eddy current damping force generated on a vibrating beam exposed to a cylindrical permanent magnet. They assume the deflection of the beam is in the transverse direction, thus the component of the magnetic field in that direction does not contribute to the generation of eddy current and eddy

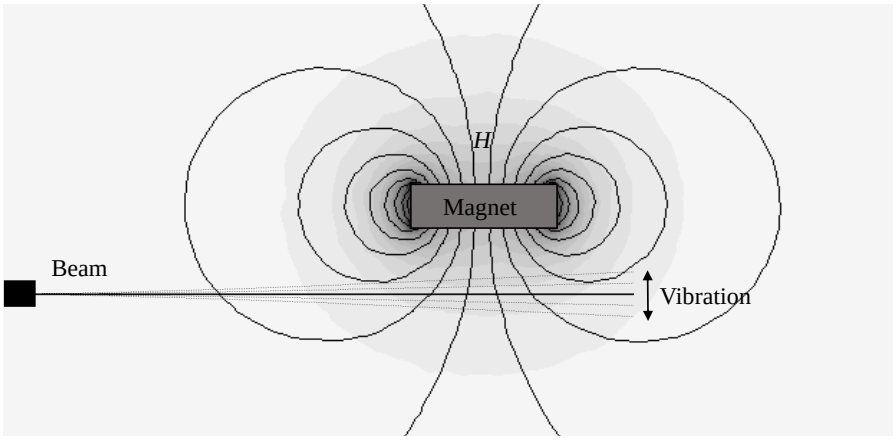

Figure 1: Scheme of the contactless eddy current damper.

force, and so only the radial magnetic flux does. Zhou and Wang [15] addressed analytically the magneto-elastic loads generated on a vibrating beam exposed to a steady-state homogenous magnetic field. In this case, they assume the magnetic field is just in the transverse direction, but, the beam has longitudinal extension and flexural deflection. Due to the lack of simple analytical models able to provide accurate results for different configurations of the contactless eddy current damper, in this work a new inverse method is proposed.

3. Experimental procedure

This section presents the experimental procedure used for measuring the dynamic response of the contactless eddy current damper. These measurements are used on the one hand to analyse the influence of induced eddy currents on the dynamic properties of the structure, and on the other hand as part of the input data of the proposed inverse method.

The analysed eddy current damper is composed of a beam made of aluminium alloy 2024-T3 and two neodymium magnets, NdFe 35 MGOe, Figure 2. The geometrical and physical properties of the beam are shown in Table 1.

The experimental tests consisted of forced vibrations with resonance in absence of and under a magnetic field [17]. The experimental setup is shown in Figure 2. The forced vibration was obtained by a base movement generated by an electrodynamic shaker. The base acceleration consisted of a

Table 1: Geometrical and physical properties of the beam

Thickness (mm)	Width (mm)	Length (mm)	Density (g/cm^3)	Storage modulus (GPa)	Loss factor
0.404 ± 0.002	9.9 ± 0.002	180 ± 0.2	2.77*	66.9 0.4**	0.0021 ± 0.0006**

*Data provided by the supplier.

**Experimental results according to the ASTM E 756-05 [16].

white noise in the frequency range from 0 to 1 kHz, and its magnitude, , was measured by a piezoelectric accelerometer and loopback controlled by a vibration controller. The response of the beam, , was measured by a laser vibrometer at a point located to 5 mm from the free end. Data acquisition and signal processing were performed with an analyser connected to a PC. In order to induce eddy currents on the vibrating beam, two neodymium magnets were placed on one side of the beam and parallel to its axis.

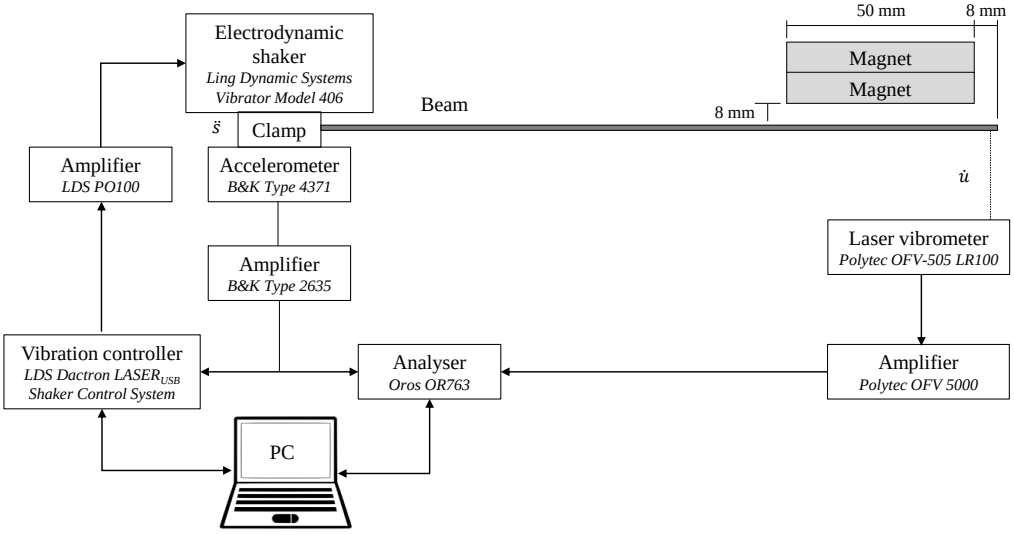

Figure 2: Scheme of the experimental set-up.

In the experimental tests, the transmissibility functions in the bandwidth of 0-1 kHz were measured. From the velocity signal of the free end, $\dot{u}$, and the

acceleration signal of the base, $\ddot{s}$, the transmissibility function is obtained as the ratio of the displacements of both points in the frequency domain, such as

$$_{\exp}T^{*}_{ij} = \frac{U_{j,\exp}}{S_{i,\exp}}\,, \tag{4}$$

where $U_{j,\exp}$ and $S_{i,\exp}$ are the Fourier transform of the displacement at the free end and the displacement applied at the base as shown in Figure 2. From the transmissibility function of all the bandwidth, the resonance frequencies were identified and the modal transmissibility functions were measured in order to obtain a higher resolution. The resolution goes from 0.003 Hz in the first mode to 0.02 Hz in the last mode.

The mode shapes of the beam were obtained from the transmissibility functions measured at several response DOF j, specifically every 5 mm along the length of the beam.

All the measurements were done at environmental temperature and in the linear range. In order to ensure the strain levels were kept within the linear range, a linearity analysis was performed before the tests. The linearity analysis involved exciting the beam with different acceleration levels and analysing the measured transmissibility functions to define the limit of the linear range. As an example, Figure 3 shows the linearity analysis conducted with a cantilever aluminium beam in the second vibration mode. It can be seen with excitation levels above 0.224 m/s^2, the transmissibility modulus and the resonance frequency are decreased, which means the deformations are over the linear range.

In Figure 4 the amplitude of the acceleration profile applied in the experimental tests is shown. Note the magnitude of the acceleration is increasing at low frequencies and remains constant after 250 Hz, in order to ensure linearity and obtain a good signal to noise ratio.

The magnetic field applied to the vibrating beam was obtained by placing two neodymium magnets, NdFe 35 MGOe, of 50 mm $\times$ 50 mm $\times$ 8 mm on one side of the beam and parallel to its axis, as seen in Figure 2. A simulation by means of finite element method (FEM) with the free software FEMM 4.2 was held to characterize the magnetic field intensity obtained with such magnets configuration. The simulation parameters were the following: 2D plane simulation, Improvised Asymptotic Boundary Condition [18] and 21408 triangular elements. In Figure 5 the magnetic field intensity distribution and the modulus of the magnetic field along the length of the beam is shown. It

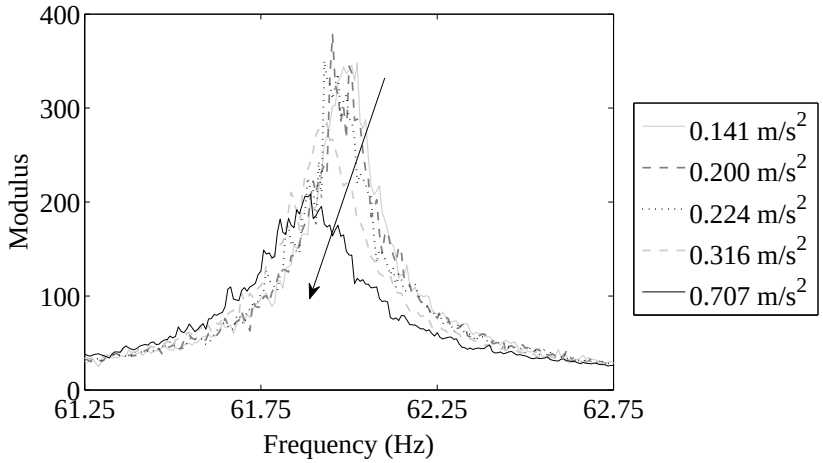

Figure 3: Linearity analysis of a 180 mm-long aluminium cantilever beam in the second vibration mode: experimental transmissibility modulus imder different base excitation levels.

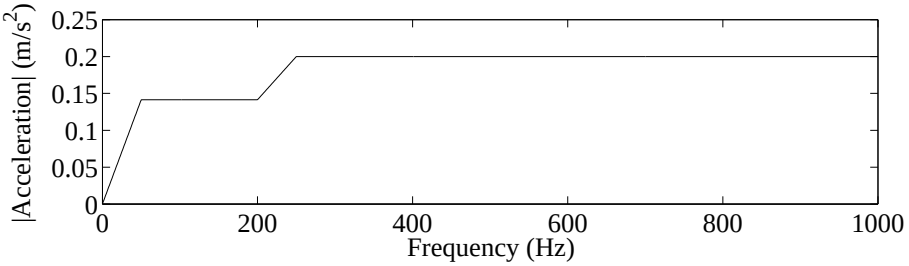

Figure 4: The amplitude pf the applied base acceleration profile in the bandwidth of 0-1 kHz.

can be seen the magnetic flux lines are almost perpendicular to the beam axis in the centre of the magnets and parallel in the boarder of the magnets. Regarding the modulus of the magnetic field, this has two maximums near the borders of the magnets and it is decreases considerably for x <100 mm.

4. Dynamic properties of the contactless eddy current damper

Following, the dynamic properties of the contactless eddy current damper are analysed. Specifically, the effect of applying a partial magnetic field to a vibrating conductive beam to induce eddy currents is studied. The

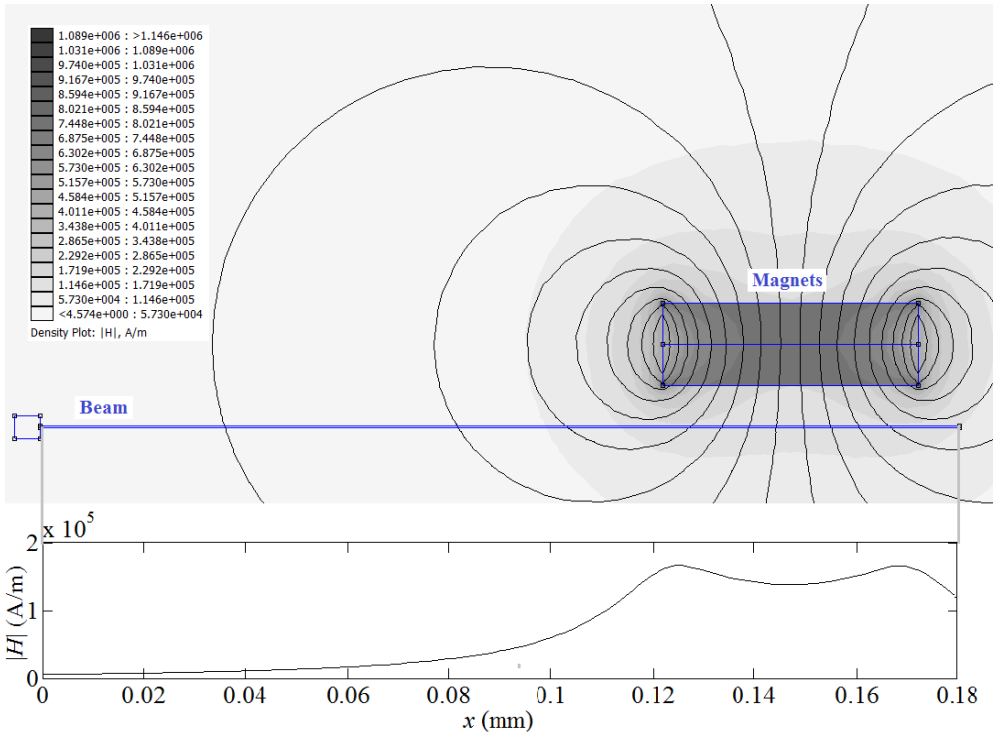

Figure 5: Simulation of the magnetic field by FEMM 4.2 software: the magnetic field intensity distribution and the modulus of the magnetic field along the length of the beam.

influence of such currents on the vibration attenuation and modal properties of the beam is analysed. Figure 6 shows the transmissibility function of the aluminium beam in absence of and under a partial magnetic field. It is observed that the natural frequencies remain unmodified in all the bandwidth of 0-1 kHz.

Table 2 shows the values of the natural frequencies and the transmissibility modulus obtained from the modal transmissibility functions. The natural frequencies of the beam are not modified when inducing eddy currents. The transmissibility modulus, instead, is decreased in all the resonances, which means the eddy currents attenuate the vibration of the beam in all the resonances in the bandwidth of 0-1 kHz. However, the relative attenuation of the beam is greater at low frequencies than at higher ones. In Table 3 the amplitude of the velocity of the beam without eddy currents in each vibration mode can be seen and it is concluded the influence of eddy currents is

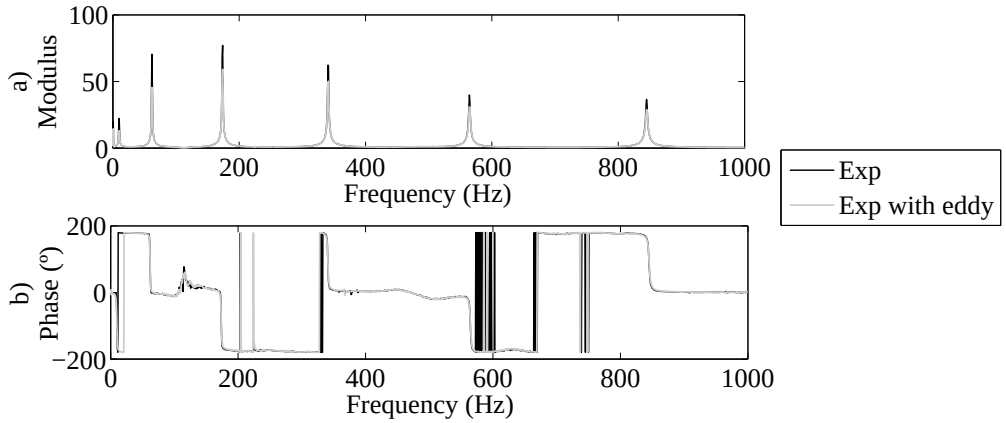

Figure 6: Experimental transmissibility function, a) modulus and b) phase, of the beam with and without eddy currents in the bandwidth of 0-1 kHz.

188 greater with higher velocities of the beam. This is consistent with what other
189 studies have shown [7, 9], such as that the induced eddy current density is
190 proportional to the transverse velocity of the beam. Note the transmissibility
191 modulus and the magnitude of the velocity in the first vibration mode are
192 lower than in the second one. This is due to a lack of resolution to properly
193 measure the first resonance.

Table 2: The natural frequencies and the transmissibility modulus of the beam in the free end with and wihout eddy currents in the bandwidth of 0-1 kHz.

	Natural frequency (Hz)		Transfer modulus	
	Without eddy currents	With eddy currents	Without eddy currents	With eddy currents
Mode 1	9.9	9.8	232	21
Mode 2	61.9	61.9	356	101
Mode 3	173.6	173.7	190	92
Mode 4	340.9	341.0	88	57
Mode 5	564.4	564.6	53	35
Mode 6	845.0	845.1	39	31

194 The attenuation of the beam due to the induced eddy currents can be
195 quantified by the loss factor, η. The loss factor is a dimensionless parameter

Table 3: The magnitude of the velocity of the beam's free end wihout eddy currents in the bandwidth of 0-1 kHz.

	Velocity (10-1 m/s)
Mode 1	1.119
Mode 2	1.293
Mode 3	0.247
Mode 4	0.082
Mode 5	0.030
Mode 6	0.016

that describes how damped an oscillator or resonator is in a vibration mode n. In this work the loss factor is obtained by the half-power bandwidth (HPB) method. As the value of the loss factor with and without eddy current are less than 0.1, the HPB method can be used to determine the loss factor with a lesser error than 0.1 % [19, 20]. In the HPB method the loss factor is obtained by the division of the bandwidth where the amplitude of the peak is reduced 3 dB, $\triangle f_n$, with the resonance frequency, f_n, such that

$$\eta_n = \frac{\triangle f_n}{f_n}\,. \tag{5}$$

In Figure 7 the influence of the eddy currents on the modal loss factor of the beam can be seen. When eddy currents are induced, the loss factor of the beam is increased in all the vibration modes in the bandwidth of 0-1 kHz. The increment of the loss factor in each vibration mode decreases with frequency. Specifically, in the first vibration mode the loss factor is increased more than 1200 % respect to the loss factor without induced eddy currents, whereas in the sixth vibration mode the increment is just of 22 %.

Figure 8 shows the experimental mode shapes, ψ, of the cantilever beam with and without induced eddy currents in the bandwidth of 0-1 kHz. The mode shapes are obtained from the modal transmissibility functions measured every 5 mm along the length of the beam. It is observed that the vibration amplitude is notably decreased in the first three vibration modes when applying a magnetic field. In addition, even if the magnetic field is applied in a partial region of the beam, Figure 2, the vibration is reduced in all the length of the beam. Figure 9 shows the theoretical [21] and the experimental mode shapes of the cantilever beam with and without eddy currents

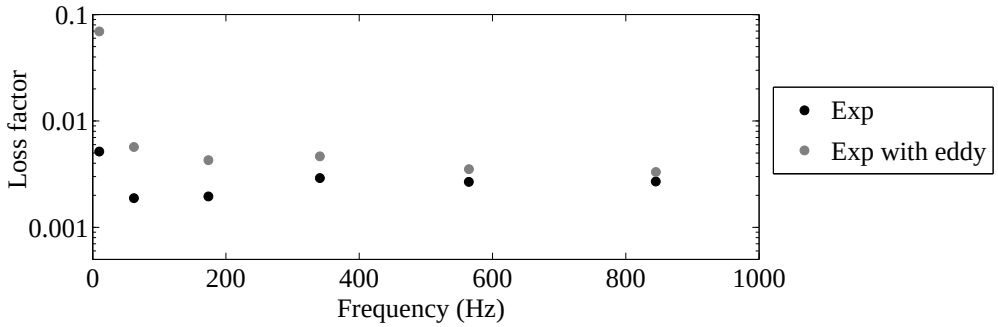

Figure 7: Experimental loss factor of the beam with and without eddy currents in the bandwidth of 0-1 kHz.

normalised to maximum displacement unit, ψ_{norm} . It is concluded that even though the vibration amplitude of the beam is decreased, the mode shape itself remains unmodified in all the analysed bandwidth.

These results show the possibility of attenuating vibrations of conductive structures by means of contactless eddy current damping mechanism without modifying the characteristics of the structure. When using the eddy current phenomenon to damp vibrations, the vibration amplitude of the structure is considerably decreased at resonances, whereas the natural frequencies and mode shapes remain unmodified. In addition, it is possible to attenuate the vibration of all the length of the beam, by applying a magnetic field only in a partial region of the beam.

5. Inverse method for modelling the contactless eddy current damper

A new inverse method is proposed in order to estimate the influence of eddy currents and facilitate the use of the contactless eddy current damper in real structures.

The proposed inverse method is based on two assumptions. First, the influence of the eddy currents on the vibrational response of the structure can be modelled by a force in the direction of the vibration actuating in the area of the structure where magnetic field is applied. Second, the eddy force is proportional to the velocity of the structure and it can be expressed by constant viscous damping matrix in frequency domain.

The inverse method minimizes the residue between the experimental and numerical transmissibility functions at certain frequencies in order to iden-

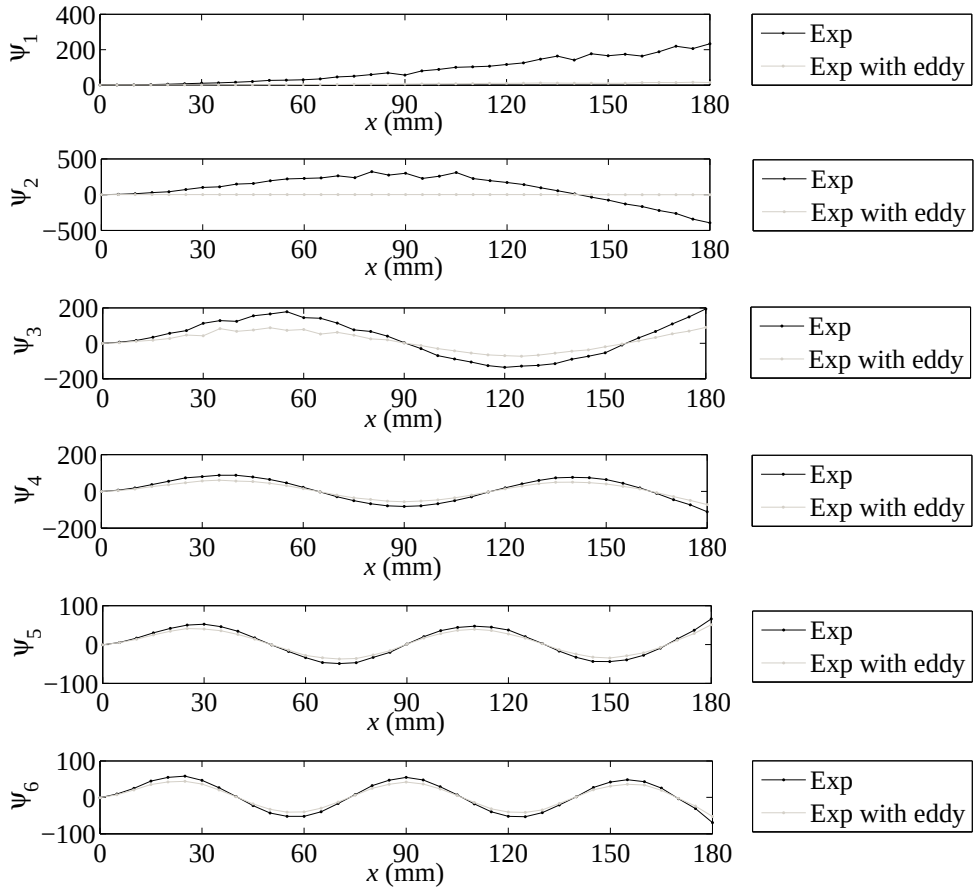

Figure 8: Experimental mode shapes of the cantilever beam with and without eddy currents in the bandwidth of 0-1 kHz.

tify the eddy damping coefficient of the proposed eddy force model. The method departs from two experimental transmissibility function, with and without induced eddy currents. Then the control frequencies, frequencies where the residue between the experimental and numerical transmissibility function will be minimized are selected and the minimization process starts. The numerical transmissibility function at the selected control frequencies is evaluated by FEM taking into account the proposed eddy force model. The minimization process is as follows: the value of the eddy damping coefficient is initialised, the FEM model is updated, the numerical transmissibility function is computed for all the control frequencies, the error between the

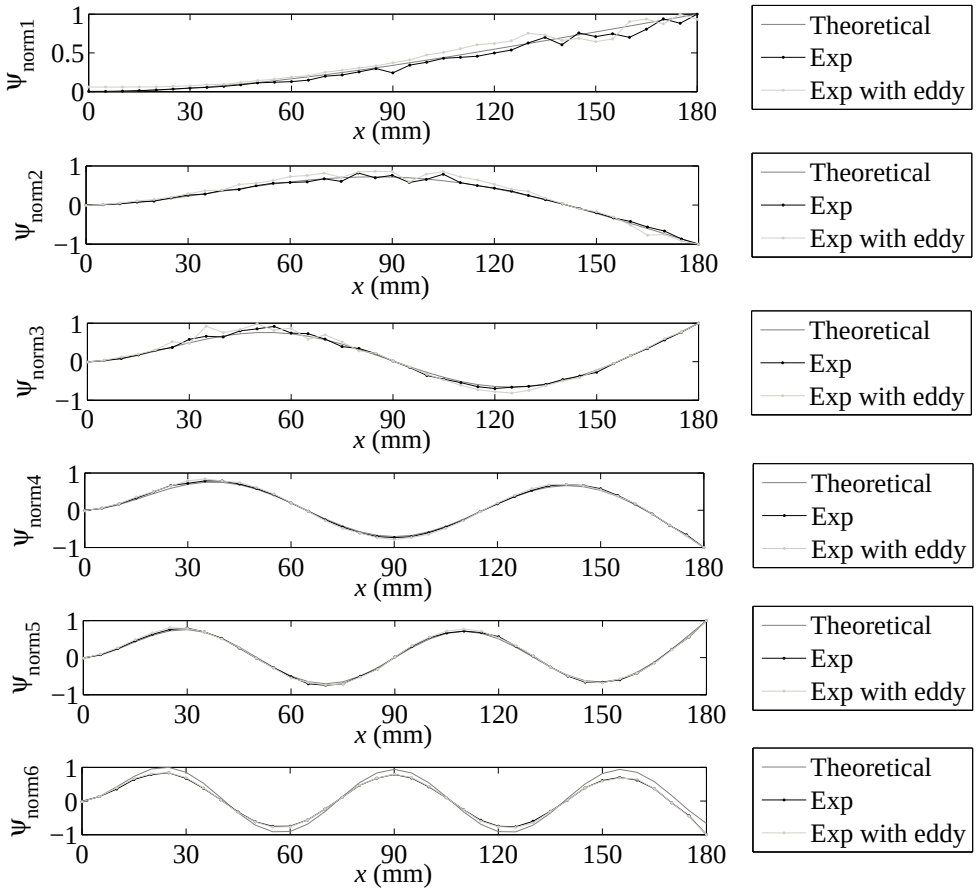

Figure 9: Experimental and theoretical mode shapes normalised to maximum displacement unit of the cantilever beam with and without eddy currents in the bandwidth of 0-1 kHz [21].

experimental and numerical transmissibility function is obtained and the iterative process is repeated until the error becomes smaller than a certain specified tolerance or the maximum number of iterations is exceeded. Figure 10 shows by way of summary a scheme of the inverse method.

Next, the input data, the selection of control frequencies, the eddy current model as a lineal viscous force, the FEM model and the minimisation procedure, is described in detail. Finally, a practical application is presented to validate the proposed numerical method.

260 *5.1. Input data*

261 The input data include the geometrical and physical properties of the
262 beam and two experimental transmissibility functions, with and without in-
263 duced eddy currents, of the same point of the beam. The transmissibility
264 functions are obtained by the forced vibration tests with resonance in ab-
265 sence of and under a magnetic field, as described in section 3, and these
266 must include at least one resonance in which the influence of eddy currents is
267 noticeable. That is to say it is enough to measure one modes transmissibility
268 function, being more appropriate the low vibration modes due to a bigger
269 influence of eddy currents in such modes. The selection of the response DOF
270 located on the free end is recommended as it does not coincide with any node
271 and provides a dynamic response with good signal-to-noise ratio.

272 *5.2. Control frequencies*

273 Control frequencies, f_k, at which the error between the experimental and
274 numerical dynamic responses is minimised must be selected by the user. The
275 use of these control frequencies improves the efficiency of the method as the
276 numerical transmissibilities are computed only at these frequencies.
277 The eddy currents affect the dynamic response of the beam mostly in the
278 vicinity of the resonance frequencies. Thus, the experimental transmissibil-
279 ity functions with and without induced currents are compared, the resonance
280 frequencies are identified and the lower and upper limits where the eddy cur-
281 rents affect the dynamic response of the beam are defined for each resonance.
282 Then control frequencies must be selected within the defined ranges, being
283 sufficient the selection of 15 frequencies. However, a greater number of points
284 may provide a better fit of the numerical dynamic response to the experi-
285 mental one.

286 *5.3. Eddy current model and finite element method*

287 The simple eddy current model proposed in this work consists on a lineal
288 viscous force. The eddy force exists just in the area where magnetic field is
289 applied, it has the direction of the structure's vibration and it is proportional
290 to the velocity of vibration. These hypothesis are in line with the theoretical
291 background presented in section 2 and the experimental results shown in
292 section 4. The proposed eddy force is given by,

$$\mathbf{F}_{\text{eddy}} = -c_{\text{e}}\mathbf{v}_z\,, \tag{6}$$

where c_e is the eddy damping coefficient and $\mathbf{v}_z$ is the transverse velocity of the structure.

In the finite element formulation, the Euler-Bernoulli beam theory is considered. The finite element is defined by two nodes with two DOF per node, the transverse displacement, w, and the rotational displacement, $\frac{\partial w}{\partial x}$, and Hermite cubic shape function, $\mathbf{N}_w$.

The governing equation of motion of a beam with induced eddy currents is given by

$$\mathbf{M}\ddot{\mathbf{u}} + \mathbf{K}\mathbf{u} = \mathbf{F} + \mathbf{F}_\mathrm{eddy}\,, \tag{7}$$

where $\mathbf{F}$, $\mathbf{F}_\mathrm{eddy}$, $\ddot{\mathbf{u}}$, and $\mathbf{u}$ are the external force, eddy force, acceleration and displacement vectors, respectively, and the dot denotes the differentiation with respect to time. $\mathbf{M}$ and $\mathbf{K}$ are the global mass and stiffness matrixes, respectively. In the finite element formulation the eddy force can be expressed by a viscous damping matrix and so the governing equation of motion results in

$$\mathbf{M}\ddot{\mathbf{u}} + \mathbf{C}_\mathrm{eddy}\dot{\mathbf{u}} + \mathbf{K}\mathbf{u} = \mathbf{F}\,, \tag{8}$$

where $\dot{u}$ is the velocity vector and $\mathbf{C}_\mathrm{eddy}$ is the global eddy damping matrix constant in frequency.

The eddy damping global matrix is obtained by assembling null matrixes for the elements where there is not an applied magnetic field and elementary eddy damping matrixes, $\mathbf{C}^e_\mathrm{eddy}$, for the elements to which a magnetic field is applied. The $\mathbf{C}^e_\mathrm{eddy}$ matrix is given by

$$\mathbf{C}^e_\mathrm{eddy} = \begin{bmatrix} \mathbf{C}_\mathrm{e} \\ \mathbf{0} \\ \mathbf{C}_\mathrm{e} \\ \mathbf{0} \end{bmatrix}\,, \tag{9}$$

where $\mathbf{C}_\mathrm{e} = c_\mathrm{e}\int_0^{l_\mathrm{e}} \mathbf{N}_w \mathrm{d}x$.

If a steady-state harmonic base excitation is considered and the motion equation is written in the frequency domain differentiating the DOF related to the base displacement and the unknown displacements, which are indicated by $(\bullet_\mathrm{s})$ and $(\bullet_\mathrm{u})$, respectively, the following is obtained

$$\left(-\omega^2 \begin{bmatrix} \mathbf{M}_{\mathrm{ss}} & \mathbf{M}_{\mathrm{su}} \\ \mathbf{M}_{\mathrm{us}} & \mathbf{M}_{\mathrm{uu}} \end{bmatrix} + \mathrm{i}\omega \begin{bmatrix} \mathbf{C}_{\mathrm{eddy,ss}} & \mathbf{C}_{\mathrm{eddy,su}} \\ \mathbf{C}_{\mathrm{eddy,us}} & \mathbf{C}_{\mathrm{eddy,uu}} \end{bmatrix} + \begin{bmatrix} \mathbf{K}_{\mathrm{ss}} & \mathbf{K}_{\mathrm{su}} \\ \mathbf{K}_{\mathrm{us}} & \mathbf{K}_{\mathrm{uu}} \end{bmatrix}\right) \begin{Bmatrix} \mathbf{S} \\ \mathbf{U} \end{Bmatrix} = \begin{Bmatrix} \mathbf{R} \\ \mathbf{0} \end{Bmatrix}, \tag{10}$$

where $\mathbf{S}$, $\mathbf{U}$ and $\mathbf{R}$ are the amplitude vectors in the frequency domain of the applied base motion, unknown displacement and reaction force on the base, respectively.

The direct frequency method is used to determine the unknown displacement amplitude vector, $\mathbf{U}$, which is computed for each control frequency in the minimisation process. The equation to be solved is derived from Equation 10 given by

$$\left(-\omega_k^2 \mathbf{M}_{\mathrm{uu}} + \mathrm{i}\omega_k \mathbf{C}_{\mathrm{eddy,uu}} + \mathbf{K}_{\mathrm{uu}}\right) \mathbf{U} = \left(\omega_k^2 \mathbf{M}_{\mathrm{us}} - \mathrm{i}\omega_k \mathbf{C}_{\mathrm{eddy,us}} - \mathbf{K}_{\mathrm{us}}\right) \mathbf{S}\,, \tag{11}$$

$$\mathbf{U} = \frac{\left(\omega_k^2 \mathbf{M}_{\mathrm{us}} - \mathrm{i}\omega_k \mathbf{C}_{\mathrm{eddy,us}} - \mathbf{K}_{\mathrm{us}}\right) \mathbf{S}}{\left(-\omega_k^2 \mathbf{M}_{\mathrm{uu}} + \mathrm{i}\omega_k \mathbf{C}_{\mathrm{eddy,uu}} + \mathbf{K}_{\mathrm{uu}}\right)}\,, \tag{12}$$

Finally, the transmissibility function, T_{ij}, can be obtained from

$$T_{ij} = \frac{U_j}{S_i}\,. \tag{13}$$

5.4. Minimisation procedure

In the minimization process the value of the eddy damping coefficient, c_{e}, is obtained by minimizing the residue between the experimental and numerical transmissibility function at the control frequencies. For that the Nelder-Mead algorithm is used [22], being the minimised function

$$\sqrt{\sum_{k=1}^{k=k_{\max}} \left(T_{ij,k} -_{\exp} T_{ij,k}\right)^2}\,, \tag{14}$$

where $k_{\max}$ is the total number of control frequencies.

In Figure 10 a summary scheme of the inverse method is shown.

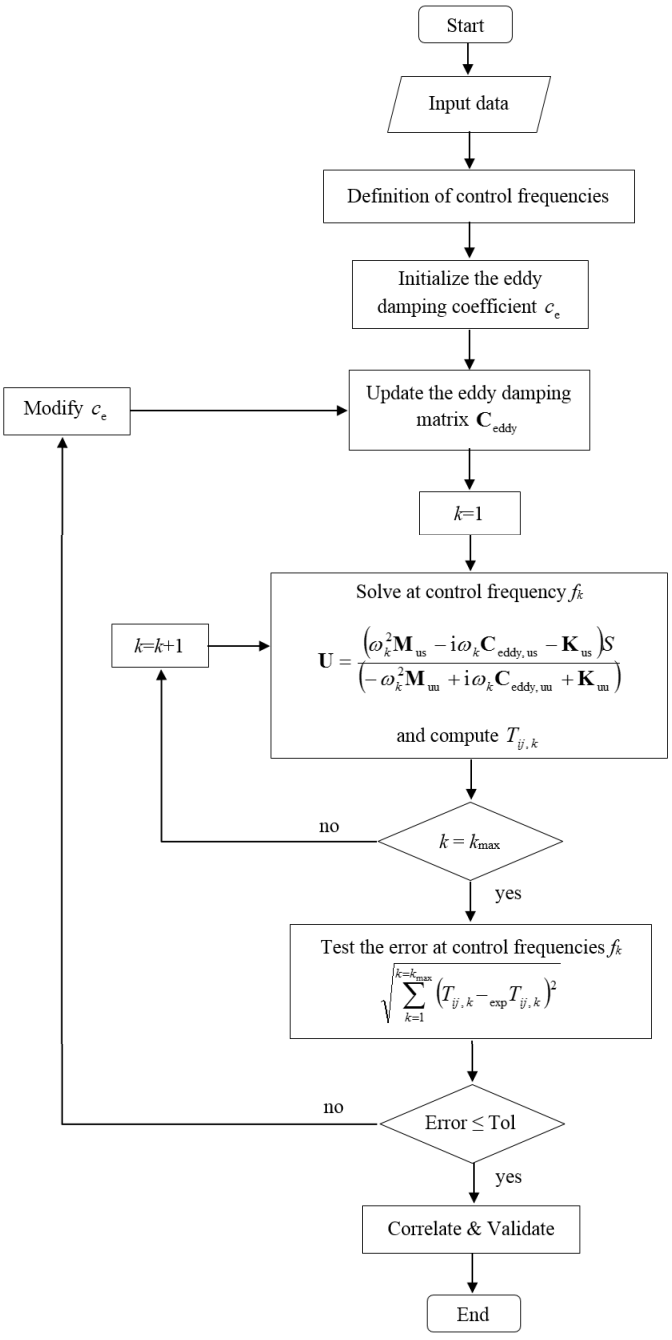

Figure 10: Scheme of the proposed inverse method for modelling the influence of induced eddy currents on vibrating structures exposed to steady-state magnetic fields.

5.5. Practical application

A practical application is presented to demonstrate the effectiveness of the proposed eddy force model and inverse method. Concretely, the dynamic response of the contactless eddy current damper described in section 3 is modelled by the inverse method.

The input data are the following: the geometrical and physical properties of the beam detailed in Table 1 and the experimental transmissibility function with and without induced eddy currents of the second vibration mode.

First, the numerical transmissibility function in absence of magnetic field is computed and compared with the experimental one in order to validate the FEM model to be used in the inverse method. As an example, in Figure 11 the numerical and experimental transmissibility modulus of the vibration modes in the bandwidth of 0-1 kHz are shown. The correlation is suitable except for the first vibration mode, being the discrepancy due to the lack of enough resolution to properly measure this mode. That is why the first modes experimental transmissibility functions are not chosen as input data and the second modes ones are used.

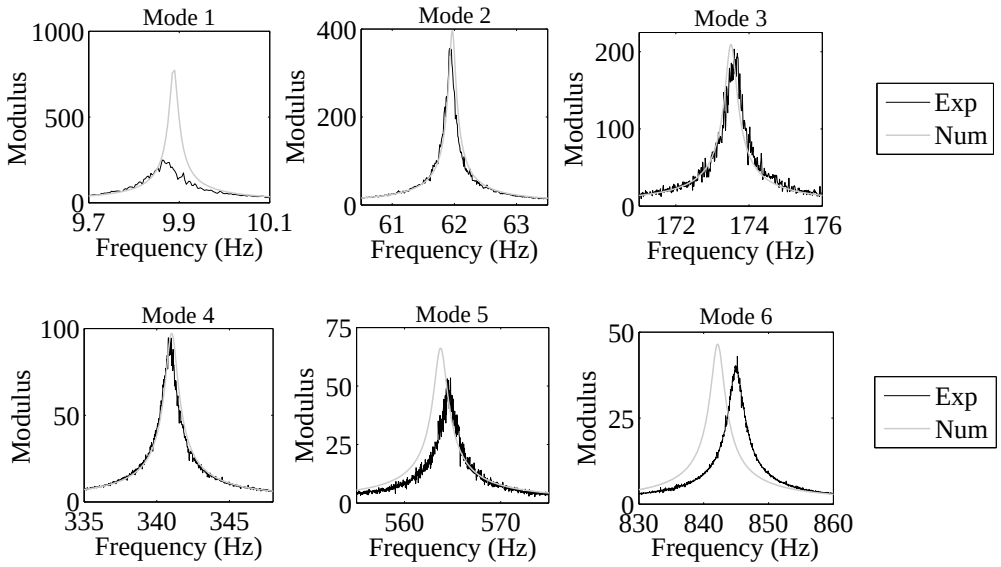

Figure 11: Numerical and experimental transmissibility modulus of the beam without eddy current in the bandwidth of 0-1 kHz.

Then, the lower and upper frequency limits where the eddy currents affect the vibrational response of the beam are defined for the second vibration

mode and 15 control frequencies are selected within the defined range. Figure 12 illustrates the transmissibility modulus of the beam with and without induced currents, the lower and upper frequency limits and the selected control frequencies.

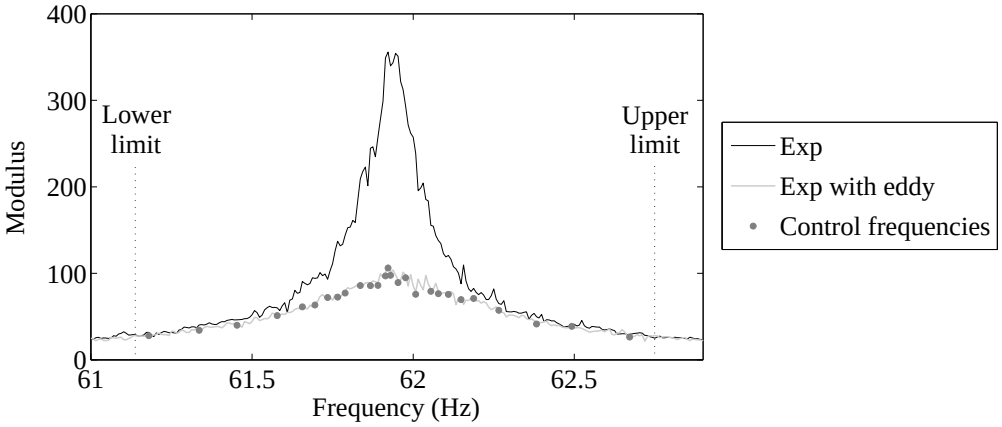

Figure 12: Experimental transmissibility modulus of the beam with and without eddy currents in the second vibration mode and the selected control frequencies.

Then the value of the eddy damping coefficient, c_e, is initialised and the minimization process starts, which consists on updating the FEM model, computing the numerical transmissibility function for all the control frequencies and obtaining the error between the experimental and numerical transmissibility function. The iterative process is repeated until an error smaller than a certain specified tolerance is obtained or the maximum number of iterations is exceeded. The value of the eddy damping coefficient obtained for the analysed contactless eddy current damper is $c_e = 0.0307$ Ns/m. Once the eddy damping coefficient is determined the dynamic properties of the contactless eddy current damper are known.

To validate the proposed eddy force model and inverse method the numerical transmissibility function of the second vibration mode is computed and compared with the experimental one. Figure 13 shows the correlation is good both in transmissibility modulus and in phase. In addition, it is observed the induced eddy currents attenuate significantly the vibration in the second vibration mode. In Figure 14 the eddy force actuating along the length of the beam in the second vibration mode, $f = 61.92$ Hz, is shown. The force exists just in the length where the magnetic field is applied and it

374 has the shape of the second vibration mode.

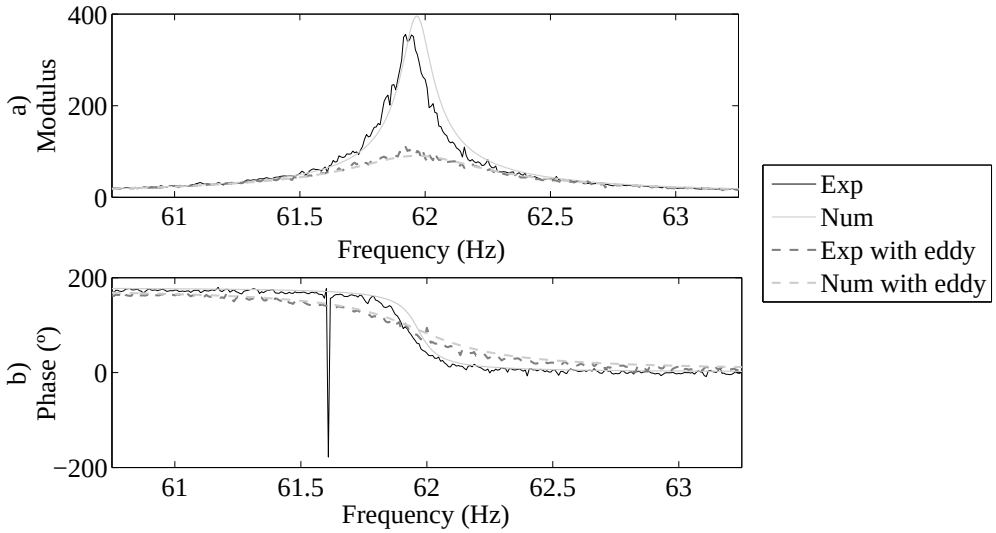

Figure 13: Experimental and numerical transmissibility function, a) modulus and b) phase, of the beam with and without eddy currents in the second vibration mode.

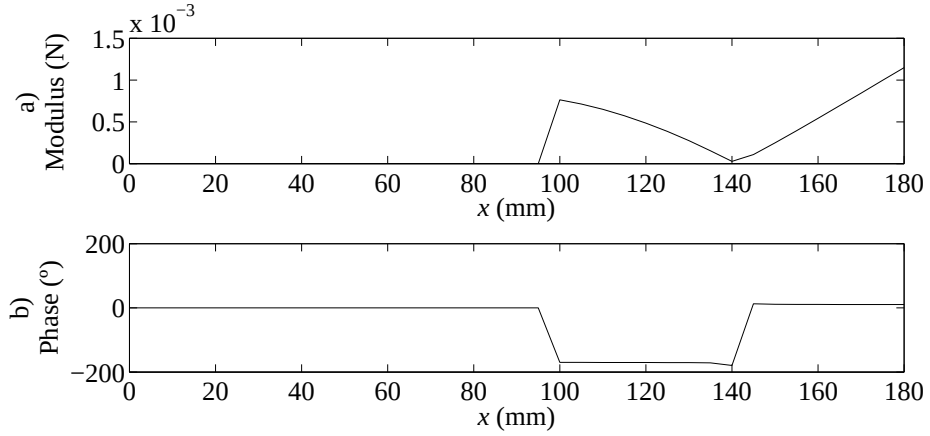

Figure 14: The eddy force, a) modulus and b) phase, along the length of the beam at $f = 61.92$ Hz with the minimised parameter $c_e = 0.0307$ Ns/m.

375 Once validated the obtained eddy damping coefficient, this can be used
376 to predict the vibrational response of the contactless eddy current damper

in any frequency bandwidth, as well as, the response of another point of the structure.

The numerical transmissibility function of the beam in the bandwidth of 0-1 kHz is computed with the c_e value obtained from the experimental results of the second vibration mode. Figure 15 show the experimental and numerical transmissibility functions of the beam with and without induced eddy currents. It is observed the correlation is good for all the bandwidth of 0-1 kHz, being the biggest deviations at high vibration modes. These results show the eddy current can be modelled by a lineal viscous force, proportional to the transverse velocity of the structure, Equation 6. This proportionality is given by the eddy damping coefficient and the eddy force can be expressed by a viscous damping coefficient not null only in the area where the magnetic field is applied and constant in frequency, Equation 8 and Equation 9.

Finally, the vibrational response of another point of the beam is predicted. In Figure 16 the influence of the induced eddy currents on the vibrational response of the beams point located at $x = 110$ mm is shown. It is observed the vibration of that point is significantly attenuated in the first two resonances.

These results highlight the proposed inverse method constitute an easy tool to model and predict the dynamic behaviour of the contactless eddy current damper of any configuration.

6. Practical application

This work brings two main contributions to the use of the contactless eddy current damper to attenuate structural vibration. On the one hand, the influence of induced eddy currents on the vibration attenuation and modal parameters of the structure was determined. On the other hand, a new numerical method was proposed to model the influence of eddy current and thus make up for the current lack of accurate theoretical models of this complex multi-physics phenomenon.

The dynamic properties of the contactless eddy current damper were analysed. For the first time, an experimental modal analysis of a cantilever beam was carried out in absence of and under a partial magnetic field in the bandwidth of 0-1 kHz. The results reveal the induced eddy currents attenuate considerably the vibration of the structure without modifying its natural frequencies and mode shapes. In addition, it is shown that it is possible to attenuate the vibration of the whole length of the beam by applying a magnetic field only in a partial region of the beam, a characteristic that makes

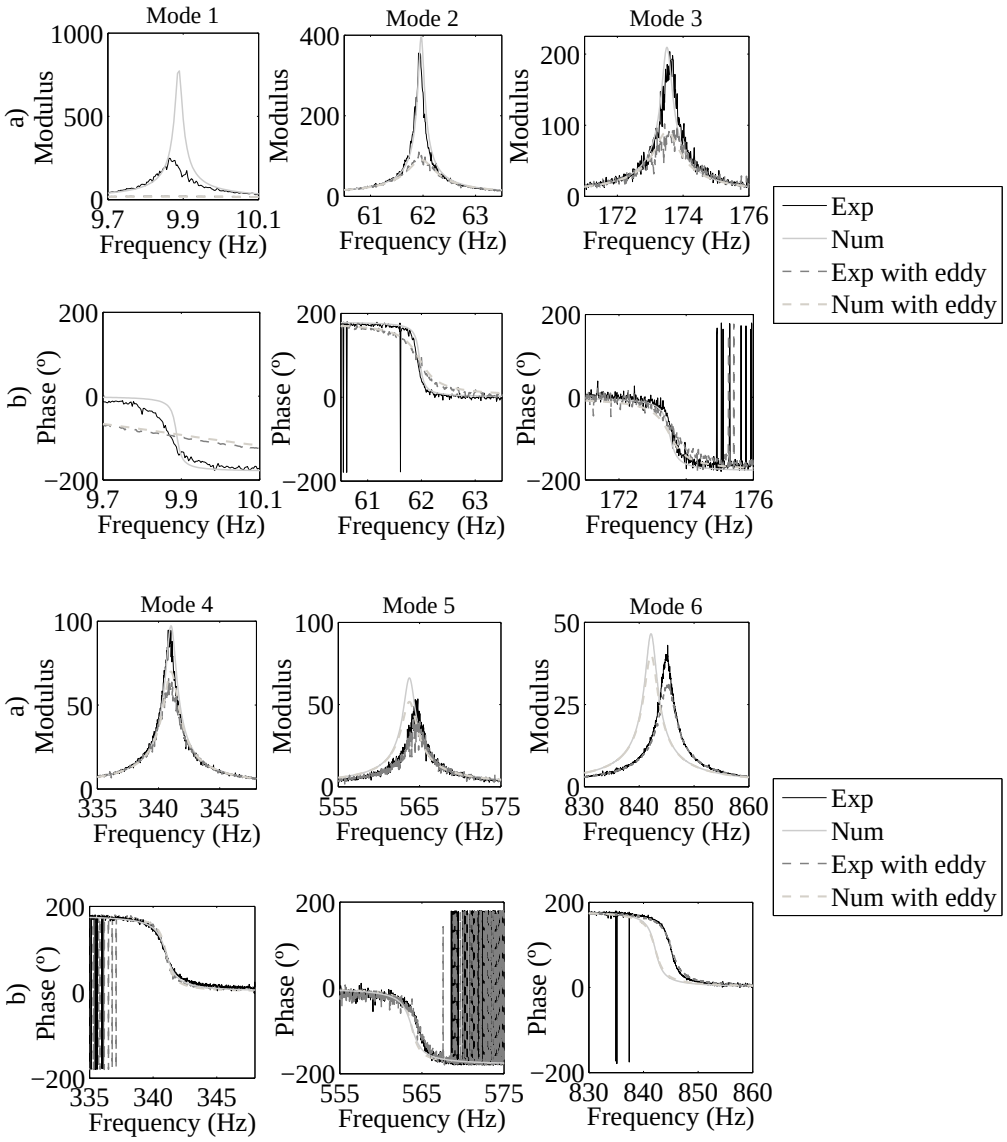

Figure 15: Experimental and numerical transmissibility function, a) modulus and b) phase, of the beam with eddy currents in the bandwidth of 0-1 kHz.

the implementation of the contactless eddy current damper even simpler.

A new inverse method was proposed in order to model the influence of induced eddy currents and facilitate the use of the contactless eddy current

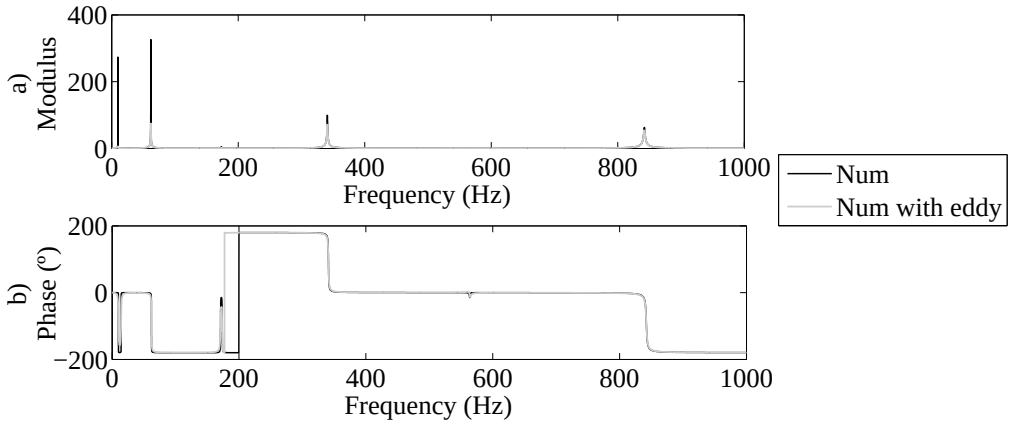

Figure 16: Numerical transmissibility function, s) modulus and b) phase, with and without eddy currents of the beams point $x = 110$ mm in the bandwidth of 0-1 kHz.

damper in several applications. The numerical method determines the eddy damping coefficient of the eddy force for any kind of contactless eddy current damper. The determined eddy damping coefficient is unique and constant in frequency, which allows to estimate the dynamic response of any point of the structure at any frequency bandwidth. The proposed eddy force model and inverse method are validated by a practical application. The numerically obtained transmissibility function correlates with the experimental one showing a good agreement in all the bandwidth of 0-1 kHz. The proposed method provides an easy and quick tool to model and predict the dynamic behaviour of the contactless eddy current damper, avoiding thus the use of complex analytical models.

Acknowledgements

The present study has been partially supported by AVISANI, DPI2015-71198-R and PI-2016-1-0026 research projects from Spanish and Basque Governments respectively.

References

[1] H. A. Sodano, J.-S. Bae, Eddy Current Damping in Structures, The Shock and Vibration Digest 36 (6) (2004) 469–478. doi:10.1177/0583102404048517.

[2] Y. Matsuzaki, D. Ishikubo, T. Kamita, T. Ikeda, Vibration Control System Using Electromagnetic Forces, Journal of Intelligent Material Systems and Structures 8 (9) (1997) 751–756. doi:10.1177/1045389X9700800904.
URL http://hjb.sagepub.com.proxy.lib.umich.edu/content/9/2/183.full.pdf+htmlhttp://journals.sagepub.com/doi/10.1177/1045389X9700800904

[3] Y. Matsuzaki, T. Ikeda, A. Nae, T. Sasaki, Electromagnetic forces for a new vibration control system: experimental verification, Smart Materials and Structures 9 (2) (2000) 127–131. doi:10.1088/0964-1726/9/2/301.
URL http://stacks.iop.org/0964-1726/9/i=2/a=301?key=crossref.e8520a4e9f1e3406e9daca8b1d2e3b29

[4] H. A. Sodano, J.-S. Bae, D. J. Inman, W. Keith Belvin, Concept and model of eddy current damper for vibration suppression of a beam, Journal of Sound and Vibration 288 (4-5) (2005) 1177–1196. doi:10.1016/j.jsv.2005.01.016.
URL http://linkinghub.elsevier.com/retrieve/pii/S0022460X05000817

[5] H. A. Sodano, J.-S. Bae, D. J. Inman, W. K. Belvin, Improved Concept and Model of Eddy Current Damper, Journal of Vibration and Acoustics 128 (3) (2006) 294. doi:10.1115/1.2172256.
URL http://reichling.physik.uos.de/download{_}paper.php?paper=JVibAcoust128p294(2006){_}Sodano.pdfhttp://vibrationacoustics.asmedigitalcollection.asme.org/article.aspx?articleid=1470848

[6] H. A. Sodano, D. J. Inman, Non-contact vibration control system employing an active eddy current damper, Journal of Sound and Vibration 305 (4-5) (2007) 596–613. doi:10.1016/j.jsv.2007.04.050.
URL http://linkinghub.elsevier.com/retrieve/pii/S0022460X07003434

[7] M. K. Kwak, M. I. Lee, S. Heo, Vibration suppression using eddy current damper, Korean Society for Noise and Vibration Engineering 13 (10) (2003) 760–766.

[8] T.-H. Cheng, I.-K. Oh, Vibration Suppression of Flexible Beam Using Electromagnetic Shunt Damper, IEEE Transactions on Magnetics 45 (6) (2009) 2758–2761. doi:10.1109/TMAG.2009.2020549.
URL http://files/414/abs{_}all.html{\%}5Cnhttp://ieeexplore.ieee.org/ielx5/20/4957672/04957720.pdf?tp={\&}arnumber=4957720{\&}isnumber=4957672http://ieeexplore.ieee.org/document/4957720/

[9] T. H. Cheng, D. J. Xuan, Z. Z. Li, Y. D. Shen, Vibration Control Using Shunted Electromagnetic Transducer, Applied Mechanics and Materials 26-28 (2010) 905–908. doi:10.4028/www.scientific.net/AMM.26-28.905.
URL http://www.scientific.net/AMM.26-28.905

[10] J.-S. Bae, J.-H. Hwang, J.-H. Roh, J.-H. Kim, M.-S. Yi, J. H. Lim, Vibration suppression of a cantilever beam using magnetically tuned-mass-damper, Journal of Sound and Vibration 331 (26) (2012) 5669–5684. doi:10.1016/j.jsv.2012.07.020.
URL http://dx.doi.org/10.1016/j.jsv.2012.07.020http://linkinghub.elsevier.com/retrieve/pii/S0022460X12005469

[11] J.-S. Bae, J.-H. Hwang, D.-G. Kwag, J. Park, D. J. Inman, Vibration Suppression of a Large Beam Structure Using Tuned Mass Damper and Eddy Current Damping, Shock and Vibration 2014 (2014) 1–10. doi:10.1155/2014/893914.
URL http://www.hindawi.com/journals/sv/2014/893914/

[12] M. Berardengo, A. Cigada, F. Guanziroli, S. Manzoni, Modelling and control of an adaptive tuned mass damper based on shape memory alloys and eddy currents, Journal of Sound and Vibration 349 (2015) 18–38. doi:10.1016/j.jsv.2015.03.036.
URL http://dx.doi.org/10.1016/j.jsv.2015.03.036http://linkinghub.elsevier.com/retrieve/pii/S0022460X15002758

[13] G. J. Stein, P. Tobolka, R. Chmurny, Ferromagnetic eddy current damper of beam transversal vibrations, Journal of Vibration and Control (2016) 1–12doi:10.1177/1077546316654791.
URL http://jvc.sagepub.com/cgi/doi/10.1177/1077546316654791

[14] A. Asghar Maddah, Y. Hojjat, M. Reza Karafi, M. Reza Ashory, Reduction of magneto rheological dampers stiffness by incorporating of an eddy current damper, Journal of Sound and Vibration 396 (2017) 51–68. doi:10.1016/j.jsv.2017.02.011.
URL http://dx.doi.org/10.1016/j.jsv.2017.02.011http://linkinghub.elsevier.com/retrieve/pii/S0022460X17301025

[15] G. Y. Zhou, Q. Wang, Use of magnetorheological elastomer in an adaptive sandwich beam with conductive skins. Part I: Magnetoelastic loads in conductive skins, International Journal of Solids and Structures 43 (17) (2006) 5386–5402. doi:10.1016/j.ijsolstr.2005.07.042.
URL http://linkinghub.elsevier.com/retrieve/pii/S0020768305004555

[16] ASTM, ASTM 756-05: Standard test method for measuring vibration-damping properties of materials (2005).

[17] L. Irazu, M. J. Elejabarrieta, Vibration attenuation of conductive beams by inducing eddy currents, Journal of Physics: Conference Series 744 (2016) 012007. doi:10.1088/1742-6596/744/1/012007.
URL http://stacks.iop.org/1742-6596/744/i=1/a=012007?key=crossref.9278021346f8149771f0217a3166f35a

[18] D. Meeker, Improvised Open Boundary Conditions for Magnetic Finite Elements, IEEE Transactions on Magnetics 49 (10) (2013) 5243–5247. doi:10.1109/TMAG.2013.2260348.
URL http://ieeexplore.ieee.org/document/6509478/

[19] F. Cortés, M. J. Elejabarrieta, Viscoelastic materials characterisation using the seismic response, Materials & Design 28 (7) (2007) 2054–2062. doi:10.1016/j.matdes.2006.05.032.
URL http://linkinghub.elsevier.com/retrieve/pii/S0261306906001816

[20] M. Martinez-Agirre, M. J. Elejabarrieta, Characterisation and modelling of viscoelastically damped sandwich structures, International Journal of Mechanical Sciences 52 (9) (2010) 1225–1233. doi:10.1016/j.ijmecsci.2010.05.010.
URL http://linkinghub.elsevier.com/retrieve/pii/S0020740310001475

[21] R. D. Blevins, Formulas for natural frequency and mode shape, Van Nostrand Reinhold Co, New York, 1979.

[22] J. A. Nelder, R. Mead, A Simplex Method for Function Minimization, The Computer Journal 7 (4) (1965) 308–313. doi:10.1093/comjnl/7.4.308.
URL http://comjnl.oxfordjournals.org/cgi/content/long/7/4/308https://academic.oup.com/comjnl/article-lookup/doi/10.1093/comjnl/7.4.308

A novel hybrid sandwich structure: viscoelastic and eddy current damping

Leire Irazu and María Jesús Elejabarrieta
Mechanical & Manufacturing Department, Mondragon Unibertsitatea, Loramendi 4, 20500 Arrasate-Mondragon, Spain

Materials and Design
(Revision)

A novel hybrid sandwich structure: viscoelastic and eddy current damping

L. Irazu, M. J. Elejabarrieta*

Mechanical & Manufacturing Department, Mondragon Unibertsitatea, 20500 Arrasate-Mondragon, Spain

Abstract

A novel hybrid damping sandwich structure (VES-ED) that can attenuate structural vibration in a wide frequency bandwidth, without adding mass to the structure or significantly modifying its mechanical properties, is proposed. The hybrid sandwich combines viscoelastic and eddy current damping and consists of a thin viscoelastic sandwich and two permanent magnets without contacting the sandwich. Experimental tests consisting of forced vibrations with resonance were carried out in the bandwidth of 0-1 kHz, and the vibrational response and the dynamic properties of the VES-ED were analysed. Finally, a numerical model of the VES-ED is presented and validated with experimental results obtained, in order to enable the use of the proposed hybrid damping sandwich in real applications.

The results show that the viscoelastic film of the VES-ED attenuated the vibration across the entire bandwidth, and the induced eddy currents suppressed the vibration to a greater extent at low frequencies. In addition, the VES-ED structure is lighter than the metallic structure. Thus, the proposed VES-ED can be used as substitute for metallic structures to obtain efficient attenuation of structural vibration across the bandwidth. In conclusion, the proposed hybrid constitutes a method of maximising the performance of conventional viscoelastic sandwiches.

Keywords: Hybrid damping, viscoelastic film, eddy current, lightweight structure, experimental characterisation, numerical model

*Email address: mjelejabarrieta@mondragon.edu (Maria Jesus Elejabarrieta)

1. Introduction

Vibration control is essential if mechanical structures are to achieve a desirable performance, such as low noise radiation, a long service life and high reliability. Passive damping techniques with viscoelastic materials are widely applied in structural vibration control, since they are cost-effective and easy to implement. These materials can be used in three different configurations to enhance the damping within a structure: free layer damping, constrained layer damping or sandwich, and tuned viscoelastic damping. Constrained layer damping, or sandwich, is the most effective of these and consists of restricting the viscoelastic material such that it lies between two elastic layers to form the sandwich structure. These sandwiches present high damping-to-weight, strength-to-weight and stiffness-to-weight ratios, and are therefore of particular interest to the aerospace, aeronautical, automotive and marine industries [1].

The dynamic behaviour of viscoelastic sandwich structures, together with their design, has been studied since the mid-20th century, as the performance and damping capabilities of sandwiches depend on various environmental factors, as well as on their design. The first studies in this field were conducted by Kerwin [2], and Ross, Ungar and Kerwin [3], who developed an analytical model to predict the damping effectiveness of viscoelastic sandwiches. Various authors subsequently analysed the influence of frequency, temperature, boundary conditions and thickness of viscoelastic and metallic layers on the damping of these sandwiches in the range of linear [4, 5] and non-linear vibration [6, 7, 8]. Recent studies have focused on the optimal design procedures for multi-layered sandwich structures [9, 10, 11, 12]. These procedures account for different variables in the design of the sandwich in order to obtain a goal, for example, to minimise mass and maximise damping. The optimal design of viscoelastic sandwiches is based on a trade-off between damping, mechanical properties and added weight, it not always being possible to achieve the required damping for a given application.

To overcome this disadvantage, the use of smart sandwiches, or the hybridisation of the sandwich, has been proposed in recent years. Smart sandwiches are able to modify their dynamic properties in response to an external stimulus, and they are obtained by replacing the conventional viscoelastic core by magnetorheological materials [13, 14], electrorheological materials [15, 16] or shape memory alloys [17]. The hybridisation of the sandwich instead consists of the simultaneous use of piezoelectric actuators and vis-

coelastic material to dampen vibration [18, 19]. The piezoelectric material can be directly attached to the sandwich structure or it can replace the constraining layer of the sandwich. These smart and hybrid sandwiches are efficient in attenuating structural vibration. Nevertheless, they present some drawbacks, such as the difficulty and cost of their manufacture, as well as their operational complexity since control strategies and a power supply are required. In addition, they are not comparable with conventional viscoelastic sandwiches, as they possess different physical properties.

Eddy currents are currents induced in conductive materials when these are subjected to time-variable magnetic fields. Different applications have been proposed with eddy currents being the most important ones braking systems and dampers of vibrations [20]. Sodano et al. studied the vibration suppression capabilities of a cantilever beam with a conductive sheet attached in the beam tip by means of different configurations of permanent magnets [21, 22, 23]. Cheng et al. [24, 25] proposed an electromagnetic shunt damper to attenuate the vibrations of beams using eddy currents. Bae et al. [26, 27] suggested combining the classical tuned mass damper with the eddy current phenomenon using a permanent magnet as a concentrated mass of the tuned mass damper. Berardengo et al. [28] developed an adaptive tuned mass damper based on shape memory alloys and eddy currents and recently Maddah et al. [29] proposed a hybrid damper consisting of an eddy current damper and a magnetorheological fluid damper. Most of the works analysing the use of the eddy current phenomenon to attenuate vibration have focused on designing eddy current devices that magnifies significantly the damping added to the structure, which sometimes results also in the modification of the original structure to be damped. However, as stated by Sodano and Bae [20] the eddy current phenomenon can be used to remove energy from the system without contacting the structure and this work is focused on such characteristic.

In the present study, a novel hybrid sandwich structure that combines viscoelastic and eddy current damping is proposed. The hybrid damping sandwich can passively attenuate the structural vibration in a wide bandwidth, without adding mass to the structure and compromising its mechanical properties. The proposed system consists of a thin viscoelastic sandwich with permanent magnets placed near, but not in contact with, the structure. The sandwich is composed of a micron-size viscoelastic adhesive and metallic layers. On the one hand, the thin viscoelastic adhesive attenuates the vibration across the entire bandwidth, with little decrement of the me-

chanical performance of the structure. On the other hand, the permanent magnets enable the induction of eddy currents in the metallic layers when the sandwich starts vibrating, which further attenuates the vibration at low frequencies. Thus, the proposed hybrid sandwich structure can efficiently suppress vibration in a wide bandwidth, and it constitutes a method of maximising the performance of conventional viscoelastic sandwiches. The field of application of the hybrid sandwich is focused on the vibration attenuation of different transport systems in the stop positions. The concept consists on substituting metallic plates of the movable structure by thin viscoelastic sandwiches and placing permanent magnets in the fixed structure of the stop positions.

First, the theoretical background of the proposed hybrid damping concept is detailed. The experimental procedure to characterise the dynamic properties of the viscoelastic sandwich (VES) and the proposed hybrid damping sandwich (VES-ED) is then presented. The vibrational response and the dynamic properties of the VES-ED in the bandwidth of 0-1 kHz are analysed via the experimental results obtained within the linear viscoelastic region. Finally, the numerical modelling of the VES-ED is presented and validated with experimental results, in order to enable the use of this hybrid damping sandwich in real applications. The numerical modelling of the VES-ED encompasses a four-parameter fractional derivative model for the viscoelastic adhesive, a finite element model for the sandwich structure and an inverse method to model the eddy force.

2. Theoretical background

The proposed hybrid damping sandwich structure consists of a combination of viscoelastic damping and eddy currents damping. In this section, the theory of the viscoelasticity and eddy currents is presented and the proposed VES-ED is described.

2.1. Viscoelastic damping

Viscoelastic damping is characteristic of many polymeric and glassy materials, showing both viscous and elastic characteristics, and it consists of the transformation of mechanical energy into heat. When a viscoelastic material is subjected to a dynamic harmonic load, the resulting deformation is also harmonic at the same frequency, but with a time delay [30]. The stress-strain relationship is characterised by a hysteresis loop, and one of the most

common ways of representing this loop is via structural damping, so that the stress-strain relationship is given by an ellipse considering the complex modulus, E^*, such as

$$\sigma(t) = E^*\epsilon(t) = (E' + \mathrm{i}E'')\,\epsilon(t) = E(1 + \mathrm{i}\eta)\,\epsilon(t)\ , \tag{1}$$

where σ is the stress, ϵ is the strain, $E = E'$ is the storage modulus, E'' is the loss modulus and $\eta = \frac{E''}{E'}$ is the loss factor. The energy dissipated by the viscoelastic material in each hysteresis loop depends on these material properties, which are affected by different factors, such as temperature, frequency, chemical composition, thermal treatments, static pre-strain or pre-stress, deformation level, etc. [31].

2.2. Eddy current damping

When a conductive material experiences a time-varying magnetic field, electrical currents, known as eddy currents, are induced in the conductor. These currents circulate in the direction in which they induce their own magnetic field with opposite polarity to the change in magnetic flux. An electromagnetic force is generated, which disappears when the induced currents are dissipated into heat. However, in dynamic systems there is a constant change in magnetic flux, which makes the eddy currents and the electromagnetic force constantly regenerate, allowing energy to be removed from the system.

The electromagnetic force, generated as a result of the induced eddy currents, can be obtained from the Lorentz force law, given by

$$\mathbf{F} = \int_V \mathbf{J} \times \mathbf{B}\mathrm{d}V\,, \tag{2}$$

where $\mathbf{J}$, $\mathbf{B}$ and V are the total eddy current density, the total magnetic flux density and the volume of the conductor, respectively. Eddy currents can be induced in the conductor through two different mechanisms: by subjecting the conductive material to a time-varying magnetic field or by a relative movement between the conductive material and magnetic field. In the first of these, the density of the induced eddy current is given by

$$\mathbf{J} = \sigma\left(-\frac{\mathrm{d}}{\mathrm{d}t}\int_S \mathbf{B}\mathrm{d}S\right)\,, \tag{3}$$

and in the second it is obtained from

$$\mathbf{J} = \sigma \left(\mathbf{v} \times \mathbf{B} \right) , \tag{4}$$

where σ is the conductivity of the conductor and S is the surface area. In addition, in the calculation of the eddy current density, $\mathbf{J}$, the surface charges generated at the end of the magnetic field projection area on the conductive material, as well as boundary conditions to account for zero current density at the edges of the conductive material, must be considered [32].

2.3. Hybrid damping sandwich

In the present study, a new hybrid damping sandwich structure based on viscoelastic and eddy current damping is proposed. The VES-ED consists of a thin VES exposed to, but not in contact with, permanent magnets, as shown in Figure 1. When the sandwich vibrates, the hybrid damping mechanism is as follows:

- The viscoelastic film is deformed in shear dissipating energy into heat, thereby attenuating the vibration across the entire bandwidth.

- Eddy currents are induced in the metallic layers and, by interacting with the magnetic field, an electromagnetic force is generated, further attenuating the vibration at low frequencies.

Thus, the VES-ED can efficiently suppress vibration in a wide frequency bandwidth. The novel hybrid damping sandwich is of particular interest for applications where structural vibration must be attenuated, without adding mass to the structure or modifying its mechanical properties.

3. Experimental procedure

The hybrid damping VES-ED consists of a thin VES and two permanent magnets, as shown in Figure 1. The VES is composed of two identical layers of aluminium alloy 1050 H18 and a micron-size polyester based adhesive. Its geometrical and physical properties are detailed in Table 1. In order to obtain the VES-ED, two neodymium magnets, NdFe 35 MGOe, were placed near, but not in contact with, the sandwich. Specifically, the magnets were placed parallel to the sandwich beam at a distance of $x_{\mathrm{m}} = 8$ mm from the surface of the sandwich and the free-end. The specifications of the magnets are detailed in Table 2, and the magnetic field along the length of the beam obtained with

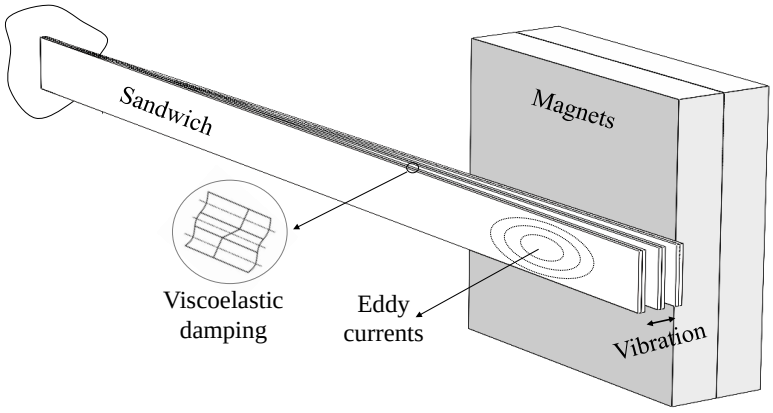

Figure 1: Scheme of the hybrid damping sandwich structure.

such a magnet configuration is shown in Figure 2. The magnetic field simulation was held by free Finite Element Method Magnetics software, version 4.2, considering a 2D planar problem and improvised asymptotic boundary conditions [33, 34] to solve the open boundary problem. It is observed that the magnetic field was at its maximum near the borders of the magnets and was almost null for $x < 90$ mm.

Table 1: Specifications of the viscoelastic sandwich and its components.

Viscoelastic sandwich			Metallic layer			Viscoelastic layer	
Thickness (mm)	Width (mm)	Density (g/cm^3)	Thickness (mm)	Density (g/cm^3)	Complex modulus (GPa)	Thickness (m)	Density (g/cm^3)
1.146 ± 0.003	9.900 ± 0.002	2.675 ± 0.008	0.564 ± 0.002	2.7*	68.11 + 0.1634i ± (0.68 + 0.0008i)**	18 ± 2	1.13*

*Data provided by the supplier, Replasa S.A.

**Data obtained from characterisation according to ASTM E 756-05.

Table 2: Specifications of the neodymium magnets.

Length (mm)	Width (mm)	Thickness (mm)	Grade
50	50	8	N35

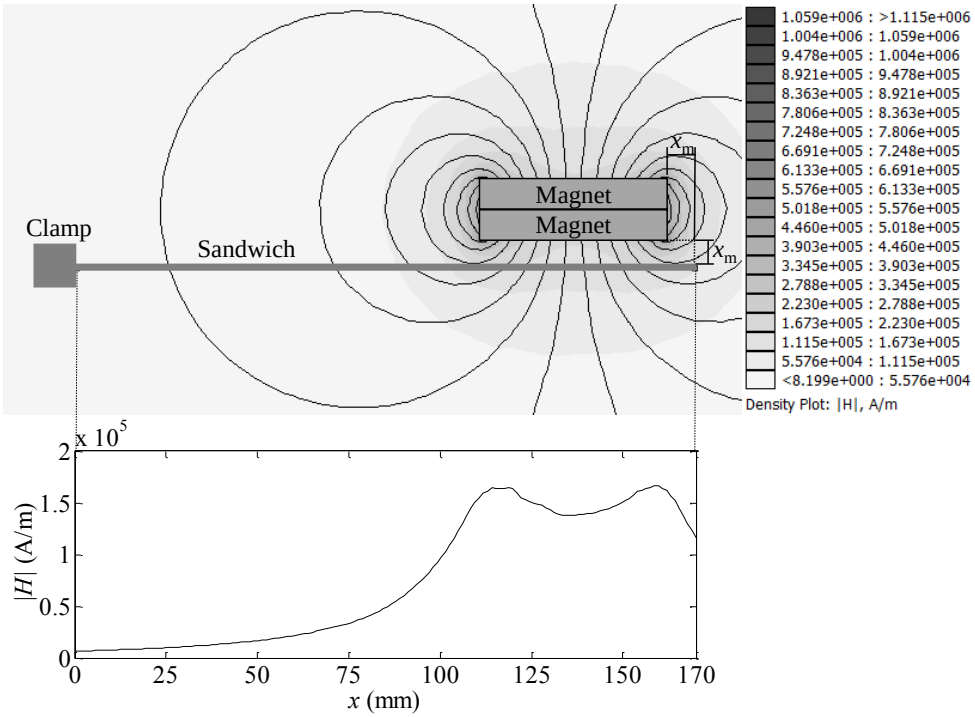

Figure 2: Simulation of the magnetic field by Finite Element Method Magnetics software, version 4.2: modulus of the magnetic field along the length of the sandwich beam.

3.1. Experimental technique

The experimental tests consisted of forced vibrations with resonance according to the ASTM E 756-05 standard [35] and the modification proposed by Cortes and Elejabarrieta [36], wherein the transmissibility functions were measured. First, tests in absence of magnets were carried out in order to obtain the dynamic properties of the VES. Magnets were then placed on one side of the sandwich beam to induce eddy currents and thus obtain the dynamic properties of the VES-ED. The VES and the VES-ED were tested in a cantilever configuration. From each sandwich, three specimens were tested, each having three different free lengths: 150 mm, 160 mm and 170 mm.

A photograph of the experimental set-up is shown in Figure 3. The seismic excitation was generated by an electrodynamic shaker (Ling Dynamic Systems Vibrator Model 406) and consisted of a white noise in the frequency

range of 0-1 kHz. The acceleration of the base was measured by a piezoelectric accelerometer (B&K Type 4371) and loopback controlled by a vibration controller (LDS Dactron LASERUSB Shaker Control System). The response of the structure was measured by a laser vibrometer (Polytec OFV-505 LR100) at the point placed 5 mm from the free end. The data acquisition and signal processing were performed using an analyser (Oros OR763) connected to a personal computer. The transmissibility functions, ${}_{\text{exp}}T^*$, were obtained by relating the acceleration of the free end of the beam with that applied at the base, so that

$$ {}_{\text{exp}}T^*(f) = \frac{U^*_{\text{exp}}(f)}{S^*_{\text{exp}}(f)}, \tag{5} $$

where $U^*_{\text{exp}}(f)$ and $s^*_{\text{exp}}(f)$ are the Fourier transform of the displacements measured by the laser vibrometer at the free end and by the accelerometer at the base.

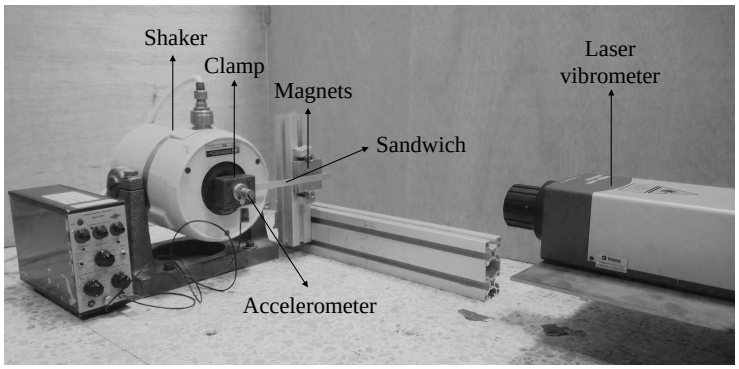

Figure 3: Scheme of the hybrid damping sandwich structure.

The dynamic properties of viscoelastic sandwiches besides depending of frequency, also depend on temperature and strain level. In this work, all measurements were made at environmental temperature and in the linear viscoelastic region. In order to ensure this, a linearity analysis was carried out, which consisted on exciting the VES with different acceleration levels. When the deformations of the VES are over the linear range, its stiffness decreases and the loss factor increases. In Figure 4 the linearity analysis carried with VES beam is shown and the acceleration value of 0.1 m/s^2 was defined as the limit to ensure linear vibration.

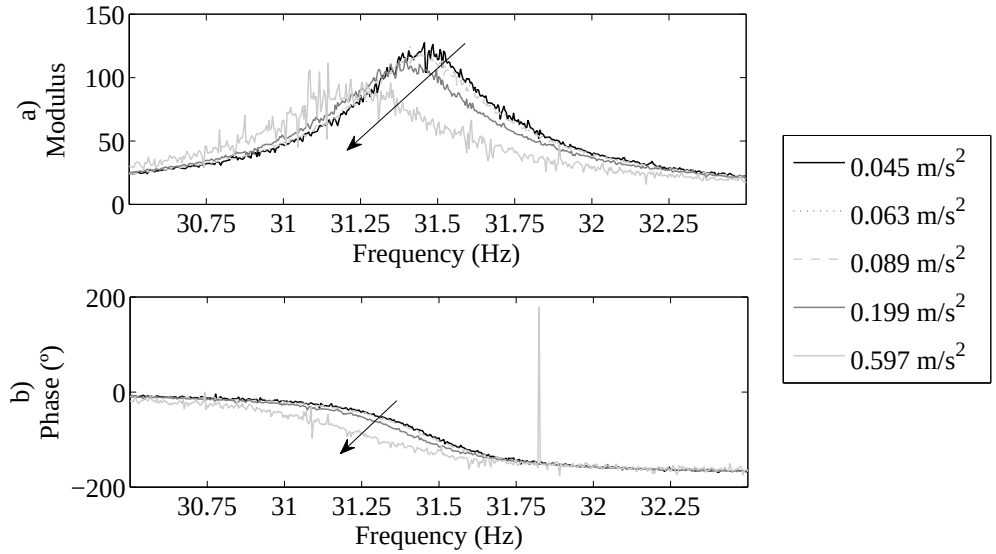

Figure 4: Linearity analysis of the viscoelastic sandwich: first mode transmissibility function of the sandwich beam with a free length o 0-1 kHz under different excitation levels.

The transmissibility functions measured in the absence of magnets were used to characterise the dynamic properties of the VES, and those measured under the magnetic field generated by the permanent magnets were used to obtain the dynamic properties of the VES-ED. The dynamic properties of both the VES and VES-ED were obtained as detailed in the ASTM E 756-05 standard [35]. The storage modulus, E, is given by

$$E\left(f\right) = \frac{12\rho L^4 f_n^2}{H^2 C_n^2}\,, \tag{6}$$

where ρ is the density of the sandwich, H is the total thickness of the sandwich, L is the free length, f_n is the resonance frequency of mode n and C_n is the coefficient for mode n of clamped-free configuration [35]. The loss factor, η, is evaluated by the half-power bandwidth method, for which the resonance frequency and the frequencies above and below the resonance frequency, where the value of the transmissibility modulus is 3 dB less than the value at resonance, must be obtained. The loss factor is the ratio of the frequency difference between the upper 3 dB and the lower 3 dB, Δf_n, to the resonance frequency, given by

$$\eta(f) = \frac{\Delta f_n}{f_n}. \tag{7}$$

Finally, assuming that the VES and VES-ED show linear viscoelastic behaviour, their homogenised complex modulus, E^*, is expressed as

$$E^*(f) = E(f)(1 + \mathrm{i}\eta(f)). \tag{8}$$

4. Dynamic analysis of the hybrid damping sandwich

In this section, the efficiency of the proposed hybrid damping VES-ED in attenuating structural vibration in a wide frequency bandwidth is analysed via the experimental results. The analysis is limited to the range of linear vibrations of the VES-ED. First, the influence on its vibrational response and dynamic properties, as a result of replacing a metallic structure with a thin VES, is shown. The effect of placing permanent magnets near the VES in order to induce eddy currents in the metallic layers of the sandwich, and thus obtain a hybrid damping VES-ED, is then analysed.

The dynamic response of a metallic beam was compared with that of a thin VES of the same thickness. The numerical transmissibility function of an aluminium beam of 1.146 mm thickness and the experimental transmissibility function of the VES (Table 1), are compared in Figure 5. The numerical transmissibility function of the aluminium beam was simulated by the finite element method (FEM) assuming a Euler-Bernoulli beam and the properties of the aluminium, as shown in Table 1. It is observed that by replacing the aluminium beam with a thin VES, the transmissibility modulus, and thereby the vibration amplitude, were decreased in all the resonances. In addition, the resonance frequencies were slightly decreased. Figure 6 shows the dynamic properties of the aluminium and the thin VES. The storage modulus of the VES was slightly smaller than that of the aluminium across the entire bandwidth, whereas the loss factor was larger. With regard to the frequency dependency of the VES, its storage modulus increased in frequency and the loss factor decreased. Finally, analysing Figure 5 and Figure 6, it is concluded that the vibrational behaviour of the VES beam was superior to that of the aluminium beam, at the expense of a small decrease in the stiffness of the structure.

In order to further improve the damping capabilities of the VES, the use of a hybrid damping VES-ED is proposed in the present study. VES-ED

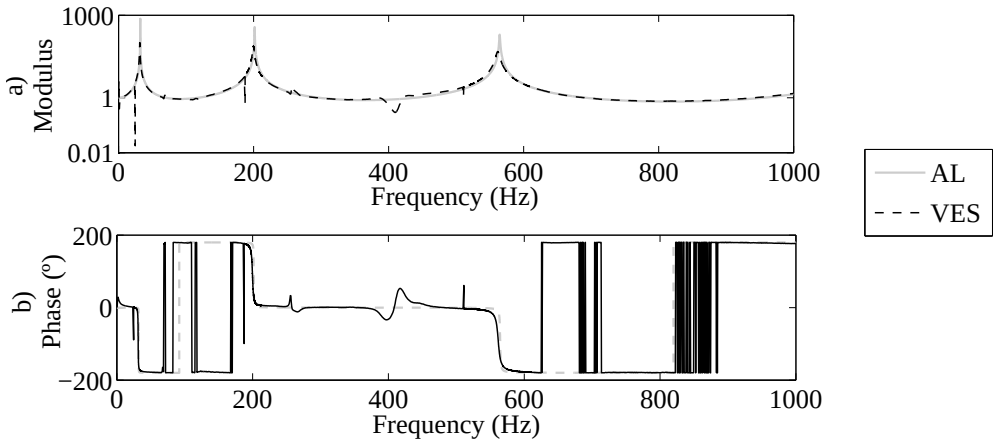

Figure 5: Numerical and experimental transmissibility functions, a) modulus and b) phase, of the aluminium and viscoelastic sandwich beams with a free length of 170 mm in the bandwidth of 0-1 kHz.

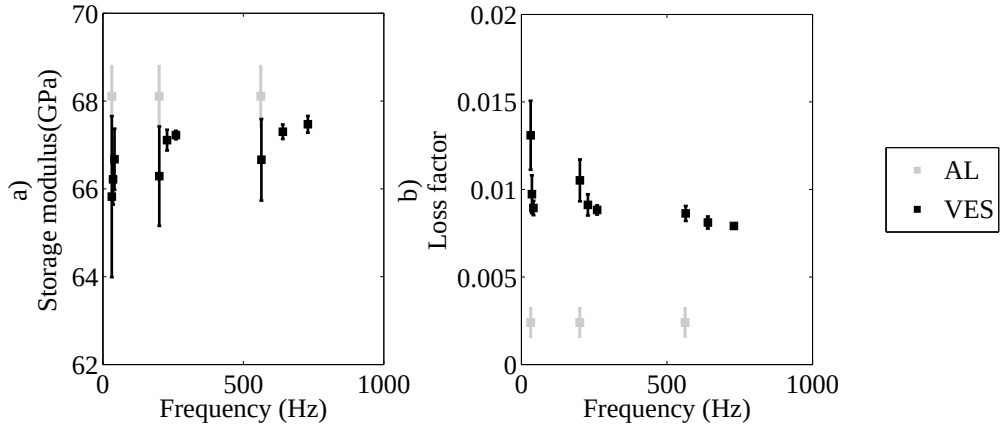

Figure 6: Experimental dynamic properties, a) storage modulus and b) loss factor, of the aluminium and viscoelastic sandwich.

consists of placing two permanent magnets near, but not in contact with, the free end of the VES, to enable the induction of eddy currents in the metallic layers of the sandwich. Thus, when the VES-ED begins vibrating, energy is dissipated by two mechanisms: shear deformation of the viscoelastic film and eddy currents. The transmissibility functions of the resonances within the bandwidth of 0-1 kHz of the VES and VES-ED are shown in Figure 7.

It is observed that the induced eddy currents decreased the transmissibility modulus of the structure in all the resonances, with this tendency being greater at low vibration modes. In addition, the induced currents did not modify the resonance frequencies of the sandwich structure or its stiffness. Figure 8 shows the loss factor of the VES and VES-ED. Due to the hybrid damping mechanism of the VES-ED, the loss factor of the sandwich increased significantly in the first vibration mode, whereas the increment was smaller in the second and third modes.

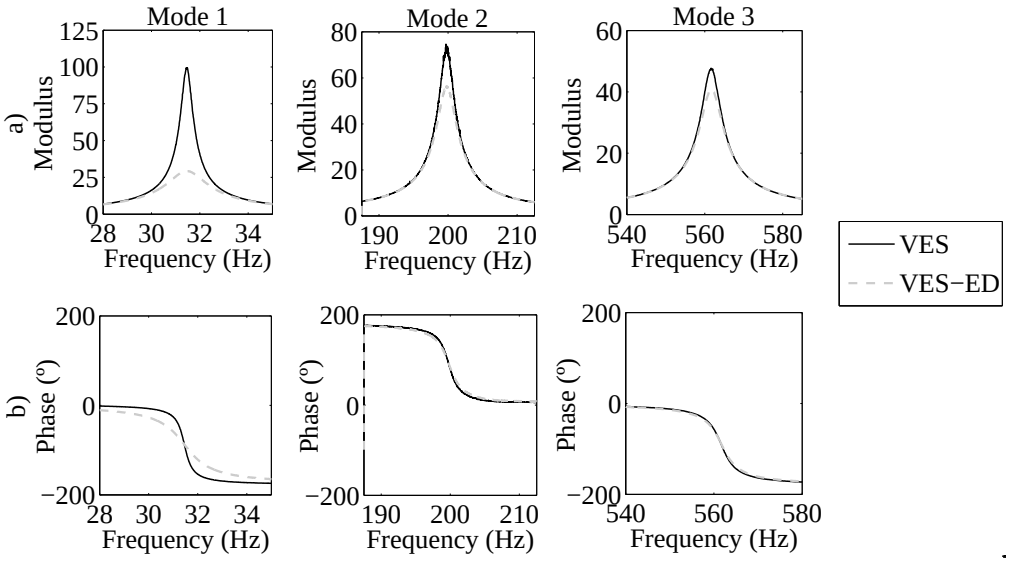

Figure 7: Experimental transmissibility function, a) modulus and b) phase, of the viscoelastic sandwich and viscoelastic sandwich with eddy currents beams with a free length of 170 mm in the bandwidth of 0-1 kHz.

Table 3 and Table 4 show all of the experimental dynamic properties of the VES and the VES-ED obtained from forced vibration tests with three different free lengths. The results are all an average of three specimens, with their corresponding standard deviations. It is clearly observed that whereas the resonance frequency and the storage modulus of the VES and VES-ED were similar, the loss factor of VES-ED was bigger than the VES loss factors.

The experimental results shown highlight the efficiency of VES-ED in attenuating vibration in a wide frequency bandwidth, without adding mass to the structure or significantly modifying its mechanical properties. For example, if an aluminium beam of 1.146 mm thickness is replaced with a

Table 3: The resonance frequencies and the homogenised complex modulus of the viscoelastic sandwich.

Viscoelastic sandwich				
f (Hz)	Mode No.	L (mm)	E (GPa)	η
31.96 ± 0.45	1	170	65.82 ± 1.83	0.0131 ± 0.0020
36.20 ± 0.16	1	160	66.22 ± 0.57	0.0097 ± 0.0011
41.35 ± 0.22	1	150	66.67 ± 0.70	0.0089 ± 0.0004
201.01 ± 1.72	2	170	66.29 ± 1.13	0.0105 ± 0.0012
228.42 ± 0.40	2	160	67.11 ± 0.24	0.0091 ± 0.0006
260.22 ± 0.19	2	150	67.23 ± 0.10	0.0088 ± 0.0003
564.43 ± 3.93	3	170	66.66 ± 0.93	0.0086 ± 0.0004
640.48 ± 0.78	3	160	67.30 ± 0.16	0.0081 ± 0.0003
729.9 ± 1.02	3	150	67.47 ± 0.19	0.0079 ± 0.0001

Table 4: The resonance frequencies and the homogenised complex modulus of the viscoelastic sandwich with eddy currents.

Viscoelastic sandwich				
f (Hz)	Mode No.	L (mm)	E (GPa)	η
31.98 ± 0.44	1	170	65.91 ± 1.82	0.0472 ± 0.0051
36.23 ± 0.15	1	160	66.30 ± 0.56	0.0413 ± 0.0021
41.37 ± 0.22	1	150	66.73 ± 0.69	0.0343 ± 0.0025
201.04 ± 1.72	2	170	66.30 ± 1.14	0.0133 ± 0.0013
228.46 ± 0.40	2	160	67.14 ± 0.24	0.0119 ± 0.0007
260.25 ± 0.20	2	150	67.24 ± 0.10	0.0114 ± 0.0000
564.52 ± 3.95	3	170	66.68 ± 0.93	0.0101 ± 0.0004
640.54 ± 0.81	3	160	67.31 ± 0.17	0.0093 ± 0.0004
730.03 ± 1.03	3	150	67.49 ± 0.19	0.0090 ± 0.0002

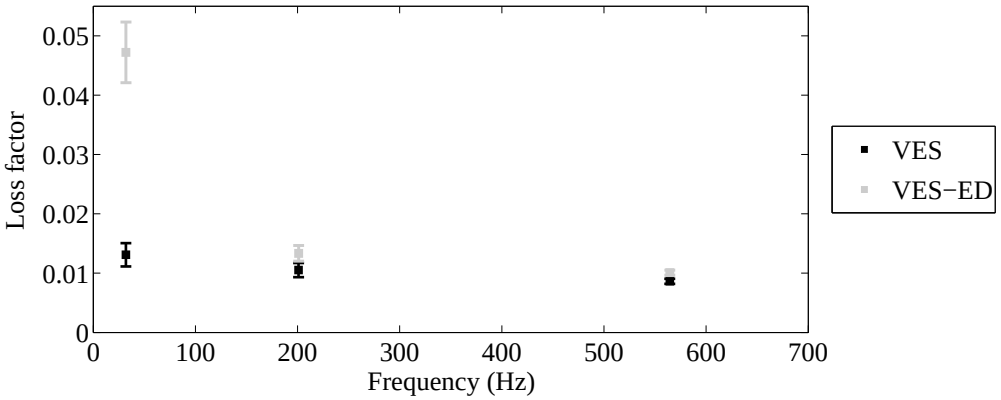

Figure 8: Experimental loss factor of the viscoelastic sandwich and viscoelastic sandwich with eddy currents obtained from beams with a free length of 170 mm in the bandwidth of 0-1 kHz.

VES of the same thickness, the loss factor of the structure increases by 445 % and the density decreases by 0.9 % at the expense of a small decrease of the storage modulus of 3 %. If permanent magnets are then placed near the VES in order to induce eddy currents, and thus obtain a VES-ED, the storage modulus is decreased just by 0.1 %, whereas the loss factor is increased by another 260 %.

5. Numerical modelling of the hybrid damping sandwich

In the following, the numerical modelling of the hybrid damping VES-ED is presented in order to facilitate its design for real applications. This modelling encompassed a four-parameter fractional derivative model for the viscoelastic adhesive, a FEM for the sandwich structure and an inverse method to model the eddy force.

5.1. Constitutive viscoelastic model

The shear dynamic properties of viscoelastic films can be directly obtained from dynamic tests in dynamic mechanical analysers or rheometers, or can be deducted from forced vibration tests with resonance carried out with sandwich specimens composed of the viscoelastic film to be characterised.

In the present study, the latter was considered and the polyester-based adhesive was characterised by the transmissibility functions of the VES measured in Section 3. The dynamic properties of the viscoelastic film were obtained in a two-step process, as detailed in the ASTM E 756-05 standard [35]. First, the homogenised complex modulus of the VES must be determined (as presented in Table 3), after which the shear complex modulus, G_{v}^{*}, of the viscoelastic film can be deducted from the Ross-Kerwin-Ungar equations [3] with Raos correction for the first mode [30, 37]. Assuming linear viscoelastic behaviour of the viscoelastic film, and that its Poisson ratio is real and constant in frequency [38, 39], the shear complex modulus is expressed as follows:

$$G_{\mathrm{v}}^{*}(f) = G_{\mathrm{v}}(f)\left(1 + \mathrm{i}\eta_{\mathrm{v}}(f)\right) , \tag{9}$$

where G_{v} is the shear modulus and η_{v} is the loss factor. Table 5 shows the experimental shear dynamic properties of the viscoelastic film obtained from the transmissibility function of the VES. All of the results shown are an average of three sandwich specimens with their corresponding standard deviations.

Table 5: The resonance frequencies of the viscoelastic sandwich and the shear complex modulus of the viscoelastic film.

Viscoelastic sandwich			Viscoelastic film	
f (Hz)	Mode No.	L (mm)	Gv (MPa)	η_{v}
31.96 ± 0.45	1	170	0.89 ± 0.45	0.5876 ± 0.3938
36.20 ± 0.16	1	160	1.11 ± 0.29	0.3681 ± 0.0657
41.35 ± 0.22	1	150	1.60 ± 0.56	0.5294 ± 0.3152
201.01 ± 1.72	2	170	6.96 ± 3.35	0.4771 ± 0.2499
228.42 ± 0.40	2	160	10.98 ± 1.35	0.6535 ± 0.1625
260.22 ± 0.19	2	150	13.40 ± 0.31	0.6939 ± 0.0977
564.43 ± 3.93	3	170	23.94 ± 10.92	0.5090 ± 0.3055
640.48 ± 0.78	3	160	35.96 ± 3.09	0.7077 ± 0.1319
729.9 ± 1.02	3	150	43.77 ± 1.54	0.8942 ± 0.2762

The mathematical models used to represent the mechanical behaviour of viscoelastic materials can be classified as either differential models, heredi-

tary models or fractional models. In the present study, fractional derivative models were considered, since they are a powerful tool with which to characterise the behaviour of real viscoelastic materials in frequency and time domains with a low number of parameters [40, 41, 42, 43]. The most known fractional derivative model is the four-parameter model, also known as the generalised Zener model, which was thoroughly analysed by Pritz [44]. It can represent the dynamic behaviour of several viscoelastic materials with just four parameters, and each parameter has a physical interpretation.

The four-parameter fractional derivative model is represented by the fractional equation

$$\sigma(t) + \tau^{\alpha} \frac{\partial^{\alpha} \sigma(t)}{\partial t^{\alpha}} = E_0 \epsilon(t) + E_{\infty} \tau^{\alpha} \frac{\partial^{\alpha} \epsilon(t)}{\partial t^{\alpha}}, \tag{10}$$

where σ, ϵ, E_0, E_{∞}, τ and α are the stress, the strain, the static modulus, the asymptotic modulus, the relaxation time and the fractional parameter, respectively. Assuming that the Poisson ratio is real and constant in frequency in the analysed bandwidth [38, 39], the shear complex modulus yields

$$G_{\mathrm{v}}^{*} = \frac{G_0 + G_{\infty} (\mathrm{i}\omega\tau)^{\alpha}}{1 + (\mathrm{i}\omega\tau)^{\alpha}}, \tag{11}$$

where G_0 and G_{∞} are the static and asymptotic shear modulus, respectively.

The Nelder-Mead minimisation algorithm was used to fit the four-parameter fractional derivative model to the experimental shear complex modulus, with the minimised function being

$$\|G_{\mathrm{v,fitted}} - G_{\mathrm{v,exp}}\| + \|G_{\mathrm{v,fitted}} \eta_{\mathrm{v,fitted}} - G_{\mathrm{v,exp}} \eta_{\mathrm{v,exp}}\|, \tag{12}$$

where $G_{\mathrm{v,fitted}}$ and $\eta_{\mathrm{v,fitted}}$ are the shear modulus and the loss factor obtained from Eq. (11) and $G_{\mathrm{v,exp}}$ and $\eta_{\mathrm{v,exp}}$ are the experimental shear modulus and the loss factor shown in Table 5. At the end of the minimisation process, satisfaction of the thermodynamic constraints must be verified: $G_{\infty} > G_0 > 0$, $\tau > 0$ and $\alpha > 0$.

In Table 6 the identified parameters of the four-parameter fractional derivative model can be seen and in Figure 9 the experimental shear complex modulus of the viscoelastic film and the fitted four-parameter fractional derivative model is shown. It is observed the shear modulus was overestimated at low frequencies and underestimated at high frequencies, while the loss factor was slightly overestimated across the entire bandwidth.

Table 6: Identified parameters of the four-parameter fractional derivative model for the viscoelastic film.

G_0 (Pa)	G_∞ (Pa)	t (s)	α
$3.24 \cdot 10^6$	$5.64 \cdot 10^8$	$1.99 \cdot 10^{-6}$	0.575

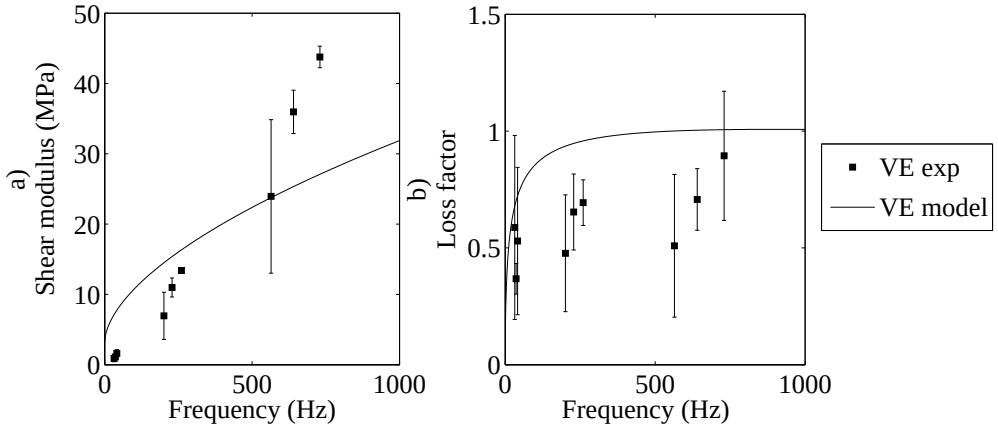

Figure 9: Experimental and the fitted shear complex modulus, a) modulus and b) loss factor of the viscoelastic film in the bandwidth of 0-1 kHz.

5.2. Finite element model

When the shear dynamic behaviour of the viscoelastic film has been modelled, a finite element is defined to model the dynamic behaviour of the thin VES. Previous studies have described the different approaches that are available to model sandwich structures, such as three-dimensional brick elements, two-dimensional multi-layer plate and shell theories and one-dimensional multi-layer beam theories. Caliri et al. [45] recently presented an extensive review of plate and shell theories for laminated structures, solved by the FEM.

In the present study, a three-layer beam finite element based on the Mead and Markus [46] theory was considered. The following assumptions were made:

- The metallic layers bend according to Euler-Bernoulli beam theory.

- The viscoelastic film is subjected only to shear deformation.

- All layers are assumed incompressible through the thickness and the transverse displacement is uniform on a cross section.

- All layers are assumed to be perfectly bonded, and there is no slippage or delamination between the layers.

The finite element is defined by two nodes with four degrees of freedom per node: the axial displacements of the top and bottom layers, u_1 and u_3, the transverse displacement, w, and the rotational displacement of the beam, $\frac{\partial w}{\partial x}$. The generalised displacements, $\mathbf{u} = \begin{bmatrix} u_1 & u_2 & u_3 \end{bmatrix}^{\mathrm{T}}$, are discretised with the Lagrange linear shape function for u_1 and u_3 and the Hermite cubic shape function for w. The formulation of the finite element is described in further detail in [47].

In the numerical modelling, the sandwich beam was discretised by elements of 5 mm in length, and the numerical transmissibility function was obtained by the direct frequency method, with a 0.02 Hz resolution in the bandwidth of 0-250 Hz and with a 0.05 Hz resolution in the bandwidth of 250-1000 Hz. Figure 10 shows the experimental and numerical transmissibility function of the VES. It is observed that the correlation was acceptable across the entire bandwidth, with the greater deviation being in the first resonance, due to overestimation of the shear modulus at low frequencies.

5.3. Inverse method

A new inverse method was developed in order to estimate the influence of induced eddy currents and facilitate the design of the proposed hybrid damping VES-ED. The inverse method and the eddy force were based on the following assumptions:

- The influence of eddy currents on the vibrational response of the sandwich structure can be modelled by an eddy force parallel to the vibration direction.

- The eddy force exists only in the area where the magnetic field is applied.

- The eddy force is proportional to the velocity of the structure and can be expressed by a constant viscous damping matrix in the frequency domain.

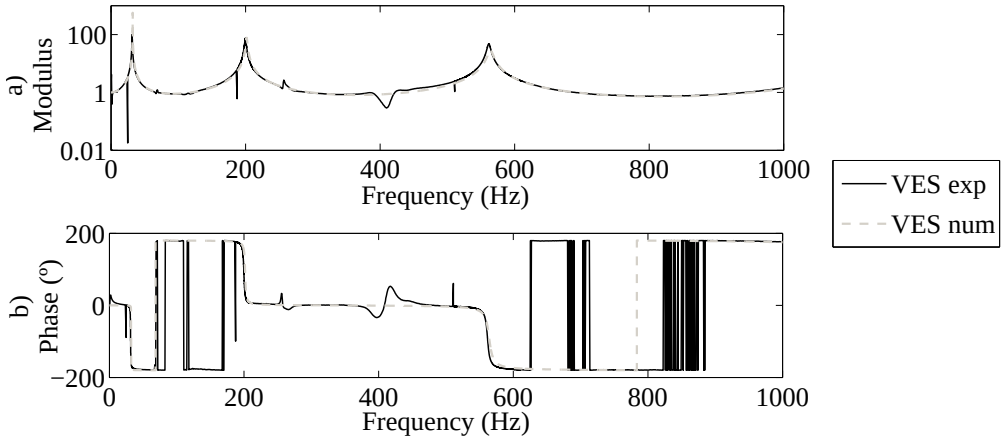

Figure 10: Experimental and numerical transmissibility function, a) modulus and b) phase, of the viscoelastic sandwich beam with a free length of 170 mm in the bandwidth of 0-1 kHz.

The proposed eddy force consists of a lineal viscous force, $\mathbf{F}^*_{\text{eddy}}$, given by

$$\mathbf{F}^*_{\text{eddy}} = -c_{\text{e}}\mathbf{v}^*_{\text{z}}\,, \tag{13}$$

where c_{e} is the eddy damping coefficient and $\mathbf{v}^*_{\text{z}}$ is the complex transverse velocity of the sandwich structure. The inverse method consists of minimising the residue between the experimental and numerical transmissibility function at certain frequencies, in order to identify the coefficient. The entire process will next be described step-by-step.

First, the input data must be provided by the user. These include the geometrical and physical properties of the sandwich structure and its components, a constitutive viscoelastic model that describes the dynamic behaviour of the viscoelastic film, a finite element model of the sandwich structure and two experimental transmissibility functions of the sandwich, with and without induced eddy currents. The transmissibility functions are obtained by forced vibration tests with resonance in the absence of, and under, a magnetic field, as described in Section 3.2. These must include at least one resonance, it not being necessary to measure the entire bandwidth under analysis. The selection of the response degree-of-freedom (DOF) located on the free end is recommended, as it does not coincide with any node and provides a dynamic response with a good signal-to-noise ratio.

The control frequencies, frequencies in which the residue between the ex-

perimental and numerical transmissibility function is minimised, must then be selected by the user. In order to do so, the experimental transmissibility functions of the sandwich structure, with and without induced eddy currents, are compared, the resonance frequency and the lower and upper limits at which the eddy currents dampen the vibration are determined and control frequencies are selected within the defined range. The selection of 15 control frequencies may be sufficient, but a greater number of control frequencies may provide greater accuracy. Their use improves the efficiency of the method, since the numerical transmissibility function is computed only at these frequencies.

Once the input data and the control frequencies have been defined, the minimisation process begins. The loop is as follows: the eddy damping coefficient is initialised, the FEM model, in which the eddy force is incorporated, is updated, the numerical transmissibility function is computed for all the control frequencies, the residue between the experimental and numerical transmissibility function is computed and the iterative process is repeated until the error becomes smaller than the specified tolerance, or until the maximum number of iterations is exceeded.

The governing equation of motion of the VES-ED in the finite element formulation is given by

$$\mathbf{M}\ddot{\mathbf{u}} + \mathbf{K}^{*}\mathbf{u} = \mathbf{F} + \mathbf{F}^{*}_{\text{eddy}}\,, \tag{14}$$

where $\mathbf{M}$, $\mathbf{K}^{*}$, $\mathbf{F}$ and $\mathbf{F}^{*}_{\text{eddy}}$, are the global mass matrix, the global stiffness matrix, the external force vector and the eddy force vector, respectively; $\ddot{\mathbf{u}}$ and $\mathbf{u}$ are the acceleration and displacement vectors, respectively, and the dot denotes differentiation with respect to time. As the proposed eddy force is linearly proportional to the transverse velocity of the sandwich, Eq. (13), it can be expressed by a viscous damping matrix. The global eddy damping matrix, $\mathbf{C}_{\text{eddy}}$, is obtained by assembling null matrices for the elements where there is not present an applied magnetic field and elementary eddy damping matrices, $\mathbf{C}^{e}_{\text{eddy}}$, for the elements to which a magnetic field is applied. Using the FEM model described in section 5.2, the $\mathbf{C}^{e}_{\text{eddy}}$ matrix is given by

$$\mathbf{C}^{e}_{\text{eddy}} = \begin{bmatrix}\mathbf{0} & \mathbf{0} & \mathbf{C}_{\text{e}} & \mathbf{0} & \mathbf{0} & \mathbf{0} & \mathbf{C}_{\text{e}} & \mathbf{0}\end{bmatrix}^{\text{T}}\,, \tag{15}$$

where $\mathbf{C}_{\text{e}} = c_{\text{e}} \int_0^{l_{\text{e}}} \mathbf{N}_{\text{w}} \mathrm{d}x$ and $\mathbf{N}_{w}$ is the Hermite cubic shape function. Thus, the governing equation of motion results in

$$\mathbf{M}\ddot{\mathbf{u}} + \mathbf{C}_{\text{eddy}}\dot{\mathbf{u}} + \mathbf{K}^{*}\mathbf{u} = \mathbf{F}\,. \tag{16}$$

If a steady-state harmonic base excitation is considered and the motion equation is written in the frequency domain differentiating the DOF related to the base displacement, $(\bullet)_s$, and the unknown displacements, $(\bullet)_s$, the following is obtained

$$\begin{aligned} &\left(-\omega^2 \begin{bmatrix} \mathbf{M}_{\text{ss}} & \mathbf{M}_{\text{su}} \\ \mathbf{M}_{\text{us}} & \mathbf{M}_{\text{uu}} \end{bmatrix} + \mathrm{i}\omega \begin{bmatrix} \mathbf{C}_{\text{eddy,ss}} & \mathbf{C}_{\text{eddy,su}} \\ \mathbf{C}_{\text{eddy,us}} & \mathbf{C}_{\text{eddy,uu}} \end{bmatrix} + \begin{bmatrix} \mathbf{K}^{*}_{\text{ss}} & \mathbf{K}^{*}_{\text{su}} \\ \mathbf{K}^{*}_{\text{us}} & \mathbf{K}^{*}_{\text{uu}} \end{bmatrix}\right) \\ &\begin{Bmatrix} \mathbf{S}^{*} \\ \mathbf{U}^{*} \end{Bmatrix} = \begin{Bmatrix} \mathbf{R}^{*} \\ \mathbf{0} \end{Bmatrix}, \end{aligned} \tag{17}$$

where $\mathbf{S}^{*}$, $\mathbf{U}^{*}$ and $\mathbf{R}^{*}$ are the amplitude vectors in the frequency domain of the applied base motion, unknown displacement and reaction force on the base, respectively.

The direct frequency method is used to compute the numerical transmissibility function at all the control frequencies. The unknown displacement amplitude vector is obtained from

$$\mathbf{U} = \frac{\left(\omega_k^2\mathbf{M}_{\text{us}} - \mathrm{i}\omega_k\mathbf{C}_{\text{eddy,us}} - \mathbf{K}^{*}_{\text{us}}\right)\mathbf{S}^{*}}{\left(-\omega_k^2\mathbf{M}_{\text{uu}} + \mathrm{i}\omega_k\mathbf{C}_{\text{eddy,uu}} + \mathbf{K}^{*}_{\text{uu}}\right)}\,, \tag{18}$$

and the numerical transmissibility function, $T^{*}_{i,j}$, is deducted from

$$T^{*}_{ij} = \frac{U^{*}_{j}}{S^{*}_{i}}\,. \tag{19}$$

Finally, the minimisation of the residue between the experimental and numerical transmissibility functions is carried out by the Nelder-Mead simplex algorithm [48] in order to obtain the eddy damping coefficient and determine the eddy force. The minimised function is given by

$$\sqrt{\sum_{k=1}^{k=k_{\max}} \left(T^{*}_{ij_k} -_{\text{exp}} T^{*}_{ij_k}\right)^2}\,, \tag{20}$$

where $k_{\max}$ is the total number of control frequencies.

The modelling of the proposed hybrid damping VES-ED (Figure 1) is next shown in order to validate the proposed eddy force model and inverse

method. The following input data were considered: the geometrical and physical properties of the sandwich structure shown in Table 1, the four-parameter fractional derivative model defined in section 5.1, the FEM model described in section 5.2 and the experimental transmissibility functions of the second vibration mode, with and without induced eddy currents, measured following the experimental technique described in section 3.2. The lower and upper frequency limits where the eddy currents dampen the vibration of the sandwich structure in the second vibration mode were then identified, and 15 control frequencies were selected within the defined range. These are shown in Figure 11.

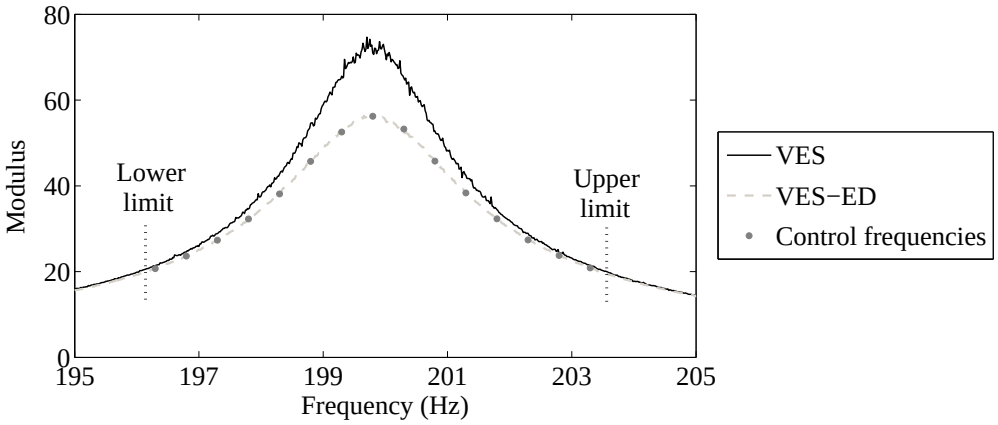

Figure 11: Experimental transmissibility modulus of the viscoelastic sandwich and viscoelastic sandwich and viscoelastic sandwich with eddy currents beams with free length of 170 mm in the second vibration mode and the selected control frequencies.

The minimisation iterative process was then held, and the value of the eddy damping coefficient $c_e = 0.131$ Ns/m was obtained. Then, the VES-ED was completely defined, since the $\mathbf{M}$, $\mathbf{K}^*$ and $\mathbf{C}_{\text{eddy}}$ of the system were known, and the dynamic response of any point of the structure in any frequency bandwidth could be obtained by the FEM.

In Figure 12 the experimental and numerical transmissibility function of the VES-ED in the bandwidth of 0-1 kHz is shown. It is observed that the correlation was good, the greatest deviation in the transmissibility modulus of the first resonance being due to the overestimated shear modulus of the viscoelastic film at low frequencies, as shown in Figure 9. In addition, it is validated $\mathbf{C}_{\text{eddy}}$ is unique and constant in all the bandwidth of 0-1 kHz.

This highlights the fact that the proposed eddy force and inverse method constitutes an easy tool with which to model and predict the vibrational response of VES-ED.

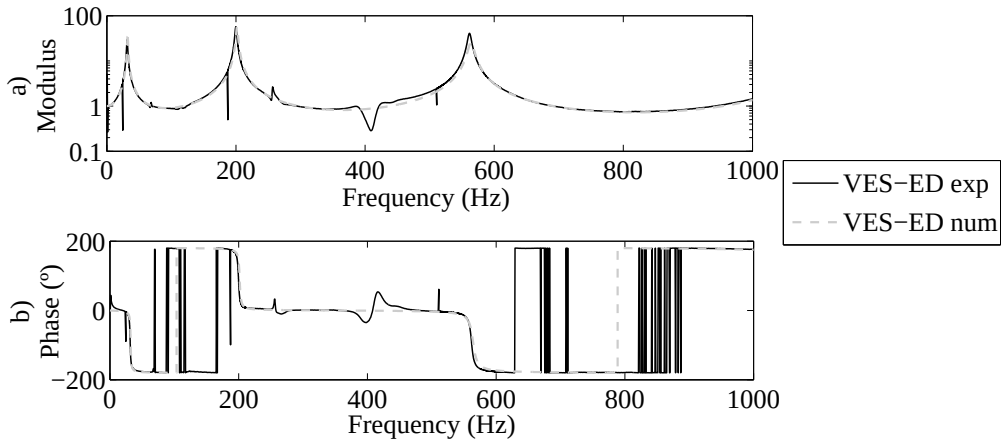

Figure 12: Experimental and numerical transmissibility function, a) modulus and b) phase, of the viscoelastic sandwich with eddy currents beam with a free length of 170 mm in the bandwidth of 0-1 kHz.

Finally, the proposed numerical model was used to predict the vibrational responses of the VES and VES-ED beams at the point $x = 100$ mm (Figure 2). In Figure 13, it is observed that the vibration amplitude of the VES-ED was much lower than that of the VES in the first vibration mode, retaining its mechanical performance. Thus, it can be said that the proposed VES-ED constitutes a method of maximising the performance of conventional viscoelastic sandwiches.

6. Conclusions

In the present study, a novel hybrid damping sandwich structure was proposed to attenuate structural vibration over an entire bandwidth without adding mass to the structure or significantly modifying its mechanical properties. The proposed hybrid damping sandwich combines viscoelastic and eddy current damping and it consists of a thin viscoelastic sandwich and two permanents magnets that are placed near, but not in contact with, the sandwich.

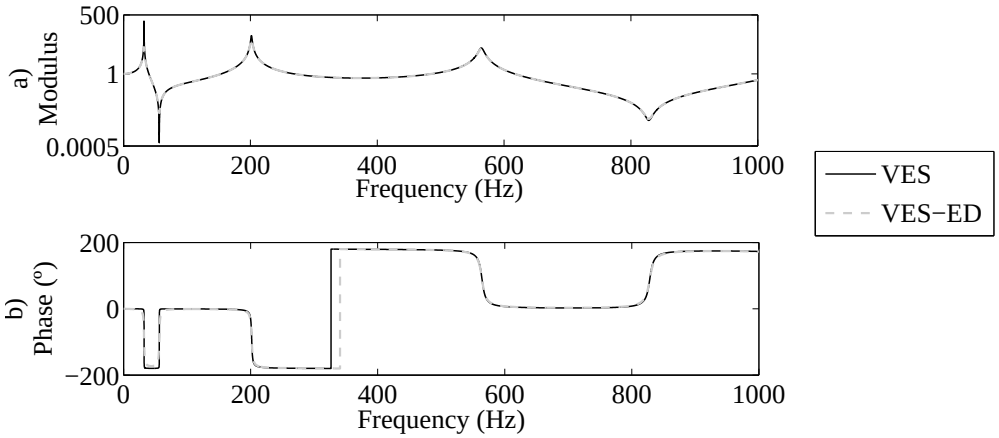

Figure 13: Numerical transmissibility function, a) modulus and b) phase, of the viscoelastic sandwich and viscoelastic sandwich with eddy currents beam with free length of 170 mm at the point $x = 100$ mm in the bandwidth of 0-1 kHz.

The vibrational response and dynamic properties of the proposed VES-ED were analysed in the bandwidth of 0-1 kHz from the experimental results. The results showed that the viscoelastic film attenuates vibration across the entire bandwidth and the induced eddy currents are responsible for even further suppression of the vibration at low frequencies. The results also highlight that the proposed VES-ED can be used as a substitute for metallic structures, without adding mass to the structure, when efficient attenuation of vibration is required.

A numerical modelling of the VES-ED was presented, which encompasses a four-parameter fractional derivative model for the viscoelastic adhesive, a finite element model for the sandwich structure and an inverse method to model the eddy force. The numerical transmissibility function correlated with that of the experiment, showing a good agreement across the entire bandwidth of 0-1 kHz. The proposed numerical modelling facilitates the use of the hybrid damping VES-ED in real applications.

In conclusion, it can be said that the proposed VES-ED constitutes a method of maximising the performance of conventional viscoelastic sandwiches.

Acknowledgements

The present study was partially supported by the AVISANI (DPI2015-71198-R, Spanish Government) and AVISANI (PI_2016_1_0026, Basque Government) projects and Replasa S.A.

References

[1] M. D. Rao, Recent applications of viscoelastic damping for noise control in automobiles and commercial airplanes, Journal of Sound and Vibration 262 (3) (2003) 457–474. doi:10.1016/S0022-460X(03)00106-8.
URL http://linkinghub.elsevier.com/retrieve/pii/S0022460X03001068

[2] E. M. Kerwin, Damping of Flexural Waves by a Constrained Viscoelastic Layer, The Journal of the Acoustical Society of America 31 (7) (1959) 952–962. doi:10.1121/1.1907821.
URL http://asa.scitation.org/doi/10.1121/1.1907821

[3] D. Ross, E. E. Ungar, E. M. Kerwin, Damping of plate flexural vibrations by means of viscoelastic laminae, Strucutral Damping (1959) 49–87.

[4] M. Leibowitz, J. M. Lifshitz, Experimental verification of modal parameters for 3-layered sandwich beams, International Journal of Solids and Structures 26 (2) (1990) 175–184. doi:10.1016/0020-7683(90)90050-6.
URL http://linkinghub.elsevier.com/retrieve/pii/0020768390900506

[5] T.-l. Teng, N.-k. Hu, Analysis of damping characteristics for viscoelastic laminated beams, Computer Methods in Applied Mechanics and Engineering 190 (29-30) (2001) 3881–3892. doi:10.1016/S0045-7825(00)00305-4.
URL http://linkinghub.elsevier.com/retrieve/pii/S0045782500003054

[6] F. Alijani, M. Amabili, Non-linear static bending and forced vibrations of rectangular plates retaining non-linearities in rotations and thickness deformation, International Journal of Non-Linear Mechanics 67 (2014) 394–404. doi:10.1016/j.ijnonlinmec.2014.10.003.

547 URL http://dx.doi.org/10.1016/j.ijnonlinmec.2014.
548 10.003http://linkinghub.elsevier.com/retrieve/pii/
549 S0020746214001978

550 [7] M. Amabili, Nonlinear vibrations of viscoelastic rectangular
551 plates, Journal of Sound and Vibration 362 (2016) 142–156.
552 doi:10.1016/j.jsv.2015.09.035.
553 URL http://dx.doi.org/10.1016/j.jsv.2015.09.035http:
554 //linkinghub.elsevier.com/retrieve/pii/S0022460X15007567

555 [8] E. M. Daya, L. Azrar, M. Potier-Ferry, An amplitude equation
556 for the non-linear vibration of viscoelastically damped sandwich
557 beams, Journal of Sound and Vibration 271 (3-5) (2004) 789–813.
558 doi:10.1016/S0022-460X(03)00754-5.
559 URL http://linkinghub.elsevier.com/retrieve/pii/
560 S0022460X03007545

561 [9] A. L. Araújo, C. M. Mota Soares, C. A. Mota Soares, J. Herskovits,
562 Optimal design and parameter estimation of frequency dependent vis-
563 coelastic laminated sandwich composite plates, Composite Structures
564 92 (9) (2010) 2321–2327. doi:10.1016/j.compstruct.2009.07.006.
565 URL http://dx.doi.org/10.1016/j.compstruct.2009.
566 07.006http://linkinghub.elsevier.com/retrieve/pii/
567 S0263822309002414

568 [10] M. Hamdaoui, G. Robin, M. Jrad, E. M. Daya, Optimal design of
569 frequency dependent three-layered rectangular composite beams for
570 low mass and high damping, Composite Structures 120 (2015) 174–182.
571 doi:10.1016/j.compstruct.2014.09.062.
572 URL http://dx.doi.org/10.1016/j.compstruct.2014.
573 09.062http://linkinghub.elsevier.com/retrieve/pii/
574 S0263822314005108

575 [11] J. F. A. Madeira, A. L. Araújo, C. M. Mota Soares, C. A. Mota Soares,
576 A. J. M. Ferreira, Multiobjective design of viscoelastic laminated
577 composite sandwich panels, Composites Part B: Engineering 77 (2015)
578 391–401. doi:10.1016/j.compositesb.2015.03.025.
579 URL http://dx.doi.org/10.1016/j.compositesb.2015.
580 03.025http://linkinghub.elsevier.com/retrieve/pii/
581 S1359836815001444

[12] J. F. A. Madeira, A. L. Araújo, C. M. Mota Soares, C. A. Mota Soares, Multiobjective optimization of viscoelastic laminated sandwich structures using the Direct MultiSearch method, Computers & Structures 147 (2015) 229–235. doi:10.1016/j.compstruc.2014.09.009.
URL http://dx.doi.org/10.1016/j.compstruc.2014.09.009http://linkinghub.elsevier.com/retrieve/pii/S0045794914002090

[13] V. Lara-Prieto, R. Parkin, M. Jackson, V. Silberschmidt, Z. Kesy, Vibration characteristics of MR cantilever sandwich beams: experimental study, Smart Materials and Structures 19 (1) (2010) 015005. doi:10.1088/0964-1726/19/1/015005.
URL http://stacks.iop.org/0964-1726/19/i=1/a=015005?key=crossref.05e4ddac9d0160c2a8e2f77776bf7a98

[14] L. Irazu, M. J. Elejabarrieta, Magneto-dynamic analysis of sandwiches composed of a thin viscoelastic-magnetorheological layer, Journal of Intelligent Material Systems and Structures (2017) 1045389X1770520doi:10.1177/1045389X17705209.
URL http://journals.sagepub.com/doi/10.1177/1045389X17705209

[15] K. Wei, Q. Bai, G. Meng, L. Ye, Vibration characteristics of electrorheological elastomer sandwich beams, Smart Materials and Structures 20 (5) (2011) 055012. doi:10.1088/0964-1726/20/5/055012.
URL http://stacks.iop.org/0964-1726/20/i=5/a=055012?key=crossref.78c5e1557a9d595fa1d4180ec3ab19eb

[16] K. Ramkumar, N. Ganesan, Vibration and damping of composite sandwich box column with viscoelastic/electrorheological fluid core and performance comparison, Materials & Design 30 (8) (2009) 2981–2994. doi:10.1016/j.matdes.2008.12.023.
URL http://dx.doi.org/10.1016/j.matdes.2008.12.023http://linkinghub.elsevier.com/retrieve/pii/S0261306909000107

[17] P. Butaud, E. Foltête, M. Ouisse, Sandwich structures with tunable damping properties: On the use of Shape Memory Polymer as viscoelastic core, Composite Structures 153 (2016) 401–408. doi:10.1016/j.compstruct.2016.06.040.
URL http://dx.doi.org/10.1016/j.compstruct.2016.

06.040http://linkinghub.elsevier.com/retrieve/pii/S0263822316309783

[18] M. A. Trindade, A. Benjeddou, Hybrid Active-Passive Damping Treatments Using Viscoelastic and Piezoelectric Materials: Review and Assessment, Modal Analysis 8 (6) (2002) 699–745. doi:10.1177/1077546029186.
URL http://journals.sagepub.com/doi/10.1177/1077546029186

[19] N. Kumar, S. P. Singh, Vibration and damping characteristics of beams with active constrained layer treatments under parametric variations, Materials & Design 30 (10) (2009) 4162–4174. doi:10.1016/j.matdes.2009.04.044.
URL http://dx.doi.org/10.1016/j.matdes.2009.04.044http://linkinghub.elsevier.com/retrieve/pii/S0261306909001836

[20] H. A. Sodano, J.-S. Bae, Eddy Current Damping in Structures, The Shock and Vibration Digest 36 (6) (2004) 469–478. doi:10.1177/0583102404048517.

[21] H. A. Sodano, J.-S. Bae, D. J. Inman, W. Keith Belvin, Concept and model of eddy current damper for vibration suppression of a beam, Journal of Sound and Vibration 288 (4-5) (2005) 1177–1196. doi:10.1016/j.jsv.2005.01.016.
URL http://linkinghub.elsevier.com/retrieve/pii/S0022460X05000817

[22] H. A. Sodano, J.-S. Bae, D. J. Inman, W. K. Belvin, Improved Concept and Model of Eddy Current Damper, Journal of Vibration and Acoustics 128 (3) (2006) 294. doi:10.1115/1.2172256.
URL http://reichling.physik.uos.de/download{_}paper.php?paper=JVibAcoust128p294(2006){_}Sodano.pdfhttp://vibrationacoustics.asmedigitalcollection.asme.org/article.aspx?articleid=1470848

[23] H. A. Sodano, D. J. Inman, Non-contact vibration control system employing an active eddy current damper, Journal of Sound and Vibration 305 (4-5) (2007) 596–613. doi:10.1016/j.jsv.2007.04.050.
URL http://linkinghub.elsevier.com/retrieve/pii/S0022460X07003434

[24] T. H. Cheng, D. J. Xuan, Z. Z. Li, Y. D. Shen, Vibration Control Using Shunted Electromagnetic Transducer, Applied Mechanics and Materials 26-28 (2010) 905–908. doi:10.4028/www.scientific.net/AMM.26-28.905.
URL http://www.scientific.net/AMM.26-28.905

[25] T.-H. Cheng, I.-K. Oh, Vibration Suppression of Flexible Beam Using Electromagnetic Shunt Damper, IEEE Transactions on Magnetics 45 (6) (2009) 2758–2761. doi:10.1109/TMAG.2009.2020549.
URL http://files/414/abs{_}all.html{\%}5Cnhttp://ieeexplore.ieee.org/ielx5/20/4957672/04957720.pdf?tp={\&}arnumber=4957720{\&}isnumber=4957672http://ieeexplore.ieee.org/document/4957720/

[26] J.-S. Bae, J.-H. Hwang, J.-H. Roh, J.-H. Kim, M.-S. Yi, J. H. Lim, Vibration suppression of a cantilever beam using magnetically tuned-mass-damper, Journal of Sound and Vibration 331 (26) (2012) 5669–5684. doi:10.1016/j.jsv.2012.07.020.
URL http://dx.doi.org/10.1016/j.jsv.2012.07.020http://linkinghub.elsevier.com/retrieve/pii/S0022460X12005469

[27] J.-S. Bae, J.-H. Hwang, D.-G. Kwag, J. Park, D. J. Inman, Vibration Suppression of a Large Beam Structure Using Tuned Mass Damper and Eddy Current Damping, Shock and Vibration 2014 (2014) 1–10. doi:10.1155/2014/893914.
URL http://www.hindawi.com/journals/sv/2014/893914/

[28] M. Berardengo, A. Cigada, F. Guanziroli, S. Manzoni, Modelling and control of an adaptive tuned mass damper based on shape memory alloys and eddy currents, Journal of Sound and Vibration 349 (2015) 18–38. doi:10.1016/j.jsv.2015.03.036.
URL http://dx.doi.org/10.1016/j.jsv.2015.03.036http://linkinghub.elsevier.com/retrieve/pii/S0022460X15002758

[29] A. Asghar Maddah, Y. Hojjat, M. Reza Karafi, M. Reza Ashory, Reduction of magneto rheological dampers stiffness by incorporating of an eddy current damper, Journal of Sound and Vibration 396 (2017) 51–68. doi:10.1016/j.jsv.2017.02.011.
URL http://dx.doi.org/10.1016/j.jsv.2017.02.011http://linkinghub.elsevier.com/retrieve/pii/S0022460X17301025

[30] D. I. G. Jones, Handbook of viscoelastic vibration damping, John Wiley and Sons Ltd, Chichester, 2001.

[31] L. E. Goodman, Material damping and slip damping, in: Shock and Vibration Handbook, c. m. harr Edition, McGrawHill, New York, 1996, p. Cap. 36.

[32] J.-S. Bae, M. K. Kwak, D. J. Inman, Vibration suppression of a cantilever beam using eddy current damper, Journal of Sound and Vibration 284 (3-5) (2005) 805–824. doi:10.1016/j.jsv.2004.07.031.
URL http://www.sciencedirect.com/science/article/pii/S0022460X04006522http://linkinghub.elsevier.com/retrieve/pii/S0022460X04006522

[33] D. Meeker, Improvised Open Boundary Conditions for Magnetic Finite Elements, IEEE Transactions on Magnetics 49 (10) (2013) 5243–5247. doi:10.1109/TMAG.2013.2260348.
URL http://ieeexplore.ieee.org/document/6509478/

[34] D. C. Meeker, Improvised Asymptotic Boundary Conditions for Electrostatic Finite Elements, IEEE Transactions on Magnetics 50 (6) (2014) 1–9. doi:10.1109/TMAG.2014.2300196.
URL http://ieeexplore.ieee.org/lpdocs/epic03/wrapper.htm?arnumber=6714455

[35] ASTM, ASTM 756-05: Standard test method for measuring vibration-damping properties of materials (2005).

[36] F. Cortés, M. J. Elejabarrieta, Viscoelastic materials characterisation using the seismic response, Materials & Design 28 (7) (2007) 2054–2062. doi:10.1016/j.matdes.2006.05.032.
URL http://linkinghub.elsevier.com/retrieve/pii/S0261306906001816

[37] D. K. Rao, Frequency and Loss Factors of Sandwich Beams under Various Boundary Conditions, Journal of Mechanical Engineering Science 20 (5) (1978) 271–282.

[38] R. S. Lakes, A. Wineman, On Poisson's Ratio in Linearly Viscoelastic Solids, Journal of Elasticity 85 (1) (2006) 45–63. doi:10.1007/s10659-

006-9070-4.
URL http://link.springer.com/10.1007/s10659-006-9070-4

[39] J. J. de Espndola, J. M. da Silva Neto, E. M. O. Lopes, A generalised fractional derivative approach to viscoelastic material properties measurement, Applied Mathematics and Computation 164 (2) (2005) 493–506. doi:10.1016/j.amc.2004.06.099.
URL http://linkinghub.elsevier.com/retrieve/pii/S0096300304003315

[40] D. Ouis, Combination of a standard viscoelastic model and fractional derivate calculus to the characterization of polymers, Materials Research Innovations 7 (1) (2003) 42–46. doi:10.1080/14328917.2003.11784758.
URL https://www.tandfonline.com/doi/full/10.1080/14328917.2003.11784758

[41] L. Rouleau, R. Pirk, B. Pluymers, W. Desmet, Characterization and Modeling of the Viscoelastic Behavior of a Self-Adhesive Rubber Using Dynamic Mechanical Analysis Tests, Journal of Aerospace Technology and Management 7 (2) (2015) 200–208. doi:10.5028/jatm.v7i2.474.
URL http://www.jatm.com.br/ojs/index.php/jatm/article/view/474

[42] Y. C. Lu, Fractional derivative viscoelastic model for frequency-dependent complex moduli of automotive elastomers, International Journal of Mechanics and Materials in Design 3 (4) (2007) 329–336. doi:10.1007/s10999-007-9039-x.
URL http://link.springer.com/10.1007/s10999-007-9039-x

[43] M. Martinez-Agirre, M. J. Elejabarrieta, Characterisation and modelling of viscoelastically damped sandwich structures, International Journal of Mechanical Sciences 52 (9) (2010) 1225–1233. doi:10.1016/j.ijmecsci.2010.05.010.
URL http://linkinghub.elsevier.com/retrieve/pii/S0020740310001475

[44] T. Pritz, ANALYSIS OF FOUR-PARAMETER FRACTIONAL DERIVATIVE MODEL OF REAL SOLID MATERIALS, Journal of Sound and Vibration 195 (1) (1996) 103–115. doi:10.1006/jsvi.1996.0406.

URL http://linkinghub.elsevier.com/retrieve/pii/S0022460X9690406X

[45] M. F. Caliri, A. J. M. Ferreira, V. Tita, A review on plate and shell theories for laminated and sandwich structures highlighting the Finite Element Method, Composite Structures 156 (2016) 63–77. doi:10.1016/j.compstruct.2016.02.036.
URL http://dx.doi.org/10.1016/j.compstruct.2016.02.036http://linkinghub.elsevier.com/retrieve/pii/S0263822316300642

[46] D. J. Mead, A comparison of some equations for the flexural vibration of damped sandwich beams, Journal of Sound and Vibration 83 (3) (1982) 363–377. doi:10.1016/S0022-460X(82)80099-0.
URL http://linkinghub.elsevier.com/retrieve/pii/S0022460X82800990

[47] L. Irazu, M. J. Elejabarrieta, The effect of the viscoelastic film and metallic skin on the dynamic properties of thin sandwich structures, Composite Structures 176 (2017) 407–419. doi:10.1016/j.compstruct.2017.05.038.
URL http://dx.doi.org/10.1016/j.compstruct.2017.05.038http://linkinghub.elsevier.com/retrieve/pii/S0263822317305214

[48] J. A. Nelder, R. Mead, A Simplex Method for Function Minimization, The Computer Journal 7 (4) (1965) 308–313. doi:10.1093/comjnl/7.4.308.
URL http://comjnl.oxfordjournals.org/cgi/content/long/7/4/308https://academic.oup.com/comjnl/article-lookup/doi/10.1093/comjnl/7.4.308

Chapter 5

Magnetorheological effect and magnetic force generated in viscoelastic-magnetorheological core

This chapter is focused on the core of viscoelastic-magnetorheological sandwiches. The influence of the magnetorheological effect and magnetic force generated in the viscoelastic-magnetorheological core on the dynamic behaviour of the sandwich is analysed. This chapter together with the previous one describe the physical phenomena governing the magneto-dynamic behaviour of smart viscoelastic-magnetorheological sandwiches.

Irazu L and Elejabarrieta MJ (Submitted October 2017). The effect of the magnetoelastic force on the magneto-dynamic model of viscoelastic-magnetorheological sandwiches. *Smart Materials and Structures*.

5.1 Introduction

When a magnetic field is applied to vibrating viscoelastic-magnetorheological sandwiches (VEMRS) two phenomena are generated in their core. On the one hand, the rheological properties of the viscoelastic-magnetorheological (VEMR) core are modified which is known as the magnetorheological effect (Chen et al. 2008). On the other hand, the VEMR core is magnetized and subjected to a distributed magnetic force (Gélinas et al. 1996; Moon and Pao 1969).

In this chapter the physical phenomena generated in vibrating VEMRSs exposed to magnetic fields due to its VEMR core are studied. The influence of the magnetorheological effect and the magnetic is analysed individually. To that end, a magnetic force model to describe the interaction generated in vibrating VEMRSs when exposed to magnetic fields is proposed. Then, a magneto-dynamic modelling of the sandwich by finite element method (FEM) including both phenomena is proposed and validated with experimental results.

Next, a brief state of the art related to the magneto-dynamic modelling of magnetorheological (MR) sandwiches in general is presented and the objectives of this chapter are defined. Then, the magnetorheological effect and the magnetic force models are described and the proposed magneto-dynamic modelling of VEMRSs by FEM is presented and validated with experimental results. The contribution of each phenomenon on the dynamic behaviour of VEMRSs is studied. Finally, the main conclusions obtained in this chapter are summarized and the scientific contribution is presented.

5.2 State of art

MR sandwiches, regardless of the nature of their core, MR fluid, MR gel or MR elastomer, they present a viscoelastic behaviour and so all the models developed for viscoelastic sandwiches are potentially applicable to MR sandwiches with the respective modifications (Eshaghi et al. 2016). Sun et al. (2003) derived a dynamic modelling of a sandwich beam composed of MR fluid by the Hamilton principle. Nayak et al. (2011) used the classical sandwich beam theory to model a MR elastomer based sandwich beam and they obtained the governing equation of motion using the Hamilton's principle along with generalized Galarkin's method. Aguib et al. (2014) proposed an approximate formulation by Ritz method for modelling the vibration behaviour of sandwich plates composed of MR elastomers. However, the FEM is the most used approach in modelling and analysing the magneto-dynamic response of MR sandwiches (Zhou et al. 2006; Rajamohan et al. 2010b; Bishay et al. 2010; Ramesh et al. 2014; Yeh 2013; Nayak et al. 2012b; Nayak et al. 2013). All the models developed for MR sandwiches account for the magnetic field dependence of the dynamic properties of their core, that is to say the magnetorheological effect, but, few takes into account other phenomena generated in vibrating MR sandwiches when exposed to magnetic

fields. Zhou and Wang (2006a) and Zhou and Wang (2006b) proposed an analytical solution for the eddy loads applied in the conductive skins of MR sandwiches due to induction of eddy currents and others incorporated these loads in the modelling of MR sandwiches (Nayak et al. 2011; Aguib et al. 2014; Nayak et al. 2012a). Lara-Prieto et al. (2010) stated the magnetic forces between the MR sandwich and the magnetic poles may play a significant role in its vibration response, however they did not propose any modelling of these magnetic forces.

The dynamic properties of MR materials depend on the intensity of the applied magnetic field due to the interactions generated between the magnetic particles resulting on a field-induced stiffening of the material. The change of modulus is usually termed as magnetorheological effect (Chen et al. 2008) and in literature different models have been proposed to describe the magnetorheological effect of MR elastomers, such as the one proposed by Jolly et al. (1996b), Jolly et al. (1996a), Shen et al. (2004), and Bica et al. (2012).

When a magnetic field is applied to a vibrating ferromagnetic material, this is magnetized and subjected to a distributed magnetic force arising from the interaction between the magnetized vibrating beam and the applied magnetic field (Moon and Pao 1969). The influence of magnetic field on vibrating ferromagnetic beam-plates have been analysed since the late twentieth century and many authors have proposed analytical and numerical models (Moon and Pao 1969; Wang 2013; Yuan et al. 2014). As VEMR materials are composed of ferromagnetic particles these are magnetized when an external magnetic field is applied (Gélinas et al. 1996). However, up today the influence of the magnetic interaction given in vibrating MR sandwiches on their vibrational response have not been analysed and there have not been proposed magnetic force models to describe such interaction.

5.3 Objectives

The main aim of this chapter is to determine the influence of the magnetorheological effect and magnetic force generated in the VEMR core on the dynamic behaviour of the sandwich. This requires:

- Proposing a magnetic force model to describe the magnetic interaction given in the vibrating sandwich due to the VEMR core.
- Developing a magneto-dynamic model of VEMRSs by FEM that includes the magnetorheological effect and the magnetic force.

5.4 Results

The thin VEMRS analysed in this chapter is composed of aluminium skins and an isotropic VEMR core synthesised by adding carbonyl iron powder (CIP) particles in

a 12 % volumetric concentration to a polyester-based adhesive. The geometrical and physical properties of the VEMRS are shown in Table 2.2.

The vibrational response of the thin VEMRS was measured in absence of and under a magnetic field following the experimental technique described in Chapter 2. The applied magnetic field, Figure 2.4, was almost completely transversal and homogeneous along the length of the beam. This configuration of magnetic field was chosen in order to minimize the induction of eddy currents in the metallic skins of the VEMRS and so analyse just the influence of the magnetic field in the VEMR core.

5.4.1 Magneto-dynamic model

When a magnetic field is applied to vibrating VEMRSs two phenomena are generated in its VEMR core, the magnetorheological effect and the magnetic force.

The rheological properties of the VEMR material depend on the intensity of the applied magnetic field due to the interactions generated between magnetic particles. A field-induced stiffening is given, and the change of shear modulus of the VEMR material is named as magnetorheological effect (Chen et al. 2008). In literature different models have been proposed to describe it, most of them being focused on anisotropic materials (Jolly et al. 1996b; Jolly et al. 1996a; Shen et al. 2004; Bica et al. 2012). The VEMR material of which is composed the smart sandwich analysed in this thesis is isotropic and so the dipole-dipole interaction based model developed by Jolly et al. (1996b) and Jolly et al. (1996a) with the correction proposed by Agirre-Olabide et al. (2017) for isotropic materials is used. This model only contemplates the influence of the magnetic field on the shear modulus of the VEMR, $G_{\mathrm{v}_B}(B)$. Thus, the shear complex modulus of the VEMR as a function of the magnetic field, $G^*_{\mathrm{v}}(B)$, can be expressed as

$$G^*_{\mathrm{v}}(B) = (G_{\mathrm{v}} + G_{\mathrm{v}_B}(B))(1 + \mathrm{i}\eta_{\mathrm{v}})\,, \tag{5.1}$$

where $G_{\mathrm{v}_B}(B)$ is given by

$$G_{\mathrm{v}_B}(B) = \frac{4\varphi J^2_{\mathrm{p}}(B) R^3}{\mu_{\mathrm{m}}\mu_0 d^3}(1-\varphi)\,, \tag{5.2}$$

where B is the magnetic field density, φ is the volume faction of particles in the composite, $J_{\mathrm{p}}(B)$ is the induced polarization of the particles, R is the radio of the particles, d is the distance between each particle, μ_0 is the magnetic permeability of the vacuum and μ_{m} is the relative magnetic permeability of the viscoelastic adhesive.

The VEMR material is magnetized under a magnetic field since it is composed of ferromagnetic, CIP, particles. Thus, when a magnetic field is applied to a vibrating VEMRS this is subjected to a magnetic force arising from the interaction between the magnetization of the VEMR and the magnetic field (Moon and Pao 1969). The model proposed by Moon and Pao (1969) for a linear ferromagnetic beam vibrating in an homogeneous transverse magnetic field was used to model the magnetic interaction

given in the VEMRS beam as a first approach. The Moon and Pao's model is based on the following assumptions:

- The effect of the induced current is negligible and so the resultant magnetic force system on the vibrating beam is assumed to consist of a magnetic couple proportional to the rotation of the beam.
- The magnetic field in the vibrating beam at any instant is given by that for a static plate configuration.

According to Moon and Pao (1969) the magnetic body couple is given by

$$C(B) = b(B)\frac{\partial w}{\partial x}\,, \tag{5.3}$$

in which $\frac{\partial w}{\partial x}$ is the rotation of the beam and the proportional coefficient b is expressed as

$$b(B) = \frac{2\chi^2 B^2 \sinh\left(\frac{kh_2}{2}\right)}{\mu_0 \mu_\mathrm{r} k \Delta}\,, \tag{5.4}$$

where χ is the magnetic susceptibility, k is the wave number, h_2 is the core thickness, μ_0 is the magnetic permeability of the vacuum, μ_r is the relative magnetic permeability of the VEMR material, and $\Delta = \mu_\mathrm{r} \sinh\left(\frac{kh_2}{2}\right) + \cosh\left(\frac{kh_2}{2}\right)$.

The magnetorheological effect and the magnetic force modifies the stiffens of the VEMRS and the governing equation of motion of the VEMRS incorporating both phenomena in the finite element form is given by

$$\mathbf{M}\ddot{\mathbf{q}} + \mathbf{K}^*(B)\mathbf{q} = \mathbf{F}\,, \tag{5.5}$$

where $\mathbf{q}$ and $\ddot{\mathbf{q}}$ are the displacement vector and the acceleration vector, and where $\mathbf{M}$, $\mathbf{K}^*(B)$ and $\mathbf{F}$ are the global mass matrix, the global complex stiffness matrix and the global force vector. The equation is the same as that for VESs, Equation 2.6, except that in the case of VEMRSs the complex stiffness matrix depends on the intensity of the magnetic field.

In order to validate the proposed magneto-dynamic modelling of VEMRSs, the numerical and experimental transfer functions of the thin VEMRS in the absence of and under the magnetic field are compared. In Figure 8.19 it is observed the correlation is good in both cases.

5.4.2 Influence of magnetorheological effect and magnetic force

Next, the influence of magnetorheological effect and magnetic force generated in the core of VEMRSs on their dynamic behaviour is analysed. Figure 8.20 shows the transfer function of the thin VEMRS in the absence of a magnetic field and the individual contribution of the magnetorheological effect and the magnetic force generated due to a magnetic field of 125 kA/m on it. The magnetic force tends to decrease the resonance

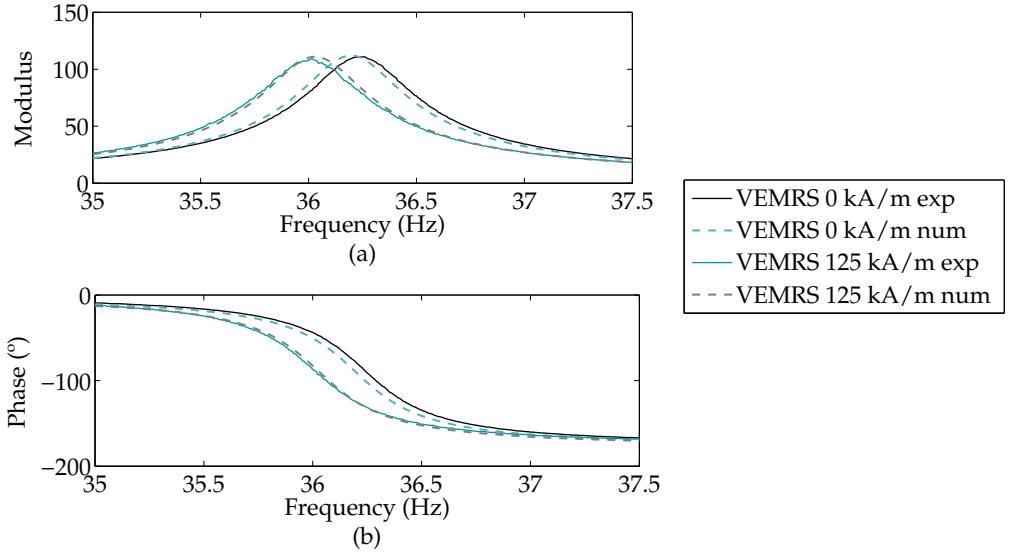

Figure 5.1. Experimental and numerical transfer function, (a) modulus and (b) phase, of the VEMRS beam with a free length of 160 mm in absence of and under a magnetic field in the first resonance.

frequency of the thin VEMRS, whereas the magnetorheological effect has no appreciable influence. The reasons why in the analysed thin VEMRS the magnetorheological effect is not appreciable are the high stiffness of the VEMR core and the low magnetic particles concentration.

A VEMRS composed of same VEMR material, but, with a core thickness of 2 mm and under a magnetic field of 2 MA/m was simulated by FEM with the aim of illustrating the contribution of the magnetorheological effect. In Figure 8.21 it can be seen the magnetorheological effect tends to increase the resonance frequency of the VEMRS. This tendency has been observed in many other numerical works in which just the magnetorheological effect was considered (Yeh 2013; Nayak et al. 2012b; Zhou and Wang 2005).

It is concluded the influence of the two phenomena present in the core of vibrating VEMRSs as a consequence of applying magnetic is opposite; the magnetorheological effect increases the resonance frequency of the sandwich, whereas the magnetic force decreases. Depending on the composition of the VEMRS and the magnetic field, each's contribution would be different and so the magneto-dynamic behaviour of the sandwich.

These results agrees with the experimental results observed with MR sandwiches in literature, since both the increment and decrement of resonance frequencies have been observed (Rajamohan et al. 2010a; Rajamohan et al. 2010b; Wei et al. 2008; Lara-Prieto et al. 2010; Choi et al. 2010; Hu et al. 2011a; Bishay et al. 2010; Irazu and Elejabarrieta 2017). Whereas the increment of the resonance frequencies have been well understood and attributed to the magnetorheological effect of the MR core, the phenomenon responsible to decrease the resonance frequencies have not been clear up-today. However, different hypothesis have been given. Choi et al. (2010) claimed the

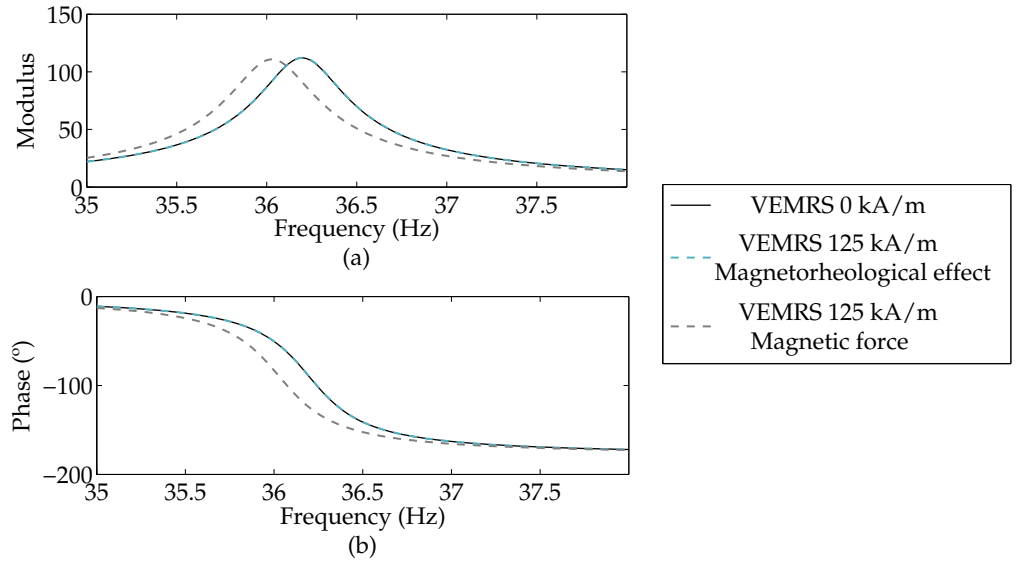

Figure 5.2. Contribution of the magnetorheological effect and magnetic force on the transfer function, (a) modulus and (b) phase, of the VEMRS with a free length of 160 mm in the first resonance.

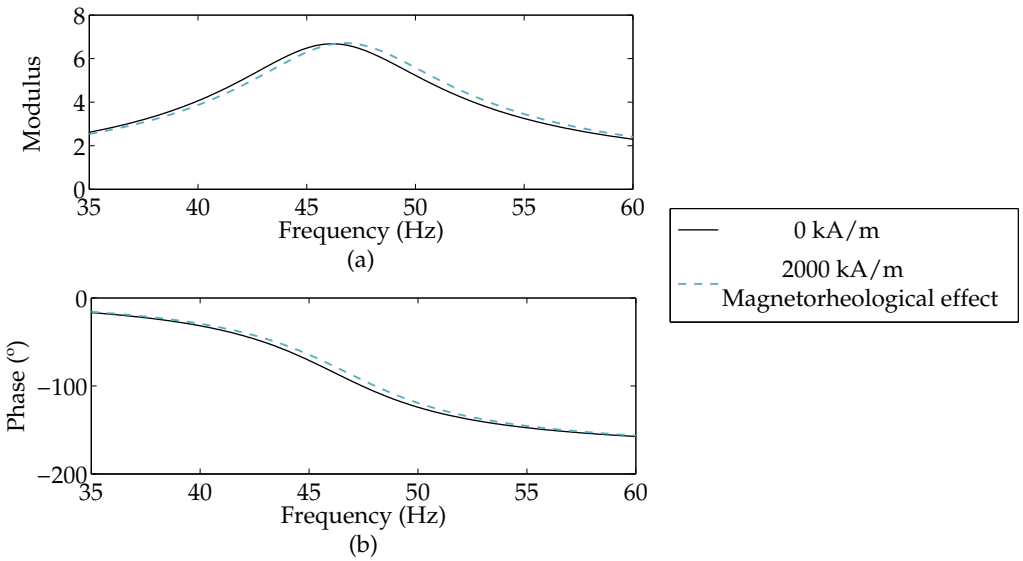

Figure 5.3. Contribution of the magnetorheological effect on the transfer function, (a) modulus and (b) phase, of the VEMRS composed of a 2 mm core and with a free length of 160 mm in the first resonance.

decrease of the natural frequency is due to the magnetic preload (Yin et al. 2006),Lara-Prieto et al. (2010) reported the non-uniform magnetic field over the sandwich lead to a non-uniform concentration of the magnetic particles and so a non-uniform stiffening effect of the MR fluid and Bishay et al. (2010) claimed the decrease of the natural frequency is attributed to a higher damping effect of the MR fluid than the stiffening effect. This Chapter gives an explanation to an experimentally observed behaviour with MR sandwiches and provides a numerical modelling able to represent such behaviour.

5.5 Conclusions

This chapter analysed the influence of the magnetorheological effect and magnetic force generated in the core of VEMRSs on their dynamic behaviour. The magnetic force model developed by Moon and Pao (1969) for a ferromagnetic beam was proposed to describe the magnetic interaction given in the VEMRS beam as a first approach. Then, a magneto-dynamic modelling of VEMRSs by FEM that includes the magnetorheological effect and magnetic force was developed and validated with experimental results. The numerical results showed the influence of the two phenomena is opposite; the magnetorheological effect tends to increase the resonance frequency of the sandwich, whereas the magnetic force tends to decrease. In the analysed thin VEMRS the predominant mechanism in its magneto-dynamic behaviour is the magnetic force. The influence of the magnetorheological effect not being appreciable due to the high stiffness of the VEMR in the absence of a magnetic field and the low magnetic particles concentration.

In addition, in this chapter an explanation was given to an experimentally observed behaviour with MR sandwiches in literature. This was the first time, to the author's knowledge, that the magnetic force generated in the MR core was identified as the mechanism responsible for decreasing the resonance frequencies of the sandwich and that a numerical modelling able to represent such behaviour was developed.

5.6 Scientific contribution

The effect of the magnetoelastic force on the magneto-dynamic model of viscoelastic-magnetorheological sandwiches

Leire Irazu and María Jesús Elejabarrieta
Mechanical & Manufacturing Department, Mondragon Unibertsitatea, Loramendi 4, 20500 Arrasate-Mondragon, Spain

Smart Materials and Structures
(Submitted October 2017)

The effect of the magnetoelastic force on the magneto-dynamic model of viscoelastic-magnetorheological sandwiches

L. Irazu and M. J. Elebajarrieta

Mech. & Manuf. Dept., Mondragon Unibertsitatea, 20500 Arrasate-Mondragon, Spain

E-mail: mjelejabarrieta@mondragon.edu

October 2017

Abstract.

A new magneto-dynamic model of viscoelastic-magnetorheological sandwiches is developed and validated with experimental results. The novelty of the model is that in addition to the magnetorheological effect of the core it also contemplates the magnetoelastic force generated in the sandwich as a result of the interaction between the magnetized vibrating sandwich and the applied magnetic field. The numerical results show the contribution of the magnetoelastic force on the magneto-dynamic behaviour of the sandwich is to decrease the natural frequency of the structure. Increasing the intensity of the magnetic field, the natural frequency and the vibration amplitude of the sandwich decrease which agrees with experimental results observed in literature. To the author's best knowledge this is the first time the magnetoelastic force is identified as the mechanism resposible for decreasing the natural frequencies of viscoelastic-magnetorheological sandwiches and that this magneto-dynamic behaviour have been represented.

Keywords: Viscoelastic-magnetorheological sandwich, micron-size core, magneto-dynamic model, magnetoelastic force, magnetorheological effect.

1. Introduction

In industrial applications, mechanical vibrations produce numerous adverse effects including acoustic radiation, excessive stresses, large deformations and progressive damage accumulation in engineering materials due to cyclic fatigue. Passive damping techniques by means of viscoelastic materials have been widely used to attenuate vibration as they result simple to implement and cost-effective. Specifically, viscoelastic sandwiches provide many advantages such as high damping-to-weight, strength-to-weight and stiffness-to-weight ratios, and so they are of special interest for the aerospace, aeronautical, automotive and marine industries [1]. However, the dynamic properties of

these sandwiches are fixed by their design and so they are unable to adapt to random sources of vibration in real time. In such cases, semi-active sandwiches in which the active control can be used to enahnce the vibration attenuation are required.

The constantly increasing requirements for the vibration control have made in recent years scientists and engineers propose different semi-active sandwiches, in which the active control can be used to enhance the vibration attenuation of the structure when needed [1]. Semi-active sandwiches can be obtained by attaching piezoelectric actuators to the sandwich structure [2, 3], or by replacing the viscoelastic core with a smart material, such as shape memory alloys [4], electrorheological materials [5, 6] or magnetorheological materials [7, 8].

Magnetorheological (MR) materials are smart materials possessing the unique ability to modify their rheological properties in response to external magnetic fields. This phenomenon is known as magnetorheological effect. MR materials are composed of micro or nanosized magnetic particles suspended in a non-magnetisable medium. These materials have variable stiffness and damping properties attributed to the magnetorheological effect and so they offer attractive features for constructing smart sandwich structures with enhanced vibration control.

In the modelling of smart MR sandwiches uptoday just the magnetorheological effect has been considered [9, 10, 11, 12, 13]. However, when a magnetic field is applied to a vibrating MR sandwich two phenomena occur: the dynamic properties of the core are modified due to the magnetorheological effect and a magnetoelastic force is generated as a result of the iteraction between the magnetized vibrating sandwich and the applied magnetic field. In this work, a new mangneto-dynamic model for viscoelastic-magnetorheological sandwiches (VEMRS) considering both phemenomena is developed. This model allows to represent magneto-dynamic behaviors that until now could not be represented.

First, the magnetorheological effect and magnetoelastic force models are proposed. Then, the magneto-dynamic model of VEMRSs by finite element method (FEM) is presented and validated with experimental results. Finally, the influence of the magnetoelastic force on the dynamic behaviour of the sandwich is studied, as well as the effect of the intensity of the magnetic field.

2. Magneto-dynamic model

Smart VEMRSs are composed of a micron-size vircoelastic-magnetorheological (VEMR) core. The dynamics these sandwich structures is modified in response to external magnetic fields. The rheological properties of the VEMR core change as a result of itneractions generated between magnetic particles, whcih is known as magnetorheological effect [14]. In particular, a field-induced stiffening co the core occurs. In addition, the VEMR core is magnetized and so a magnetoelastic force is generated in the VEMRS due to the itneraction between the magnetized virbating sandwich and the applied magnetic field[15].

Next, the magnetorheological effect and magnetic force models are described and their implementation in the FEM model of the sandwich is presented. Afterwards, the developed magneto-dynamic model of VEMRSs is validated with experimental results.

2.1. Magnetorheological effect

The rheological properties of the VEMR core depend on the intensity of the applied magnetic field due to the interactions generated between magnetic particles [14]. In literature different models have been proposed to describe the magnetic field dependence of magnetorheological materials [16, 17, 18, 19]. In this work the dipole-dipole interaction based model developed by Jolly et al. [16, 17] with the correction proposed by Agirre-Olabide et al. [20] for isotropic materials is used. This model only contemplates the influence of the magnetic field on the shear modulus of the VEMR film.

Assuming a linear viscoelastic behaviour of the VEMR core, its the shear complex modulus in the absence of a magnetic field, G_{v}^{*}, can be expressed as

$$G_{\mathrm{v}}^{*} = G_{\mathrm{v}}\left(1 + \mathrm{i}\eta_{\mathrm{v}}\right), \tag{1}$$

where G_{v} is the shear modulus and η_{v} is the loss factor. When a magnetic field is applied the shear modulus of the VEMR film is increased due to the interactions generated between magnetic particles. Thus, the shear complex modulus as a function of the magnetic field, $G_{\mathrm{v}}^{*}(H)$, can be expressed as

$$G_{\mathrm{v}}^{*}(H) = \left(G_{\mathrm{v}} + G_{\mathrm{v_H}}(H)\right)\left(1 + \mathrm{i}\eta_{\mathrm{v}}\right), \tag{2}$$

where $G_{\mathrm{v_H}}(H)$ is the field-induced change. According to the model developed by Jolly et al. [16, 17] with the correction proposed by Agirre-Olabide et al. [20] for isotropic magnetorheological materials $G_{\mathrm{v_H}}(H)$ is given by

$$G_{\mathrm{v_H}}(H) = \frac{4\varphi J_{\mathrm{p}}^{2} R^{3}}{\mu_{\mathrm{m}}\mu_{0} d^{3}}(1-\varphi), \tag{3}$$

where φ is the volume faction of particles in the composite, R is the radio of the particles, μ_0 is the magnetic permeability of the vacuum and μ_{m} is the relative magnetic permeability of the viscoelastic medium. The distance between each particle, d, is obtained from

$$d = \sqrt{\upsilon \frac{\frac{4}{3}\pi R^{3}}{\varphi}}, \tag{4}$$

where υ is the particle lattice coefficient [21, 22]. The induced polarisation of the particle, J_{p}, is obtained from

$$J_{\mathrm{p}} = \frac{3}{2}\alpha^{3}\mu_{0}H + (1-\alpha^{3})J_{\mathrm{s}}, \tag{5}$$

where H is the applied magnetic field intensity, J_{s} is the magnetic saturation and α is the saturation ratio of each particle [16].

2.2. Magnetoelastic force

The VEMR core is magnetized under a magnetic field since it is composed of ferromagnetic particles [23]. Thus, when a magnetic field is applied to a vibrating VEMRS this is subjected to a distributed magnetic force arising from the interaction between the magnetization of its core and the magnetic field [15]. The model developed by Moon and Pao [15] for a linear ferromagnetic beam vibrating in an homogeneous transverse magnetic field is proposed to describe the magnetoelastic force as a first approach. The Moon and Pao's model is based on the following assumptions:

- The effect of the induced current is negligible and so the resultant magnetic force system on the vibrating beam is assumed to consist of a magnetic couple proportional to the rotation of the beam.
- The magnetic field in the vibrating beam at any instant is given by that for a static beam configuration.

The Moon and Pao's model is acceptable when the ratio length-to-thickness of the ferromagnetic beam is greater than 100-200 [24, 25], requirement met by the VEMR core.

According to Moon and Pao [15] the resultant magnetic force is a body couple given by

$$C(H) = b\,(H)\,\frac{\partial w}{\partial x}, \tag{6}$$

in which $\frac{\partial w}{\partial x}$ is the rotation of the beam, Figure 1, and the proportional coefficient b is expressed as

$$b(B) = \frac{2\chi^2 H^2 \mu_0 \mu_{\mathrm{r}} \sinh\left(\frac{kh_2}{2}\right)}{k\Delta}, \tag{7}$$

where χ is the magnetic susceptibility, k is the wave number, h_2 is the core thickness, μ_0 is the magnetic permeability of the vacuum, μ_{r} is the relative magnetic permeability of the VEMR core and $\Delta = \mu_{\mathrm{r}} \sinh\left(\frac{kh_2}{2}\right) + \cosh\left(\frac{kh_2}{2}\right)$.

2.3. Finite element model

The proposed magnetorheological effect and magnetoelastic force models are implemented in FEM in order to obtain the magneto-dynamic model of VEMRSs.

A three-layer beam finite element based on the following assumptions is considered:

- The skin layers bend according to Euler-Bernoulli beam theory and the VEMR core is subjected only to shear deformation.
- The transverse displacement is uniform on a cross section of the sandwich.
- All layers are assumed to be perfectly bonded, not having slippage between layers during deformation.

The three-layer finite element is defined by two nodes with four degrees of freedom (DOF) per node, which are: the axial displacements of the top and bottom skin layer, u_1 and u_2, the transverse displacement of the beam, w, and the rotational displacement of the beam, $\frac{\partial w}{\partial x}$. In Figure 1 the configuration of the sandwich and the assume displacement field is shown. Note that $(\bullet)_1$, $(\bullet)_2$ and $(\bullet)_3$ refer to the top, core, and bottom layers, respectively.

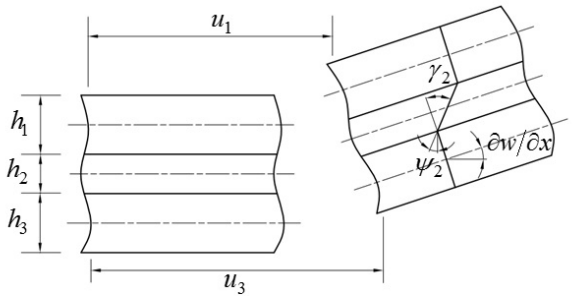

Figure 1. Displacement field of the sandwich beam.

The total angular rotation of the core, ψ_2, is given by

$$\psi_2 = -\gamma_2 - \frac{\partial w}{\partial x}, \tag{8}$$

and the shear strain in the core, γ_2, is derived from [26]

$$\gamma_2 = \left(1 + \frac{h_1 + h_3}{2h_2}\right)\frac{\partial w}{\partial x} + \frac{u_1 - u_3}{h_2} \tag{9}$$

The generalized displacement vector can be determined in terms of displacements of two nodes, such as

$$\begin{Bmatrix} u_1 \\ u_2 \\ w \end{Bmatrix} = \begin{Bmatrix} \mathbf{N}_{\mathrm{u1}} \\ \mathbf{N}_{\mathrm{u3}} \\ \mathbf{N}_{\mathrm{w}} \end{Bmatrix} \mathbf{q}^e \tag{10}$$

where $\mathbf{q}^e$ is the displacement vector of the element, $\mathbf{N}_{\mathrm{u1}}$ and $\mathbf{N}_{\mathrm{u3}}$ are the Lagrange linear shape functions and $\mathbf{N}_{\mathrm{w}}$ is the Hermite cubic shape function.

The stiffness matrix for the sandwich element is obtained from the strain energy. This includes extension of the skin layers, bending of the skin layers, a negative bending stiffness due to the magnetic body couple generated in the VEMR core and shear deformation of the core which is modified in the presence of a magnetic field due to the magnetorheological effect of the VEMR core. Thus, the element stiffness matrix, $\mathbf{k}^{e^*}(H)$, depends on magnetic field and it is given by

$$\mathbf{k}^{e^*} = \mathbf{k}^{e^*}_{\mathrm{extension}} + \mathbf{k}^{e^*}_{\mathrm{bending}}(H) + \mathbf{k}^{e^*}_{\mathrm{shear}}(H), \tag{11}$$

where

$$\mathbf{k}^{e^*}_{\text{extension}} = \int_0^{l_e} \left(E_1 A_1 \frac{\partial \mathbf{N}_{\text{u}_1}^{\text{T}}}{\partial x} \frac{\partial \mathbf{N}_{\text{u}_1}}{\partial x} + E_3 A_3 \frac{\partial \mathbf{N}_{\text{u}_3}^{\text{T}}}{\partial x} \frac{\partial \mathbf{N}_{\text{u}_3}}{\partial x} \right) \mathrm{d}x, \tag{12}$$

$$\mathbf{k}^{e^*}_{\text{bending}}(H) = \int_0^{l_e} \left(E_1 I_1 + E_3 I_3 - \frac{b(H)}{k^2} \right) \frac{\partial^2 \mathbf{N}_{\text{w}}^{\text{T}}}{\partial x^2} \frac{\partial^2 \mathbf{N}_{\text{w}}}{\partial x^2} \mathrm{d}x, \tag{13}$$

$$\begin{aligned} \mathbf{k}^{e^*}_{\text{shear}}(H) = \int_0^{l_e} & G_{\text{v}}^*(H) A_2 \left(1 + \frac{h_1 + h_3}{2h_2} \right) \\ & \left(\frac{\partial \mathbf{N}_{\text{w}}}{\partial x} + \frac{\mathbf{N}_{\text{u}_1} - \mathbf{N}_{\text{u}_3}}{h_2} \right)^{\text{T}} \left(\frac{\partial \mathbf{N}_{\text{w}}}{\partial x} + \frac{\mathbf{N}_{\text{u}_1} - \mathbf{N}_{\text{u}_3}}{h_2} \right) \mathrm{d}x, \end{aligned} \tag{14}$$

l_e is the length of the element, I_1 and I_3 are the second moment of inertia at the centroid of the skin layers and A_1, A_3 and A_2 are the cross-sectional area of the skin layers and the core.

The mass matrix for the sandwich element is obtained from the kinetic energy, which includes the transverse displacement of all layers, the axial displacement of skin layers and the rotation of the core. The element mass matrix, $\mathbf{m}^e$, is constant and it is given by

$$\mathbf{m}^e = \mathbf{m}^e_{\text{axial translation}} + \mathbf{m}^e_{\text{transverse translation}} + \mathbf{m}^e_{\text{rotation}}, \tag{15}$$

where

$$\mathbf{m}^e_{\text{axial translation}} = \int_0^{l_e} \left(\rho_1 A_1 \mathbf{N}_{\text{u}_1}^T \mathbf{N}_{\text{u}1} + \rho_3 A_3 \mathbf{N}_{\text{u}_3}^T \mathbf{N}_{\text{u}3} \right) \mathrm{d}x, \tag{16}$$

$$\mathbf{m}^e_{\text{transverse translation}} = \int_0^{l_e} \rho A \mathbf{N}_{\text{w}}^T \mathbf{N}_{\text{w}} \mathrm{d}x, \tag{17}$$

$$\begin{aligned} \mathbf{m}^e_{\text{rotation}} = \int_0^{l_e} & \rho_2 I_2 \left(- \left(\left(1 + \frac{h_1 + h_3}{h_2} \right) \frac{\partial \mathbf{N}_{\text{w}}}{\partial x} + \frac{\mathbf{N}_{\text{u}1} - \mathbf{N}_{\text{u}3}}{h_2} \right) \frac{\partial \mathbf{N}_{\text{w}}}{\partial x} \right)^{\text{T}} \\ & \left(- \left(\left(1 + \frac{h_1 + h_3}{h_2} \right) \frac{\partial \mathbf{N}_{\text{w}}}{\partial x} + \frac{\mathbf{N}_{u1} - \mathbf{N}_{\text{u}3}}{h_2} \right) \frac{\partial \mathbf{N}_{\text{w}}}{\partial x} \right) \mathrm{d}x, \end{aligned} \tag{18}$$

I_2 is the second moment of inertia at the centroid of the core and ρ, ρ_1, ρ_2, and ρ_3 are the total density of the sandwich, skin layers and core layer, respectively.

The governing equation of motion of the VEMRS in the finite element form is written as

$$\mathbf{M}\ddot{\mathbf{q}} + \mathbf{K}^*\mathbf{q} = \mathbf{F}, \tag{19}$$

where $\mathbf{q}$ and $\ddot{\mathbf{q}}$ are the displacement vector and the acceleration vector, and where $\mathbf{M}$, $\mathbf{K}^*$ and $\mathbf{F}$ are the global mass matrix, the global stiffness matrix and the global force

vector, obtained by assembling the corresponding matrices for all of the elements. If a steady-state harmonic base excitation is considered, and the motion equation is written differentiating the DOF related to the base displacement vector, indicated by $(\bullet)_{\mathrm{s}}$, and the unknown displacement vector, indicated by $(\bullet)_{\mathrm{u}}$, the following is obtained

$$\left(-\omega^2 \begin{bmatrix} \mathbf{M}_{\mathrm{ss}} \mathbf{M}_{\mathrm{su}} \\ \mathbf{M}_{\mathrm{us}} \mathbf{M}_{\mathrm{uu}} \end{bmatrix} + \begin{bmatrix} \mathbf{K}^*_{\mathrm{ss}} \mathbf{K}^*_{\mathrm{su}} \\ \mathbf{K}^*_{\mathrm{us}} \mathbf{K}^*_{\mathrm{uu}} \end{bmatrix}\right) \begin{Bmatrix} \mathbf{S}^* \\ \mathbf{U}^* \end{Bmatrix} = \begin{Bmatrix} \mathbf{R}^* \\ 0 \end{Bmatrix}, \tag{20}$$

where $\mathbf{S}^*$, $\mathbf{U}^*$ and $\mathbf{R}^*$ are the amplitude vector of the applied base motion, unknown displacements and reaction forces on the base, respectively. The unknown displacement amplitude vector, $\mathbf{U}^*$, is obtained from

$$\mathbf{U}^* = \frac{\left(\omega^2 \mathbf{M}_{\mathrm{us}} - \mathbf{K}^*_{\mathrm{us}}\right) \mathbf{S}^*}{-\omega^2 \mathbf{M}_{\mathrm{uu}} + \mathbf{K}^*_{\mathrm{uu}}}, \tag{21}$$

and the transmissibility function is determined by dividing the transverse displacement of the response DOF U^*_j by the transverse displacement applied at the base DOF S^*_i , as

$$T^*_{ij} = \frac{U^*_j}{S^*_i} \tag{22}$$

The FEM first has to be computed in the absence of a magnetic field, $H = 0\mathrm{kA/m}$ in Equation 19 to Equation 22, in order to identify the natural frequencies of the VEMRS structure to be analysed. Then, the FEM model under different magnetic field intensities, H, can be computed for each vibration mode.

2.4. Experimental Validation

A thin VEMRS was tested in order to validate the developed magneto-dynamic model. The VEMRS was composed of two identical 1050 H18 aluminium alloy skins and an isotropic viscoelastic-magnetorheological film. The micron-size isotropic VEMR film was synthesised by adding spherical carbonyl iron powder (CIP) particles of 1.25 ± 0.55 m in a 12% volumetric concentration to a polyester-based adhesive. The geometrical and physical properties of the VEMRS and its components are shown in Table 1 and Table 2.

Table 1. Geometrical and physical properties of the VEMRS.

VEMRS			
Length (mm)	Thickness (mm)	Width (mm)	Density (g/cm3)
160 ± 0.5	1.162 ± 0.003	9.900 ± 0.002	2.676 ± 0.008

Table 2. Geometrical and physical properties of the components of the VEMRS.

Skins			Core		
Thickness (mm)	Density (g/cm3)	Complex modulus (GPa)	Thickness (m)	Density (g/cm3)	Shear complex modulus (MPa)
0.564 ± 0.002	2.7*	68.11 + 0.1634i**	35 ± 2	1.91*	1.675 + 0.54i**

*Data provided by the manufacturer, Replasa S.A.

**Data obtained from forced vibration test according to ASTM E 756-05 standard.

The experimental technique consisted of forced vibrations with resonance according to ASTM E 756-05 standard with the modification proposed by Cortes and Elejabarrieta [27, 28]. The sandwich beam was tested in a cantilever configuration. The base excitation was generated by an electrodynamic shaker and the acceleration of the base was measured by a piezoelectric accelerometer and loopback controlloed by a vibration controller. The response of the beam was measured in the free end by a laser vibrometer and the data acquisition and signal processing were performed with an analyser connected to a computer. The transmissibility function was determined by relating the response movement of the beams free end with that applied at the base [29].

The transmissibility function of the cantilever sandwich beam was measured in the absence of and under a magnetic field. The magnetic field was implemented in the forced vibrations test by means of a device composed of twelve magnets, NdFeB 35 MGOe 42 x 42 x 8 mm^3, distributed symmetrically along the length of the beam. A photograph of the VEMRS beam with the magnets device can be seen in Figure 2. The magnetic field obtained with such magnets configuration was determined by a simulation in the Finite Element Method Magnetics 4.2 software. In Figure 3 it can be seen the magnetic field is almost completely transversal and homogeneous along the length of the beam.

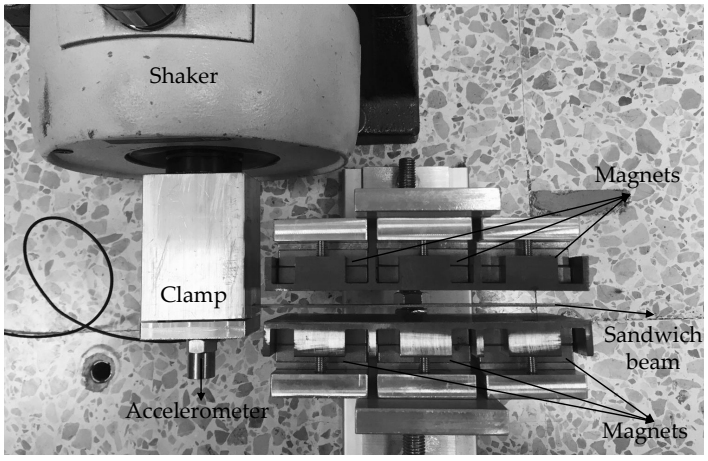

Figure 2. Photograph of the thin VEMRS with the magnets device.

Following, the numerical transmissibility function of the VEMRS in the absence of and under the magnetic field is compared with the experimental ones in order to validate the proposed magneto-dynamic model of thin VEMRSs.

To that end, first the magnetorheological effect of the VEMR core, $G_{v_H}(H)$, was determined. The field-induced change was calculated from Equation 3 to Equation 5 considering the parameters shown in Table 3. For the magnetic field of 125 kA/m its value is $G_{v_H}(H) = 2.9 \cdot 10^3$ Pa.

Then, the distributed magnetic force to which is subjected the vibrating thin

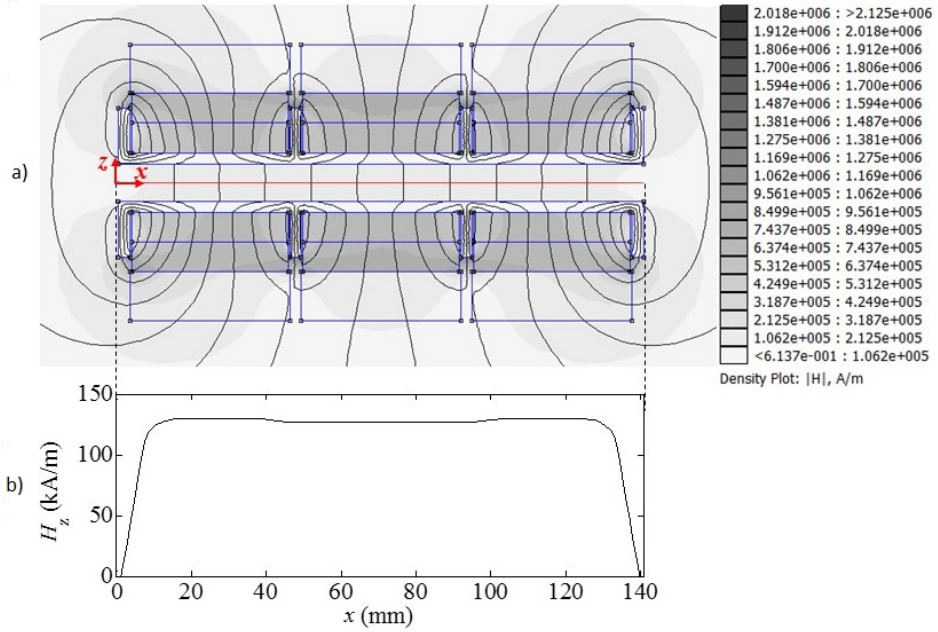

Figure 3. Simulation of the magnetic field: a) magnetic flux distribution and b) magnetic field intensity along the length of the magnets device.

Table 3. Parameters of the magnetorheological effect model.

φ	R (µm)	μ_{m}	υ	J_{s}	α
0.12	1.25 ± 0.55	1	1	2.1 T	0.94

VEMRS is determined. For that, first the relative magnetic permeability of the VEMR core is obtained according to Bruggeman mixing rule $\mu_{\mathrm{r}} = 1.48$ [30, 31]. Then, the magnetic body couple coefficient, $b(H)$, is obtained from Equation 7, which for a magnetic field of 125 kA/m its value is $b = 0.107$.

Finally, in the FEM model the sandwich beam is discretised by 5 mm long elements and the transmissibility function of VEMRS in the first resonance is obtained with a 0.02 Hz resolution.

Figure 4 shows the numerical and experimental transmissibility functions of the VEMRS in the absence of and under the magnetic field of 125 kA/m. It can be observed the correlation is good in both cases. Applying the magnetic field, the natural frequency of the VEMRS is decreased, the developed magneto-dynamic model being able to represent such behaviour. This result highlights the validity of the proposed magneto-dynamic model of VEMRSs.

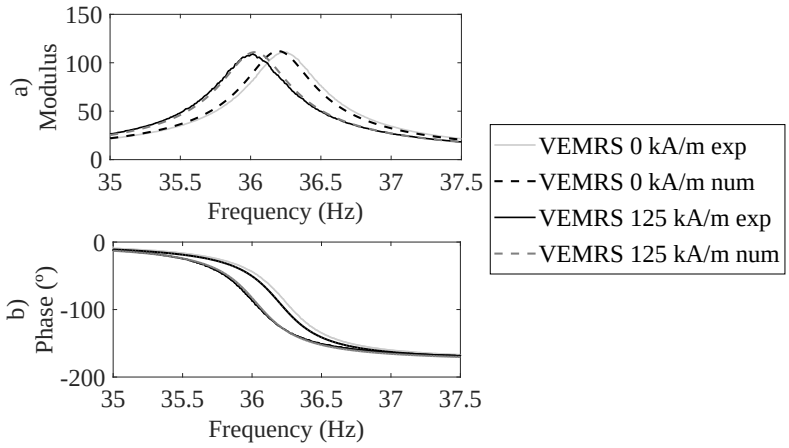

Figure 4. Numerical and experimental transmissibility function, a) Modulus and b) Phase, of the VEMRS in the absence of and under a magnetic field in the first resonance.

3. Effect of the magnetoelastic force

Next, the effect of the magnetoelastic force on the magneto-dynamic response of VERMSs is studied and then the influence of the magnetic field intensity.

Figure 5 shows the transmissibility function of the VEMRS in the absence of magnetic field and the individual contribution of the magnetorheological effect and magnetoelastic force generated by a magnetic field of 125 kA/m. The magnetoelastic force tends to decrease the resonance frequency of the VEMRS, whereas the magnetorheological effect has no appreciable influence. From literature it is known the magnetorheological effect tends to increase the resonance frequency of the sandwich [32, 33, 34] thus it is concluded the influence of the magnetorheological effect and the magnetoelastic force is opposite. Depending on the nature of the VEMR core and the sandwich configuration, the influence of one will predominate over the other. In the analysed thin VEMRS the magnetorheological effect is not appreciable due to low magnetic particles concentration, isotropic configuration and high stiffness of the VEMR core.

In literature several authors have observed experimentally the decrement of natural frequencies of magnetorheological sandwiches when applying magnetic fields [7, 35, 36, 11, 8] and different hypothesis have been given to justify this behaviour. Choi et al. [35] claimed the decrease of the natural frequency is due to the magnetic preload of the magnetorheological elastomer [37], Lara-Prieto et al. [7] reported the non-uniform magnetic field over the sandwich lead to a non-uniform concentration of the magnetic particles and so a non-uniform stiffening of the magnetorheological fluid and Bishay et al. [11] claimed the decrease of the natural frequency is attributed to a higher damping effect of the magnetorheological fluid than the stiffening effect. However, the mechanism

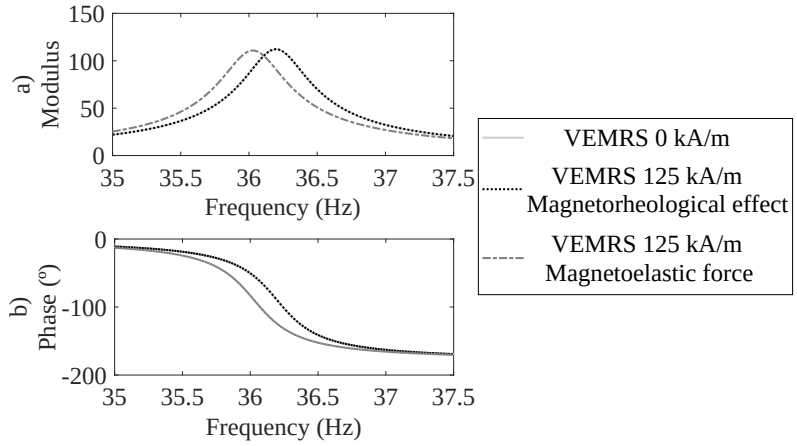

Figure 5. Contribution of the magnetorheological effect and magnetoelastic force on the transmissibility function of the first resonance, a) Modulus and b) Phase, of the VEMRS.

responsible to decrease the resonance frequencies of the structure have not been clear and no numerical models have been proposed to describe such behaviour up-today.

Finally, the influence of the magnetic field intensity on the dynamic response of the VEMRS is analysed. Figure 6 shows the transmissibility function of the analysed thin VEMRS under different intensities of magnetic field. Note, even with a magnetic field of 500 kA/m the magnetorheological effect has no substantial influence. Increasing the magnetic field, the natural frequency is decreased. In addition the transmissibility modulus is slightly decreased. The influence of the magnetic field intensity is not linear, being the influence of the increment of the magnetic field bigger at higher intensities.

4. Conclusions

In this work a new magneto-dynamic model of viscoelastic-magnetorheological sandwiches by FEM was developed. The novelty of the model is that in addition to the magnetorheological effect of the core, it also contemplates the magnetoelastic force generated in the sandwich as a result of the interaction between the magnetized vibrating sandwich and the applied magnetic field. The magnetoelastic force is described by the force model developed by Moon and Pao [15] for ferromagnetic beams as a first approach. The proposed magneto-dynamic model of VEMRSs correlates well with the experimental results in the first resonance.

The numerical results show the contribution of the magnetoelastic force on the magneto-dynamic behaviour of the VEMRS is to decrease the natural frequency of the structure. Increasing the intensity of the magnetic field, the natural frequency and the vibration amplitude of the sandwich decrease which agrees with experimental results observed in literature. These results lead to the conclude the influence of the

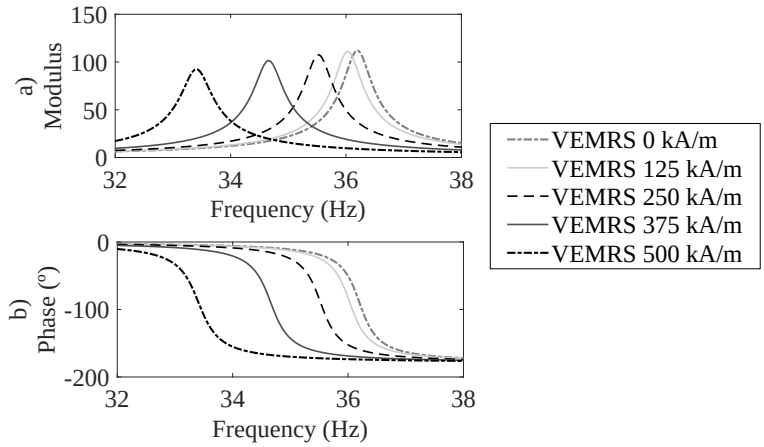

Figure 6. Numerical transmissibility functions, a) Modulus and b) Phase, of the VEMRS under different intensities of magnetic field, 0 kA/m, 125 kA/m, 250 kA/m, 375 kA/m and 500 kA/m, in the first resonance.

magnetorheological effect and the magnetoelastic force is opposite. To the author's best knowledge, this is the first time that the magnetoelastic force is identified as the mechanism responsible for decreasing the natural frequency and a numerical model to describe such behaviour is proposed.

Acknowledgements

The present study was partially supported by the AVISANI (DPI2015-71198-R, Spanish Government) and AVISANI (PI_2016_1_0026, Basque Government) projects and Replasa S.A.

References

[1] M. D. Rao. Recent applications of viscoelastic damping for noise control in automobiles and commercial airplanes. *Journal of Sound and Vibration*, 262(3):457–474, may 2003.

[2] M. A. Trindade and A. Benjeddou. Hybrid active-passive damping treatments using viscoelastic and piezoelectric materials: Review and assessment. *Modal Analysis*, 8(6):699–745, jun 2002.

[3] N. Kumar and S. P. Singh. Vibration and damping characteristics of beams with active constrained layer treatments under parametric variations. *Materials & Design*, 30(10):4162–4174, dec 2009.

[4] P. Butaud, E. Foltête, and M. Ouisse. Sandwich structures with tunable damping properties: On the use of Shape Memory Polymer as viscoelastic core. *Composite Structures*, 153:401–408, oct 2016.

[5] K. Ramkumar and N. Ganesan. Vibration and damping of composite sandwich box column with viscoelastic/electrorheological fluid core and performance comparison. *Materials & Design*, 30(8):2981–2994, sep 2009.

[6] K. Wei, Q. Bai, G. Meng, and L. Ye. Vibration characteristics of electrorheological elastomer sandwich beams. *Smart Materials and Structures*, 20(5):055012, may 2011.

[7] V. Lara-Prieto, R. Parkin, M. Jackson, V. Silberschmidt, and Z. Kesy. Vibration characteristics of MR cantilever sandwich beams: experimental study. *Smart Materials and Structures*, 19(1):015005, jan 2010.

[8] L. Irazu and M. J. Elejabarrieta. Magneto-dynamic analysis of sandwiches composed of a thin viscoelastic-magnetorheological layer. *Journal of Intelligent Material Systems and Structures*, page 1045389X1770520, may 2017.

[9] G Y Zhou, K C Lin, and Q Wang. Finite element studies on field-dependent rigidities of sandwich beams with magnetorheological elastomer cores. *Smart Materials and Structures*, 15(3):787–791, jun 2006.

[10] V. Rajamohan, R. Sedaghati, and S. Rakheja. Vibration analysis of a multi-layer beam containing magnetorheological fluid. *Smart Materials and Structures*, 19:015013, 2010.

[11] P. L. Bishay, M. Tawfik, and H. M. Negm. Experimental and finite element models of an adaptive magnetorheological sandwich beam. In *The 17th International Congress on Sound and Vibration*, Cairo, 2010.

[12] Babu V. Ramesh, R. Vasudevan, and Naveen B. Kumar. Vibration analysis of a laminated composite magnetorheological elastomer sandwich beam. *Applied Mechanics and Materials*, 592-594:2097–2101, jul 2014.

[13] S. Aguib, A. Nour, H. Zahloul, G. Bossis, Y. Chevalier, and P. Lancon. Dynamic behavior analysis of a magnetorheological elastomer sandwich plate. *International Journal of Mechanical Sciences*, 87:118–136, oct 2014.

[14] L. Chen, X. L. Gong, and W. H. Li. Effect of carbon black on the mechanical performances of magnetorheological elastomers. *Polymer Testing*, 27(3):340–345, may 2008.

[15] F. C. Moon and Y. Pao. Vibration and dynamic instability of a beam-plate in a transverse magnetic field. *Journal of Applied Mechanics*, 36(1):92, 1969.

[16] M. R Jolly, J. D. Carlson, B. C. Muñoz, and T. A. Bullions. The magnetoviscoelastic response of elastomer composites consisting of rerrous particles embedded in a polymer matrix. *Journal of Intelligent Material Systems and Structures*, 7(6):613–622, nov 1996.

[17] M. R. Jolly, J. D. Carlson, and B. C Muñoz. A model of the behaviour of magnetorheological materials. *Smart Materials and Structures*, 5(5):607–614, oct 1996.

[18] Y. Shen, M. F. Golnaraghi, and G. R. Heppler. Experimental research and modeling of magnetorheological elastomers. *Journal of Intelligent Material Systems and Structures*, 15(1):27–35, jan 2004.

[19] I. Bica, M. Balasoiu, and A. I. Kuklin. Anisotropic silicone rubber based magnetorheological elastomer with oil silicone and iron microparticles. *Solid State Phenomena*, 190:645–648, jun 2012.

[20] I. Agirre-Olabide, A. Lion, and M. J. Elejabarrieta. A new three-dimensional magneto-viscoelastic model for isotropic magnetorheological elastomers. *Smart Materials and Structures*, 26(3):035021, mar 2017.

[21] D. Ivaneyko, V. P. Toshchevikov, M. Saphiannikova, and G. Heinrich. Magneto-sensitive elastomers in a homogeneous magnetic field: A regular rectangular lattice model. *Macromolecular Theory and Simulations*, 20(6):411–424, jul 2011.

[22] D. Ivaneyko, V. P. Toshchevikov, M. Saphiannikova, and G. Heinrich. Effects of particle distribution on mechanical properties of magneto-sensitive elastomers in a homogeneous magnetic field. *Condensed Matter Physics*, 15(3):33601, sep 2012.

[23] C. Gélinas, F. Chagnon, and S. Pelletier. Development of an iron-resin composite material for soft magnetic applications. In *World Congress*, pages 85–97, Washington, 1996.

[24] Y. Zhou and X. Zheng. A theoretical model of magnetoelastic bucking for soft ferromagnetic thin plates. *Acta Mechanica Sinica*, 12(3):213–224, aug 1996.

[25] X. J. Zheng, Y. H. Zhou, X. Z. Wang, and J. S. Lee. Bending and buckling of ferroelastic plates. *Journal of Engineering Mechanics*, 125(2):180–185, feb 1999.

[26] D. J. Mead and S. Markus. The forced vibration of a three-layer, damped sandwich beam with

arbitrary boundary conditions. *Journal of Sound and Vibration*, 10(2):163–175, sep 1969.

[27] ASTM E 756-05. Standard test method for measuring vibration-damping properties of materials, 2005.

[28] F. Cortés and M. J. Elejabarrieta. Viscoelastic materials characterisation using the seismic response. *Materials & Design*, 28(7):2054–2062, jan 2007.

[29] L. Irazu and M. J. Elejabarrieta. The effect of the viscoelastic film and metallic skin on the dynamic properties of thin sandwich structures. *Composite Structures*, 176:407–419, sep 2017.

[30] D. A. G. Bruggeman. Berechnung verschiedener physikalischer Konstanten von heterogenen Substanzen. III. Die elastischen Konstanten der quasiisotropen Mischkörper aus isotropen Substanzen. *Annalen der Physik*, 421(2):160–178, 1937.

[31] A. Sihvola. Homogenization principles and effect of mixing on dielectric behavior. *Photonics and Nanostructures - Fundamentals and Applications*, 11(4):364–373, nov 2013.

[32] J. Yeh. Vibration analysis of sandwich rectangular plates with magnetorheological elastomer damping treatment. *Smart Materials and Structures*, 22(3):035010, mar 2013.

[33] G. Y. Zhou and Q. Wang. Magnetorheological elastomer-based smart sandwich beams with nonconductive skins. *Smart Materials and Structures*, 14(5):1001–1009, oct 2005.

[34] Biswajit Nayak, Bhanu Subramanya Sastri, Santosha Kumar Dwivedy, and Krishna Murthy. A comparative study of hte classical and higher order theory for free vibration analysis of MRE cored sandwich beam with composite skins using finite element method. In *IEEE-International Conference On Advances In Engineering*, pages 172–178, 2012.

[35] W. J. Choi, Y. P. Xiong, and R. A. Shenoi. Vibration characteristics of sandwich beams with steel skins and magnetorheological elastomer cores. *Advances in Structural Engineering*, 13(5):837–847, oct 2010.

[36] G. L. Hu, M. Guo, and W. H. Li. Analysis of vibration characteristics of magnetorheological elastomer sandwich beam under non-homogeneous magnetic field. *Applied Mechanics and Materials*, 101-102:202–206, sep 2011.

[37] H. Yin, L. Sun, and J. Chen. Magneto-elastic modeling of composites containing chain-structured magnetostrictive particles. *Journal of the Mechanics and Physics of Solids*, 54(5):975–1003, may 2006.

Chapter 6

Thin viscoelastic-magetorheological sandwich

This chapter analyses the dynamics of a thin viscoelastic-magnetorheological sandwich experimentally. The smart sandwich is obtained by adding magnetic particles to the viscoelastic adhesive of a conventional thin sandwich, and the influence of this process is analysed. The effect of the intensity and position of the magnetic field on the magneto-dynamic response of the thin viscoelastic-magnetorheological sandwich is analysed. The resulting behaviours are related to the physical phenomena generated in these sandwiches and studied in Chapter 4 and Chapter 5.

Irazu L and Elejabarrieta MJ (2017). Magneto-dynamic analysis of sandwiches composed of a thin viscoelastic-magnetorheological layer. *Journal of Intelligent Material Systems and Structures*. DOI:10.1177/1045389X17705209.

6.1 Introduction

Smart thin viscoelastic-magnetorheological sandwiches (VEMRS) can be obtained by adding magnetic particles to the viscoelastic (VE) adhesive of thin conventional sandwiches. Unlike other magnetorheological (MR) sandwiches analysed in the literature, these are analogous to thin viscoelastic sandwiches (VES). Thus, they preserve their main advantages, such as high stiffness-to-weight and damping-to-weight ratios and the possibility to use them on classic sheet metal forming processes. In the absence of a magnetic field they behave in a similar way to thin VESs. When magnetic fields are applied, instead, their magneto-dynamic behaviour is the result of the coupling of different physical effects generated in the skins and core. Depending on the composition of the sandwich and the configuration of the magnetic field the contribution of these phenomena is different and so the magneto-dynamic behaviour of the thin VEMRS. The effect of the induced eddy currents on the metallic skins, Chapter 4, and the influence of the magnetorheological effect and magnetic force generated in the viscoelastic-magnetorheological (VEMR) core, Chapter 5, have been already studied.

In this chapter, the dynamics of a thin VEMRS is assessed experimentally. The influence of adding magnetic particles to a VE adhesive of a thin VES on the dynamic properties of the VEMRS is analysed. Then, the effect of the intensity and position of the magnetic field on the magneto-dynamic response of the thin VEMRS is studied. The resulting behaviours are related to the physical phenomena generated in these sandwiches.

Following, a brief state of the art about MR elastomer based sandwiches is presented and the objectives of this chapter are defined. Then, the influence of adding magnetic particles to the VE adhesive of a thin VES on the dynamic properties of the sandwich is analysed. Afterwards, the magneto-dynamic behaviour of the thin VEMRS is studied, analysing the influence of the intensity and position of the magnetic field. Finally, the main conclusions obtained in this chapter are summarized and the scientific contribution is presented.

6.2 State of art

Zhou and Wang (2005) were the first ones proposing the use of MR elastomers as core of sandwich structures to obtain smart sandwiches whose dynamic properties can be modified in response to magnetic fields and since them different authors have analysed these sandwiches.

Review of literature shows that MR elastomer based sandwiches are mostly composed of aluminium skins (Hu et al. 2011b; Megha et al. 2016; Choi et al. 2009; Wei et al. 2008; Aguib et al. 2014). Aluminium is chosen, on the one hand, due to its low damping properties and relatively high stiffness properties compared to those of MR elastomers. On the other hand, because its relative magnetic permeability is equal to 1, which means it does not affect the distribution and the strength of the applied

magnetic field (Hu et al. 2011b). Choi et al. (2010) fabricated MR elastomer based sandwiches composed of steel skins. They observed in these sandwiches the changes on the resonance frequencies and damping under a same applied magnetic field are bigger with bigger skin thickness, since thick steel skins induce a higher value of magnetic field on the MR elastomer. Babu and Vasudevan (2016) fabricated a tapered MR sandwich plate with composite face layers. When it comes to core, isotropic (Aguib et al. 2014; Babu and Vasudevan 2016; Hu et al. 2011b) and anisotropic (Choi et al. 2009; Choi et al. 2010; Wei et al. 2008) MR elastomers have been used to form the sandwiches, in most cases composed of magnetic particles in a 30 % volume fraction.

The smart sandwiches composed of MR elastomers overcome the drawbacks of the ones composed of MR fluids, such as the sealing problems and the settling of magnetic particles. However, in general they are composed of thick elastomers, which may compromise the main advantages of conventional thin VESs. In literature, MR elastomers of thicknesses ranging from 1 to 3 mm have been used to form smart sandwiches (Aguib et al. 2014; Babu and Vasudevan 2016; Hu et al. 2011b; Wei et al. 2008), whereas in some cases even MR elastomers of 10 mm thick have been used (Choi et al. 2009; Choi et al. 2010).

The most conducted experimental test to characterize the magneto-dynamic response of sandwiches composed of MR elastomers has been the forced vibration test under permanent magnets. In most cases, the sandwich was tested in a cantilever configuration (Babu and Vasudevan 2016; Hu et al. 2011b; Wei et al. 2008). However, other boundary conditions, such as simply supported or clamped-clamped, were also studied (Choi et al. 2009).

Experimentally different behaviours have been observed when it comes to resonance frequencies of the sandwich. Wei et al. (2008), Wei et al. (2010), and Babu and Vasudevan (2016) experimentally observed the natural frequencies of sandwiches composed of MR elastomers increase when a global magnetic field along the length of the beam is applied. In contrast, Hu et al. (2011a), Hu et al. (2011b), and Irazu and Elejabarrieta (2017) observed the first resonance frequency of MR elastomer based sandwiches decreases under partial magnetic fields. Choi et al. (2009) and Choi et al. (2010), instead, observed both behaviours. Decrement of the first resonance frequency and increment of the second to fifth ones under global magnetic fields. The increment of the resonance frequencies has been well understood and attributed to the magnetorheological effect of the MR elastomer. Instead, the mechanism responsible to decrease the resonance frequencies have not been clear.

The damping of MR elastomer based sandwiches have been studied analysing the vibration amplitude and loss factor of the sandwich. Most of experimental results have shown the vibration amplitude of the sandwich is decreased when a magnetic field is applied and the loss factor is increased (Choi et al. 2010; Wei et al. 2010; Irazu and Elejabarrieta 2017).

From the reviewed bibliography it can be concluded the analysed smart sandwiches are not analogous to thin VESs since thick MR elastomers have been used to

form the sandwiches. In this way, smart sandwiches able to modify their dynamic properties in response to magnetic fields are obtained, but, the main characteristics of conventional thin VESs may be compromisedExperimental tests have been conducted with MR elastomer based sandwiches in order to analyse their magneto-dynamic behaviour. However, most of these studies have focused on analysing the global behaviour of the sandwich, rather than studying the different phenomena generated in these sandwiches.

6.3 Objectives

The main aim of this chapter is to study experimentally the dynamics of a thin VEMRS. This involves:

- Analysing the influence of adding magnetic particles to the viscoelastic adhesive of a thin VES to obtain a VEMRS.
- Studying the effect of the intensity and position of magnetic fields on the global magneto-dynamic behaviour of the thin VEMRS and relating the resulting behaviours to the physical phenomena generated in these sandwiches.

6.4 Results

In this chapter two sandwich structures are analysed, a VES and a VEMRS. The thin VES is composed of aluminium skins and a polyester-based adhesive and the thin VEMRS was obtained by adding carbonyl iron powder (CIP) particles in a 12% volumetric concentration to the polyester-based adhesive. In the fabrication stage the core thickness of both sandwiches was the same; however, once the vulcanization processes finished the core thickness of the VEMRS was bigger than the VES ones. Both sandwiches geometrical and physical properties are shown in Table 2.2.

The dynamic response of both sandwiches, VES and VEMRS, were measured by the experimental technique detailed in Chapter 2. The forced vibration tests with resonance were carried out in the absence of a magnetic field with both sandwiches, as well as under different intensities and positions of a partial magnetic field with the VEMRS. The partial magnetic field was obtained by placing neodymium magnets in both sides of the beam in a partial region, Figure 2.5. Note with this magnets device the axial alignment of the magnets is not guaranteed and so the actual applied magnetic field may be less homogeneous than the one shown by the simulation. The intensity and position of the magnetic field was modified by varying the amount of magnets and changing the distance of the magnets to the free end, x_{m}. When referring to the magnetic field intensity it is referred to the maximum intensity.

6.4.1 Influence of magnetic particles

Next, the influence of adding magnetic particles to the VE adhesive of a thin VES in order to obtain a smart VEMR is analysed. In Figure 8.22 the experimental dynamic properties of the VES and the VEMRS in the bandwidth of 0-1 kHz are shown. As a consequence of adding magnetic particles, the storage modulus of the sandwich decreases in all the bandwidth and the loss factor increases in medium to high frequencies. The loss factor of the VEMRS is more frequency dependent than the VES ones. It should be noted that the modifications observed in the dynamic properties of the sandwich are due to two reasons. On the one hand, due to the modification of the shear dynamic properties of the VE adhesive when adding magnetic particles. On the other hand, due to a thicker core of the VEMRS than the VES one once vulcanization is finished. Specifically, the core of the VEMRS is 35 µm , whereas the VES ones is 18 µm, Table 2.2.

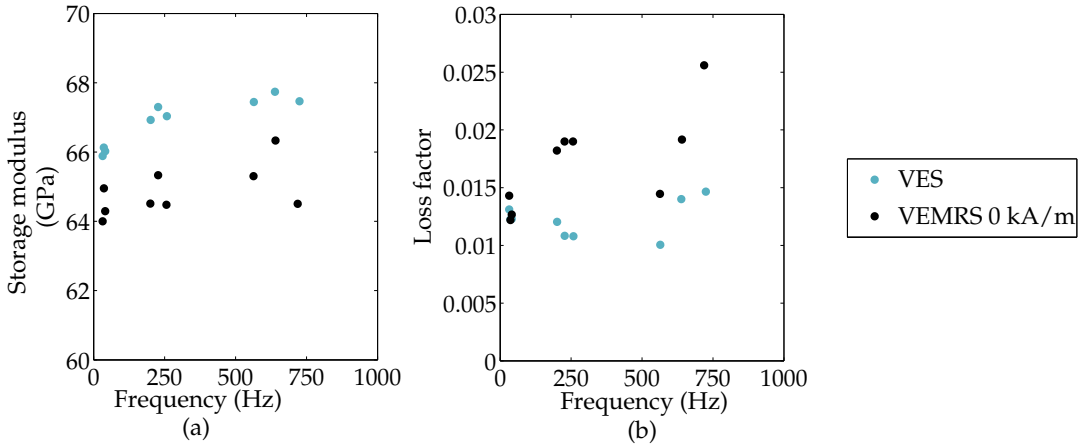

Figure 6.1. Experimental homogenised complex modulus, (a) storage modulus and (b) loss factor, of the VES and the VEMRS in the bandwidth between 0 and 1 kHz.

6.4.2 Influence of magnetic field

Following, the magneto-dynamic behaviour of the thin VEMRS is analysed from experimental results and the observed behaviours are related to the physical phenomena studied in Chapter 4 and Chapter 5. In addition, the influence of the intensity and position of the magnetic field on the vibrational response of the thin VEMRS is analysed.

In Figure 8.23 the influence of applying a partial magnetic field of 360 kA/m in the free end of the VEMRS beam on its resonances within the bandwidth of 0-1 kHz is shown. It is observed the vibrational response of the VEMRS is modified in the first vibration mode, whereas remains constant in the second and third modes. In particular, in the first vibration mode the resonance frequency and the modulus of the transfer function are decreased, meaning that the sandwich structure losses rigidity and the vibration is attenuated. The mechanism responsible for the decrement of the resonance frequency is the magnetic force generated in the VEMR core, and for the

vibration attenuation the eddy currents induced in the metallic skins and the magnetic force in a lesser extent. The influence of the magnetic field is appreciated just in the first resonance, since the transverse displacement of the beam and so the rotation and the velocity on which depend the magnetic force, Equation 5.3, and the eddy damping force, Equation 4.1, are maximum in this resonance. It is concluded in the analysed system, thin VEMRS beam exposed to a partial magnetic field applied at its free end, the phenomena governing its magneto-dynamic behaviour is the magnetic force generated in the VEMR core and eddy currents induced in the metallic skins.

The results shown in Figure 8.23 emphasise the capacity of sandwich structures composed of micron-size VEMR layers to modify their vibratonal response under external magnetic fields. Moreover, its vibrational response is fully reversible once removed the magnetic field.

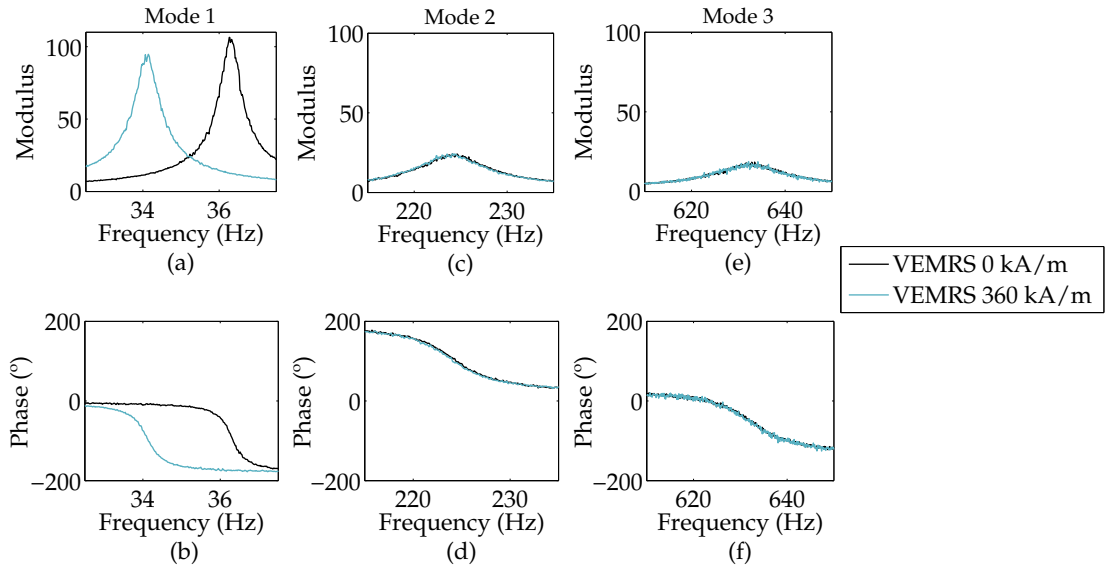

Figure 6.2. Experimental modal transfer functions, (a) modulus and (b) phase, of the VEMRS beam with 160 mm of free length, in absence of and under a partial magnetic field of 360 kA/m placed at 8 mm from the free end in the bandwidth of 0-1 kHz.

The influence of the magnetic field intensity on the vibrational response of the thin VEMRS is shown in Figure 8.24. The resonance frequency and the modulus of the transfer function are decreased when increasing the magnetic field intensity since both the amplitude of the magnetic force and eddy damping force are bigger.

Finally, Figure 8.25 shows the effect of the position of the partial magnetic field on vibrational response the thin VEMRS. Changing the position of the magnetic field from the clamped end of the sandwich beam towards the free end, the resonance frequency is decreased notably, whereas the transfer modulus is decreased slightly. The magnetic force generated in the VEMR core is proportional to the rotation of the sandwich beam and so in the first vibration mode its magnitude is maximum if the magnetic field is placed in the free end. The influence of the induced eddy currents is also maximum placing the magnetic field in the free end, since it is the velocity of the beam in the first vibration mode.

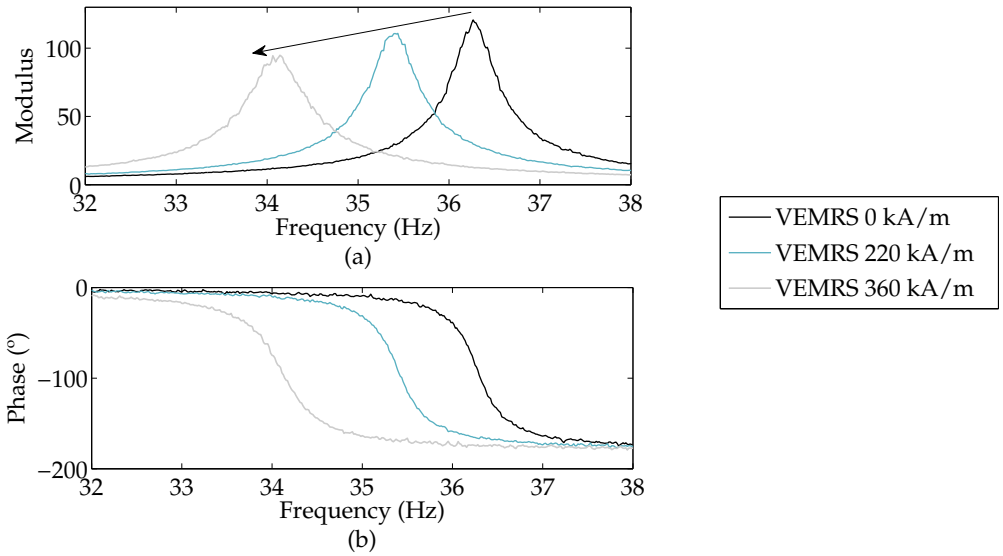

Figure 6.3. Experimental transfer functions, (a) modulus and (b) phase, of the VEMRS beam with 160 mm of free length in absence of and under different intensities of partial magnetic field (220 kA/m and 360 kA/m) placed at 8 mm from the free end in the first resonance

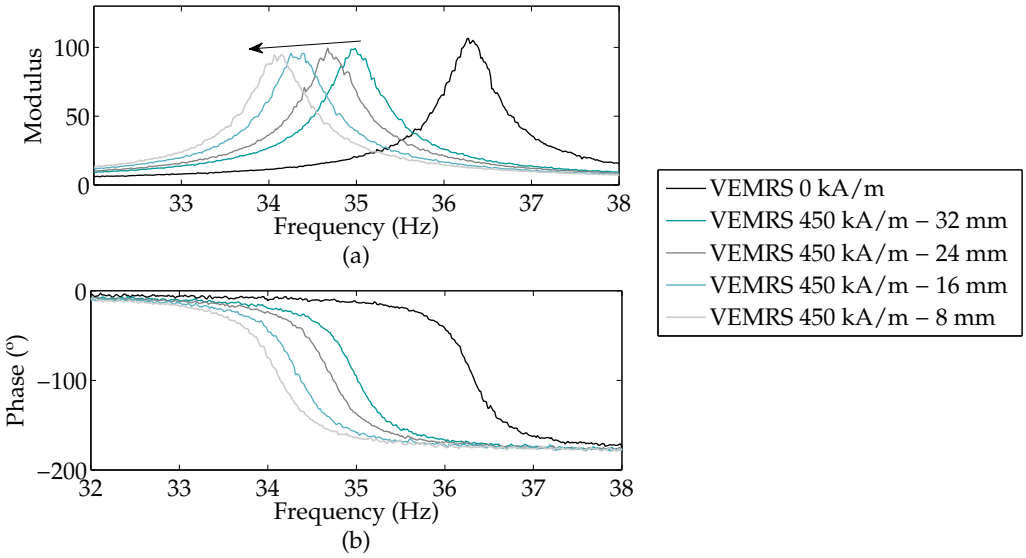

Figure 6.4. Experimental transfer functions, (a) modulus and (b) phase, of the VEMRS beam with 160 mm of free length in absence of and under a magnetic field of 360 kA/m placed at different positions (8mm, 16 mm, 24 mm and 32 mm) from the free end in the first resonance

6.5 Conclusions

In this chapter the magneto-dynamic behaviour of thin VEMRSs was experimentally analysed.

The results showed when magnetic particles are added to the VE adhesive of a thin VES to obtain a smart VEMRS the geometrical and physical properties of the sandwich are slightly modified. As a consequence, the storage modulus of the sandwich is decreased slightly across all the bandwidth, whereas the loss factor is increased in medium to high frequencies.

The vibrational response of the obtained thin VEMRS is modified instantaneously and reversibly in its first vibration mode when partial magnetic fields are applied. Specifically, the resonance frequency and the vibration amplitude of the sandwich are decreased. The magneto-dynamic behaviour of the analysed thin VEMRS is governed mostly by the magnetic force generated in the VEMR core and to a lesser extent by the induced eddy currents on the metallic skins. The former decreases the resonance frequency of the sandwich and the latter attenuate the vibration. The dynamic response of the thin VEMRS can be modified by the intensity and position of the partial magnetic field. When the intensity of the magnetic field is increased, the resonance frequency and the vibration amplitude of the sandwich are decreased. When the magnetic field is moved towards the free end, the resonance frequency is decreased.

The experimental results highlighted the smartness and the vibration suppression capacity of thin VEMRS without compromising the main advantages of thin VESs.

6.6 Scientific contribution

Magneto-dynamic analysis of sandwiches composed of a thin viscoelastic-magnetorheological layer

Leire Irazu and María Jesús Elejabarrieta
Mechanical & Manufacturing Department, Mondragon Unibertsitatea, Loramendi 4, 20500 Arrasate-Mondragon, Spain

Journal of Intelligent Material Systems and Structures (2017)
DOI: 10.1177/1045389X17705209.

Impact factor - JCR: 2.255
Ranking - JCR: 108/275

Journal of Intelligent Material Systems and Structures

Original Article

Journal of Intelligent Material Systems and Structures
1–9
© The Author(s) 2017
Reprints and permissions:
sagepub.co.uk/journalsPermissions.nav
DOI: 10.1177/1045389X17705209
journals.sagepub.com/home/jim
SAGE

Magneto-dynamic analysis of sandwiches composed of a thin viscoelastic-magnetorheological layer

Leire Irazu and Maria Jesus Elejabarrieta

Abstract

This study's relevance lies in the possibility of obtaining a smart sandwich structure with controllable dynamic properties, without compromising the main characteristics of conventional thin viscoelastic sandwiches. The proposed sandwich is composed of a micron-size viscoelastic-magnetorheological layer, which is obtained by adding spherical iron particles to a viscoelastic layer. Thin sandwiches with identical base layers and a viscoelastic core, with and without magnetic particles, are fabricated. Both the viscoelastic sandwich structure and viscoelastic-magnetorheological sandwich structure are experimentally characterised by a forced vibration test with resonance in a bandwidth between 0 and 1 kHz. This work analyses the influence of adding iron particles to obtain a smart thin sandwich. In addition, the vibrational response of the viscoelastic-magnetorheological sandwich structure under an external partial magnetic field, and the controllability of its dynamic properties by means of the magnetic field intensity and position, are studied.

Keywords

Magnetorheological sandwich, micron-size layer, magneto-dynamic characterisation

Introduction

Thin viscoelastic sandwich (VES) structures are widely used in aerospace and automotive industries as a structural vibration control technique (Rao, 2003). These sandwiches provide many advantages such as high-energy absorption, lightweight and high-specific stiffness. In addition, due to their small thickness, VES can be formed by classical sheet metal forming processes to obtain damped parts with complex geometries. However, these sandwiches are unable to adapt to an application's requirements in real time, unlike smart materials and structures.

In recent years, the use of magnetorheological (MR) materials in smart devices and structures has increased (Çeşmeci and Engin, 2010; Li et al., 2014; Wang and Meng, 2001). MR materials possess the unique ability to modify their rheological properties instantaneously and reversibly in response to an external magnetic field. They are composed of micro or nanosized magnetic particles suspended in a non-magnetisable medium, and depending on the nature of the medium, they are classified as MR fluids, MR gels or MR elastomers (Carlson and Jolly, 2000).

MR fluids and MR elastomers have replaced the viscoelastic (VE) core of conventional sandwiches in order to obtain smart sandwich structures (Aguib et al., 2014; Eshaghi et al., 2015, 2016; Hu et al., 2011; Korobko et al., 2012; Lara-Prieto et al., 2010; Rajamohan et al., 2010; Zhou and Wang, 2006). These MR sandwiches are able to modify their dynamic response under an external magnetic field. The sandwiches composed of MR fluids have the disadvantages of sealing problems and the settling of magnetic particles (Goncalves et al., 2006). The sandwiches composed of MR elastomers overcome these drawbacks, but they are not as thin as the conventional VES. Thin sandwiches are defined as when the core is equal or thinner than the base layers. While the VE layer of conventional sandwiches can be measured in microns (Irazu and Elejabarrieta, 2015; Martinez-Agirre and Elejabarrieta, 2010) with a core-skin thickness ratio of 0.15 or less, at the time of writing there are no MR sandwiches composed of such thin layers. In most studies, the MR sandwiches are composed of elastomers with thicknesses ranging from 0.88 to 3.5 mm with core-skin thickness ratios ranging from

Mechanical and Manufacturing Department, Mondragon Unibertsitatea, Arrasate-Mondragon, Spain

Corresponding author:
Maria Jesus Elejabarrieta, Mechanical and Manufacturing Department, Mondragon Unibertsitatea, 20500 Arrasate-Mondragon, Spain.
Email: mjelejabarrieta@mondragon.edu

Table 1. Geometrical and physical properties of the VES and VEMRS specimens.

	H_e(±0.002 mm)	$H_{v,wet}$[a](μm)	H_v(μm)	b (±0.002 mm)	H (±0.003 mm)	ρ (±0.008 g/cm^3)
VES	0.564	80	18	9.900	1.146	2.675
VEMRS	0.564	80	35	9.900	1.162	2.676

VES: viscoelastic sandwich; VEMRS: viscoelastic-magnetorheological sandwich.
[a]Manufacturer's data, Replasa S.A.

1.15 to 3 (Aguib et al., 2016; Babu and Vasudevan, 2016; Hu et al., 2012; Kozlowska et al., 2016; Long et al., 2013; Wei et al., 2008). Other authors have used even thicker elastomers, with layers measuring 10 or 20 mm, to form the MR sandwiches, leading to a core-skin thickness ratio that can reach 20 (Aguib et al., 2014; Choi et al., 2009, 2010). The use of thick MR elastomers to fabricate sandwich structures compromises some of the main characteristics of these structures, such as the low added weight to the structure or the possibility to form them by classical sheet metal forming processes.

This work focuses on the magneto-dynamic properties of a sandwich structure composed of a micron-size viscoelastic-magnetorheological (VEMR) layer. The VEMR layer is obtained by adding spherical iron particles to the viscoelastic material used in conventional sandwiches. The main aim is to analyse the advantages this smart thin sandwich can provide as a structural vibration control technique over the conventional sandwiches. To this purpose, two sandwich structures, a VES and a viscoelastic-magnetorheological sandwich (VEMRS), composed of identical base layers and a viscoelastic core, with and without magnetic particles, are fabricated and characterised. The storage modulus and loss factor of the VES and the VEMRS are obtained in a bandwidth between 0 and 1 kHz. The influence of adding iron particles to obtain a smart sandwich is analysed. The vibrational response of the VEMRS under an external partial magnetic field, as well as the possibility to control its dynamic properties by means of intensity and position of the magnetic field, is also studied.

Experimental characterisation

VES and VEMRS are characterised in a bandwidth between 0 and 1 kHz by a forced vibration test, consisting of a base movement as proposed by Cortés and Elejabarrieta (2007). Then, a variable external magnetic field, in terms of intensity and position, is added to the experimental test in order to analyse the vibration suppression capabilities and the dynamic properties of the smart thin VEMRS.

Specimens

Two different sandwich structures are fabricated by a coil-coating process in collaboration with Replasa S.A.: a conventional VES and a smart VEMRS. Both sandwiches are symmetrical and they are composed of the same base layers and a viscoelastic layer, with and without magnetic particles. The base layers are made of a 1050 H18 aluminium alloy, due to its low damping properties and high stiffness compared to those of their cores. The VE core of the VES is a polyester-based adhesive, while the VEMR core of the VEMRS is synthesised by adding spherical carbonyl iron powder particles of 1.25 ± 0.55 μm in a 12% volumetric concentration to the polyester-based adhesive.

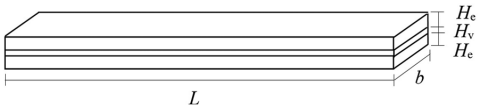

Figure 1. Sandwich configuration.

Three specimens from each sandwich structure are tested, each of them with free lengths of 150, 160 and 170 mm. The configuration of both sandwich structures is shown in Figure 1, and their geometrical and physical properties are shown in Table 1, where L, H, b and ρ are the free length, thickness, width and density of the sandwich structure, and where H_e, H_v and $H_{v,wet}$ are the base layer thicknesses, core and wet core. Note that $(\bullet)_e$ and $(\bullet)_v$ refer to the elastic and viscoelastic materials, respectively. The $H_{v,\,wet}$ of both sandwiches is the same; however, once the curing process is finished, the H_v of the VEMRS is slightly larger than the H_v of the VES. Thus, as a consequence of adding magnetic particles, H_v, H and ρ of both sandwiches differ somewhat, as seen in Table 1.

Experimental technique

A forced vibration test with resonance, consisting of a base movement as proposed by Cortés and Elejabarrieta (2007), is the experimental technique used. The transmissibility functions of the cantilever sandwich specimens' free ends are then obtained.

Figure 2 shows an image and a scheme of the experimental set-up. The base excitation is generated by an electrodynamic shaker (Ling Dynamic Systems Vibrator, Model 406) and consists of a white noise in the frequency range from 0 to 1 kHz. The defined acceleration's amplitude is as follows

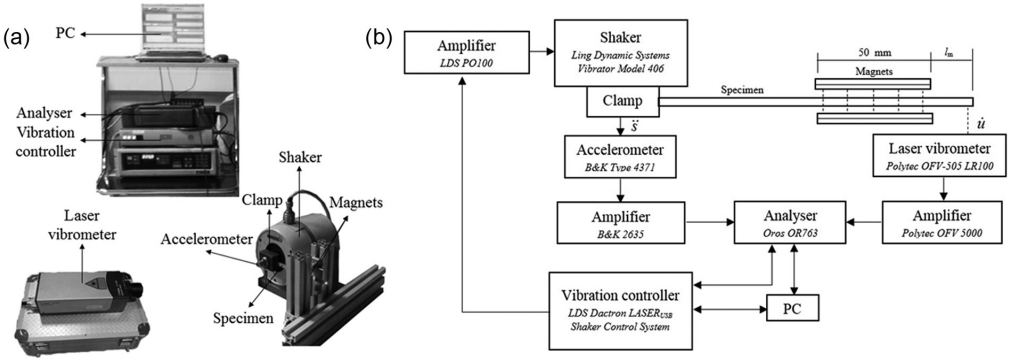

Figure 2. Experimental set-up: (a) image and (b) scheme.

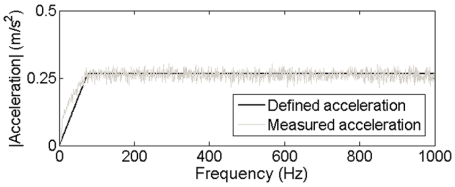

Figure 3. Defined and measured acceleration's modulus of the base in a bandwidth between 0 and 1 kHz.

$$\text{Acceleration Amplitude} \begin{cases} 0.035 \cdot f & 0 \text{ Hz} \leq f < 75 \text{ Hz} \\ 0.265 & 75 \text{ Hz} \leq f \leq 1000 \text{ Hz} \end{cases} \quad (1)$$

where f is the frequency. The acceleration of the base, $\ddot{s}$, is measured and loopback controlled by a piezoelectric accelerometer (B&K Type 4371) and a vibration controller (LDS Dactron LASER Shaker Control System). In Figure 3, the defined and measured acceleration's modulus of the base is shown. The velocity of the specimens' free end, $\dot{u}$, is measured by a laser vibrometer (Polytec OFV 5000). Finally, the signal acquisition and treatment are carried out by a four-channel analyser (OROS OR763) connected to a PC. The applied magnetic field is always parallel to the base motion and it is obtained by placing pairs of neodymium magnets (NdFeB 35 MGOe) in a partial region of the sandwich beam. The intensity and position of the magnetic field are modified by varying the number of magnets and by changing the distance of the magnets to the free end, l_m, respectively.

The transmissibility functions are determined relating the acceleration of the beam's free end with that applied at the base, so that

$$T^* = \frac{U^*}{S^*} \quad (2)$$

where U^* and S^* are the Fourier transform of the derivative of the velocity measured at beam's free end, $\dot{u}$, and the acceleration applied at the base, $\ddot{s}$ (Figure 2). First, the transmissibility functions in the frequency range from 0 to 1 kHz are obtained and the resonance frequencies are identified. Specifically, in this bandwidth, three vibration modes of the VES and the VEMRS are observed. Subsequently, the modal transmissibility functions are measured in order to obtain a higher resolution, ranging from 0.016 Hz in the first mode to 0.06 Hz in the last mode. This process is repeated for different intensities and locations of the external magnetic field. All measurements are made in the linear range and at a room temperature of 20°C.

Dynamic properties, storage modulus and loss factor of the VES and the VEMRS are obtained from the modal transmissibility functions. The storage modulus, E, is deduced from

$$E = \frac{12\rho L^4 f_n^2}{H^2 C_n^2} \quad (3)$$

where ρ is the sandwich's density, f_n is the sandwich's resonance frequency of mode n and C_n is the coefficient for mode n of clamped-free configuration (ASTM E756-05, 2005).

The loss factor, η, is evaluated by the half-power bandwidth (HPB) method. The values of the loss factor in the absence and under the magnetic field are <0.1, so the HPB method can be used to determine the loss factor with an error $<0.1\%$ (Martinez-Agirre and Elejabarrieta, 2010). In order to do so, the resonant frequency and the frequencies above and below the resonant frequency where the value of the transmissibility modulus is 3 dB less than the value at resonance must be obtained from the modal transmissibility functions. The loss factor is the ratio of the frequency difference between the upper 3 dB and the lower 3 dB, Δf_n, to the resonant frequency, given by

Table 2. Resonance frequency (f), storage modulus (E) and loss factor (η) of the VES, with three free lengths (L) and for three vibration modes in a bandwidth between 0 and 1 kHz.

VES				
L (mm)	Mode no.	f (Hz)	E (GPa)	η
170 ± 1	1	31.8 ± 0.2	65.9 ± 0.8	0.0131 ± 0.0005
160 ± 1	1	36.0 ± 0.3	66.1 ± 1.0	0.0123 ± 0.0011
150 ± 1	1	40.9 ± 0.3	66.0 ± 1.0	0.0123 ± 0.0015
170 ± 1	2	220.8 ± 0.9	66.9 ± 0.6	0.0120 ± 0.0003
160 ± 1	2	227.3 ± 1.2	67.3 ± 0.7	0.0108 ± 0.0005
150 ± 1	2	258.1 ± 1.4	67.0 ± 0.7	0.0108 ± 0.0004
170 ± 1	3	564.4 ± 3.0	67.4 ± 0.7	0.0100 ± 0.0005
160 ± 1	3	638.6 ± 2.9	67.7 ± 0.6	0.0140 ± 0.0014
150 ± 1	3	725.1 ± 3.6	67.5 ± 0.7	0.0147 ± 0.0009

VES: viscoelastic sandwich.

Table 3. Resonance frequency (f), storage modulus (E) and loss factor (η) of the VEMRS, with three free lengths (L) and for three vibration modes in a bandwidth between 0 and 1 kHz.

VEMRS				
L (mm)	Mode no.	f (Hz)	E (GPa)	η
170 ± 1	1	31.8 ± 0.1	64.0 ± 0.6	0.0143 ± 0.0038
160 ± 1	1	36.1 ± 0.1	65.0 ± 0.4	0.0122 ± 0.0039
150 ± 1	1	40.9 ± 0.3	64.3 ± 1.1	0.0127 ± 0.0045
170 ± 1	2	199.8 ± 2.2	64.5 ± 1.4	0.0182 ± 0.0071
160 ± 1	2	227.0 ± 2.0	65.3 ± 1.2	0.0190 ± 0.0099
150 ± 1	2	256.6 ± 1.0	64.5 ± 0.5	0.0190 ± 0.0127
170 ± 1	3	563.0 ± 0.6	65.3 ± 1.4	0.0145 ± 0.0054
160 ± 1	3	640.6 ± 5.0	66.3 ± 1.1	0.0192 ± 0.0068
150 ± 1	3	718.7 ± 3.7	64.5 ± 0.7	0.0256 ± 0.0175

VEMRS: viscoelastic-magnetorheological sandwich.

$$\eta = \frac{\Delta f_n}{f_n} \tag{4}$$

Finally, as the study is performed in the linear viscoelastic range, the homogenised complex modulus, E^*, of the sandwich structure can be expressed as

$$E^* = E(1 + i\eta) \tag{5}$$

where the storage modulus and the loss factor are frequency dependent (Nashif et al., 1985).

Results and discussion

The influence of adding magnetic particles to the viscoelastic core of conventional sandwiches in order to obtain smart thin sandwiches is analysed. The vibration suppression capabilities of the VEMRS structures in response to an external partial magnetic field are also studied, as well as the controllability of the dynamic properties of the VEMRS, analysing the influence of the location and intensity of the magnetic field on its dynamic properties.

The experimental results of the dynamic properties of the VES and the VEMRS are presented in Tables 2 to 4. All the results shown are an average of the three different specimens' measures. The deviations shown are standard deviations.

Figure 4 shows the evolution of the homogenised complex modulus of the VES and the VEMRS in the frequency domain in accordance with the results shown in Tables 2 and 3. The storage modulus and loss factor of both sandwiches are increased slightly with frequency. In Figure 4(a), it is observed that when adding magnetic particles to the viscoelastic core of conventional sandwiches, the storage modulus is decreased over the whole bandwidth, and Figure 4(b) shows that the loss factor is increased at high frequencies. At low frequencies, the influence of the magnetic particles is not appreciated in the loss factor. Note that these tendencies are due to a slightly larger core thickness, as seen in Table 1, and the modification of the dynamic properties of the core is observed when magnetic particles are added.

The vibrational response of the smart sandwich, composed of a micron-size VEMR layer, under a

Table 4. Resonance frequency (f), storage modulus (E) and loss factor (η) of the VEMRS, with three free lengths (L) and under different intensities and locations of the magnetic field for the first vibration mode.

VEMRS					
Magnetic field (kA/m)/l_m (mm)	L (mm)	Mode no.	f (Hz)	E (GPa)	η
220/8	170 ± 1	1	30.8 ± 0.2	60.1 ± 0.7	0.0162 ± 0.004
220/8	160 ± 1	1	35.2 ± 0.1	61.8 ± 0.4	0.0139 ± 0.0038
220/8	150 ± 1	1	40.1 ± 0.3	61.9 ± 1.0	0.0144 ± 0.0059
220/16	170 ± 1	1	30.9 ± 0.2	60.7 ± 0.9	0.0165 ± 0.0041
220/16	160 ± 1	1	35.34 ± 0.1	62.3 ± 0.3	0.0137 ± 0.0042
220/16	150 ± 1	1	40.2 ± 0.3	62.3 ± 1.1	0.0141 ± 0.0056
220/24	170 ± 1	1	31.1 ± 0.2	61.3 ± 1.0	0.0157 ± 0.0041
220/24	160 ± 1	1	35.5 ± 0.1	62.8 ± 0.3	0.0138 ± 0.0042
220/24	150 ± 1	1	40.4 ± 0.3	62.6 ± 1.0	0.0141 ± 0.0066
220/32	170 ± 1	1	31.2 ± 0.2	61.7 ± 0.8	0.0158 ± 0.0035
220/32	160 ± 1	1	35.6 ± 0.1	63.0 ± 0.5	0.0134 ± 0.0040
360/8	170 ± 1	1	29.2 ± 0.2	54.2 ± 0.7	0.0207 ± 0.0063
360/8	160 ± 1	1	33.9 ± 0.1	57.3 ± 0.5	0.0179 ± 0.0053
360/8	150 ± 1	1	39.2 ± 0.3	59.2 ± 0.8	0.0159 ± 0.005
360/16	170 ± 1	1	29.6 ± 0.2	55.7 ± 0.7	0.0193 ± 0.0063
360/16	160 ± 1	1	34.2 ± 0.1	58.4 ± 0.5	0.0174 ± 0.0047
360/16	150 ± 1	1	39.5 ± 0.2	60.1 ± 0.7	0.0164 ± 0.006
360/24	170 ± 1	1	30.1 ± 0.2	57.4 ± 0.7	0.0189 ± 0.0057
360/24	160 ± 1	1	34.7 ± 0.2	59.8 ± 0.5	0.0166 ± 0.005
360/24	150 ± 1	1	39.9 ± 0.2	61.1 ± 0.7	0.0157 ± 0.0057
360/32	170 ± 1	1	30.3 ± 0.1	58.4 ± 0.6	0.0184 ± 0.0072
360/32	160 ± 1	1	34.9 ± 0.1	60.6 ± 0.3	0.0167 ± 0.005

VEMRS: viscoelastic-magnetorheological sandwich.

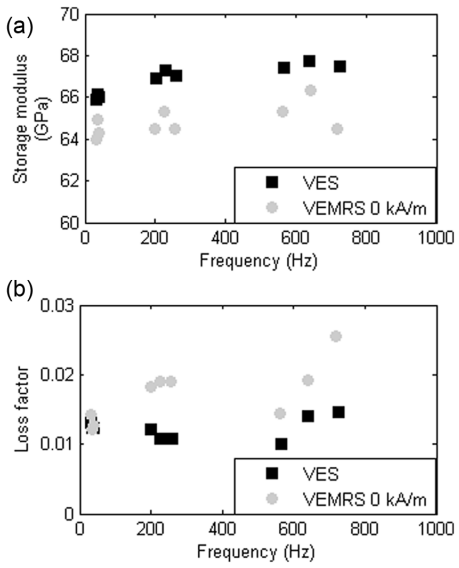

Figure 4. Homogenised complex modulus: (a) storage modulus and (b) loss factor of the VES and the VEMRS in a bandwidth between 0 and 1 kHz.

partial magnetic field placed at the free end of the sandwich beam, is analysed. The maximum value of the magnetic field intensity is 360 kA/m. Figure 5 shows the modal transmissibility functions of the VEMRS in a bandwidth between 0 and 1 kHz. As it can be seen, the magnetic field placed around the sandwich beam's free end modifies its vibrational response at the first vibration mode. In particular, in this mode, the resonant frequency and the transmissibility modulus are decreased, meaning that the sandwich structure loses rigidity and the damping is greater. In the second and third vibration modes, the dynamic response of the VEMRS remains unmodified. Figure 6 shows the displacement's amplitude of the VEMRS beam's free end in the absence of magnetic field, and it can be seen the displacement decreases in frequency. Specifically, there is a difference of two orders of magnitude between the displacement amplitude in the first and second resonances. For this reason, the influence of the magnetic field is much smaller in the second and third vibration modes and as no significant changes are appreciated in the vibrational response of the VEMRS at those vibration modes, the rest of the analyses are focused on the first vibration mode.

The results shown in Figure 5 emphasise the smartness and the vibration suppression capabilities of sandwich structures composed of micron-size VEMR layers under external magnetic fields. Moreover, its vibrational response is fully reversible once the magnetic field is removed.

The possibility of shifting the natural frequencies of sandwiches composed of MR fluid or elastomer to a

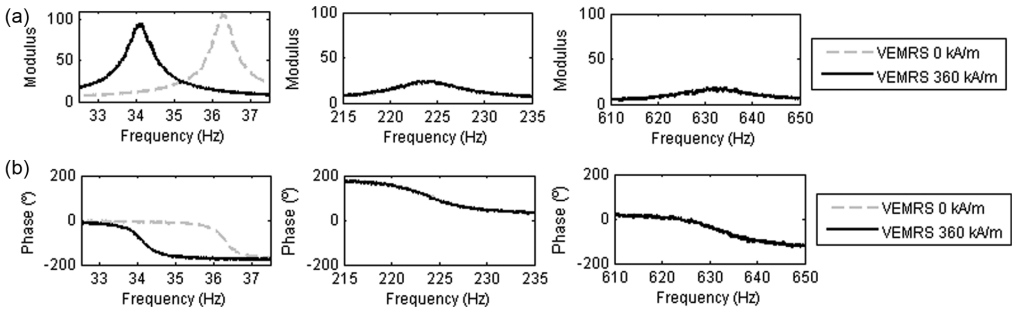

Figure 5. The first three modal transmissibility functions: (a) modulus and (b) phase of the VEMRS beam with free length of 160 mm, with and without a magnetic field of 360 kA/m placed at 8 mm from the free end.

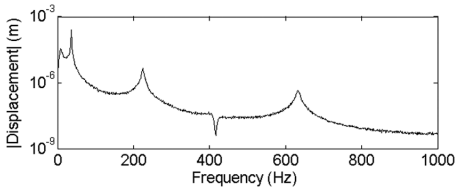

Figure 6. Displacement amplitude of the VEMRS beam's free end without magnetic field and in a bandwidth between 0 and 1 kHz.

lower ones by applying partial magnetic fields had been observed previously by other authors (Hu et al., 2011; Lara-Prieto et al., 2010; Megha et al., 2016). This is due to the fact that when a steady magnetic field is applied to a vibrating MR sandwich, more phenomena despite the modification of the rheological properties of the MR material are involved, such as induction of eddy currents on conductive skins or magnetic forces due to the magnetic nature of the core or skins (Sodano et al., 2005). In addition, the contribution of each phenomenon to the final dynamic response of the sandwich would be different depending on the geometrical and physical properties of the sandwich structure and the configuration of the applied magnetic field.

Figures 7 and 8 show the influence of the magnetic field intensity on the transmissibility function and dynamic properties of the VEMRS in accordance with the results shown in Table 4. In Figure 7, it is observed that the first resonant frequency and its modulus decreased with increasing magnetic field intensity. In Figure 8, it can be seen that by increasing the magnetic field intensity, the storage modulus is decreased and the loss factor is increased, being these tendencies more appreciable with larger free lengths. As both the storage modulus and the loss factor are modified by the magnetic field intensity, the dynamic properties of the VEMRS can be controlled by adjusting the magnetic field intensity.

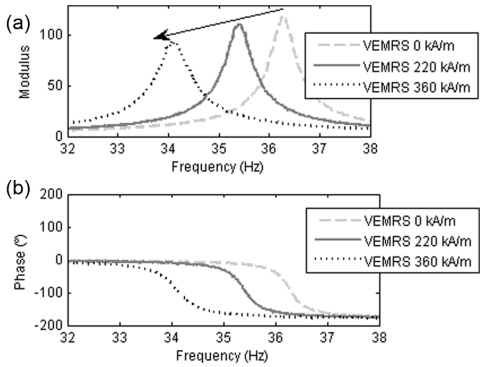

Figure 7. Influence of the magnetic field intensity (0, 220 and 360 kA/m) placed at 8 mm from the free end on the transmissibility function of the first mode, (a) modulus and (b) phase, of the VEMRS beam with free length of 160 mm.

Figures 9 and 10 show the influence of the position of partial magnetic fields, with two different intensities, on the transmissibility function of the VEMRS. It is observed that moving the magnetic field from the clamped end of the sandwich beam towards the free end, the resonant frequency is decreased and the transmissibility modulus remains quite constant, being the influence of the magnetic field position more remarkable with a higher intensity.

Figure 11 shows the dynamic properties of VEMRS at different locations of a magnetic field of 360 kA/m. It shows that the storage modulus is decreased when the magnetic field is moved towards the free end of the sandwich beam, as expected, by decreasing the resonance frequency. With respect to the loss factor, it seems the loss factor is increased slightly, moving the magnetic field towards the free end. However, the position has no remarkable influence on the loss factor. The influence of the position of the magnetic field is bigger with a larger free length of the beam.

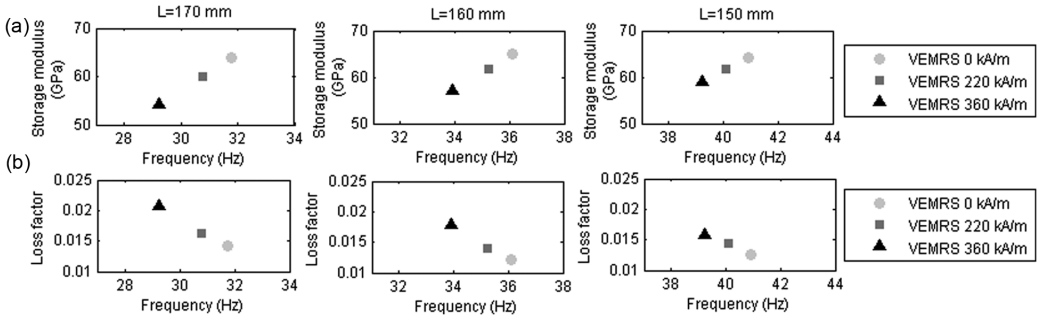

Figure 8. Influence of the magnetic field intensity (0, 220 and 360 kA/m) placed at 8 mm from the free end on the homogenised complex modulus, (a) storage modulus and (b) loss factor, of the VEMRS beam with free length of 170, 160 and 150 mm.

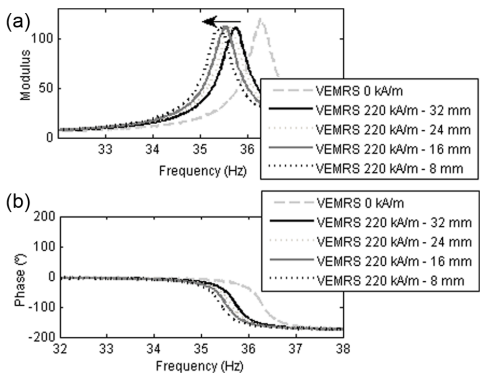

Figure 9. Influence of the 220 kA/m magnetic field's position (32, 24, 16 and 8 mm from the free end) on the transmissibility function of the first mode, (a) modulus and (b) phase, of the VEMRS beam with free length of 160 mm.

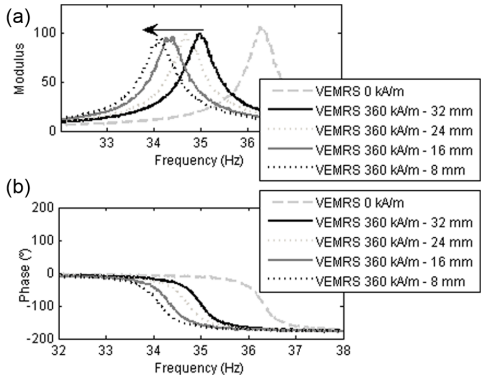

Figure 10. Influence of the 360 kA/m magnetic field's position (32, 24, 16 and 8 mm from the free end) on the transmissibility function of the first mode, (a) modulus and (b) phase, of the VEMRS beam with free length of 160 mm.

Conclusion

In this work, a new smart thin sandwich structure is fabricated and experimentally characterised. Besides being smart, it continues to have the main characteristics of conventional thin VES, such as low added weight to the structure and the possibility to be formed by sheet metal forming processes. The smart sandwich is composed of a micron-size viscoelastic-MR layer, which is obtained by adding spherical carbonyl iron powder particles to a viscoelastic layer of a conventional sandwich. Both the VES and the VEMRS are characterised by the forced vibration test with resonance in a bandwidth between 0 and 1 kHz.

The dynamic properties of the VES and the VEMRS, with the same configuration and composed of same base materials, are compared, and the influence of adding magnetic particles to obtain a smart thin sandwich is analysed. The storage modulus and loss factor of both sandwiches, VES and VEMRS, are increased in frequency. When magnetic particles are added to the viscoelastic core, the storage modulus of the sandwich is decreased across all the bandwidth, whereas the loss factor is increased at high frequencies.

The vibrational response of the smart sandwich structure with a micron-size VEMR layer can be modified instantaneously and reversibly by the application of an external partial magnetic field in its first vibration mode. When the magnetic field is applied, the natural frequency and the transmissibility modulus are decreased, which means the sandwich structure loses rigidity and increases the damping. By increasing the intensity of the magnetic field, the storage modulus is decreased, whereas the loss factor is increased, and by moving the partial magnetic field from the clamped end of the sandwich beam towards the free end, the storage modulus is decreased.

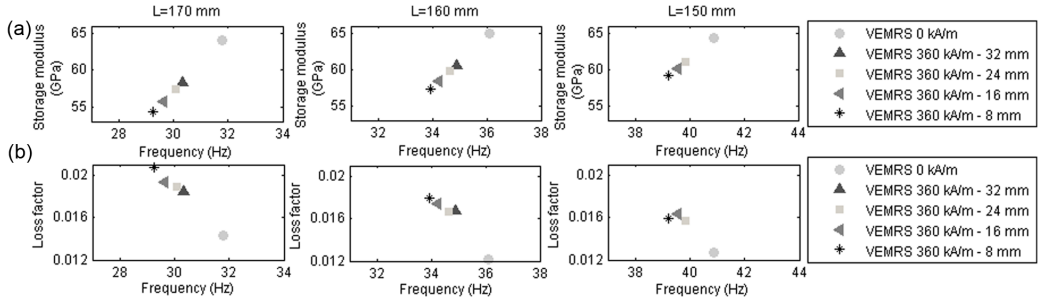

Figure 11. Influence of the 360 kA/m magnetic field's position (32, 24, 16 and 8 mm from the free end) on the homogenised complex modulus, (a) storage modulus and (b) loss factor, of the VEMRS beam with free length of 170, 160 and 150 mm.

Acknowledgements

The authors would like to thank Modesto Mateos from Mondragon Unibertsitatea for the help provided with English grammar.

Declaration of Conflicting Interests

The author(s) declared no potential conflicts of interest with respect to the research, authorship and/or publication of this article.

Funding

The author(s) disclosed receipt of the following financial support for the research, authorship, and/or publication of this article: This study has been partially supported by AVISANI (DPI2015-71198-R, Spanish Government and PI-2016-1-0026, Basque Government) research project and Replasa S.A.

References

Aguib S, Nour A, Djedid T, et al. (2016) Forced transverse vibration of composite sandwich beam with magnetorheological elastomer core. *Journal of Mechanical Science and Technology* 30(1): 15–24.

Aguib S, Nour A, Zahloul H, et al. (2014) Dynamic behavior analysis of a magnetorheological elastomer sandwich plate. *International Journal of Mechanical Sciences* 87: 118–136.

ASTM E756-05 (2005) Standard test method for measuring vibration-damping properties of materials.

Babu VR and Vasudevan R (2016) Dynamic analysis of tapered laminated composite magnetorheological elastomer (MRE) sandwich plates. *Smart Materials and Structures* 25(3): 035006-1–035006-19.

Carlson JD and Jolly MR (2000) MR fluid, foam and elastomer devices. *Mechatronics* 10(4–5): 555–569.

ÇeşmeciŞ and Engin T (2010) Modeling and testing of a field-controllable magnetorheological fluid damper. *International Journal of Mechanical Sciences* 52(8): 1036–1046.

Choi WJ, Xiong YP and Shenoi RA (2009) *Experimental Study on Vibration Characteristics of Sandwich Beams with Aluminum Skins and Magnetorheological Elastomer Cores*. Edinburgh: International Committee on Composite Materials.

Choi WJ, Xiong YP and Shenoi RA (2010) Vibration characteristics of sandwich beams with steel skins and magnetorheological elastomer cores. *Advances in Structural Engineering* 13(5): 837–847.

Cortes F and Elejabarrieta MJ (2007) Viscoelastic materials characterisation using the seismic response. *Materials & Design* 28(7): 2054–2062.

Eshaghi M, Sedaghati R and Rakheja S (2015) The effect of magneto-rheological fluid on vibration suppression capability of adaptive sandwich plates: experimental and finite element analysis. *Journal of Intelligent Material Systems and Structures* 26(14): 1920–1935.

Eshaghi M, Sedaghati R and Rakheja S (2016) Dynamic characteristics and control of magnetorheological/electrorheological sandwich structures: a state-of-the-art review. *Journal of Intelligent Material Systems and Structures* 27: 2003–2037.

Goncalves FD, Koo J-H and Ahmadian M (2006) A review of the state of the art in magnetorheological fluid technologies part I: MR fluid and MR fluid models. *Shock and Vibration Digest* 38(3): 203–219.

Hu G, Guo M and Li W (2012) Analysis of vibration characteristics of magnetorheological elastomer sandwich beam under non-homogeneous magnetic field. *Applied Mechanics and Materials* 101–102: 202–206.

Hu G, Guo M, Li W, et al. (2011) Experimental investigation of the vibration characteristics of a magnetorheological elastomer sandwich beam under non-homogeneous small magnetic fields. *Smart Materials and Structures* 20(12): 127001-1–127001-7.

Irazu L and Elejabarrieta MJ (2015) The influence of viscoelastic film thickness on the dynamic characteristics of thin sandwich structures. *Composite Structures* 134: 421–428.

Korobko EV, Mikhasev GI, Novikova ZA, et al. (2012) On damping vibrations of three-layered beam containing magnetorheological elastomer. *Journal of Intelligent Material Systems and Structures* 23(9): 1019–1023.

Kozlowska J, Boczkowska A, Czulak A, et al. (2016) Novel MRE/CFRP sandwich structures for adaptive vibration

control. *Smart Materials and Structures* 25(3): 035025-1–035025-14.

Lara-Prieto V, Parkin R, Jackson M, et al. (2010) Vibration characteristics of MR cantilever sandwich beams: experimental study. *Smart Materials and Structures* 19(1): 015005-1–015005-9.

Li Y, Li J, Li W, et al. (2014) A state-of-the-art review on magnetorheological elastomer devices. *Smart Materials and Structures* 23(12): 123001-1–123001-24.

Long M, Hu G and Wang S (2013) *Vibration Response Analysis of MRE Cantilever Sandwich Beam under Non-Homogeneous Magnetic Fields*. Guilin, China: Trans Tech Publications.

Martinez-Agirre M and Elejabarrieta MJ (2010) Characterisation and modelling of viscoelastically damped sandwich structures. *International Journal of Mechanical Sciences* 52(9): 1225–1233.

Megha S, Kumar NS and D'Silva R (2016) Vibration analysis of magnetorheological elastomer sandwich beam under different magnetic fields. *Journal of Mechanical Engineering and Automation* 6: 75–80.

Nashif AD, Jones DIG and Henderson JP (1985) *Vibration Damping*. New York: John Wiley & Sons.

Rajamohan V, Sedaghati R and Rakheja S (2010) Vibration analysis of a multi-layer beam containing magnetorheological fluid. *Smart Materials and Structures* 19(1): 015013-1–015013-12.

Rao MD (2003) *Recent Applications of Viscoelastic Damping for Noise Control in Automobiles and Commercial Airplanes*. London: Academic Press.

Sodano HA, Bae J, Inman DJ, et al. (2005) Concept and model of eddy current damper for vibration suppression of a beam. *Journal of Sound and Vibration* 288(4–5): 1177–1196.

Wang J and Meng G (2001) Magnetorheological fluid devices and their applications in mechanical engineering. *Journal of Mechanical Strength* 23(1): 50–56.

Wei K, Meng G, Zhang W, et al. (2008) Experimental investigation on vibration characteristics of sandwich beams with magnetorheological elastomers cores. *Journal of Central South University of Technology* 15(1): 239–242.

Zhou GY and Wang Q (2006) Study on the adjustable rigidity of magnetorheological-elastomer-based sandwich beams. *Smart Materials and Structures* 15(1): 59–74.

Chapter 7

Conclusions and future works

In this chapter the outcomes of the thesis are summarised and proposals for further work are given.

7.1 Conclusions

The main goal of the present dissertation was to study the dynamics of thin viscoelastic-magnetorheological sandwich (VEMRS) structures analysing the physical phenomena generated in these sandwiches when magnetic fields are applied.

The dynamic behaviour of thin VESs and the influence of the design of the sandwich on it was studied. To that end, thin VESs composed of different VE adhesives and metallic skins were characterized and numerical models were defined. The joint analysis of the experimental and numerical results led to the following conclusions:

- VE adhesives with high shear modulus and loss factor or metallic skins with high storage modulus lead to thin VESs with higher stiffness and damping.
- The thickness of the VE core influences the dynamic behaviour of the sandwich in the bandwidth up to 4 kHz. Increasing the core thickness, the loss factor of the sandwich increases and the vibration amplitude decreases. In contrast, the storage modulus decreases, whereas the bending stiffness increases.
- The thickness of the metallic skins has no remarkable influence on the dynamic properties of the sandwich. However, its thickness modifies the bending stiffness of the structure.

The influence of eddy currents induced in metallic skins on the dynamic behaviour of the sandwich was analysed. The following conclusions were obtained:

- Eddy currents induced in non-magnetic metallic beams attenuate the vibration of the beam in all the bandwidth of 0-1 kHz without modifying its natural frequencies and mode shapes. In addition, the vibration of all the length of the beam is attenuated even if the magnetic field is applied only in a partial region.
- A new hybrid sandwich structure (VES-ED) was defined. The VES-ED consists of a thin VES and permanent magnets placed near, but not in contact with, the sandwich. When the sandwich begins vibrating, energy is dissipated by two mechanisms: shear deformation of the viscoelastic film and eddy currents. The VES-ED attenuates structural vibration in a wide frequency bandwidth, without adding mass to the structure and compromising its mechanical properties. This newly proposed VES-ED provides a method of maximising the performance of thin VESs at low frequencies.
- A new inverse method was developed in order to estimate and model the influence of induced eddy currents in metallic and sandwich structures.

The influence of magnetorheological effect and magnetic force generated in the VEMR core on the dynamic behaviour of sandwich was analysed. The following conclusions were obtained:

- The magnetic force model developed by Moon and Pao (1969) for a ferromagnetic beam was proposed to describe the magnetic interaction given in the VEMRS beam.
- A magneto-dynamic modelling of VEMRSs by FEM that includes the magnetorheological effect and magnetic force was developed and validated with experimental results.
- The influence of the two phenomena is opposite; the magnetorheological effect tends to increase the resonance frequency of the sandwich, whereas the magnetic force tends to decrease.
- An explanation was given to an experimentally observed behaviour with MR sandwiches in literature. This is the first time, to the author's knowledge, that the magnetic force generated in the in the MR core was identified as the mechanism responsible for decreasing the resonance frequencies of the sandwich and that a numerical modelling able to represent such behaviour was developed.

Finally, the the dynamics of a thin VEMRS was experimentally studied and the following conclusions were obtained:

- When magnetic particles are added to the VE adhesive of a thin VES to obtain a smart VEMRS the geometrical and physical properties of the sandwich are slightly modified. As a consequence, the storage modulus of the sandwich is decreased slightly across all the bandwidth, whereas the loss factor is increased in medium to high frequencies.
- The vibrational response of the the thin VEMRS is modified instantaneously and reversibly in its first vibration mode when partial magnetic fields are applied.
- The magneto-dynamic behaviour of the analysed thin VEMRS is governed mostly by the magnetic force generated in the VEMR core and to a lesser extent by the induced eddy currents on the metallic skins. The former decreases the resonance frequency of the sandwich and the latter attenuate the vibration.
- The dynamic response of the thin VEMRS can be modified by the intensity and position of the partial magnetic field. When the intensity of the magnetic field is increased, the resonance frequency and the vibration amplitude of the sandwich are decreased. When the magnetic field is moved towards the free end, the resonance frequency is decreased.

7.2 Future works

This dissertation provided new insight into the dynamics of thin viscoelastic-magnetorheological sandwiches. However, further research work is recommended in order to completely understand some open questions outlined in this thesis.

A new inverse method was developed to estimate and model the influence of eddy currents induced in metallic skins of sandwiches. This method requires two experimental transfer functions, with and without induced eddy currents, and so experimental tests must be carried out at least in a narrow bandwidth. It would be valuable to propose an analytical model to describe the phenomenon of eddy currents in sandwich structures.

A magneto-dynamic modelling of VEMRSs that includes the phenomena of magnetorheological effect and magnetic force was developed. The magnetic interaction given in the VEMRS beam was described by the magnetic force model developed by Moon and Pao (1969) for ferromagnetic beams exposed to homogeneous transverse magnetic fields and further studies are needed to extend the model to non-homogeneous and oblique magnetic fields.

The magneto-dynamic behaviour of thin VEMRSs is the result of the coupling of different physical effects generated in the skins and core. Depending on the composition of VEMRS and configuration of magnetic field the contribution of each is different and so the magneto-dynamic behaviour of the sandwich. Hence, it would be of great interest to carry out a design analysis similar to that carried with thin VESs, but, extending it to magnetic fields. The influence of the composition of VEMR material, nature of VE adhesive and concentration of magnetic particles, thickness of the VEMR core, nature and thickness of metallic skins, and configuration of the magnetic field could be analysed. This analyses would enable to design a thin VEMRS in which the phenomena of eddy currents, magnetorheological effect and magnetic force could be generated depending on the requirements of the application.

Chapter 8

FIGURAS

8.1 Figuras

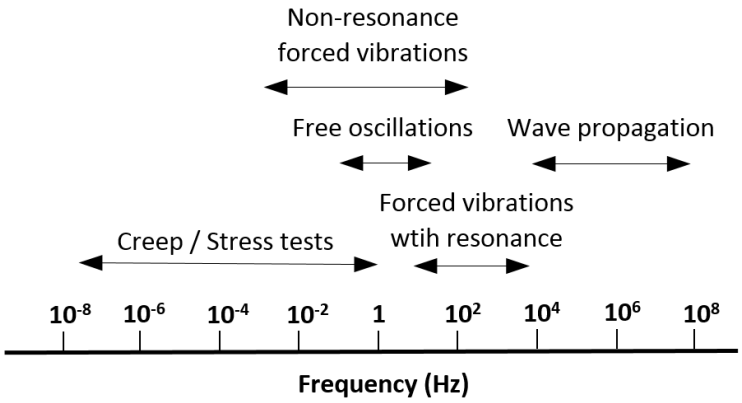

Figure 8.1. Viscoelastic materials characterization techniques classified according to the frequency range under study.

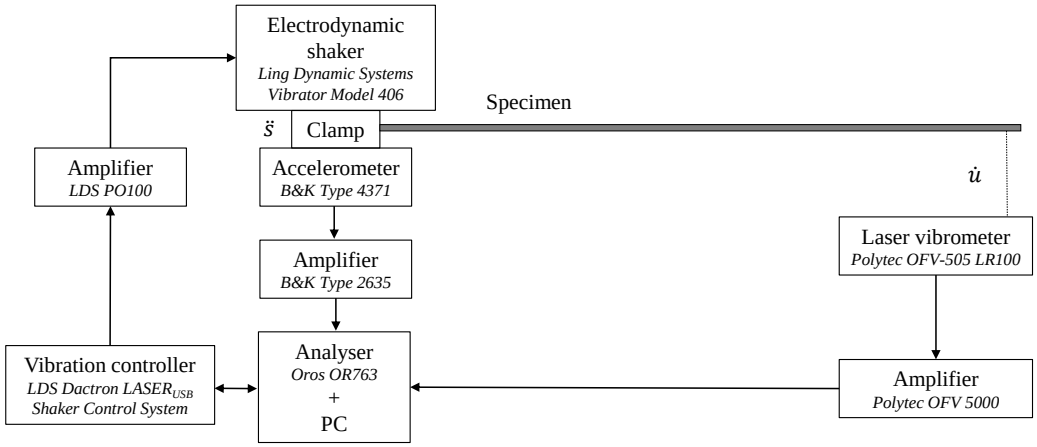

Figure 8.2. Experimental set-up.

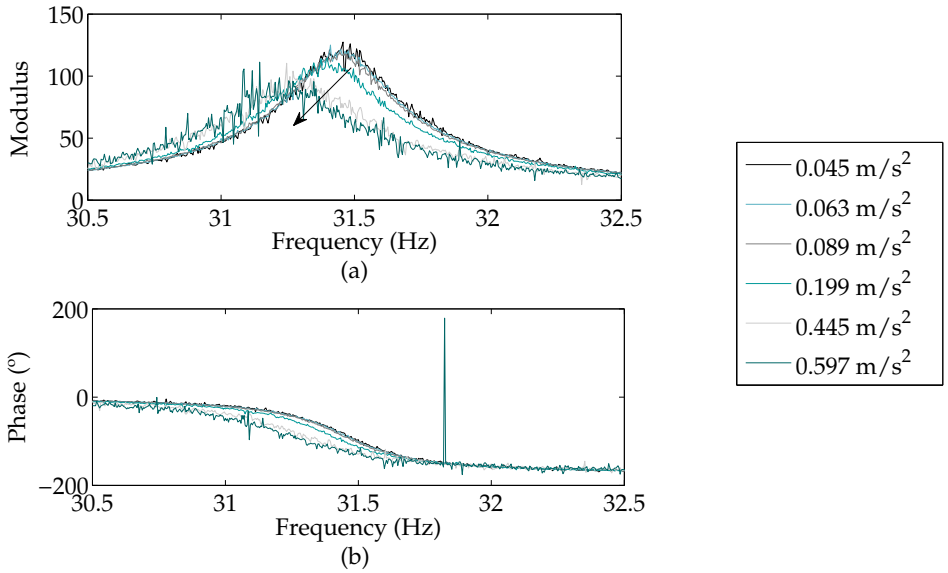

Figure 8.3. Linearity analysis of the VES with 170 mm of free length: First mode transfer function, (a) modulus and (b) phase, under different excitation levels.

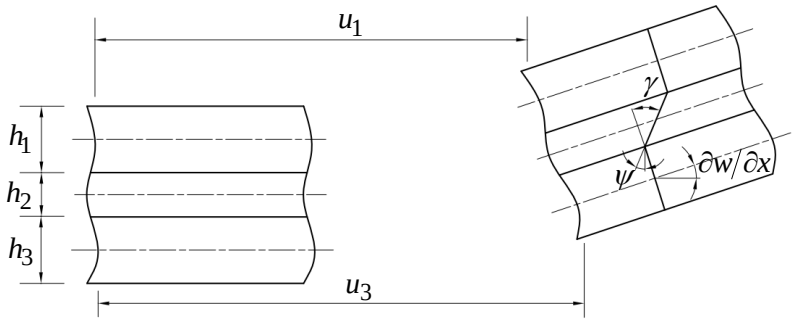

Figure 8.4. Displacement field of the sandwich beam.

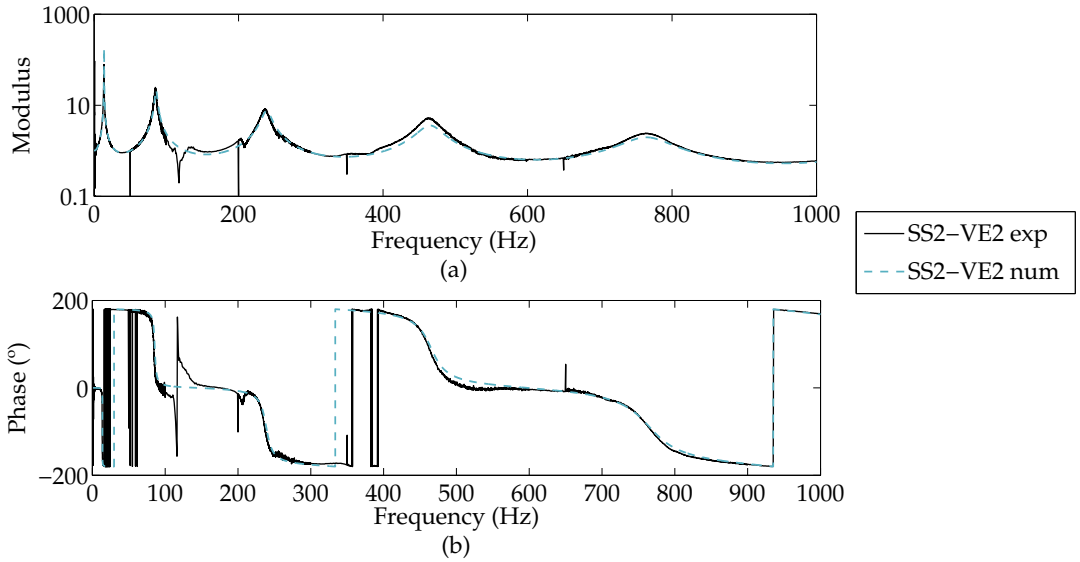

Figure 8.5. Experimental and numerical transfer function, (a) modulus and (b) phase, of the SS2-VE2 beam with 170 mm of free length in the bandwidth of 0-1 kHz.

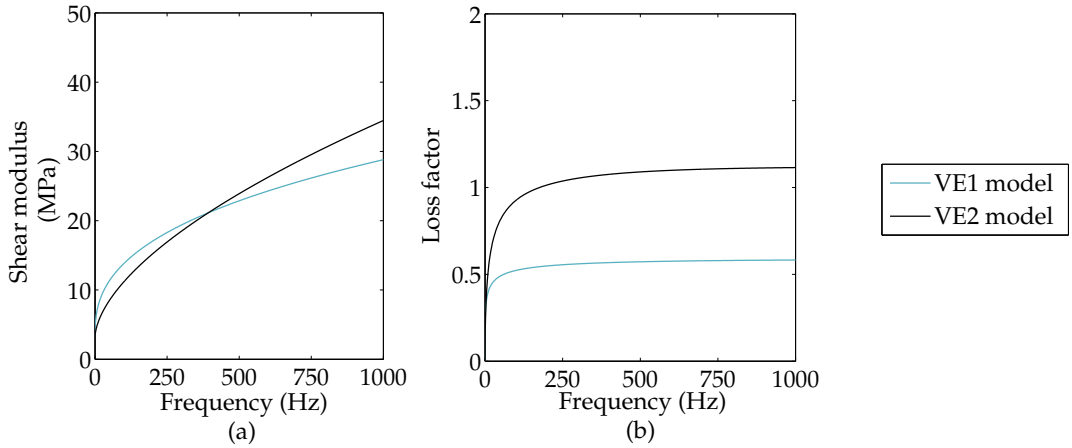

Figure 8.6. Shear complex modulus models, (a) shear modulus and (b) loss factor, of VE1 and VE2 films in the bandwidth of 0-1 kHz.

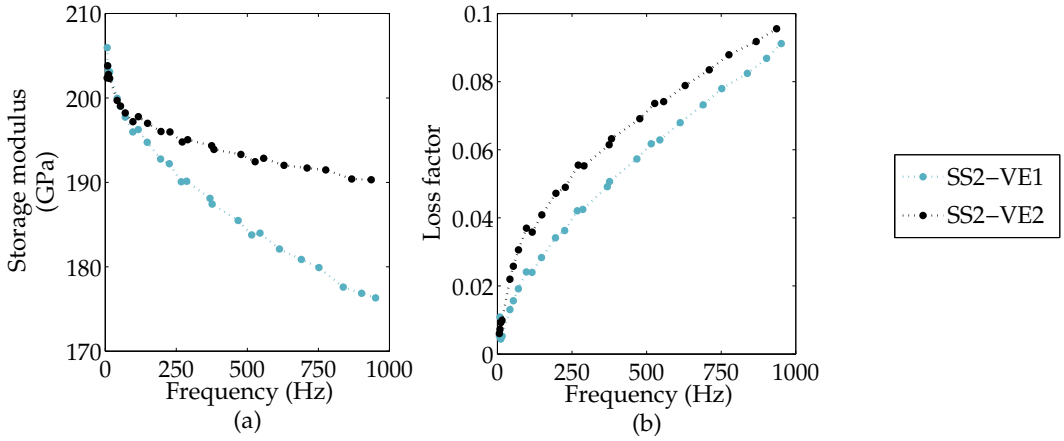

Figure 8.7. Influence of the VE film nature on the homogenised complex modulus, (a) storage modulus and (b) loss factor, of thin VESs in the bandwidth of 0-1 kHz. The composition of the sandwiches is the following: 0.25 mm of SS2 skins, and 40 µm of VE1 or VE2.

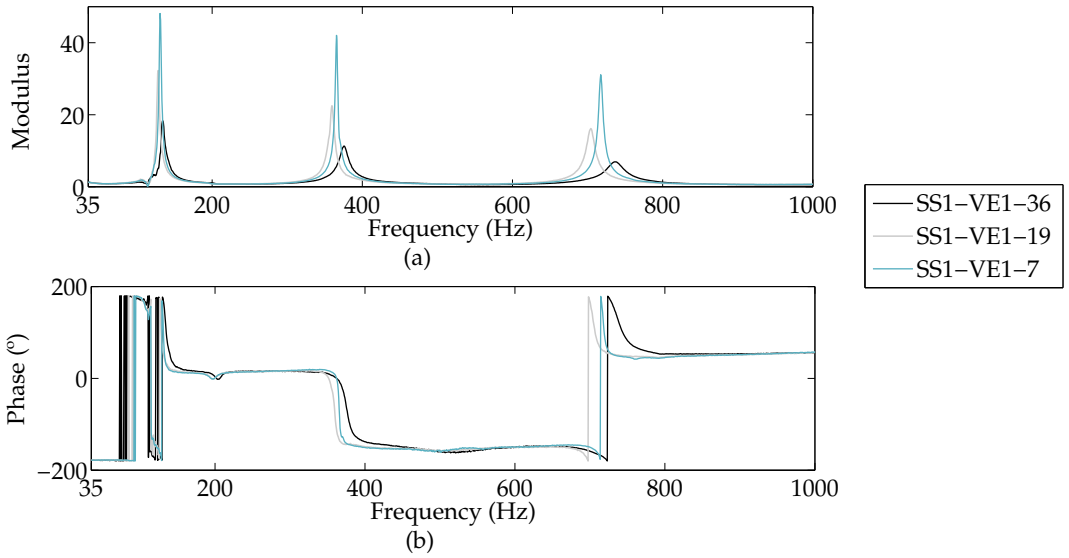

Figure 8.8. Experimental transfer functions, (a) Modulus and (b) Phase, of the SS1-VE1-36, SS1-VE1-19 and SS1-VE1-7 beams with with 140 mm of free length in the bandwidth of 35-1000 Hz.

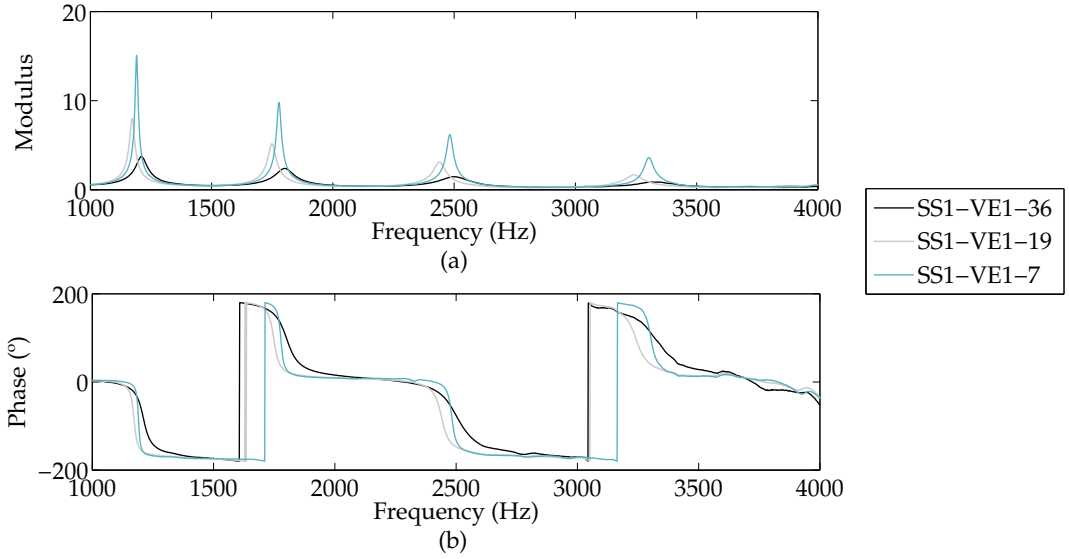

Figure 8.9. Experimental transfer functions, (a) Modulus and (b) Phase, of the SS1-VE1-36, SS1-VE1-19 and SS1-VE1-7 beams with with 140 mm of free length in the bandwidth of 1-4 kHz.

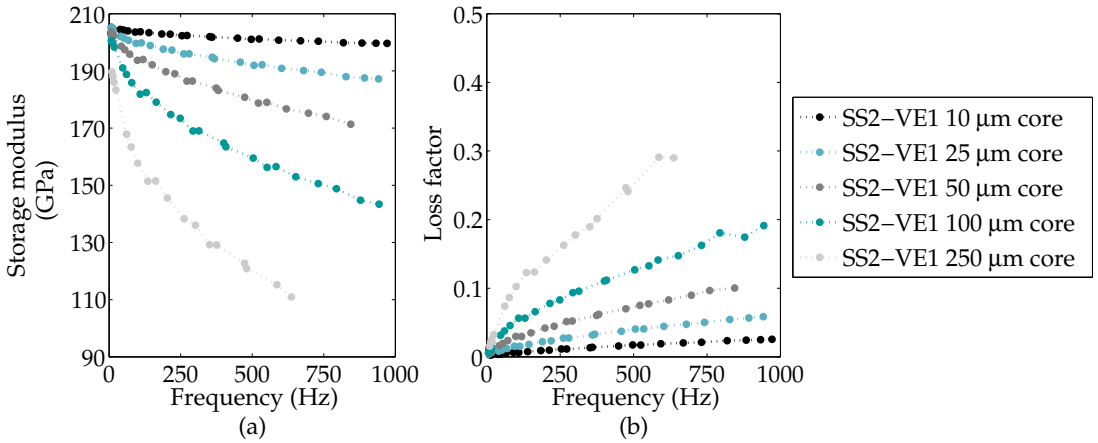

Figure 8.10. Influence of the VE1 film thickness on the homogenised complex modulus, (a) storage modulus and (b) loss factor, of thin VESs in the bandwidth of 0-1 kHz. The composition of the sandwiches is the following: 0.25 mm of SS2 skins, and 5 µm, 25 µm, 50 µm, 100 µm or 250 µm of VE1.

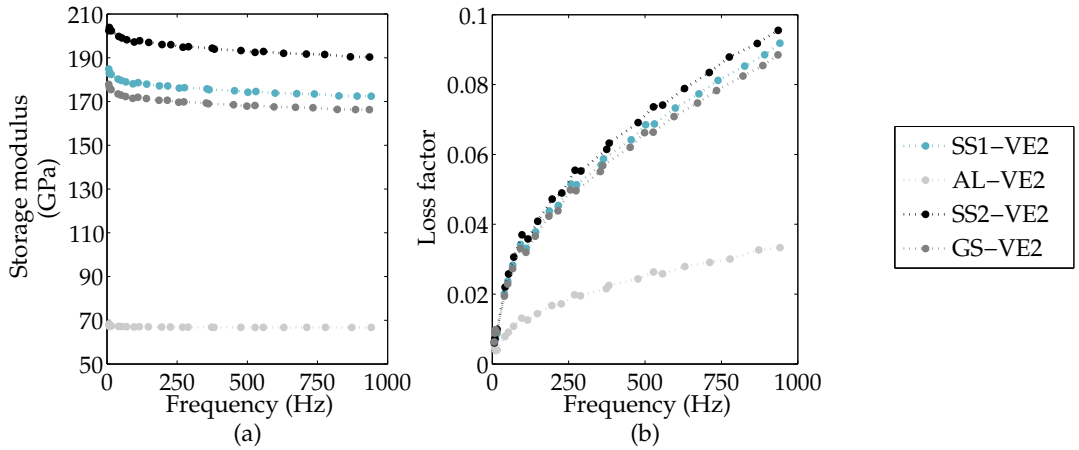

Figure 8.11. Influence of the type of metallic skin on the homogenised complex modulus, (a) storage modulus and (b) loss factor, of thin VESs in the bandwidth of 0-1 kHz. The composition of the sandwiches is the following: 0.25 mm of SS1, AL, SS2 or GS skins and 40 µm of VE2.

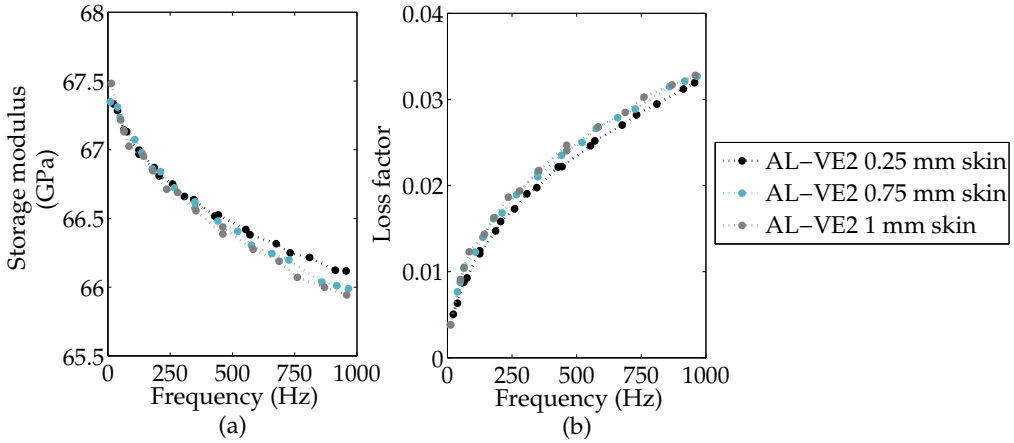

Figure 8.12. Influence of the AL skin thickness on the homogenised complex modulus, (a) storage modulus and (b) loss factor, of thin VESs in the bandwidht of 0-1 kHz. The composition of the sandwiches is the following: 0.25 mm, 0.75 mm or 1 mm of AL skins, and 40 µm of VE2.

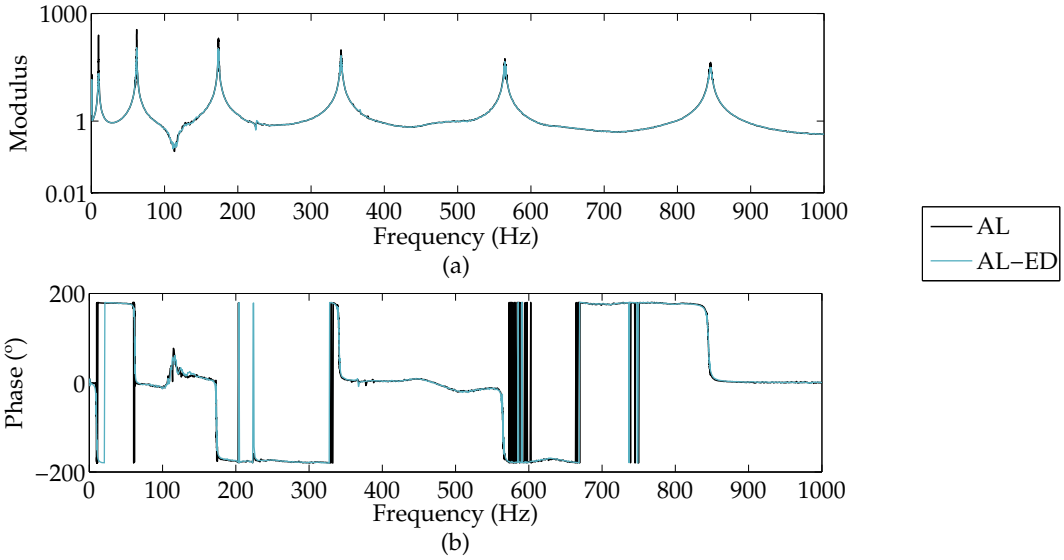

Figure 8.13. Experimental transfer function, (a) modulus and (b) phase, of the AL beam with 180 mm of free length whit and without induced eddy currents in the bandwidth of 0-1 kHz.

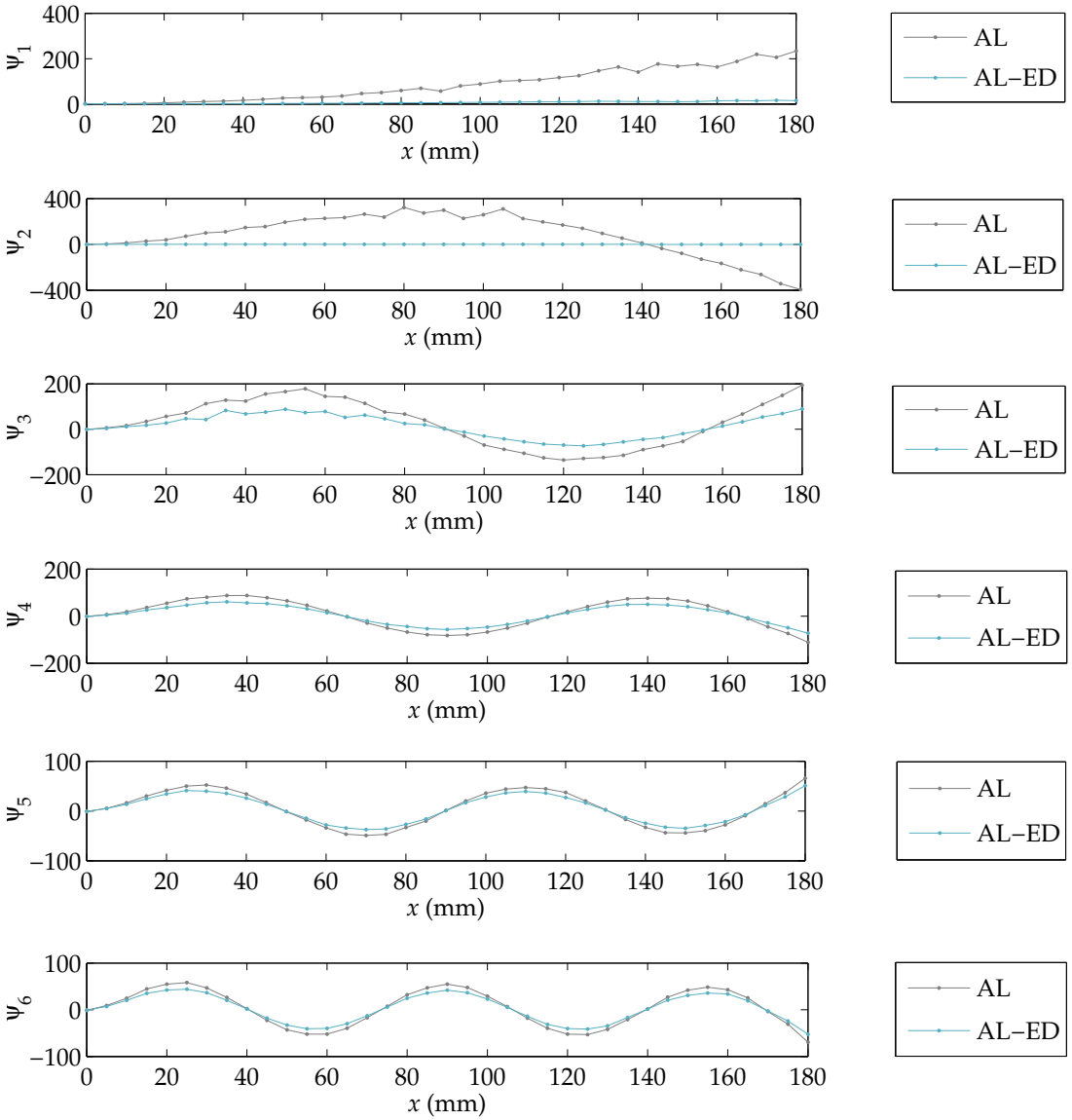

Figure 8.14. Experimental mode shapes of the AL cantilever beam with 180 mm of free length with and without eddy currents in the bandwidth of 0-1 kHz.

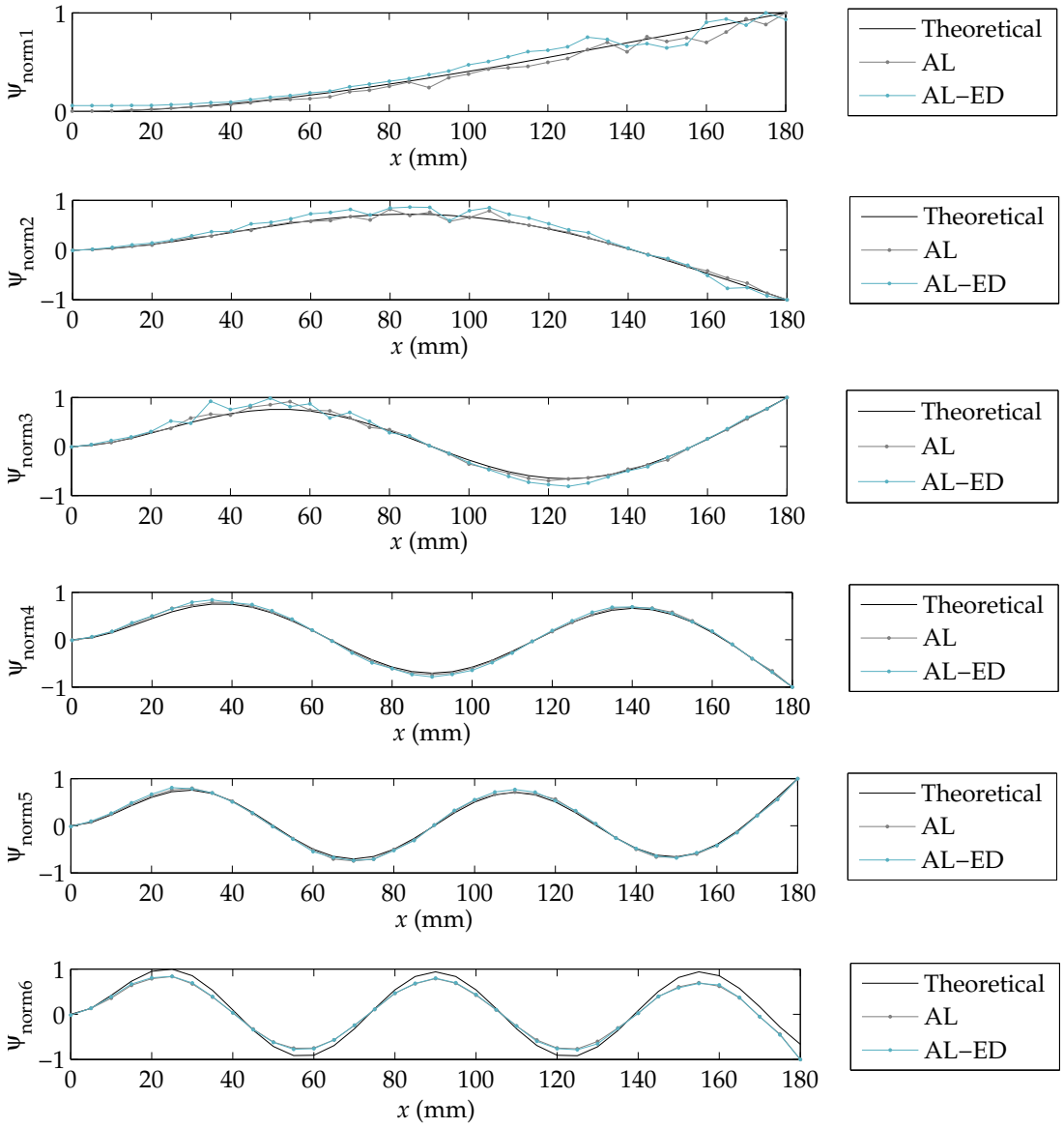

Figure 8.15. Experimental and theoretical mode shapes normalised to maximum displacement unit of the AL cantilever beam with 180 mm of free length with and without eddy currents in the bandwidth of 0-1 kHz (Blevins 1979)

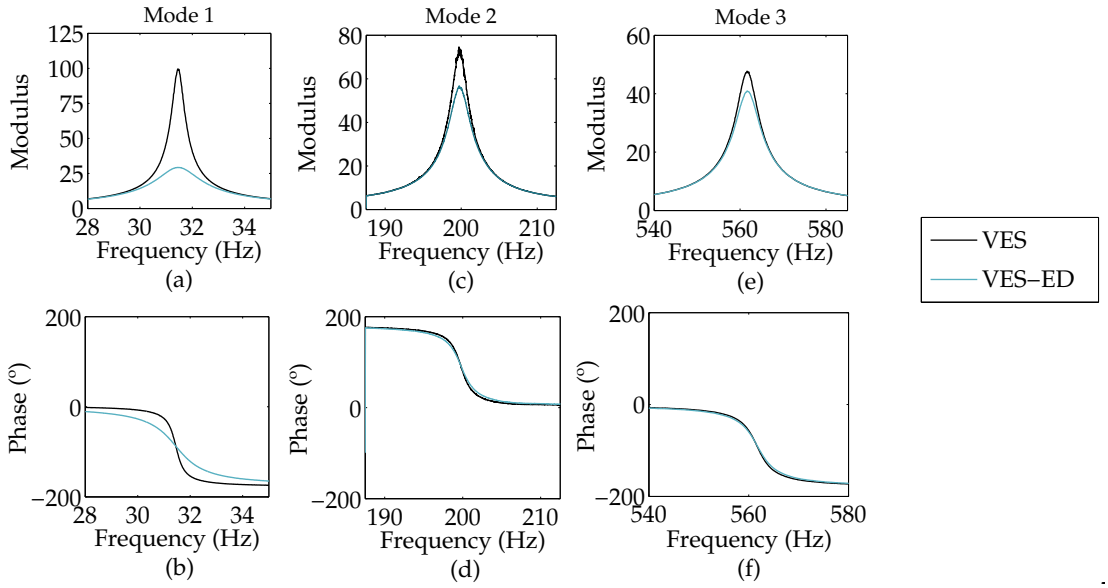

Figure 8.16. Experimental modal transfer functions, (a) modulus and (b) phase, of the VES and VES-ED beams with 170 mm of free length in the bandwidth of 0-1 kHz.

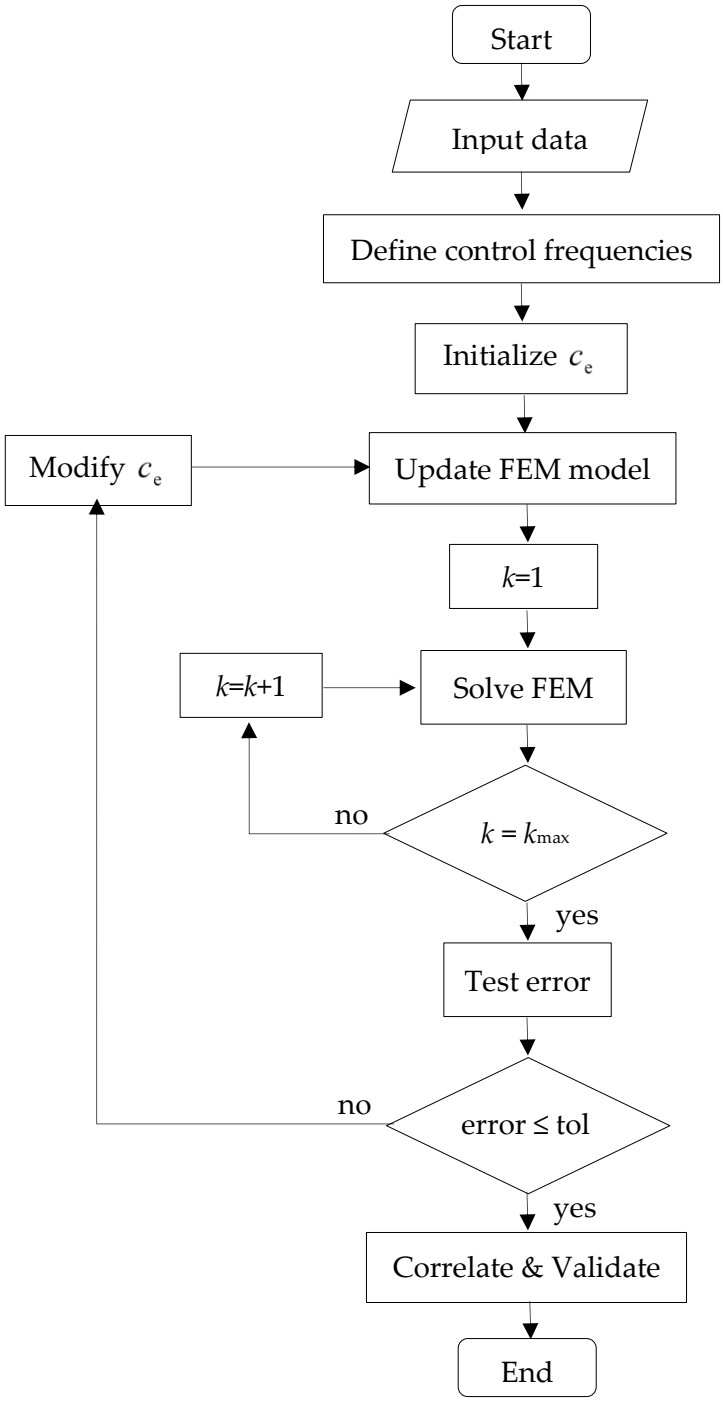

Figure 8.17. Scheme of the proposed inverse method for modelling the influence of induced eddy currents on conductive vibrating structures exposed to steady-state magnetic fields.

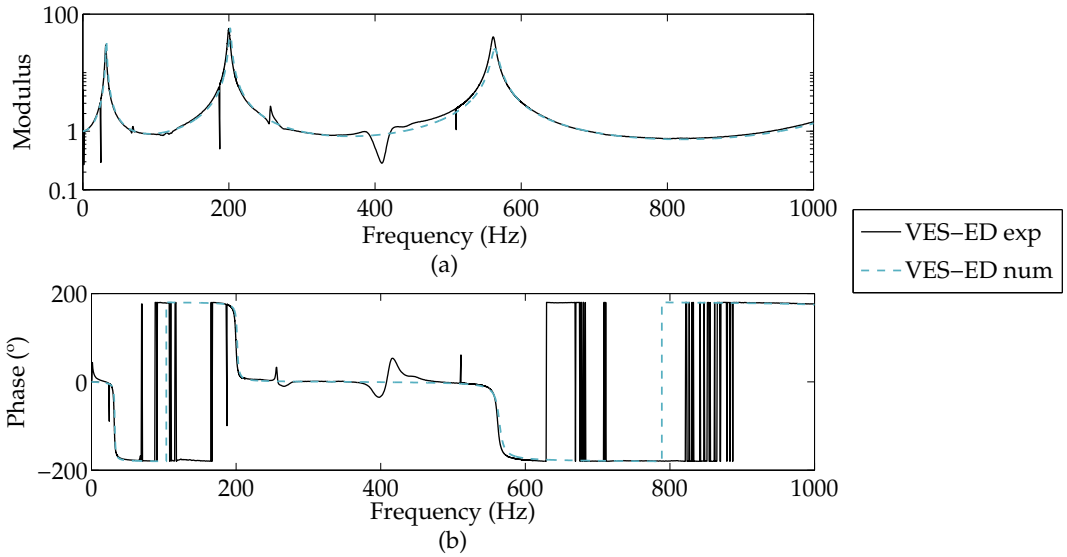

Figure 8.18. Experimental and numerical transmissibility function, a) modulus and b) phase, of the VES-ED beam with a free length of 170 mm in the bandwidth of 0-1 kHz.

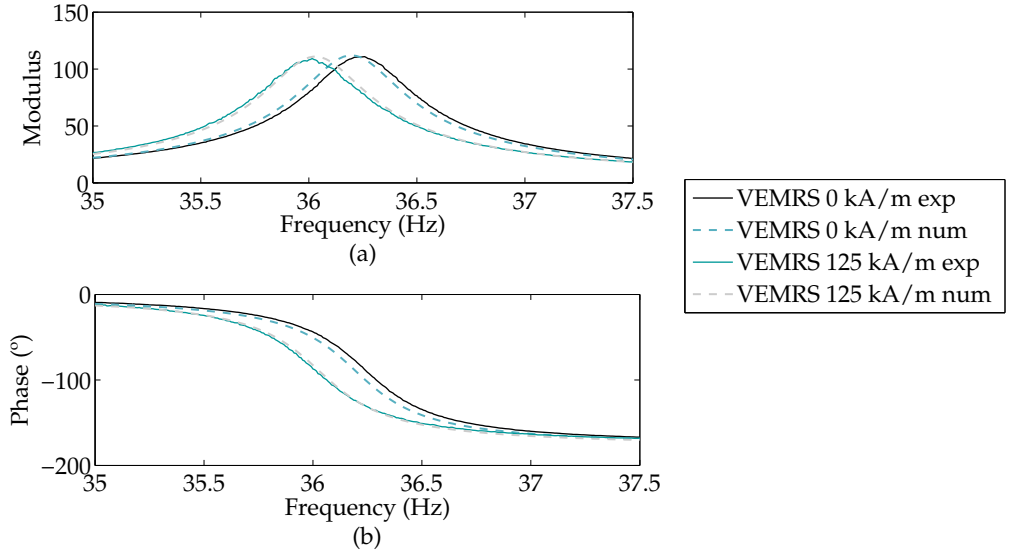

Figure 8.19. Experimental and numerical transfer function, (a) modulus and (b) phase, of the VEMRS beam with a free length of 160 mm in absence of and under a magnetic field in the first resonance.

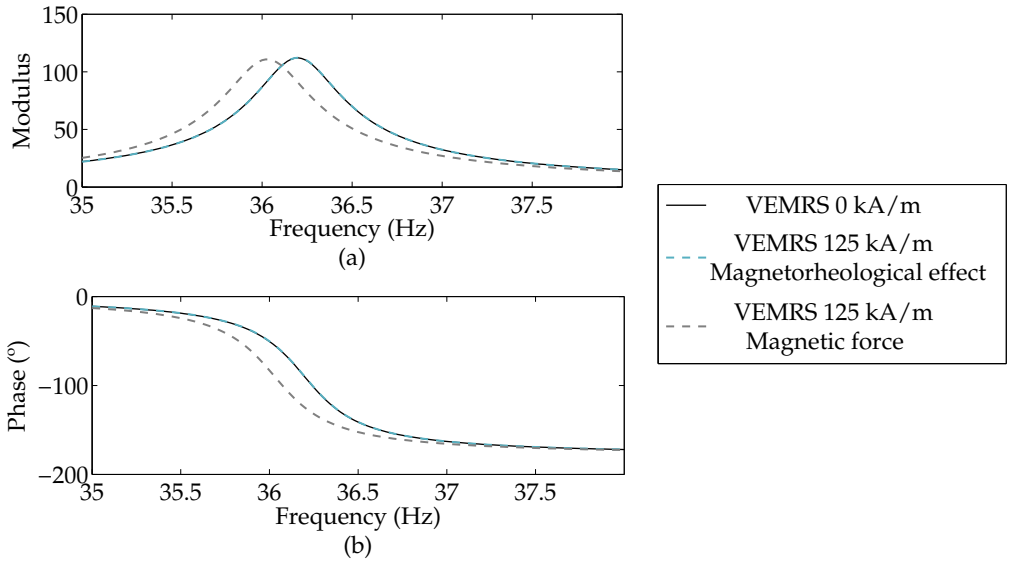

Figure 8.20. Contribution of the magnetorheological effect and magnetic force on the transfer function, (a) modulus and (b) phase, of the VEMRS with a free length of 160 mm in the first resonance.

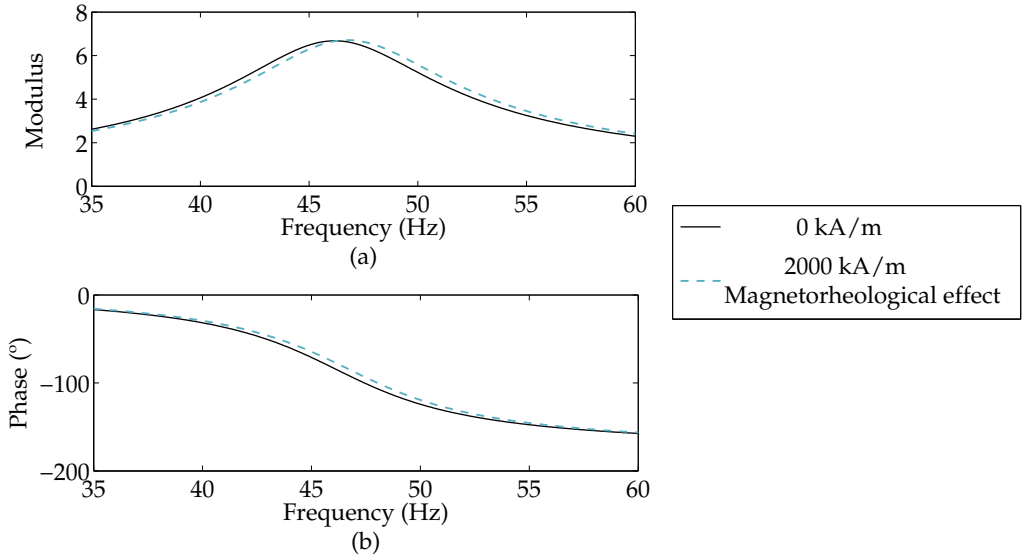

Figure 8.21. Contribution of the magnetorheological effect on the transmissibility function, (a) modulus and (b) phase, of the VEMRS composed of a 2 mm core and with a free length of 160 mm in the first resonance.

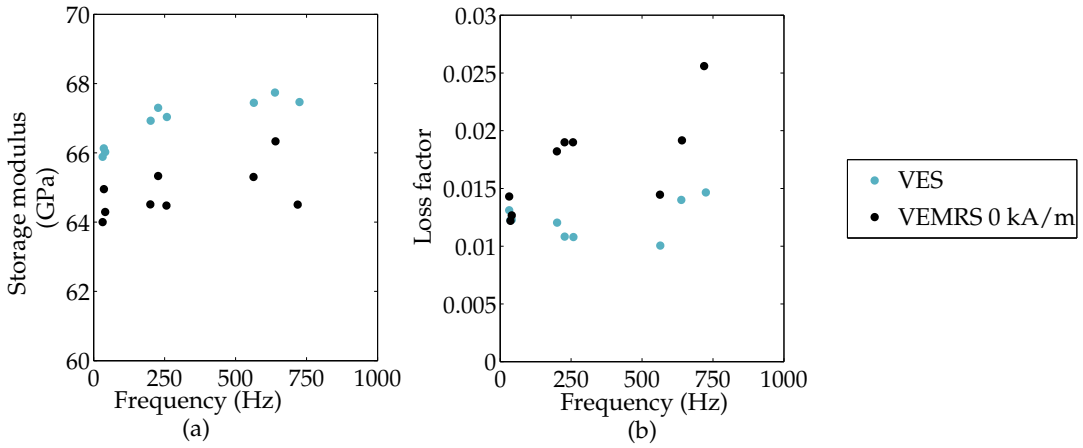

Figure 8.22. Experimental homogenised complex modulus, (a) storage modulus and (b) loss factor, of the VES and the VEMRS in the bandwidth between 0 and 1 kHz.

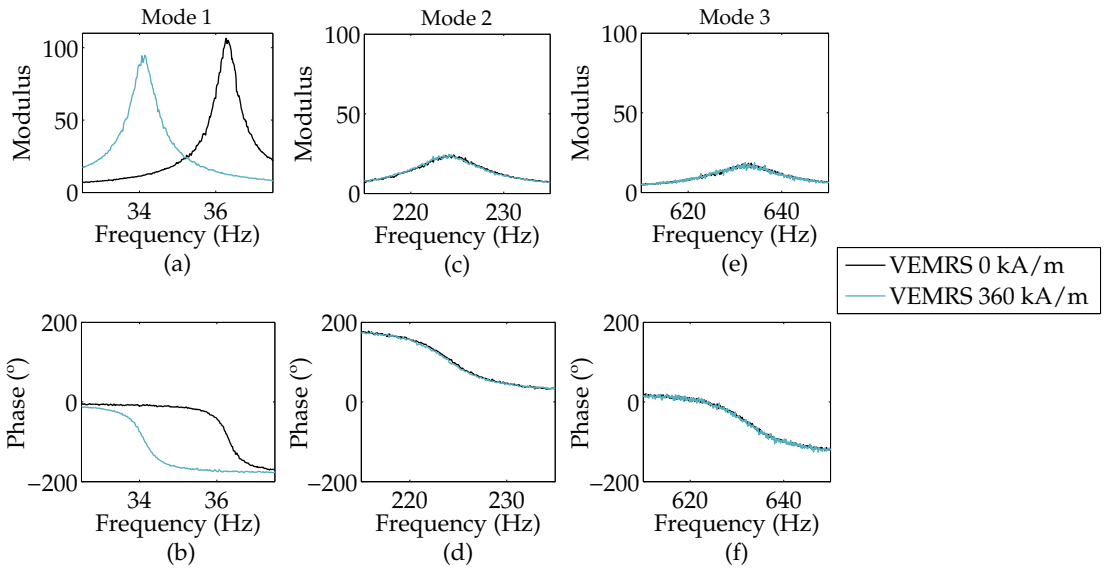

Figure 8.23. Experimental modal transfer functions, (a) modulus and (b) phase, of the VEMRS beam with 160 mm of free length, in absence of and under a partial magnetic field of 360 kA/m placed at 8 mm from the free end in the bandwidth of 0-1 kHz.

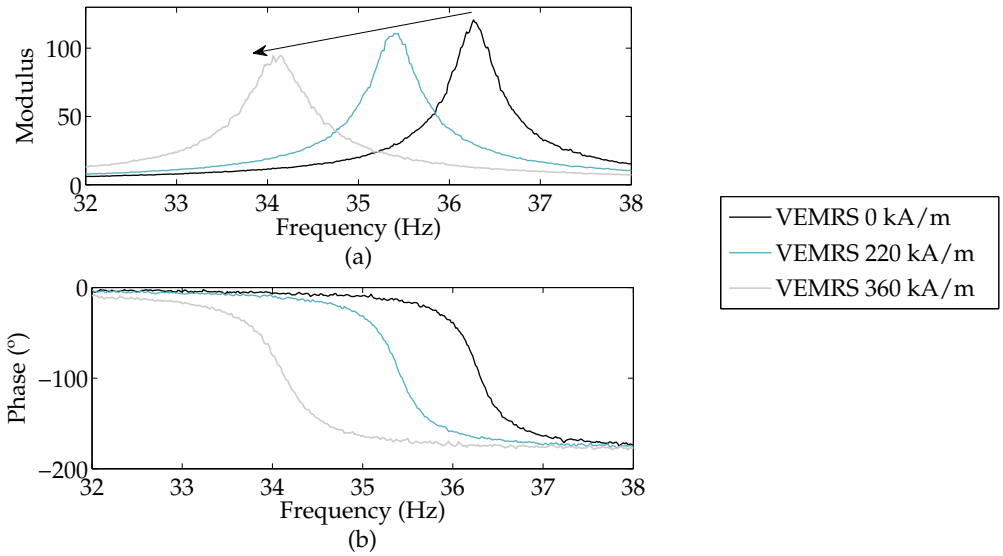

Figure 8.24. Experimental transfer functions, (a) modulus and (b) phase, of the VEMRS beam with 160 mm of free length in absence of and under different intensities of partial magnetic field (220 kA/m and 360 kA/m) placed at 8 mm from the free end in the first resonance

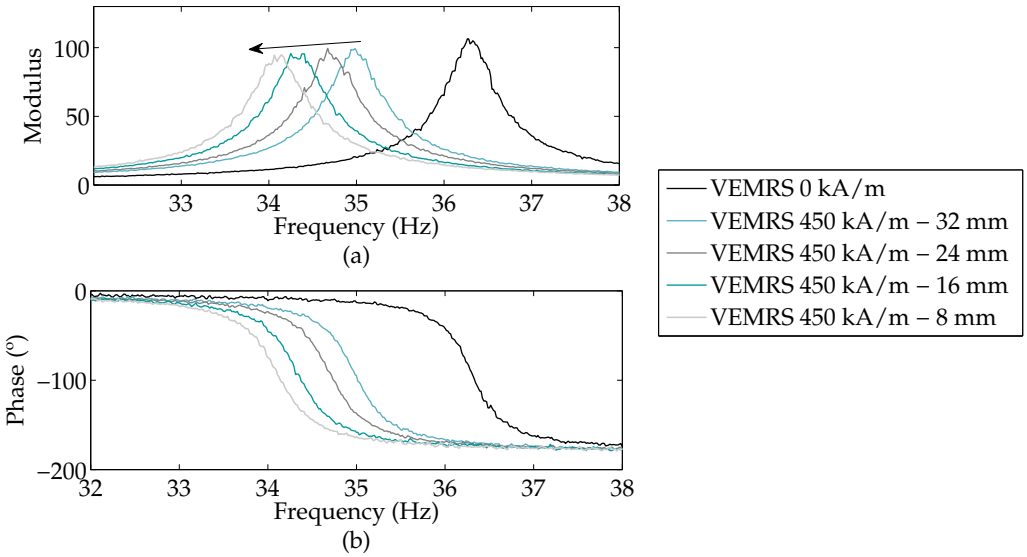

Figure 8.25. Experimental transfer functions, (a) modulus and (b) phase, of the VEMRS beam with 160 mm of free length in absence of and under a magnetic field of 360 kA/m placed at different positions (8mm, 16 mm, 24 mm and 32 mm) from the free end in the first resonance

Bibliography

Agirre-Olabide I, Lion A, and Elejabarrieta MJ (2017). A new three-dimensional magneto-viscoelastic model for isotropic magnetorheological elastomers. *Smart Materials and Structures* 26 (3):035021. DOI: 10.1088/1361-665X/26/3/035021.

Aguib S, Nour A, Zahloul H, Bossis G, Chevalier Y, and Lancon P (2014). Dynamic behavior analysis of a magnetorheological elastomer sandwich plate. *International Journal of Mechanical Sciences* 87:118–136. DOI: 10.1016/j.ijmecsci.2014.05.014.

Araújo AL, Mota Soares CM, Mota Soares CA, and Herskovits J (2010). Optimal design and parameter estimation of frequency dependent viscoelastic laminated sandwich composite plates. *Composite Structures* 92 (9):2321–2327. DOI: 10.1016/j.compstruct.2009.07.006.

Asghar Maddah A, Hojjat Y, Reza Karafi M, and Reza Ashory M (2017). Reduction of magneto rheological dampers stiffness by incorporating of an eddy current damper. *Journal of Sound and Vibration* 396:51–68. DOI: 10.1016/j.jsv.2017.02.011.

ASTM E 756 05 (2005). Standard test method for measuring vibration-damping properties of materials.

Babu VR and Vasudevan R (2016). Dynamic analysis of tapered laminated composite magnetorheological elastomer (MRE) sandwich plates. *Smart Materials and Structures* 25 (3):035006. DOI: 10.1088/0964-1726/25/3/035006.

Bae JS, Hwang JH, Kwag DG, Park J, and Inman DJ (2014). Vibration suppression of a large beam structure using tuned mass damper and eddy current damping. *Shock and Vibration* 2014:1–10. DOI: 10.1155/2014/893914.

Bae JS, Hwang JH, Roh JH, Kim JH, Yi MS, and Lim JH (2012). Vibration suppression of a cantilever beam using magnetically tuned-mass-damper. *Journal of Sound and Vibration* 331 (26):5669–5684. DOI: 10.1016/j.jsv.2012.07.020.

Bae JS, Kwak MK, and Inman DJ (2005). Vibration suppression of a cantilever beam using eddy current damper. *Journal of Sound and Vibration* 284 (3-5):805–824. DOI: 10.1016/j.jsv.2004.07.031.

Bagley RL and Torvik PJ (1983). A theoretical basis for the application of fractional calculus to viscoelasticity. *Journal of Rheology* 27 (3):201–210. DOI: 10.1122/1.549724.

Bagley RL and Torvik PJ (1986). On the fractional calculus model of viscoelastic behavior. *Journal of Rheology* 30 (1):133–155. DOI: 10.1122/1.549887.

Berardengo M, Cigada A, Guanziroli F, and Manzoni S (2015). Modelling and control of an adaptive tuned mass damper based on shape memory alloys and eddy currents. *Journal of Sound and Vibration* 349:18–38. DOI: 10.1016/j.jsv.2015.03.036.

Bica I, Balasoiu M, and Kuklin AI (2012). Anisotropic silicone rubber based magnetorheological elastomer with oil silicone and iron microparticles. *Solid State Phenomena* 190:645–648. DOI: 10.4028/www.scientific.net/SSP.190.645.

Bishay PL, Tawfik M, and Negm HM (2010). Experimental and finite element models of an adaptive magnetorheological sandwich beam. *The 17th International Congress on Sound and Vibration*. Cairo.

Blevins RD (1979). *Formulas for natural frequency and mode shape*. New York: Van Nostrand Reinhold Co.

Butaud P, Foltête E, and Ouisse M (2016). Sandwich structures with tunable damping properties: On the use of Shape Memory Polymer as viscoelastic core. *Composite Structures* 153:401–408. DOI: 10.1016/j.compstruct.2016.06.040.

Caliri MF, Ferreira AJM, and Tita V (2016). A review on plate and shell theories for laminated and sandwich structures highlighting the Finite Element Method. *Composite Structures* 156:63–77. DOI: 10.1016/j.compstruct.2016.02.036.

Carlson JD and Jolly MR (2000). MR fluid, foam and elastomer devices. *Mechatronics* 10 (4-5):555–569. DOI: 10.1016/S0957-4158(99)00064-1.

Chen L, Gong XL, and Li WH (2008). Effect of carbon black on the mechanical performances of magnetorheological elastomers. *Polymer Testing* 27 (3):340–345. DOI: 10.1016/j.polymertesting.2007.12.003.

Cheng TH, Xuan DJ, Li ZZ, and Shen YD (2010). Vibration control using shunted electromagnetic transducer. *Applied Mechanics and Materials* 26-28:905–908. DOI: 10.4028/www.scientific.net/AMM.26-28.905.

Cheng TH and Oh IK (2009). Vibration suppression of flexible beam using electromagnetic shunt damper. *IEEE Transactions on Magnetics* 45 (6):2758–2761. DOI: 10.1109/TMAG.2009.2020549.

Choi WJ, Xiong YP, and Shenoi RA (2009). Experimental study on vibration characteristics of sandwich beams with aluminum skins and magnetorheological elastomer cores. *17 International conference on composite materials*. Edinburgh. DOI: 10.1260/1369-4332.13.5.837.

Choi WJ, Xiong YP, and Shenoi RA (2010). Vibration characteristics of sandwich beams with steel skins and magnetorheological elastomer cores. *Advances in Structural Engineering* 13 (5):837–847. DOI: 10.1260/1369-4332.13.5.837.

Cortés F and Elejabarrieta MJ (2007). Viscoelastic materials characterisation using the seismic response. *Materials & Design* 28 (7):2054–2062. DOI: 10.1016/j.matdes.2006.05.032.

Davis LC (1999). Model of magnetorheological elastomers. *Journal of Applied Physics* 85 (6):3348–3351. DOI: 10.1063/1.369682.

De Espíndola JJ, da Silva Neto JM, and Lopes EMO (2005). A generalised fractional derivative approach to viscoelastic material properties measurement. *Applied Mathematics and Computation* 164 (2):493–506. DOI: 10.1016/j.amc.2004.06.099.

Eshaghi M, Sedaghati R, and Rakheja S (2016). Dynamic characteristics and control of magnetorheological/electrorheological sandwich structures: A state-of-the-art review. *Journal of Intelligent Material Systems and Structures* 27 (15):2003–2037. DOI: 10.1177/1045389X15620041.

Gélinas C, Chagnon F, and Pelletier S (1996). Development of an iron-resin composite material for soft magnetic applications. *World Congress*. Washington, p. 85–97.

Goncalves FD, Koo JH, and Ahmadian M (2006). A review of the state of the art in magnetorheological fluid technologies - Part I: MR fluid and MR fluid models. *The Shock and Vibration Digest* 38 (3):203–219. DOI: 10.1177/0583102406065099.

Goodman LE (1996). Material damping and slip damping. *Shock and Vibration Handbook*. C. M. Harr. New York: McGraw–Hill, p. Cap. 36.

Hamdaoui M, Robin G, Jrad M, and Daya EM (2015). Optimal design of frequency dependent three-layered rectangular composite beams for low mass and high damping. *Composite Structures* 120:174–182. DOI: 10.1016/j.compstruct.2014.09.062.

Hu GL, Guo M, and Li WH (2011a). Analysis of vibration characteristics of magnetorheological elastomer sandwich beam under non-homogeneous magnetic field. *Applied Mechanics and Materials* 101-102:202–206. DOI: 10.4028/www.scientific.net/AMM.101-102.202.

Hu GL, Guo M, Li WH, Du H, and Alici G (2011b). Experimental investigation of the vibration characteristics of a magnetorheological elastomer sandwich beam under non-homogeneous small magnetic fields. *Smart Materials and Structures* 20 (12):127001. DOI: 10.1088/0964-1726/20/12/127001.

Irazu L and Elejabarrieta MJ (2017). Magneto-dynamic analysis of sandwiches composed of a thin viscoelastic-magnetorheological layer. *Journal of Intelligent Material Systems and Structures*:1045389X1770520. DOI: 10.1177/1045389X17705209.

Jolly MR, Carlson JD, and Muñoz BC (1996a). A model of the behaviour of magnetorheological materials. *Smart Materials and Structures* 5 (5):607–614. DOI: 10.1088/0964-1726/5/5/009.

Jolly MR, Carlson JD, Muñoz BC, and Bullions TA (1996b). The magnetoviscoelastic response of elastomer composites consisting of rerrous particles embedded in a polymer matrix. *Journal of Intelligent Material Systems and Structures* 7 (6):613–622. DOI: 10.1177/1045389X9600700601.

Jones DIG (2001). *Handbook of viscoelastic vibration damping*. Chichester: John Wiley and Sons Ltd.

Kergourlay G, Balmès E, and Legal G (2006). A characterization of frequency–temperature–prestress effects in viscoelastic films. *Journal of Sound and Vibration* 297 (1-2):391–407. DOI: 10.1016/j.jsv.2006.04.003.

Kerwin EM (1959). Damping of flexural waves by a constrained viscoelastic layer. *The Journal of the Acoustical Society of America* 31 (7):952–962. DOI: 10.1121/1.1907821.

Kumar N and Singh SP (2009). Vibration and damping characteristics of beams with active constrained layer treatments under parametric variations. *Materials & Design* 30 (10):4162–4174. DOI: 10.1016/j.matdes.2009.04.044.

Kwak MK, Lee MI, and Heo S (2003). Vibration suppression using eddy current damper. *Korean Society for Noise and Vibration Engineering* 13 (10):760–766.

Lakes RS and Wineman A (2006). On Poisson's ratio in linearly viscoelastic solids. *Journal of Elasticity* 85 (1):45–63. DOI: 10.1007/s10659-006-9070-4.

Lara-Prieto V, Parkin R, Jackson M, Silberschmidt V, and Kesy Z (2010). Vibration characteristics of MR cantilever sandwich beams: experimental study. *Smart Materials and Structures* 19 (1):015005. DOI: 10.1088/0964-1726/19/1/015005.

Leibowitz M and Lifshitz JM (1990). Experimental verification of modal parameters for 3-layered sandwich beams. *International Journal of Solids and Structures* 26 (2):175–184. DOI: 10.1016/0020-7683(90)90050-6.

Li J, Gong X, Xu Z, and Jiang W (2008). The effect of pre-structure process on magnetorheological elastomer performance. *International Journal of Materials Research* 99 (12):1358–1364. DOI: 10.3139/146.101775.

Lifshitz JM and Leibowitz M (1987). Optimal sandwich beam design for maximum viscoelastic damping. *International Journal of Solids and Structures* 23 (7):1027–1034. DOI: 10.1016/0020-7683(87)90094-1.

Lu YC (2007). Fractional derivative viscoelastic model for frequency-dependent complex moduli of automotive elastomers. *International Journal of Mechanics and Materials in Design* 3 (4):329–336. DOI: 10.1007/s10999-007-9039-x.

Madeira JFA, Araújo AL, Mota Soares CM, and Mota Soares CA (2015a). Multiobjective optimization of viscoelastic laminated sandwich structures using the Direct MultiSearch method. *Computers & Structures* 147:229–235. DOI: 10.1016/j.compstruc.2014.09.009.

Madeira JFA, Araújo AL, Mota Soares CM, Mota Soares CA, and Ferreira AJM (2015b). Multiobjective design of viscoelastic laminated composite sandwich panels. *Composites Part B: Engineering* 77:391–401. DOI: 10.1016/j.compositesb.2015.03.025.

Martinez-Agirre M and Elejabarrieta MJ (2010). Characterisation and modelling of viscoelastically damped sandwich structures. *International Journal of Mechanical Sciences* 52 (9):1225–1233. DOI: 10.1016/j.ijmecsci.2010.05.010.

Martinez-Agirre M, Illescas S, and Elejabarrieta MJ (2014). Characterisation and modelling of prestrained viscoelastic films. *International Journal of Adhesion and Adhesives* 50:183–190. DOI: 10.1016/j.ijadhadh.2014.01.029.

Matsuzaki Y, Ikeda T, Nae A, and Sasaki T (2000). Electromagnetic forces for a new vibration control system: experimental verification. *Smart Materials and Structures* 9 (2):127–131. DOI: 10.1088/0964-1726/9/2/301.

Matsuzaki Y, Ishikubo D, Kamita T, and Ikeda T (1997). Vibration control system using electromagnetic forces. *Journal of Intelligent Material Systems and Structures* 8 (9):751–756. DOI: 10.1177/1045389X9700800904.

Megha S, N SK, and Silva RD (2016). Vibration analysis of magnetorheological elastomer sandwich beam under different magnetic fields. *Journal of Mechanical Engineering and Automation* 6:75–80. DOI: 10.5923/c.jmea.201601.14.

Moon FC and Pao YH (1969). Vibration and dynamic instability of a beam-plate in a transverse magnetic field. *Journal of Applied Mechanics* 36 (1):92. DOI: 10.1115/1.3564592.

Moreira RAS and Dias Rodrigues J (2010). Multilayer damping treatments: Modeling and experimental assessment. *Journal of Sandwich Structures & Materials* 12 (2):181–198. DOI: 10.1177/1099636209104530.

Nashif AD, Jones DIG, and Henderson JP (1985). *Vibration Damping*. New York: Wiley.

Nayak B, Dwivedy SK, and Murthy KSRK (2011). Dynamic analysis of magnetorheological elastomer-based sandwich beam with conductive skins under various boundary conditions. *Journal of Sound and Vibration* 330 (9):1837–1859. DOI: 10.1016/j.jsv.2010.10.041.

Nayak B, Dwivedy SK, and Murthy KSRK (2012a). Multi-frequency excitation of magnetorheological elastomer-based sandwich beam with conductive skins. *International Journal of Non-Linear Mechanics* 47 (5):448–460. DOI: 10.1016/j.ijnonlinmec.2011.08.007.

Nayak B, Dwivedy SK, and Murthy KSRK (2013). Dynamic stability of magnetorheological elastomer based adaptive sandwich beam with conductive skins using FEM and the harmonic balance method. *International Journal of Mechanical Sciences* 77:205–216. DOI: 10.1016/j.ijmecsci.2013.09.010.

Nayak B, Sastri BS, Dwivedy SK, and Murthy K (2012b). A comparative study of hte classical and higher order theory for free vibration analysis of MRE cored sandwich beam with composite skins using finite element method. *IEEE-International Conference On Advances In Engineering*, p. 172–178.

Nelder JA and Mead R (1965). A simplex method for function minimization. *The Computer Journal* 7 (4):308–313. DOI: 10.1093/comjnl/7.4.308.

Ouis D (2003). Combination of a standard viscoelastic model and fractional derivate calculus to the characterization of polymers. *Materials Research Innovations* 7 (1):42–46. DOI: 10.1080/14328917.2003.11784758.

Pritz T (1996). Analysis of four-parameter fractional derivative model of real solid materials. *Journal of Sound and Vibration* 195 (1):103–115. DOI: 10.1006/jsvi.1996.0406.

Rajamohan V, Rakheja S, and Sedaghati R (2010a). Vibration analysis of a partially treated multi-layer beam with magnetorheological fluid. *Journal of Sound and Vibration* 329 (17):3451–3469. DOI: 10.1016/j.jsv.2010.03.010.

Rajamohan V, Sedaghati R, and Rakheja S (2010b). Vibration analysis of a multi-layer beam containing magnetorheological fluid. *Smart Materials and Structures* 19:015013. DOI: 10.1088/0964-1726/19/1/015013.

Ramesh BV, Vasudevan R, and Kumar NB (2014). Vibration analysis of a laminated composite magnetorheological elastomer sandwich beam. *Applied Mechanics and Materials* 592-594:2097–2101. DOI: 10.4028/www.scientific.net/AMM.592-594.2097.

Ramkumar K and Ganesan N (2009). Vibration and damping of composite sandwich box column with viscoelastic/electrorheological fluid core and performance comparison. *Materials & Design* 30 (8):2981–2994. DOI: 10.1016/j.matdes.2008.12.023.

Rao MD (2003). Recent applications of viscoelastic damping for noise control in automobiles and commercial airplanes. *Journal of Sound and Vibration* 262 (3):457–474. DOI: 10.1016/S0022-460X(03)00106-8.

Ross D, Ungar EE, and Kerwin EM (1959). Damping of plate flexural vibrations by means of viscoelastic laminae. *Strucutral Damping*:49–87.

Rouleau L, Pirk R, Pluymers B, and Desmet W (2015). Characterization and modeling of the viscoelastic behavior of a self-adhesive rubber using dynamic mechanical analysis Tests. *Journal of Aerospace Technology and Management* 7 (2):200–208. DOI: 10.5028/jatm.v7i2.474.

Sargianis J and Suhr J (2012). Effect of core thickness on wave number and damping properties in sandwich composites. *Composites Science and Technology* 72 (6):724–730. DOI: 10.1016/j.compscitech.2012.01.024.

Shen Y, Golnaraghi MF, and Heppler GR (2004). Experimental research and modeling of magnetorheological elastomers. *Journal of Intelligent Material Systems and Structures* 15 (1):27–35. DOI: 10.1177/1045389X04039264.

Sher BR and Moreira RAS (2013). Dimensionless analysis of constrained damping treatments. *Composite Structures* 99:241–254. DOI: 10.1016/j.compstruct.2012.11.037.

Sodano HA and Bae JS (2004). Eddy current damping in structures. *The Shock and Vibration Digest* 36 (6):469–478. DOI: 10.1177/0583102404048517.

Sodano HA, Bae JS, Inman DJ, and Belvin WK (2006). Improved concept and model of eddy current damper. *Journal of Vibration and Acoustics* 128 (3):294. DOI: 10.1115/1.2172256.

Sodano HA, Bae JS, Inman DJ, and Keith Belvin W (2005). Concept and model of eddy current damper for vibration suppression of a beam. *Journal of Sound and Vibration* 288 (4-5):1177–1196. DOI: 10.1016/j.jsv.2005.01.016.

Sodano HA and Inman DJ (2007). Non-contact vibration control system employing an active eddy current damper. *Journal of Sound and Vibration* 305 (4-5):596–613. DOI: 10.1016/j.jsv.2007.04.050.

Stein GJ, Tobolka P, and Chmurny R (2016). Ferromagnetic eddy current damper of beam transversal vibrations. *Journal of Vibration and Control*:1–12. DOI: 10.1177/1077546316654791.

Sun Q, Zhou JX, and Zhang L (2003). An adaptive beam model and dynamic characteristics of magnetorheological materials. *Journal of Sound and Vibration* 261 (3):465–481. DOI: 10.1016/S0022-460X(02)00985-9.

Teng Tl and Hu Nk (2001). Analysis of damping characteristics for viscoelastic laminated beams. *Computer Methods in Applied Mechanics and Engineering* 190 (29-30):3881–3892. DOI: 10.1016/S0045-7825(00)00305-4.

Trindade MA and Benjeddou A (2002). Hybrid active-passive damping treatments using viscoelastic and piezoelectric materials: Review and assessment. *Modal Analysis* 8 (6):699–745. DOI: 10.1177/1077546029186.

Ubaidillah S, Sutrisno J, Purwanto A, and Mazlan SA (2015). Recent progress on magnetorheological solids: Materials, fabrication, testing, and applications. *Advanced Engineering Materials* 17 (5):563–597. DOI: 10.1002/adem.201400258.

Wang X (2013). Dynamic analysis of magnetoelasticity for ferromagnetic plates with nonlinear magnetization in magnetic fields. *Journal of Engineering Mechanics* 139 (5):559–568. DOI: https://doi.org/10.1061/(ASCE)EM.1943-7889.0000518.

Ward IM and Sweeney J (2004). *An introduction to the mechanical properties of solid polymers*. Second edi. Chichester: John Wiley & Sons Ltd.

Wei KX, Meng G, Zhang WM, and Zhu SS (2008). Experimental investigation on vibration characteristics of sandwich beams with magnetorheological elastomers cores. *Journal of Central South University* 15:239–242.

Wei KX, You H, and Xia P (2010). Vibration suppression of flexible beams using MR elastomers. *Advanced Materials Research* 97-101:1578–1581. DOI: 10.4028/www.scientific.net/AMR.97-101.1578.

Wei K, Bai Q, Meng G, and Ye L (2011). Vibration characteristics of electrorheological elastomer sandwich beams. *Smart Materials and Structures* 20 (5):055012. DOI: 10.1088/0964-1726/20/5/055012.

Yeh JY (2013). Vibration analysis of sandwich rectangular plates with magnetorheological elastomer damping treatment. *Smart Materials and Structures* 22 (3):035010. DOI: 10.1088/0964-1726/22/3/035010.

Yin H, Sun L, and Chen J (2006). Magneto-elastic modeling of composites containing chain-structured magnetostrictive particles. *Journal of the Mechanics and Physics of Solids* 54 (5):975–1003. DOI: 10.1016/j.jmps.2005.11.007.

Yuan Z, Li W, Pei C, Wu W, and Chen Z (2014). Dynamic analysis of a ferromagnetic structure in strong magnetic field with electromagneto-mechanical coupling. *International Journal of Applied Electromagnetics and Mechanics* 45:387–394. DOI: 10.3233/JAE-141855.

Zhou GY, Lin KC, and Wang Q (2006). Finite element studies on field-dependent rigidities of sandwich beams with magnetorheological elastomer cores. *Smart Materials and Structures* 15 (3):787–791. DOI: 10.1088/0964-1726/15/3/014.

Zhou GY and Wang Q (2005). Magnetorheological elastomer-based smart sandwich beams with nonconductive skins. *Smart Materials and Structures* 14 (5):1001–1009. DOI: 10.1088/0964-1726/14/5/038.

Zhou GY and Wang Q (2006a). Use of magnetorheological elastomer in an adaptive sandwich beam with conductive skins. Part I: Magnetoelastic loads in conductive skins. *International Journal of Solids and Structures* 43 (17):5386–5402. DOI: 10.1016/j.ijsolstr.2005.07.042.

Zhou GY and Wang Q (2006b). Use of magnetorheological elastomer in an adaptive sandwich beam with conductive skins. Part II: Dynamic properties. *International Journal of Solids and Structures* 43 (17):5403–5420. DOI: 10.1016/j.ijsolstr.2005.07.044.